CRC Report No. A-65

Accuracy of Regional Simulations of Background Ozone and Particulate Matter

Final Report

September 2009

COORDINATING RESEARCH COUNCIL, INC.
3650 MANSELL ROAD·SUITE 140·ALPHARETTA, GA 30022

The Coordinating Research Council, Inc. (CRC) is a non-profit corporation supported by the petroleum and automotive equipment industries. CRC operates through the committees made up of technical experts from industry and government who voluntarily participate. The four main areas of research within CRC are : air pollution (atmospheric and engineering studies); aviation fuels, lubricants, and equipment performance, heavy-duty vehicle fuels, lubricants, and equipment performance (e.g., diesel trucks); and light-duty vehicle fuels, lubricants, and equipment performance (e.g., passenger cars). CRC's function is to provide the mechanism for joint research conducted by the two industries that will help in determining the optimum combination of petroleum products and automotive equipment. CRC's work is limited to research that is mutually beneficial to the two industries involved, and all information is available to the public.

Foreword

Under CRC Project A-65 “Accuracy of Regional Simulations of Background Ozone and Particulate Matter (PM),” ENVIRON International Corporation, in collaboration with researchers at University of California at Riverside, conducted research to investigate the effects of natural sources on background concentrations of ozone and PM and on their sensitivities to emission control strategies using a regional scale air quality model. Based on the research results, a draft journal manuscript entitled “Natural Emissions for Regional Modeling of Background Ozone and Particulate Matter and Impacts on Emissions Control Strategies” was produced. It will be submitted to Atmospheric Environment.

The draft manuscript is included in this report along with an Executive Summary.

Final Report

CRC PROJECT A-65

Accuracy of Regional Simulations of Background Ozone and Particulate Matter

Prepared for

CRC Atmospheric Impacts Committee
Coordinating Research Council
3650 Mansell Road, Suite 140
Alpharetta, GA 30022

Prepared by

Bonyoung Koo
Jeremiah Johnson
Tanarit Sakulyanontvittaya
Piti Piyachaturawat
Ralph E. Morris
Greg Yarwood
ENVIRON International Corporation
773 San Marin Drive, Suite 2115
Novato, CA 94998

and

Chao-Jung Chien
Gail Tonnesen
Center for Environmental Research & Technology
University of California at Riverside
1084 Columbia Avenue
Riverside, CA 92507

September 9, 2009

Executive Summary

Background

Air quality modeling for tropospheric ozone and particulate matter (PM) relies upon emission inventories for both anthropogenic and natural sources. While considerable effort has been devoted to quantifying emissions from these sources for the purpose of air quality management, significant uncertainties remain, especially for natural sources. There are many natural sources of ozone precursors and PM, including both direct emissions of primary PM (such as windblown dust) and emissions of gaseous species that undergo photochemical transformation and condensation to secondary PM. Natural sources are of concern because they provide background ozone and PM that cannot be controlled by attainment strategies designed to meet the National Ambient Air Quality Standard (NAAQS). Current modeling practice for the State Implementation Plans (SIPs) usually either neglects (e.g., lightning NOx) or simplifies (e.g., biogenics) many natural sources of ozone and PM. Natural contributions to ozone and PM will become more important as the NAAQS are revised and tightened. As SIP control measures reduce future emissions from anthropogenic sources, correctly quantifying the impact of natural sources will become more important.

There are four issues related to natural sources and background conditions that are important in air quality management planning:

1. Are natural sources alone able to result in exceedances of the ozone and/or PM NAAQS?
2. Are non-U.S. anthropogenic sources sufficient to cause exceedances of the NAAQS?
3. What are the levels of background ozone and PM concentrations in the absence of anthropogenic sources (or U.S. anthropogenic sources)?
4. What effects do natural sources and background concentrations have on the development of ozone and PM attainment emission control strategies?

The focus of the current CRC project (Project A-65) is on the fourth issue. To answer this question, we first focused on improving and refining the current natural source emissions. We reviewed the available literature to identify potentially important sources of natural background ozone, PM and precursors that are usually missing from regulatory modeling, and developed estimates for their contributions. Then, we conducted model sensitivity studies to investigate how revised natural sources influence the effectiveness of future anthropogenic emission control strategies.

Revised Natural Emissions

We identified and evaluated the following updates for natural sources:

- Organosulfur emissions from the ocean – dimethyl sulfide (DMS) and methanesulfonic acid (MSA)
- Nitric oxide (NO) emissions from lightning
- Alternative sea salt emissions

- Updated biogenic emissions of ozone and secondary organic aerosol (SOA) precursors from the Model of Emissions of Gases and Aerosols from Nature (MEGAN)
- Background methane reduced to pre-industrial level

These revisions were applied incrementally so that the impact of each revision could be evaluated separately. Each simulation was conducted with the 2002 annual ozone and PM modeling database developed for the Western Regional Air Partnership (WRAP) using EPA's Community Multiscale Air Quality (CMAQ) model version 4.6.

The largest impact on background ozone concentrations was from including lightning NO. However, ozone impacts were mostly limited to the southeastern US and Gulf of Mexico regions. Another natural component that had significant impact on background ozone was biogenic NO emissions (related to crop fertilization). MEGAN estimates much lower biogenic NO emissions than SMOKE BEIS3 in the central and western US resulting in significant ozone decreases in these regions. Background $PM_{2.5}$ concentrations generally increased with the revised natural sources. Additional SOA from biogenic sources (e.g., SOA from sesquiterpenes and polymerization) was the major part of $PM_{2.5}$ increases in the southeastern US while lower estimates of monoterpenes by MEGAN result in $PM_{2.5}$ decreases in the western US. However, the magnitude of the overall impact of the revised natural emissions is relatively small (Figure ES-1). Over inland areas, the changes in annual average ozone concentrations were within ~3 ppb and increases in annual average $PM_{2.5}$ were less than 2 $\mu g/m^3$.

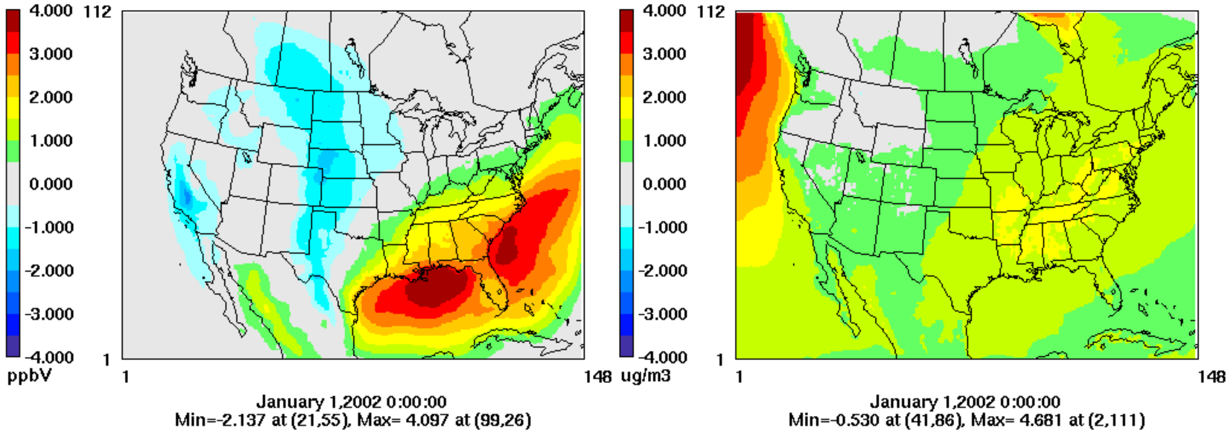
(a) Ozone difference (Revised – Current)

(b) $PM_{2.5}$ difference (Revised – Current)

Figure ES-1. Differences in annual average concentrations of ozone and $PM_{2.5}$ due to all the revised natural emissions combined.

The model simulations for this study limited the ozone concentration in the top layers (i.e., the stratosphere) of the lateral boundary condition files to prevent overly vigorous vertical velocities that incorrectly transport too much stratospheric ozone to the ground (for more details on this issue, see Appendix A). The vertical transport issue uncovered in this study prompted further study, sponsored by American Petroleum Institute, where ENVIRON is currently investigating improvements to vertical transport algorithms.

Impacts on Sensitivity to Emission Controls

To assess the impacts of revised natural emissions on ozone and PM responses to anthropogenic emission reductions, annual simulations were performed with both the current and revised natural emissions for a 2002 base year and 2018 future year. The modeling database had 36 km and 12 km nested grids and was developed by the Visibility Improvement State and Tribal Association of the Southeast (VISTAS). For ozone, we reduced by 30% future year (2018) anthropogenic emissions of NOx, VOC, and both NOx and VOC and evaluated model responses for the 4-th highest 8-hour ozone at monitoring sites. This metric was selected for its regulatory significance to ozone Design Values (DVs). For $PM_{2.5}$ and regional haze, we reduced the 2018 anthropogenic emissions of NOx, VOC, SO_2, NH_3, and primary $PM_{2.5}$ by 30% and calculated annual $PM_{2.5}$ DVs at monitoring sites and Class I area visibility projected to the 2018 future year using EPA's Modeled Attainment Test Software (MATS). MATS implements procedures developed by the EPA to combine base and future year model results with base year observed concentrations to project future-year concentrations.

The revised natural emissions had marginal impact on ozone response to emissions reductions and both the current and revised natural emission scenarios showed very similar ozone responses. This indicates that the anthropogenic emissions still play a major role in ozone formation in 2018 and/or that the changes to natural emissions were modest. The 4-th highest 8-hour ozone was slightly less responsive to anthropogenic NOx emission reductions with the revised natural emissions (Figure ES-2). The response to reducing both NOx and VOC was very similar to the NOx reduction case because reducing VOC had almost no impact on the 4-th highest 8-hour ozone concentrations.

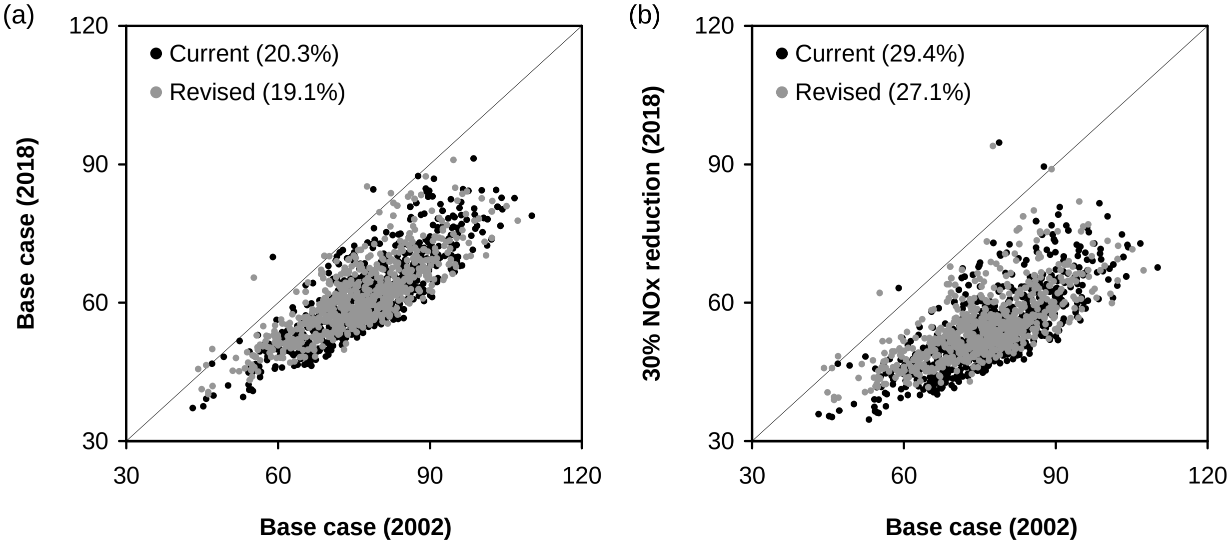

Figure ES-2. Scatter plots of the 4-th highest 8-hour ozone (in ppb) for the sites in the 12 km domain: (a) 2002 vs. 2018 with base case emissions; (b) 2002 base case vs. 2018 with 30% NOx reduction. The ozone concentrations from simulations with the current (black) and revised (gray) natural emissions are shown. Numbers in parentheses represent average percent reductions in the 4-th highest 8-hour ozone concentrations between the base year and future year simulations.

In all the anthropogenic emission reduction cases, the responses of annual $PM_{2.5}$ DVs to the emissions changes are very similar between the current and revised natural emission scenarios

(30% anthropogenic NOx reduction case is shown in Figure ES-3). Like ozone, it appears natural emissions have minor impact on $PM_{2.5}$ level in 2018. Similarly, both natural emission cases show no noticeable difference in the model response of visibility to the anthropogenic emission reductions in 2018.

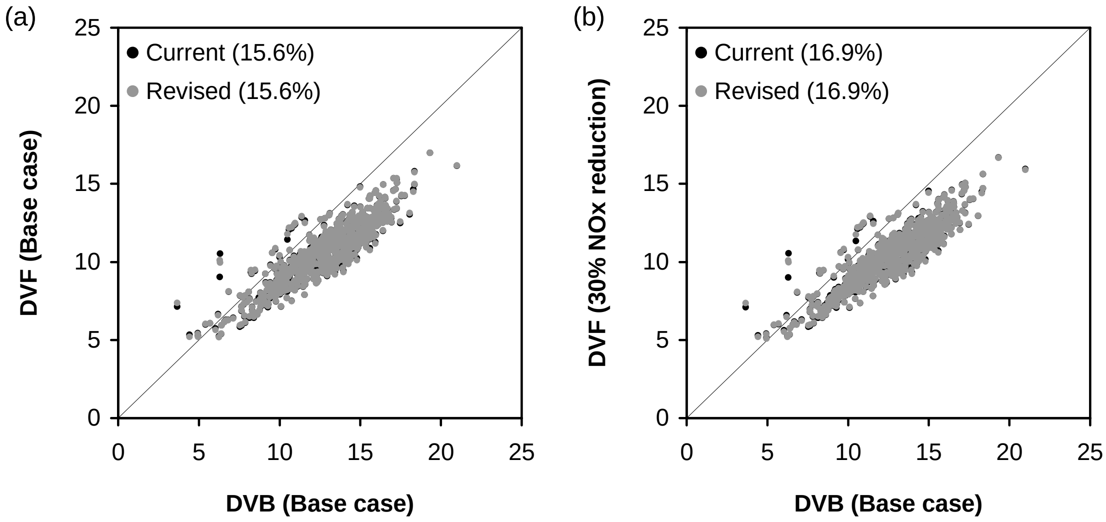

Figure ES-3. Scatter plots of $PM_{2.5}$ DVs (in $\mu g/m^3$): (a) Base year DV (DVB) vs. future year DV (DVF) with base case emissions; (b) DVB with base case emissions vs. DVF with 30% NOx reduction. DV projections using simulations with the current (black) and revised (gray) natural emissions are shown. Numbers in parentheses represent average percent reductions in DVs between the base year and future year simulations.

Recommendations

Although we have made significant improvements to the representation of natural sources in regulatory air quality modeling, large uncertainties remain. These include:

- SOA formation mechanisms – SOA formation is an area of active research. While a simple mechanism introduced in this study resulted in relatively minor SOA formation from isoprene, recent studies have proposed alternative mechanisms. For example, it has been reported that the SOA yields from isoprene photooxidation were enhanced in the presence of acidic seed particles. Other studies provided evidences of in-cloud SOA formation from oxidation products of isoprene. In addition, laboratory studies have reported NOx-dependent SOA yields for isoprene and terpenes. The latest version of CMAQ, which was released too late to be considered in this study, implemented some of these mechanisms, and can be used to test the effects of the updated mechanism on our revised natural simulations.
- Estimation of lightning NOx – Considerable uncertainties exist in the parameters for lightning NOx estimation (emission factor per flash, number of flashes, etc.). A further study is needed to refine the lightning NOx emission processor developed in this study, which will provide a simple and effective way to incorporate this important natural emission into current regulatory modeling.
- Wild fires and dust emissions – Wild fires and dust can significantly affect local and regional PM and large uncertainties exist in current emission inventories.

- Stratospheric ozone – This is a major source of ozone in the upper troposphere but should have much less influence at ground level. The ability of current models to correctly represent the stratospheric source of ground level ozone is limited by deficiencies in vertical transport schemes, especially for mountainous regions.
- Mineral nitrate – Current regional modeling has been underestimating summer nitrate due to almost complete evaporation of ammonium nitrate at high temperature. This is partly due to the fact that current models do not include nitrate uptake on mineral dust particles, which leads to non-volatile nitrate. In areas where naturally-occurring dust is abundant, this process may have a significant impact on the natural background nitrate concentrations.

Other sources of emissions uncertainty:

- Effects of international transport – This study considered natural background air quality by excluding world-wide anthropogenic emissions. A related issue is the contribution of anthropogenic sources outside North America which are both uncertain and changing. While global models have previously been used for simulating future-year scenarios (e.g., Wang et al., 2009), their applications are limited and not readily available for specific needs of regulatory modelers.
- Ammonia emissions – PM nitrate formation is strongly influenced by availability of ammonia from both natural and anthropogenic sources, and current emission inventories have large uncertainties, e.g., seasonal distribution of emissions.

This study has shown the impact of several important natural sources on background concentrations of ozone and $PM_{2.5}$ and the effectiveness of anthropogenic emission control strategies. However, the natural sources considered in this study are neither complete nor comprehensive. Further study of the issues listed above will improve understanding of natural background ozone and PM and help to establish the most effective air quality management plans.

Draft Journal Manuscript

Natural Emissions for Regional Modeling of Background Ozone and Particulate Matter and Impacts on Emissions Control Strategies

Bonyoung Koo[1*], Chao-Jung Chien[2], Gail Tonnesen[2], Ralph Morris[1], Jeremiah Johnson[1], Tanarit Sakulyanontvittaya[1], Piti Piyachaturawat[1], and Greg Yarwood[1]

[1]ENVIRON International Corporation, Novato, California
[2]Center for Environmental Research & Technology, University of California at Riverside

Abstract

Natural emissions adopted in current regional air quality modeling are updated to better describe natural background ozone and PM concentrations for North America. The revised natural emissions include organosulfur from the ocean, NO from lightning, sea salt, biogenic secondary organic aerosol (SOA) precursors, and pre-industrial levels of background methane. The model algorithm for SOA formation was also revised. Natural background ozone concentrations increase by up to 4 ppb in annual average over the southeastern US and Gulf of Mexico due to added NO from lightning while the revised biogenic emissions produced less ozone in the central and western US. Natural $PM_{2.5}$ concentrations generally increased with the revised natural emissions. Future year (2018) simulations were conducted for several anthropogenic emission reduction scenarios to assess the impact of the revised natural emissions on anthropogenic emission control strategies. Overall, the revised natural emissions did not significantly alter the ozone responses to the emissions reductions in 2018. With revised natural emissions, ozone concentrations were slightly less sensitive to reducing NOx in the southeastern US than with the current natural emissions due to higher NO from lightning. The revised natural emissions have little impact on modeled $PM_{2.5}$ responses to anthropogenic emission reductions.

Introduction

Natural background concentrations can be defined as those concentrations of ozone, particulate matter (PM) and their precursors that would occur as a result of only natural (i.e., biogenic and geogenic) emissions. Contributions to background ozone include both photochemical production from natural ozone precursors and stratospheric intrusion of ozone into the troposphere, while background contributions to PM include direct emissions of primary PM (such as windblown dust) and secondary PM formed from photochemical transformation and/or condensation of gaseous precursors from natural sources.

Air quality modeling for atmospheric ozone and PM must include emission inventories for both anthropogenic and natural sources. While extensive efforts have been given to investigate and quantify natural emissions, significant uncertainties remain. Natural sources become more important as air quality standards are tightened because they cause background levels of ozone and PM that cannot be controlled by attainment strategies. With the US EPA's current 35 $\mu g/m^3$ 24-hour $PM_{2.5}$ National Ambient Air Quality Standard (NAAQS) and recently revised 75 ppb 8-hour ozone NAAQS, it is questionable whether violations of the NAAQS may occur due to natural sources alone and whether the selected emissions control path may be affected by neglecting or over-simplifying the representation of natural sources. The impact of the natural sources will become more significant in the future as adopted control measures reduce anthropogenic emissions.

Modeling studies for natural ozone and PM have been completed at both the global and regional scale. Global scale simulations are necessary even when the focus is on local or regional emissions because international transport is rapid, with time scales of days to weeks. Global scale models, however, typically have coarse spatial resolution which limits their usefulness for evaluating local scale variability in pollutant concentrations. Global model simulations of background ozone and PM have been performed with the GEOS-CHEM model (Fiore et al., 2003; Park et al., 2004). Global scale model simulations of international transport have been performed with both GEOS-CHEM (Heald et al., 2006) and the MOZART model (Liu and Mauzerall, 2007). Heald et al. (2006) found enhancement of sulfate in North America caused by transport from Asia, with average enhancement of sulfate of 0.16 $\mu g/m^3$ during spring 2001. This was 33% greater than the 0.12 $\mu g/m^3$ sulfate concentration used to represent total background sulfate in the western US (EPA, 2003). In global scale studies of background ozone, Fiore et al. (2003) found that natural ozone levels were typically between 10 to 25 ppb and never exceeded 40 ppb. When including international transport, they found that background ozone in the US was between 15 to 30 ppb with some incidences between 40 to 50 ppb in the western US. They also concluded that stratospheric intrusion of ozone was always less than 20 ppb and that it represented a minor contribution to background ozone. Another GEOS-CHEM study performed by Wang et al. (2009) yielded a mean surface ozone concentration of 26 ppb in the absence of anthropogenic emissions from North America during summer 2001. They also found that Canadian and Mexican pollution increased US ozone concentrations by 3 ppb in average.

At the same time, several Regional Planning Organizations (RPOs) have developed anthropogenic emission control strategies for regional $PM_{2.5}$ and visibility in the US. One RPO, the Western Regional Air Partnership (WRAP), performed a regional scale simulation to evaluate $PM_{2.5}$ and visibility in the absence of anthropogenic emissions (Tonnesen et al., 2006). The WRAP “Clean Condition” scenario does not represent true natural conditions because it lacks several natural sources (e.g., lightning, sea salt), but nevertheless found that natural emissions did contribute to visibility impairment because of large wildfires. These results call for additional investigation of the impacts of missing natural emissions in future modeling studies.

The primary objectives of this study are to address two issues related to natural sources and background conditions that are of importance in air quality management planning: (1) What are the background concentrations of ozone and PM in the absence of anthropogenic sources? (2) What effects do natural sources and background concentrations have on emission control strategies?

First, we assess the impact of potentially important sources of natural background ozone, PM and their precursors that are usually missing from regulatory modeling in the US. Subsequently, we discuss how these revised natural emissions affect current emissions control strategies to achieve the ambient standards.

Updating Natural Emissions in Current Air Quality Modeling

We evaluated the following updates to the current representation of natural sources:

- Organosulfur emissions from the ocean – dimethyl sulfide (DMS) and methanesulfonic acid (MSA)
- NO emissions from lightning
- Alternative sea salt emissions
- Updated biogenic secondary organic aerosol (SOA) formation with emissions from the Model of Emissions of Gases and Aerosols from Nature (MEGAN)
- Pre-industrial level of background methane

To evaluate the effect of these revisions separately, we conducted a series of regional scale simulations using US EPA's Community Multiscale Air Quality (CMAQ) modeling system version 4.6 and the WRAP 2002 annual modeling database (Tonnesen et al., 2006). The modeling domain is the RPO Unified Continental 36 km modeling grid covering the contiguous 48 US states, southern Canada and northern Mexico (Figure 1). The vertical grid has 19 layers that extend to the lower stratosphere (~15 km) with a surface layer thickness of 40 m. The boundary conditions (BCs) for the modeling domain were from a GEOS-CHEM global simulation without anthropogenic emissions. The CB05 gas-phase chemistry mechanism and AERO4 aerosol scheme were used in CMAQ. We present results for two natural condition cases, a "current" case with natural emissions from WRAP and a "revised" case with updated natural emissions.

Organosulfur from Oceans

Oceanic dimethylsulfide (DMS) is a major natural source of sulfur to the atmosphere and contributes to sulfate aerosol. Global DMS emissions are believed to account for 15% of the total global sulfur emissions of 3.2 Tg S/year (Bates et al., 1992). DMS is also emitted in biomass burning (Meinardi et al., 2003). In the CMAQ modeling system, sulfur emissions from the ocean are treated as sulfate and speciated from sea salt emissions. CMAQ version 4.5 was the first release to include sea salt aerosols which were implemented in the AERO4 aerosol module. The emissions of sea salt aerosols from the open ocean are calculated based on wind speed and relative humidity (Shankar et al., 2005). In the AERO4 module, sea salt sulfate is speciated from the sea salt aerosols using a mass ratio of 0.0755. Emissions of DMS and MSA outside of the US modeling domain need to be represented as boundary conditions (BCs). For the revised natural case, DMS and MSA from the GEOS-CHEM simulation were mapped to sulfur dioxide (SO_2) and sulfate (SO_4) in CMAQ, respectively.

Including DMS and MSA in the BCs resulted in slight decreases (less than 0.1 ppb) in annual average ozone over the Pacific Ocean and downwind (Figure 2 (c)). DMS was represented as SO_2 which reacts with hydroxyl radical (OH) and produces less ozone than other reaction partners for OH over the Pacific Ocean (e.g., methane). Annual average $PM_{2.5}$ increased slightly due to added sulfur from the ocean (Figure 3 (c)).

NO from Lightning

Lightning NO emissions can be estimated directly based on the number of lightning flashes, the intensity of each flash, the lightning type (cloud to ground versus cloud to cloud), and the emissions factor per flash. While the number of lightning flashes and flash intensity can be estimated from the National Lightning Detection Network (NLDN), there is uncertainty in the estimates of emissions factors per flash. As a result, there remains at least a factor of ten uncertainty in estimates of lightning NOx emissions, with estimates typically within the range 1-20 Tg N/year globally (Schumann and Huntrieser, 2007; Zhang et al., 2003a, 2003b; Lee et al., 1997). Orville et al. (2002) estimated about 30 million flashes per year for North America cloud-to-ground lightning. Using a multiplier of 2.8 to get intracloud flashes (Boccippio et al., 2001), we estimate a total of 114 million flashes per year. Using a high-end estimate for NO emissions per flash of 9.3 Kg N per flash from the EULINOX study (Holler and Schumann, 2000), we obtained 1.06 Tg N/year for North America. This high-end estimate of annual total lightning NO emissions was then spatially and temporally allocated to the model grid cells using convective precipitation activity as a surrogate. The hourly and gridded 3-D lightning NO emissions are calculated as follows:

$$E(\bar{x},t) = R_{NO} P_c(\bar{x},t) D(\bar{x},t) p'(\bar{x},t)$$

where:

$E(\bar{x},t)$	NO emission rate (mol/hr) at time t and grid location $\bar{x}$
R_{NO}	NO emission factor
$P_c(\bar{x},t)$	Convective precipitation (m/hr) at time t and grid location $\bar{x}$
$D(\bar{x},t)$	Convective cloud depth (m) at time t and grid location $\bar{x}$
$p'(\bar{x},t)$	Pressure (Pa) at time t and grid location $\bar{x}$

Setting $\sum E(\bar{x},t)$ to 1.06 Tg N/year returns a value of R_{NO} equal to 3.9 x 10^{-12} which was used to generate the hourly and gridded lightning NOx emissions for the 2002 year. Figure 4 shows the vertical profile of the WRAP domain average lightning NO emissions for January and July 2002. Lightning NO emission rates are higher in July due to much stronger and widespread convective activity. Figure 5 shows the spatial column total lightning NO emissions for January and July 2002.

Adding lightning NO emissions resulted in significant ozone increases over the southeastern US where biogenic VOC emissions are high and convective activity is strong (Figure 2 (d)). Increased NO emissions also can lead to more nitrate formation. However, excess nitrate could replace chloride in sea salt (similar to sulfate replacing chloride) resulting in less chloride in the particle phase. The combined effect resulted in slightly increased $PM_{2.5}$ with lightning NO emissions (Figure 3 (d)). Because we used a high-end estimate of lightning NO emissions these concentration changes also should be regarded as high-end values.

Alternative Sea Salt Emissions

Previous modeling studies conducted for WRAP and Visibility Improvement State and Tribal Association of the Southeast (VISTAS) have shown that the internally generated sea salt emissions with the CMAQ AERO4 module generally underestimate measured chlorine concentrations although there may be other chlorine sources contributing to the measurement data. To obtain revised sea salt emissions, we developed sea salt emission from meteorological data and published emission algorithms. The emitted particle flux was calculated using the parameterization of Gong (2003) with an upper limit for the sea salt aerosol size range set to 2.5 microns. The flux represents the rate of production of marine aerosol droplets per unit area of the sea surface per increment of droplet radius. From the particle flux, the emitted particle mass is calculated assuming spherical particle geometry, and a density of 1150 kg m^{-3} (Grini et al. 2002). Sulfate emissions were calculated using a sulfate-to-sodium ratio of 0.25. The externally generated sea salt (and sulfate) emissions were then supplied to a modified CMAQ code where the internal sea salt generation code was disabled.

Figure 2 (e) shows that ozone concentrations are slightly decreased over the ocean with the alternative sea salt and sulfate emissions. This is because increased sodium chloride emissions reduced nitric acid over the ocean by forming sodium nitrate. In very low NOx environments, nitric acid can be a significant source of NOx via nitric acid photolysis and reaction with OH. In this situation, reduced nitric acid due to increased sea salt resulted in lower ozone. $PM_{2.5}$ increased with the new sea salt emissions with effects seen mostly over the ocean (Figure 3 (e)).

Updated SOA Scheme and Biogenic Emissions

Modeling studies conducted for the VISTAS RPO in the southeastern US using the CMAQ model have shown poor performance organic aerosol (OA) with a tendency toward under prediction. To improve the model performance, Morris et al. (2006) modified the SOA scheme in CMAQ to incorporate potentially important SOA forming processes that were missing: (1) SOA formation from isoprene, (2) SOA formation from sesquiterpenes, and (3) Polymerization of SOA. Since sesquiterpenes are not accounted for in the SMOKE BEIS3 model, Morris et al. (2006) estimated sesquiterpenes from monoterpene emissions. For the revised natural case, we used the same modified SOA scheme to add the new processes. Also, the biogenic emissions from SMOKE BEIS3 were replaced by those from the latest MEGAN biogenic emissions model which provided more biogenic VOC species (including sesquiterpenes) using updated land use data with higher resolution. However, we used isoprene emissions from SMOKE BEIS3 instead of MEGAN because previous modeling studies showed that the MEGAN isoprene emissions, which are significantly higher than SMOKE BEIS3, result in overestimation of ozone. Some recent measurement studies suggest that current isoprene chemistry mechanisms significantly underpredict OH radical concentrations under a low NOx condition and thus cause isoprene to accumulate in the boundary layer (Kuhn et al., 2007; Lelieveld et al., 2008). However, uncertainties remain as to whether and how the proposed additional OH is produced. Figure 6 compares NO and monoterpene emissions from SMOKE BEIS3 and MEGAN. Biogenic NO emissions from MEGAN are generally lower than those from SMOKE BEIS3, especially in the central and western US. Monoterpene emissions are higher with MEGAN in the southeastern US, but less in the western US.

Using an updated biogenic SOA scheme combined with MEGAN biogenic emissions resulted in an overall decrease in ozone concentrations in the central US (Figure 2 (f)) due mainly to lower biogenic NO emissions with MEGAN. Figure 3 (f) shows higher $PM_{2.5}$ concentrations over the eastern US due to greater OA formation from the updated SOA scheme, mainly from sesquiterpene emissions and SOA polymerization. Lower NO emissions from MEGAN did reduce nitrate concentrations in some areas but overall $PM_{2.5}$ increased because SOA increases outweighed nitrate decreases.

Pre-industrial Level of Background Methane

CMAQ uses a constant background methane concentration of 1.85 ppm which we changed to 0.70 ppm to reflect pre-industrial level estimated by Blunier et al. (1993). Methane reacts with OH to form hydroperoxy radical (HO_2) and organic peroxy radicals (RO_2) which leads to ozone formation in the presence of NO. Therefore, reducing background methane concentration should lower ozone formation and Figure 2 (g) confirms that ozone decreased. The locations of ozone decreases due to reduced methane and ozone increases due to lightning NO emissions are similar but the magnitude of the former is much smaller than that of the latter. $PM_{2.5}$ concentration slightly increased with lowered methane (Figure 3 (g)). No PM is formed when OH reacts with methane so reducing methane can result in more OH available to react with PM precursors.

Combined Effect of Revised Natural Emissions

The overall impact of the revised natural emissions on annual average ozone concentrations is shown in Figure 2 (h). The impact of lightning NO emissions is dominant with the biggest increases shown over the Gulf of Mexico (up to 4 ppb in annual average ozone). The ozone decreases over the central US are mainly due to lower biogenic NO emissions from MEGAN. $PM_{2.5}$ concentrations are generally higher with revised natural emissions (Figure 3 (h)) with major contributions coming from the alternative sea salt emissions and the updated SOA scheme. The impact of alternative sea salt emissions is mostly seen over the northern Pacific Ocean with relatively minor increases inland. Increases in $PM_{2.5}$ over the eastern US are primarily due to additional SOA formation. However, note that the overall impact over inland area is relatively small (less than ~3 ppb for ozone and less than ~2 $\mu g/m^3$ for $PM_{2.5}$).

Comparison with Previous Estimates of Natural Background Ozone and $PM_{2.5}$

Although there is large uncertainty in the natural ozone levels, estimates of pre-industrial US ozone levels typically range from 20 to 30 ppb. Our revised natural emission scenario predicted annual average ozone over the US of 14 to 23 ppb compared to 13 to 24 ppb in the current natural emission scenario.

Estimates of natural haze levels have been developed by the US EPA for visibility planning purposes and are described in *Guidance for Estimating Natural Visibility Conditions under the Regional Haze Rule* (EPA, 2003). The EPA's natural haze levels were based on ambient data analysis for days with good visibility. The sum of the average natural concentrations of $PM_{2.5}$

species in the EPA guidance is 1.21 μg/m^3 for the western US and 2.25 μg/m^3 for the eastern US. The modeled annual mean $PM_{2.5}$ concentrations averaged over IMPROVE monitoring sites are 2.01 μg/m^3 (West) and 0.99 μg/m^3 (East) with the current natural emissions. With the revised natural emissions, they increased to 2.09 μg/m^3 (West) and 1.90 μg/m^3 (East), respectively. In both natural emissions scenarios, the model predicted much higher $PM_{2.5}$ in the western US than the EPA guidance as wild fires heavily affected some of the IMPROVE sites. In the eastern US, the modeled $PM_{2.5}$ concentrations are almost doubled using the revised natural emissions, primarily due to lightning NOx and increased biogenic emissions, although still lower than the EPA estimate.

Impact of Revised Natural Emissions on Emission Controls

To assess impact of the revised natural emissions on ozone and PM responses to emissions control strategies, sensitivity simulations were conducted using the CMAQ modeling database developed for VISTAS. The modeling domain consists of the same 36-km grid as used in the previous section with an additional 12-km grid covering the southeastern US (Figure 1). The CMAQ model was applied for the 2002 base year and 2018 future year with the current and revised natural emissions. Various emissions reduction scenarios were tested in future year simulations with two sets of natural emissions (Table 1). The 36-km simulations were conducted for the annual period and used for evaluating $PM_{2.5}$ responses to the emissions reductions. Although the 36-km grid covers the entire continental US, the following analyses exclude the results for the WRAP states because there are uncertainties in the VISTAS modeling database over the western US. For ozone, the sensitivity runs were performed for the third quarter (July – September) with the 12-km grid resolution to follow EPA guideline that recommends the model grid resolution not to exceed 12 km for 8-hour ozone attainment demonstration (EPA, 2007). Annual emissions from anthropogenic and biogenic sources over the 36-km domain are summarized in Table 2.

Figure 7 shows the 4-th highest 8-hour ozone concentrations with the current and revised natural emissions. The first scatter plot compares the ozone concentrations for the 2002 and 2018 simulations at each AQS monitoring site for the base case. Both the current and revised natural emission simulations resulted in similar reductions in the 4-th highest 8-hour ozone from 2002 to 2018 indicating that the revised natural emissions have minor impact on the modeled ozone response to the base case emission changes between 2002 and 2018. The rest of the scatter plots compare the ozone concentrations between the 2018 base case and cases with reduced 2018 anthropogenic NOx and/or VOC emissions. The ozone concentrations with the revised natural emissions are slightly less responsive to reduction in anthropogenic NOx emissions because additional NO from lightning was added. Reducing anthropogenic VOC emissions makes almost no changes in both natural emission cases indicating NOx-limited ozone in 2018. The ozone reductions from reducing both NOx and VOC emissions are very similar to those in the NOx reduction case.

For $PM_{2.5}$ and visibility, EPA's Modeled Attainment Test Software (MATS) was used to forecast 2018 annual average $PM_{2.5}$ Design Values (DVs) and regional haze at Class I areas (EPA, 2007). Responses of annual average $PM_{2.5}$ DVs with revised natural emissions to emission changes between 2002 and 2018 are almost identical to those with current natural emissions (Figure 8). Reduction in either of 2018 NOx, VOC or NH_3 emissions has little impact on DVFs with both the current and revised natural emissions. Simulations with the current and revised natural emissions both resulted in a slight decrease in DVF when 2018 anthropogenic SO_2 emissions were reduced by 30% and the responses were similar since effects of the changes in natural sulfur emissions are mostly limited over the ocean. Reducing primary $PM_{2.5}$ emission is effective in lowering DVFs in our simulations and both the current and revised natural emission cases exhibit similar sensitivities to the emission reduction as expected.

Figure 9 presents model responses of Haziness (visibility) on worst 20% days at Class I areas to the future year emissions reductions. Like $PM_{2.5}$ DVs shown above, the visibility responses to 2018 emission reductions are similar for both natural emission cases. Visibility in 2018 is little affected by reductions in most anthropogenic emissions tested while slightly improved with reductions in SO_2 emissions.

Table 3 summarizes percent reductions in the 8-hour ozone and annual average $PM_{2.5}$ DVs and Haziness between 2002 and 2018 for each RPO region. In general, the 8-hour ozone DVs are slightly more sensitive to the future year emissions reductions in the current natural case than in the revised natural case. However, the $PM_{2.5}$ DVs and visibility show little difference between the current and revised natural cases.

Table 4 shows the number of sites violating either the 8-hour ozone standard (75 ppb) or annual $PM_{2.5}$ standard (15 $\mu g/m^3$) in 2018 under various emission control scenarios. The revised natural emissions did not significantly alter the number of violating sites in most cases. The MRPO region has much fewer ozone standard violating sites in the base case simulation with the revised natural emissions which has lower biogenic NO emissions in the region. However, further reduction in anthropogenic NOx and/or VOC emissions eliminates this difference.

Conclusions

Natural emissions used in current US modeling practice for ozone and PM were updated and evaluated. The largest impact on background ozone concentrations was from inclusion of lightning NO emissions which resulted in widespread ozone increases over the southeastern US and Gulf of Mexico. MEGAN estimates less NO emissions from biogenic sources than SMOKE BEIS3 and caused ozone decreases in the central and western US. Background $PM_{2.5}$ generally increased with the revised natural sources. Additional SOA from new biogenic precursor emissions and updated modeling scheme (e.g., SOA from sesquiterpenes and polymerization) is the major part of $PM_{2.5}$ increases in the southeastern US.

For $PM_{2.5}$ and visibility, the model responses to anthropogenic emission reductions are similar in both the current and revised natural emission cases. Ozone is slightly less responsive to NOx reductions with the revised natural emissions indicating that slightly more anthropogenic reduction will be needed to lower ozone. Overall, the revised natural emissions resulted in only small differences in the future year ozone and $PM_{2.5}$, thus their impacts on the effectiveness of anthropogenic emissions reductions remain relatively small.

Although we have incorporated and updated important natural sources in this study (e.g., lightning NOx, organosulfur emissions, new biogenic SOA), they are neither complete nor comprehensive. For example, we did not include acid-catalyzed heterogeneous SOA formation (Jang et al., 2002; Czoschke et al., 2003; Surratt et al., 2007), NOx-dependent SOA yields (Kroll et al., 2006; Ng et al., 2007), or in-cloud SOA formation (Lim et al., 2005; Chen et al., 2007). Heterogeneous reaction of nitric acid on dust particles to form mineral nitrate (Astitha et al., 2007) was also not considered in our study. Also, there still remain significant uncertainties in the natural emissions considered here. For example, estimates of sea salt emissions are highly uncertain as well as wild fires and dust. Lightning NO is also a critical uncertainty, especially for the southeastern US where biogenic VOC emissions are large and ozone formation is especially sensitive to changes in NOx emissions. Assumptions for lightning NO emissions can significantly change modeled natural ozone levels and may also change the relative effectiveness of VOC and NOx emissions controls.

References

Astitha, M., G. Kallos, P. Katsafados, and E. Mavromatidis (2007) Heterogeneous chemical processes and their role on particulate matter formation in the Mediterranean region, 29th NATO/SPS ITM on Air Pollution Modelling and its Applications, Aveiro, Portugal.

Bates, T. S., B. K. Lamb, A. Guenther, J. Dignon, and R. E. Stoiber (1992) Sulfur emissions to the atmosphere from natural sources, J. Atmos. Chem., 14, 315-337.

Blunier, T., J. A. Chappellaz, J. Schwander, J.-M. Barnola, T. Desperts, B. Stauffer, and D. Raynaud (1993) Atmospheric methane, record from a Greenland ice core over the last 1000 year, Geophys. Res. Lett., 20(20), 2219.

Boccippio, D. J., K. L. Cummins, H. J. Christian, and S. J. Goodman (2001) Combined Satellite- and Surface-Based Estimation of the Intracloud-Cloud-to-Ground Lightning Ratio over the Continental United States, Mon. Wea. Rev., 129, 108-122.

Chen, J., R. J. Griffin, A. Grini, and P. Tulet (2007) Modeling secondary organic aerosol formation through cloud processing of organic compounds, Atmos. Chem. Phys., 7, 5343-5355.

Czoschke, N. M., M. Jang, and R. M. Kamens (2003) Effect of acidic seed on biogenic secondary organic aerosol growth, Atmos. Environ., 37, 4287-4299.

EPA (2003) Guidance for Estimating Natural Visibility Conditions Under the Regional Haze Rule, U.S. Environmental Protection Agency, Research Triangle Park, NC. EPA-454/B-03-005. September.

EPA (2007) Guidance on the Use of Models and Other Analyses for Demonstrating Attainment of Air Quality Goals for Ozone, $PM_{2.5}$ and Regional Haze, U.S. Environmental Protection Agency, Research Triangle Park, NC. EPA-454/B-07-002. April.

Fiore, A., D. J. Jacob, H. Liu, R. M. Yantosca, T. D. Fairlie, and Q. Li (2003) Variability in surface ozone background over the United States: Implications for air quality policy, J. Geophys. Res., 108, ACH 19-1 - ACH 19-12.

Gong, S. L. (2003) A parameterization for sea-salt aerosol source function for sub- and super-micron particle sizes, Biogeochemical Cycles, 17, 1097-1104.

Grini, A., G. Myhre, J. K. Sundet, and I. S. A. Isaksen (2002) Modeling the annual cycle of sea salt in the global 3D model Oslo CTM2: concentrations, fluxes and radiative impact, J. Climate, 15, 1717-1730.

Heald, C. L., D. J. Jacob, R. J. Park, B. Alexander, T. D. Fairlie, R. M. Yantosca, and D. A. Chu (2006) Transpacific transport of Asian anthropogenic aerosols and its impact on surface air quality in the United States, J. Geophys. Res., 111(D14), 1-13.

Holler, H. and U. Schumann (2000) EULINOX (European Lightning Nitrogen Oxides Project) Final Report (http://www.pa.op.dlr.de/eulinox/publications/finalrep/index.html).

Jang, M., N. M. Czoschke, S. Lee, and R. M. Kamens (2002) Heterogeneous atmospheric aerosol production by acid-catalyzed particle-phase reactions, Science, 298, 814-817.

Kroll, J. H., N. L. Ng, S. M. Murphy, R. C. Flagan, and J. H. Seinfeld (2006) Secondary organic aerosol formation from isoprene photooxidation, Environ. Sci. Technol., 40, 1869-1877.

Kuhn, U., M. O. Andreae, C. Ammann, A. C. Araujo, E. Brancaleon, P. Ciccioli, T. Dindorf, M. Frattoni, L. V. Gatti, L. Ganzeveld, B. Kruijt, J. Lelieveld, J. Lloyd, F. X. Meixner, A. D. Nobre, U. Poschl, C. Spirig, P. Stefani, A. Thielmann, R. Valentini, and J. Kesselmeier (2007) Isoprene and monoterpene fluxes from Central Amazonian rainforest inferred from tower-based and airborne measurements, and implications on the atmospheric chemistry and the local carbon budget, Atmos. Chem. Phys., 7, 2855-2879.

Lee, D. S., I. Kohler, E. Grobler, F. Rohrer, R. Sausen, L. Gallardo-Klenner, J. G. J. Olivier, F. J. Dentener, and A. F. Bouwman (1997) Estimations of global NOx emissions and their uncertainties, Atmospheric Environment, 31(12), 1735.

Lelieveld, J., T. M. Butler, J. N. Crowley, T. J. Dillon, H. Fischer, L. Ganzeveld, H. Harder, M. G. Lawrence, M. Martinez, D. Taraborrelli, and J. Williams (2008) Atmospheric oxidation capacity sustained by a tropical forest, Nature, 452, 737-740.

Lim, H.-J.; A. G. Carlton, and B. J. Turpin (2005) Isoprene forms secondary organic aerosol through cloud processing: model simulations, Environ. Sci. Technol., 39, 4441-4446.

Liu, J. and D. L. Mauzerall (2007) Potential influence of inter-continental transport of sulfate aerosols on air quality, Environ. Res. Lett., 2(4), 045029.

Meinardi, S., I. J. Simpson, N. J. Blake, D. R. Blake, and F. S. Rowland (2003) Dimethyl disulfide (DMDS) and dimethyl sulfide (DMS) emissions from biomass burning in Australia, Geophys. Res. Lett., 30(9), 1454, doi:10.1029/2003GL016967.

Morris, R. E., B. Koo, A. Guenther, G. Yarwood, D. McNally, T. W. Tesche, G. Tonnesen, J. Boylan, and P. Brewer (2006) Model Sensitivity Evaluation for Organic Carbon using Two Multi-Pollutant Air Quality Models that Simulate Regional Haze in the Southeastern United States, Atmos. Environ., 40, 4960-4972.

Ng, N. L., P. S. Chhabra, A. W. H. Chan, J. D. Surratt, J. H. Kroll, A. J. Kwan, D. C. McCabe, P. O. Wennberg, A. Sorooshian, S. M. Murphy, N. F. Dalleska, R. C. Flagan, and J. H. Seinfeld (2007) Effect of NOx level on secondary organic aerosol (SOA) formation from the photooxidation of terpenes, Atmos. Chem. Phys., 7, 5159-5174.

Orville, R. E., G. R. Huffines, W. R. Burrows, R. L. Holle, and K. L. Cummins (2002) The North American Lightning Detection Network (NALDN)-First Results: 1998-2000, Mon. Wea. Rev., 130, 2098-2109.

Park, R. J., D. J. Jacob, B. D. Field, R. M. Yantosca, and M. Chin (2004) Natural and transboundary pollution influences on sulfate-nitrate-ammonium aerosols in the United States: Implications for policy, J. Geo-phys Res., 109, D15204, doi:10.1029/2003JD004473.

Schumann, U. and H. Huntrieser (2007) The global lightning-induced nitrogen oxides source, Atmos. Chem. Phys. Discuss, 7, 2623-2818.

Shankar, U., P. V. Bhave, J. M. Vukovich, and S. J. Roselle (2005) Initial applications of sea salt aerosol emissions and chemistry algorithms in the CMAQ v4.5 - AERO4 module, Presented at 4th Annual CMAS Models-3 Users' Conference, Chapel Hill, NC.

Surratt, J. D., M. Lewandowski, J. H. Offenberg, M. Jaoui, T. E. Kleindienst, E. O. Edney, and J. H. Seinfeld (2007) Effect of acidity on secondary organic aerosol formation from isoprene, Environ. Sci. Technol., 41, 5363-5369.

Tonnesen, G., M. Omary, Z. Wang, C. J, Jung, R. Morris, G. Mansell, Y. Jia, B. Wang, and Z. Adelman (2006) Report for the Western Regional Air Partnership Regional Modeling Center, University of California Riverside, Riverside, California, November. (http://pah.cert.ucr.edu/aqm/308/reports/final/2006/WRAP-RMC_2006_report_FINAL.pdf)

Wang, H., D. J. Jacob, P. L. Sager, D. G. Streets, R. J. Park, A. B. Gilliland, and A. van Donkelaar (2009) Surface ozone background in the United States: Canadian and Mexican pollution influences, Atmos. Environ., 43, 1310-1319.

Zhang, X., J. J. H. Helsdon, and R. D. Farley (2003a) Numerical modeling of lightning-produced NOx using an explicit lightning scheme: 1. Two-dimensional simulation as a 'proof of concept', J. Geophys. Res., 108(D18), ACH 5-1 - ACH 5-20.

Zhang, X., J. J. H. Helsdon, and R. D. Farley (2003b) Numerical modeling of lightning-produced NOx using an explicit lightning scheme: 2. Three-dimensional simulation and expanded chemistry, J. Geophys. Res., 108(D18), ACH 6-1 - ACH 6-17.

Tables

Table 1. Level of anthropogenic emission reductions selected for the future year sensitivity runs.

	NOx	VOC	SO_2	NH_3	$PM_{2.5}$
For $PM_{2.5}$ DV and Visibility	30%	-	-	-	-
36 km grid (Annual)	-	30%	-	-	-
	-	-	30%	-	-
	-	-	-	30%	-
	-	-	-	-	30%
For 8-hour ozone DV and 4th	30%	-	-	-	-
highest 8-hour ozone	-	30%	-	-	-
12 km grid (Q3)	30%	30%	-	-	-

Table 2. Annual emissions from anthropogenic and biogenic sources over the 36-km modeling domain (10^6 tons per year)

	Anthropogenic		Biogenic[a]	
	2002	2018	Current	Revised
NOx	15.8	9.6	1.8	3.5
VOC	16.5	13.3	79.3	58.6
SO_2	17.8	11.3	0.2	0.2
NH_3	3.8	4.8	0.6	0.6
$PM_{2.5}$	4.2	4.3	3.8	3.9

[a] Biogenic emissions are assumed to be the same for the base and future year scenarios.

Table 3. Percent reductions in 8-hour ozone and annual average PM2.5 DVs and visibility projected to 2018 by RPO region.

	VISTAS		MANE-VU		MRPO		CENRAP	
	Current	Revised	Current	Revised	Current	Revised	Current	Revised
Ozone[a]								
Base case	25.8%	24.2%	23.4%	23.6%	19.6%	19.9%	14.5%	13.5%
30% reduction in								
NOx	36.1%	33.7%	32.9%	32.9%	28.2%	28.5%	25.0%	23.4%
VOC	25.7%	24.2%	23.8%	24.1%	20.2%	20.6%	15.0%	14.1%
NOx/VOC	36.5%	33.1%	34.9%	32.2%	30.1%	28.1%	25.5%	23.5%
# of sites[b]	214	205	125	120	167	162	83	78
PM$_{2.5}$[c]								
Base case	21.6%	21.6%	21.0%	21.1%	13.9%	14.0%	10.6%	10.4%
30% reduction in								
NOx	22.4%	22.3%	21.7%	22.0%	15.8%	16.1%	12.4%	12.4%
VOC	22.1%	22.0%	21.6%	21.7%	14.6%	14.6%	11.0%	10.7%
SO$_2$	28.2%	28.3%	26.7%	26.9%	20.2%	20.3%	17.1%	17.0%
NH$_3$	22.0%	22.3%	22.0%	22.3%	15.6%	15.8%	11.7%	11.7%
PM$_{2.5}$	29.4%	28.5%	30.6%	30.2%	24.5%	23.6%	22.4%	21.1%
# of sites	222	222	157	157	159	159	168	168
Visibility[d]								
Base case	18.2%	18.1%	13.3%	13.2%	7.04%	7.14%	10.3%	10.1%
30% reduction in								
NOx	19.2%	18.9%	14.5%	14.2%	9.50%	9.72%	12.5%	12.4%
VOC	18.3%	18.1%	13.4%	13.2%	7.08%	7.16%	10.3%	10.1%
SO$_2$	23.6%	23.5%	17.7%	17.5%	11.6%	11.7%	14.7%	14.5%
NH$_3$	18.4%	18.4%	13.9%	13.9%	8.63%	8.88%	10.9%	10.8%
PM$_{2.5}$	20.4%	19.3%	15.6%	14.9%	9.88%	9.38%	13.1%	12.0%
# of sites	15	15	8	8	2	2	7	7

[a] Average percent reductions in 8-hour ozone DV.

[b] Different numbers of sites are accounted for the current and revised natural emission runs because MATS discards sites that do not have enough days with ozone concentration above a threshold.

[c] Average percent reductions in annual average PM$_{2.5}$ DV.

[d] Average percent reduction in Haziness on 20% worst days at Class I areas.

Table 4. Number of sites with exceedance of 8-hour ozone and annual $PM_{2.5}$ standards.

	VISTAS		MANE-VU		MRPO		CENRAP	
	Current	Revised	Current	Revised	Current	Revised	Current	Revised
Ozone[a]								
Base case	1	0	19	20	24	17	25	24
30% reduction in								
NOx	0	0	0	0	5	5	4	5
VOC	0	0	13	15	17	15	22	22
NOx/VOC	0	0	0	0	2	3	4	4
$PM_{2.5}$[b]								
Base case	1	1	1	1	4	4	0	0
30% reduction in								
NOx	1	1	1	1	2	2	0	0
VOC	1	1	1	1	3	3	0	0
SO_2	0	0	1	1	1	1	0	0
NH_3	1	1	1	1	3	2	0	0
$PM_{2.5}$	0	0	0	0	0	0	0	0

[a] Number of sites whose 2018 8-hour ozone DVFs exceed 75 ppb.

[b] Number of sites whose 2018 annual average $PM_{2.5}$ DVFs exceed 15 μg/m^3.

Figures

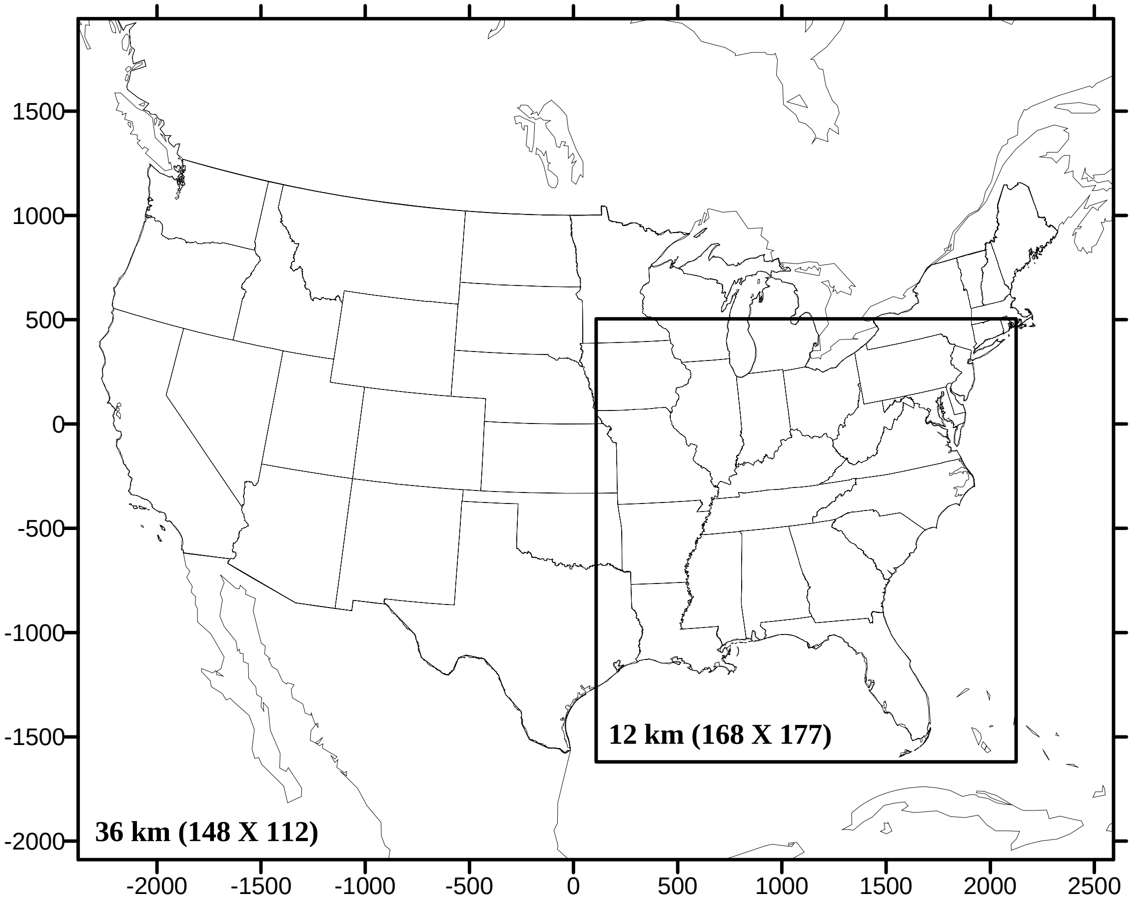

Figure 1. RPO United Continental 36 km modeling domain used by WRAP and VISTAS and 12 km nested grid for VISTAS.

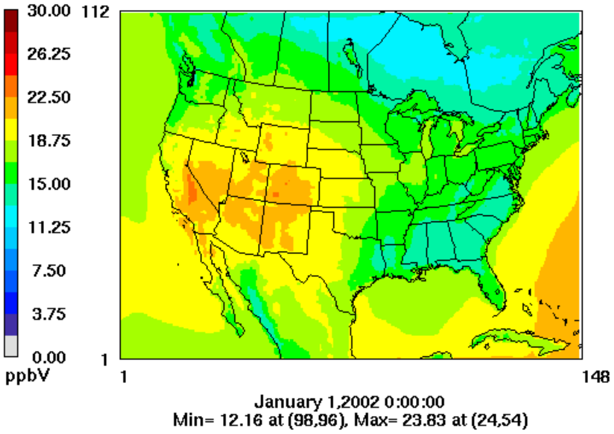

(a) Current natural case

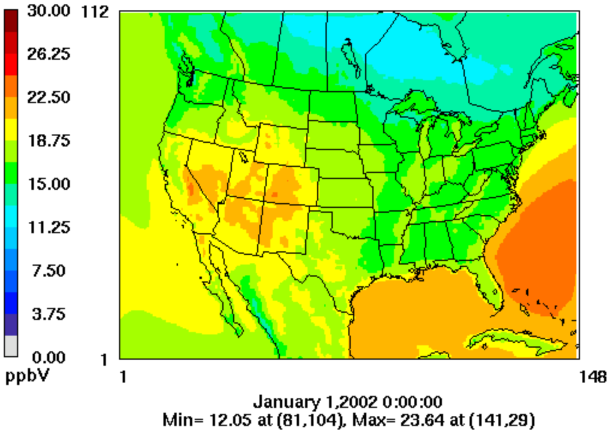

(b) Revised natural case

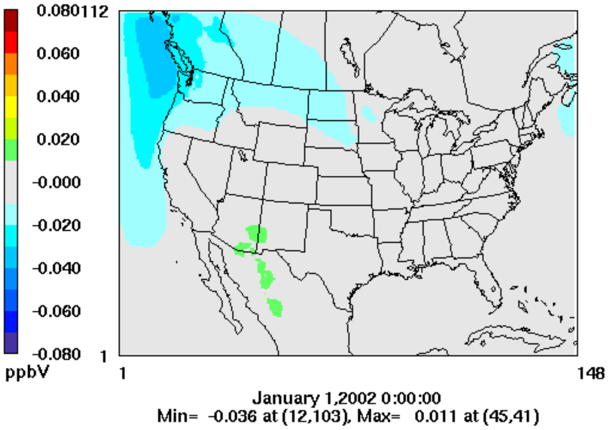

(c) Changes due to DMS/MSA

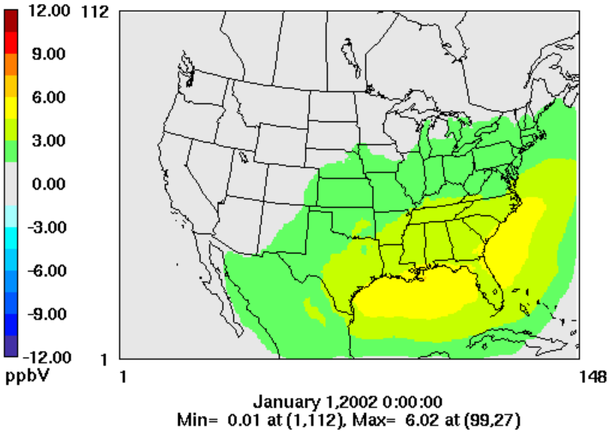

(d) Changes due to lightning NO

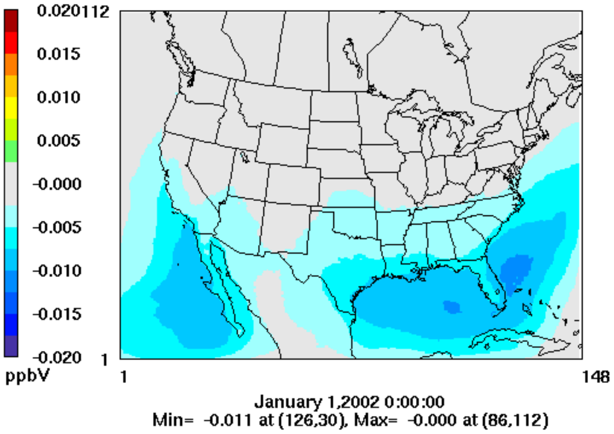

(e) Changes due to alternative sea salt

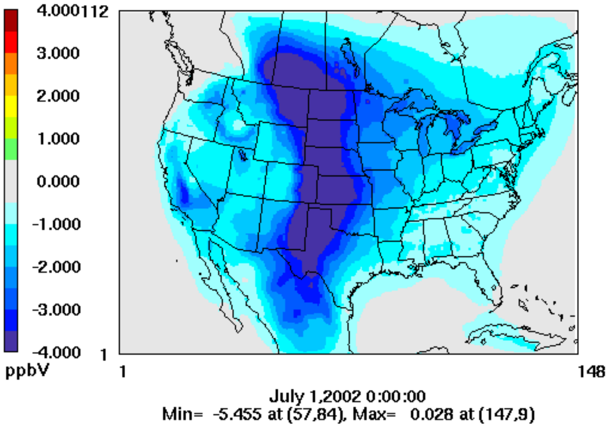

(f) Changes due to revised SOA scheme

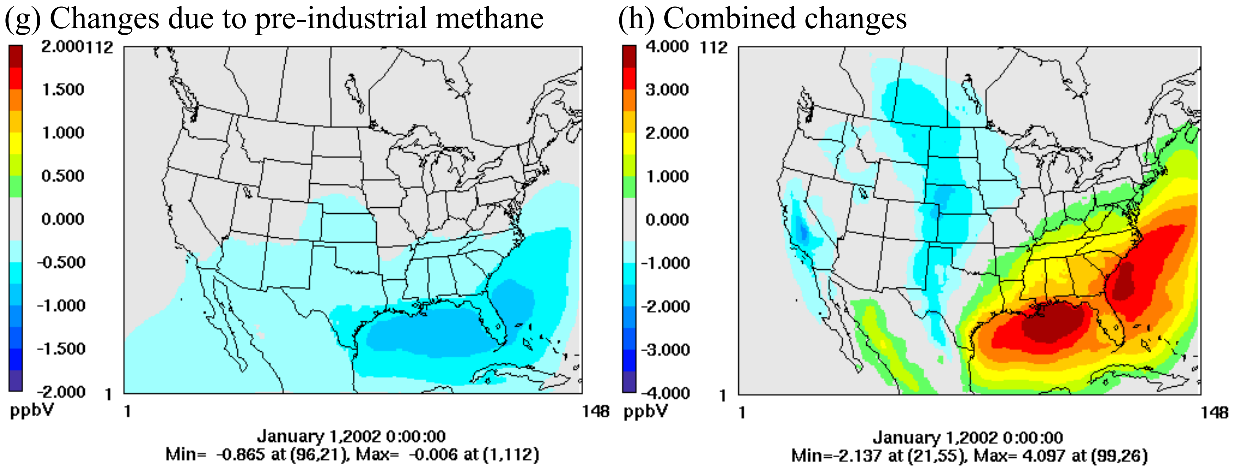

(g) Changes due to pre-industrial methane

(h) Combined changes

Figure 2. Annual average ozone concentrations (in ppb) for (a) current natural and (b) revised natural cases; (c)-(g) present changes in annual average ozone due to each of the revised natural emissions; (h) shows changes due to all the revised natural emissions combined.

(a) Current natural case

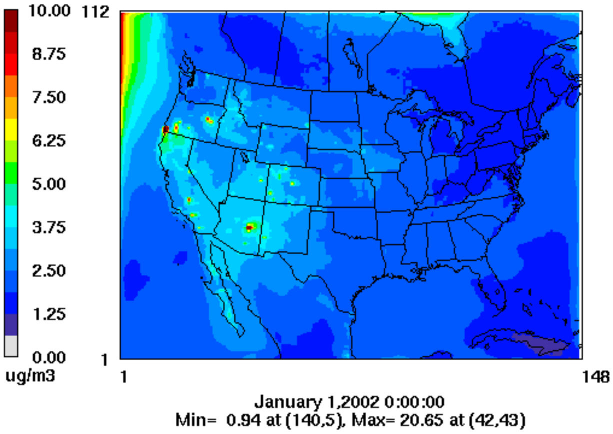

(b) Revised natural case

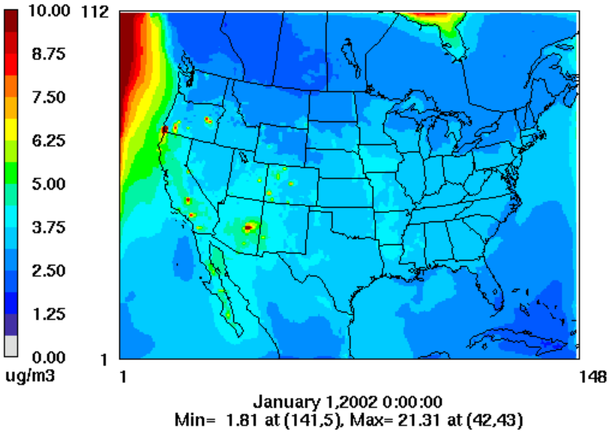

(c) Changes due to DMS/MSA

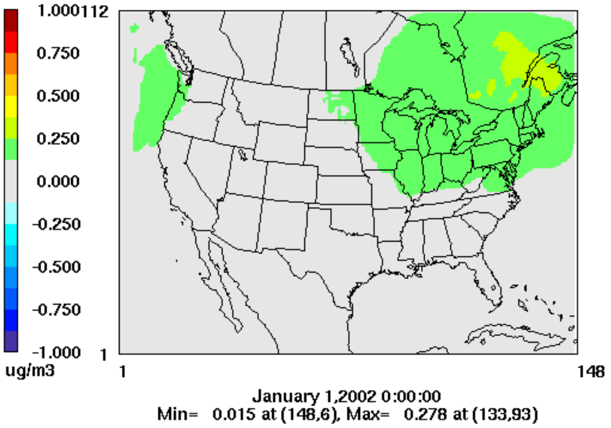

(d) Changes due to lightning NO

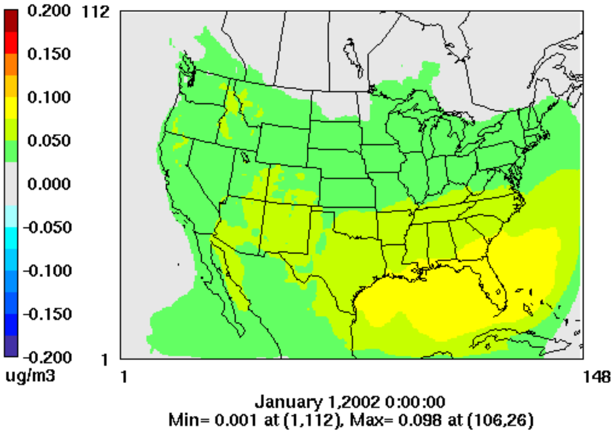

(e) Changes due to alternative sea salt

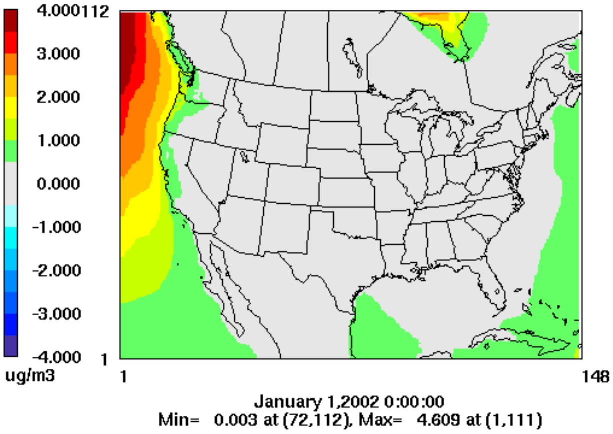

(f) Changes due to revised SOA scheme

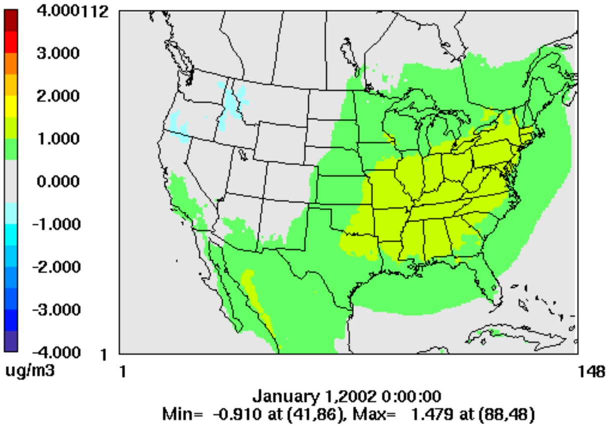

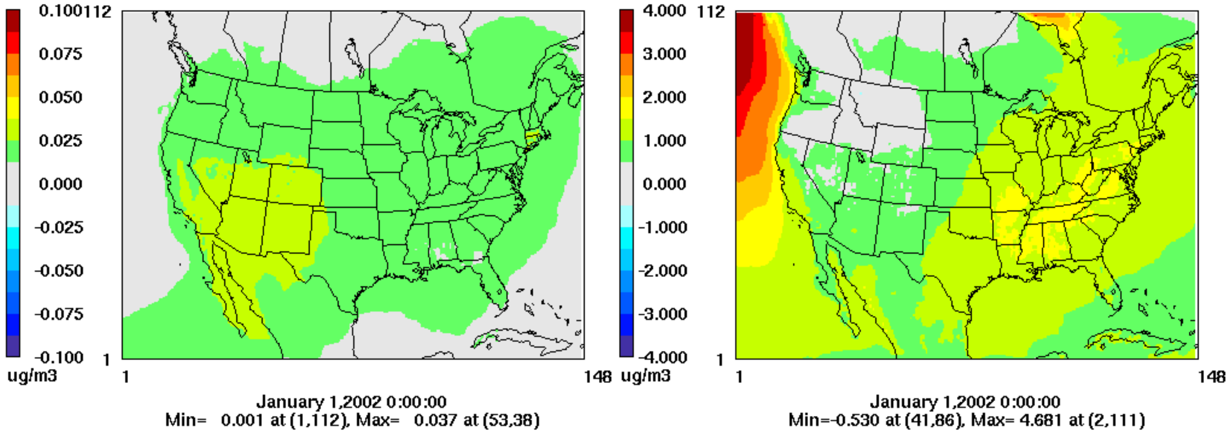

(g) Changes due to pre-industrial methane

(h) Combined changes

Figure 3. Annual average $PM_{2.5}$ concentrations (in μg/m^3) in (a) current natural and (b) revised natural cases; (c)-(g) present changes in annual average $PM_{2.5}$ due to each of the revised natural emissions; (h) shows changes due to all the revised natural emissions combined.

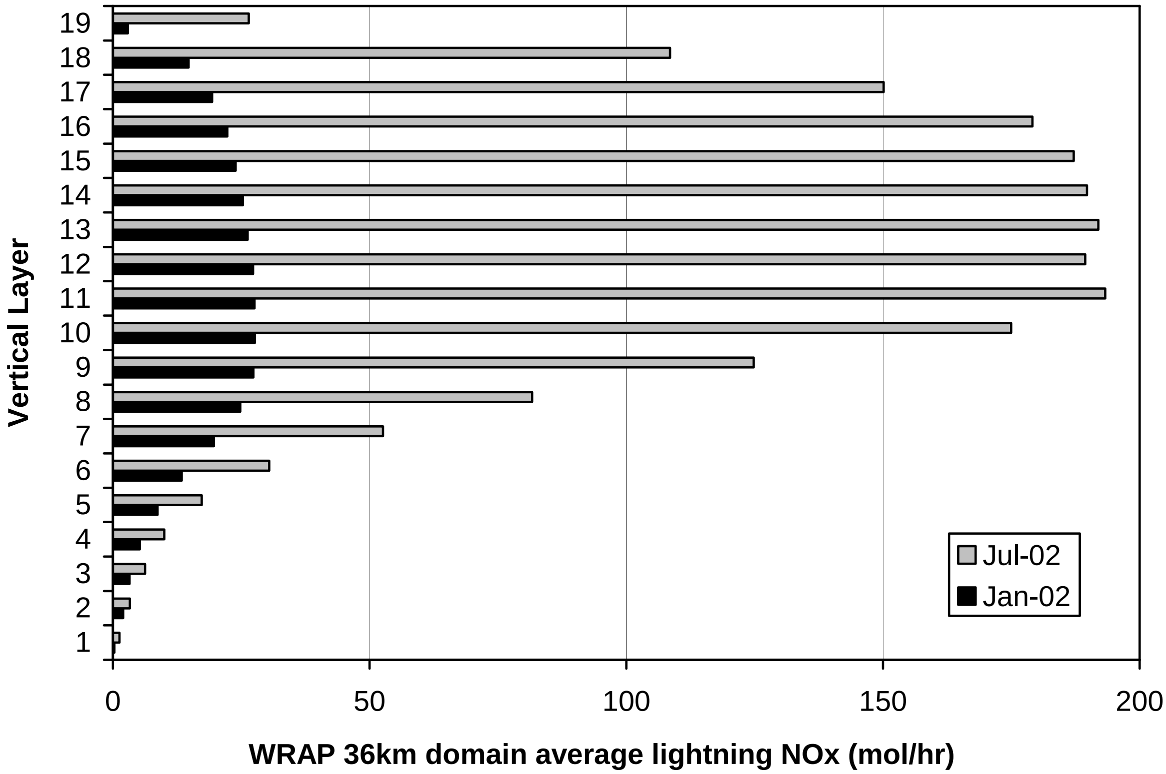

Figure 4. Vertical profile of the WRAP domain average lightning NOx emissions, averaged over the months of January and July, 2002.

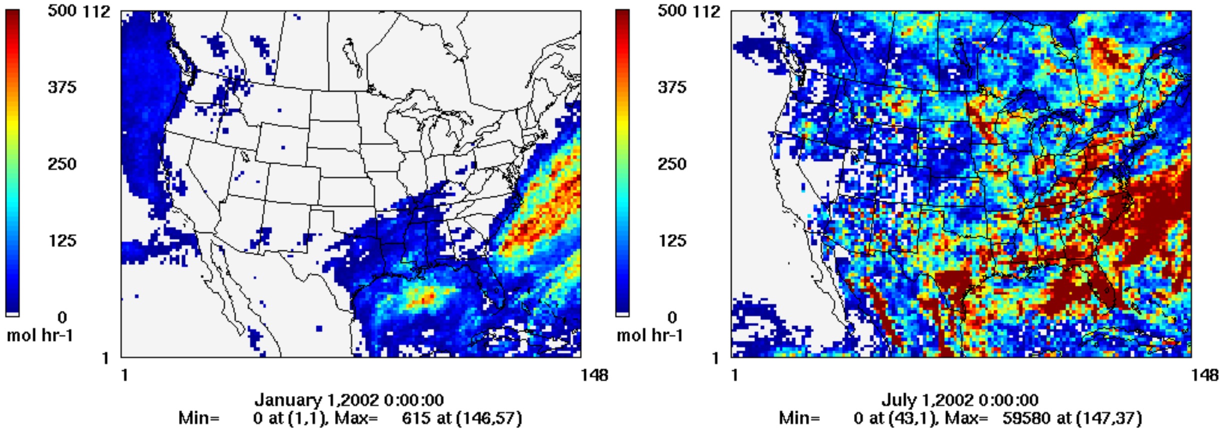
(a) January 2002

(b) July 2002

Figure 5. Spatial plots of the total vertical column lightning NOx emissions, averaged over the months of January and July, 2002.

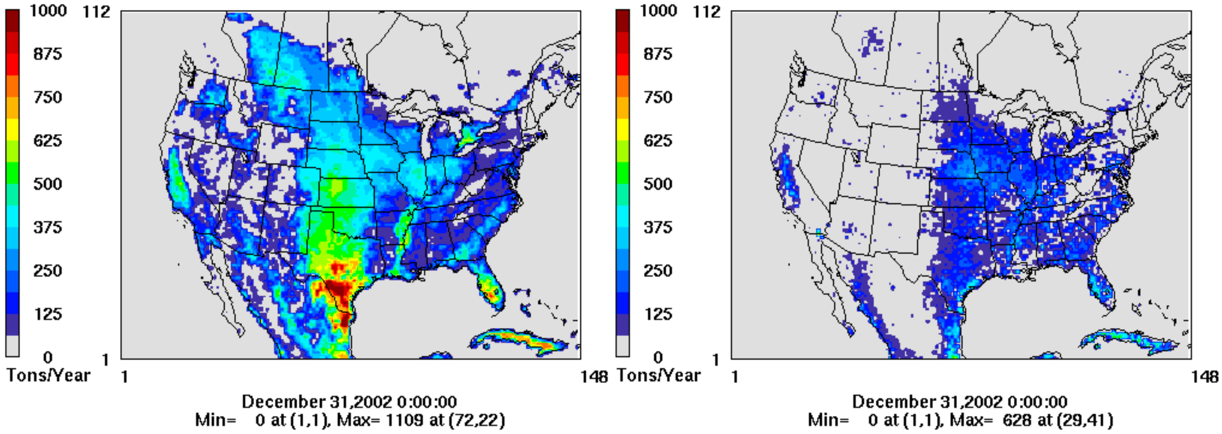
(a) NO (SMOKE BEIS3)
(b) NO (MEGAN)

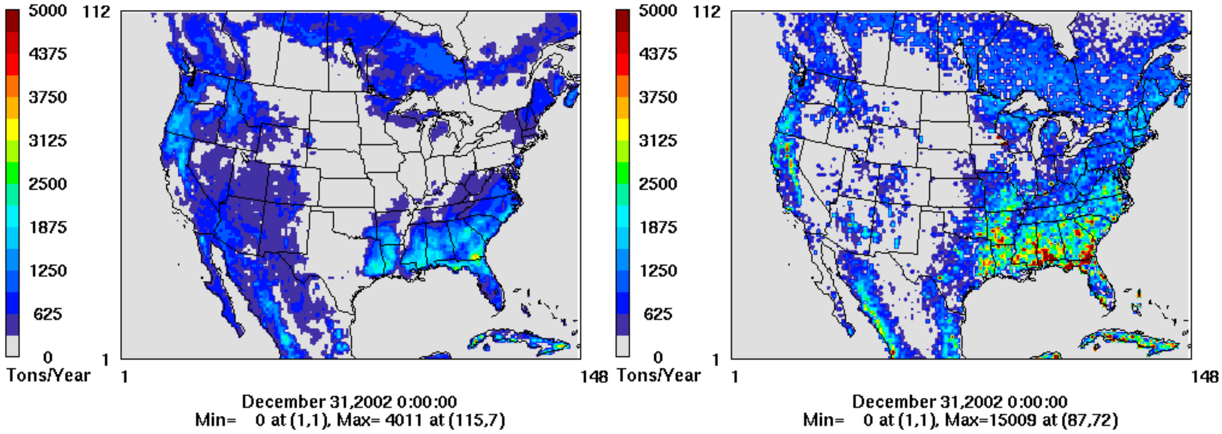
(c) Monoterpenes (SMOKE BEIS3)
(d) Monoterpenes (MEGAN)

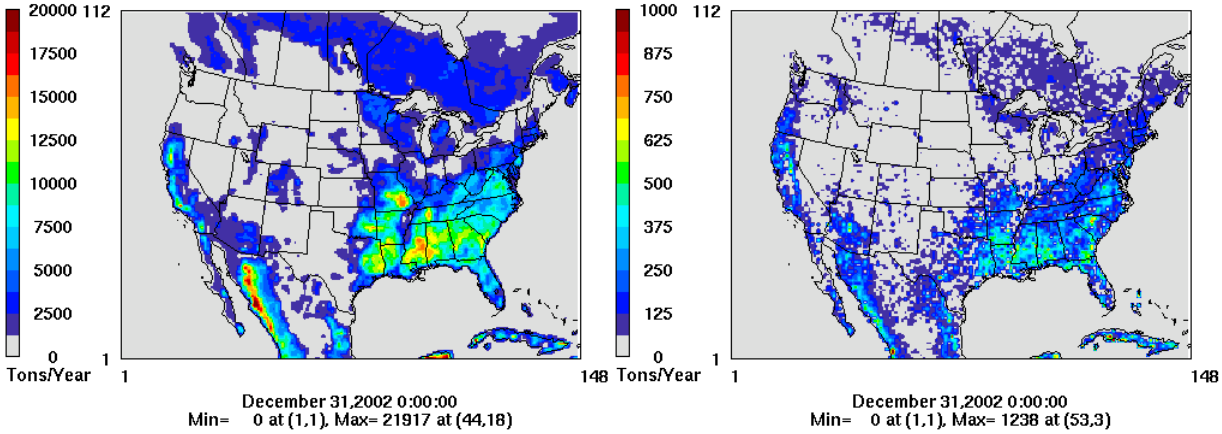
(e) Isoprene (SMOKE BEIS3)
(f) Sesquiterpenes (MEGAN)

Figure 6. Annual total biogenic emissions by SMOKE BEIS3 and MEGAN emission models.

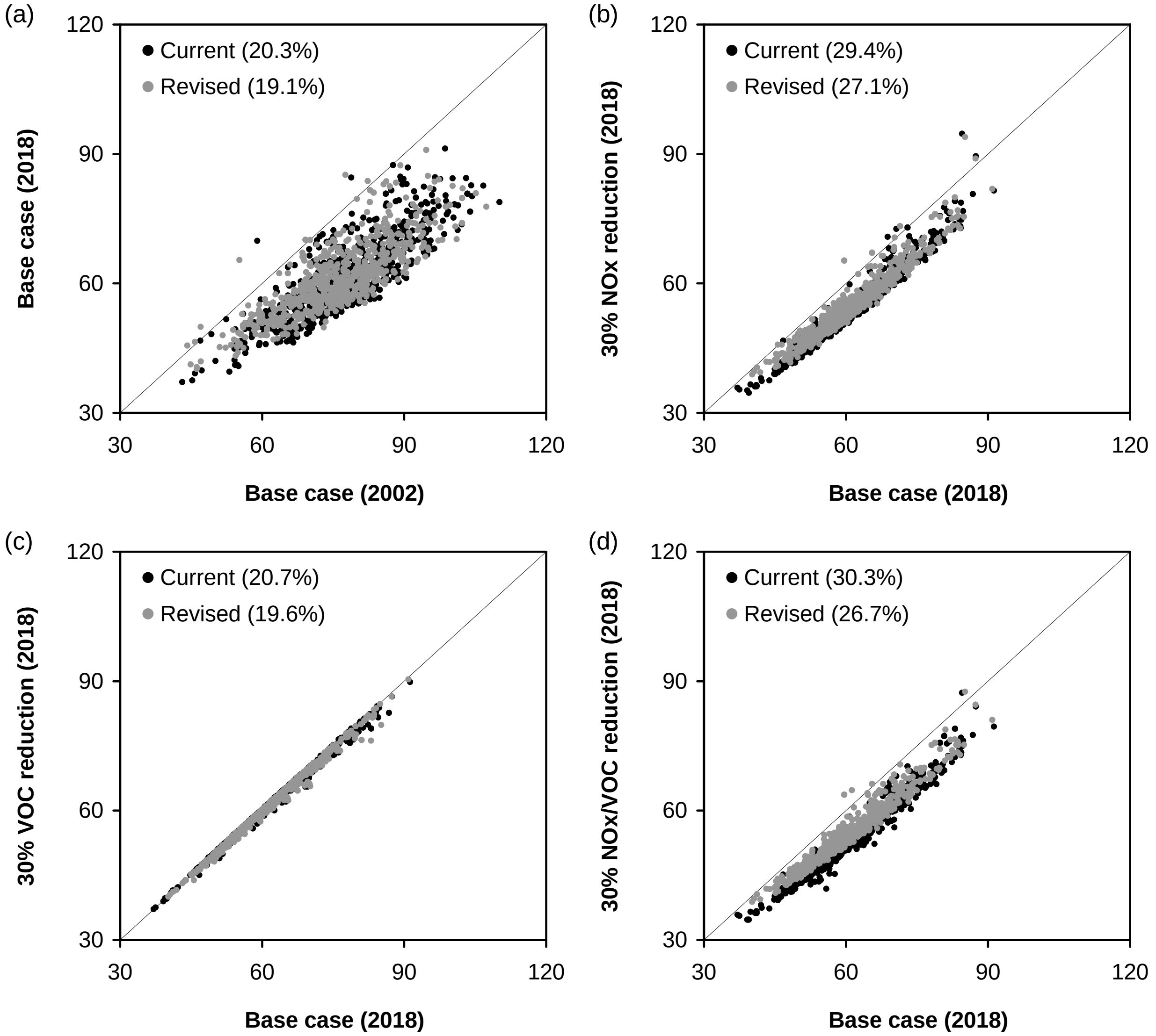

Figure 7. Scatter plots of the 4-th highest 8-hour ozone (in ppb) for the sites in the 12 km domain: (a) 2002 vs. 2018 with base case emissions; (b)-(d) 2018 with base case emissions vs. 2018 with 30% reduction in various anthropogenic emissions. The ozone concentrations from simulations with the current (black) and revised (gray) natural emissions are shown. Numbers in parentheses represent average percent reductions in the 4-th highest 8-hour ozone concentrations, defined as follows:

$$\frac{1}{N}\sum_{i=1}^{N}\frac{B_i - F_i}{B_i}$$

where B_i and F_i are the base year and future year ozone concentrations at the i-th monitoring site, respectively, and N is the number of monitoring sites.

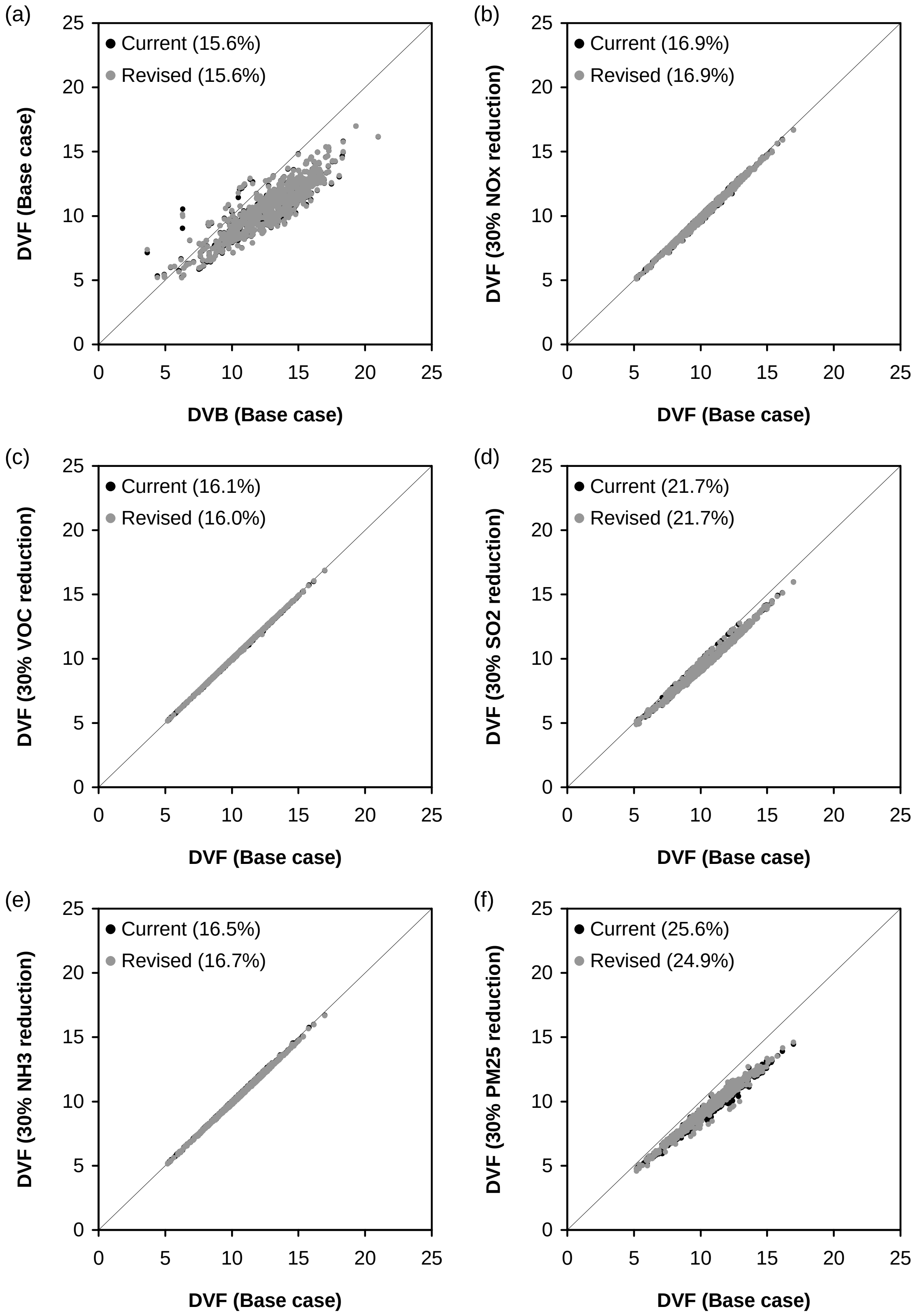

Figure 8. Scatter plots of PM$_{2.5}$ DVs (in μg/m^3): (a) DVB vs. DVF with base case emissions; (b)-(f) DVF with base case emissions vs. DVF with 30% reduction in various anthropogenic

emissions. DV projections using simulations with the current (black) and revised (gray) natural emissions are shown. Numbers in parentheses represent average percent reductions in DVs (same definition as in the caption of Figure 7 only with DV instead of the concentration).

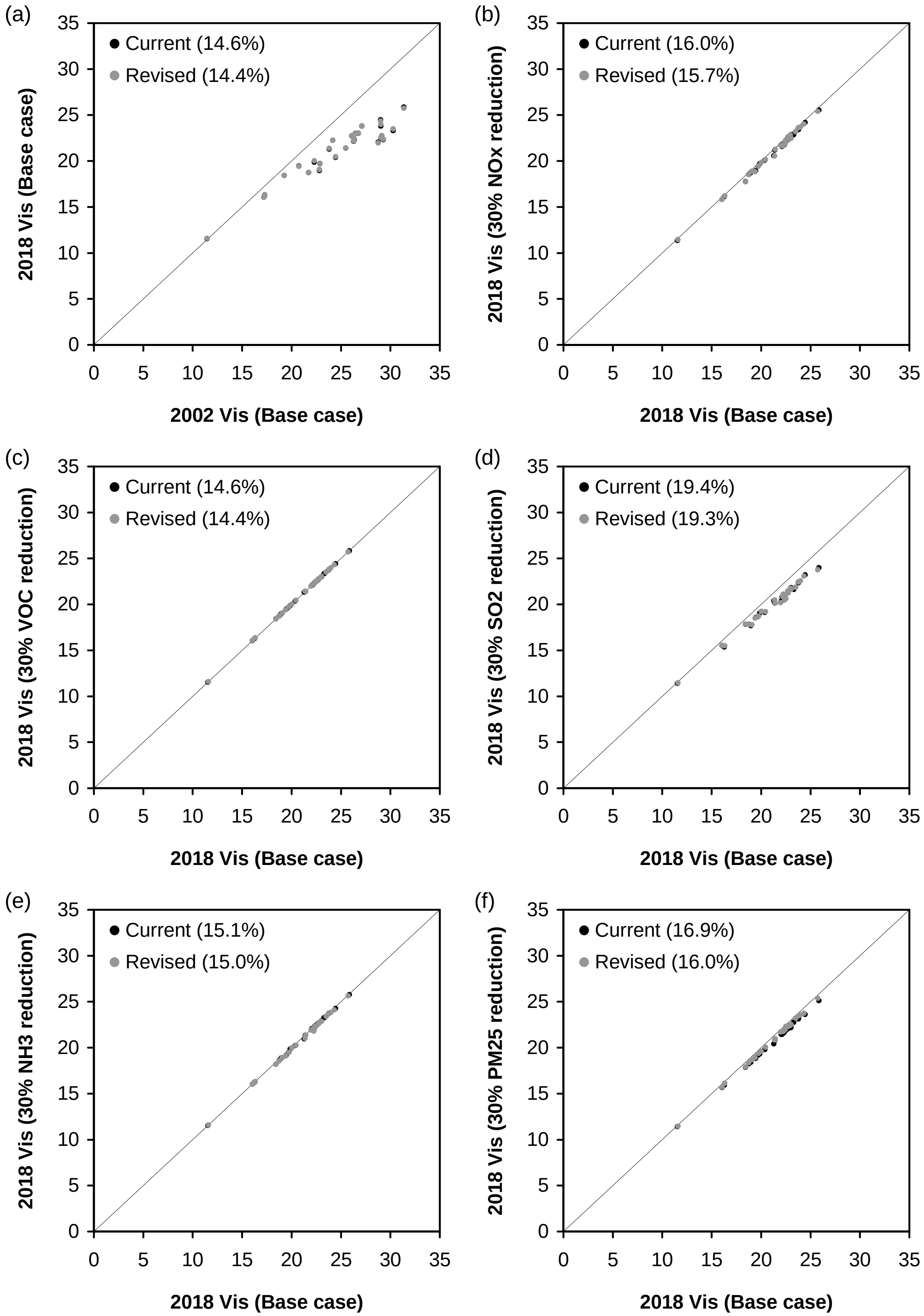

Figure 9. Scatter plots of Haziness on 20% worst days (in deciview): (a) 2002 vs. 2018 Haziness with base case emissions; (b)-(f) 2018 Haziness with base case emissions vs. 2018 Haziness with

30% reduction in various anthropogenic emissions. Haziness projections using simulations with the current (black) and revised (gray) natural emissions are shown. Numbers in parentheses represent average percent reductions in Haziness (same definition as in the caption of Figure 7 only with Haziness instead of DV).

APPENDIX A

Progress Report #1

Progress Report

CRC Project No. A-65

Accuracy of Regional Simulations of Background Ozone and PM

Prepared for

Coordinating Research Council
3650 Mansell Road, Suite 140
Alpharetta, GA 30022

Prepared by

Bonyoung Koo
Greg Yarwood
Ralph Morris
ENVIRON International Corporation
773 San Marin Drive, Suite 220
Novato, CA 94998

And

Gail Tonnesen
University of California at Riverside
1084 Columbia Avenue
Riverside, CA 92507

March 28, 2008

1. INTRODUCTION

1.1. Background

As ozone and particulate matter (PM) National Ambient Air Quality Standards (NAAQS) are revised and lowered, “background” concentrations due to “natural sources” will have increasing importance. With the new 35 $\mu g/m^3$ 24-hour $PM_{2.5}$ NAAQS and recently revised 75 ppb 8-hour ozone NAAQS, there are questions whether violations of the NAAQS may occur due to natural sources alone and whether the selected emissions control path may be affected by neglecting or over simplifying the representation of natural sources. Current standard modeling practice for 8-hour ozone and $PM_{2.5}$ State Implementation Plans (SIPs) either neglects (e.g., lightning, geogenic, some biogenic and stratospheric sources) or simplifies (e.g., biogenics and wildfires) many natural sources of ozone and PM. Although some of these deficiencies may not affect current year base case modeling and model performance evaluation, they may affect the future-year control strategy modeling potentially leading to incorrect emission control levels or even incorrect pathways for attainment of the NAAQS.

There are four issues related to natural sources and background conditions that are of importance in air quality management planning:

1. Are natural sources alone able to result in exceedances of the ozone and/or PM NAAQS: In the case of wildfires, wind blown dust and stratospheric ozone intrusion the evidence is yes. EPA has a Natural Events Policy to address this issue where exceedances due to natural events can be discounted in attainment classification so long as Best Available Control Measures (BACM) on anthropogenic sources are in place.

2. Are non-U.S. anthropogenic sources sufficient to cause exceedances of the NAAQS: This issue is related to the previous issue but includes anthropogenic emissions from international sources as well as natural sources. Again, EPA has a policy whereby a state can prepare a “but for” State Implementation Plan (SIP) to demonstrate that they would have attained the NAAQS “but for” international transport. “but for” SIPs have been developed for El Paso Texas and Imperial County California.

3. What are the levels of background ozone and PM concentrations in the absence of anthropogenic sources (or U.S. anthropogenic sources): A lot of recent research of this issue has been undertaken as part of the development of the Regional Haze Rule (RHR) SIPs whose objective is return to natural visibility conditions (i.e., no man-made impairment) at Class I areas by 2064. EPA has developed default background natural PM estimates (EPA, 2007) based on the work of Trijonis from the 1985 NAPAP study.

4. What effects do natural sources and background concentrations have on the development of ozone and PM attainment emission control strategies: This issue has seen less study than the previous issues but as standards are tightened and anthropogenic emissions are reduced will be of increasing importance.

These issues are interrelated, but require different modeling study designs to address. The Coordinating Research Council (CRC) retained ENVIRON and personnel from the University of California at Riverside (UCR) to study these issues. The last issue is the primary objective of the proposed CRC A-65 study.

1.2. Overview of Approach

From the previous WRAP clean condition study, we know the current natural background emissions inventories do not yield background concentrations that are consistent with the current estimates. Therefore, we will first focus on refining the current natural background emissions. In Section 1, we reviewed and summarized the available literature to identify potentially important sources of natural background ozone, PM and precursors that are usually missing in the regulatory modeling, and obtain estimates of their natural background concentrations. To assess impacts of these potential natural sources, we will conduct a series of regional scale annual simulations where these sources are incrementally added and evaluated against the natural background estimates identified in the review task.

With the revised natural background emissions determined in the above step, we will proceed to conduct sensitivity simulations to answer how the refined natural background emissions will affect current emissions control strategies to achieve the ambient standards. In this task, we will test various anthropogenic emissions reductions under the current and refined natural source conditions with a future year scenario. Then, the 8-hour ozone and $PM_{2.5}$ Design Values and regional haze metrics under the two natural conditions will be compared.

This document is the first Quarterly Progress Report for the CRC A-65 study that reviews the literature on natural sources and recommends a modeling approach for the study.

2. LITERATURE REVIEW

There are natural emissions of both primary and secondary $PM_{2.5}$, however, there are large uncertainties in natural emissions inventories and in the chemical reactions that convert natural precursors to secondary $PM_{2.5}$. Natural sources are of concern because they represent sources of ozone and of $PM_{2.5}$ that cannot be reduced in efforts to attain ambient air quality standards. Estimates of natural haze levels have been developed by EPA for visibility planning purposes and are described in “Guidance for Estimating Natural Visibility Conditions Under the Regional Haze Rule” (EPA, 2003). Table 2-1 shows the estimates of natural PM concentrations used in that report. Although it may be possible to use mass isotope analyses to identify some $PM_{2.5}$ species as being of either biogenic or anthropogenic origin, it is generally not possible to make this determination using monitoring data for observed concentrations of $PM_{2.5}$ because these ambient monitoring typically measures only the total mass and does not include isotopic analysis. Moreover, it is not possible to use observations to classify photochemically produced ozone as biogenic or anthropogenic. Therefore, modeling studies are the primary method available for estimating the relative contribution of natural versus anthropogenic emissions contributions to ozone and $PM_{2.5}$. In this section we review literature for natural emissions of $PM_{2.5}$ and its precursors and natural emissions of ozone precursors, and we also summarize finding of previous modeling studies.

Table 2-1. Natural PM concentrations used in the USEPA evaluation of natural haze (from EPA, 2003, Table 2-1).

PM component	West (ug/m3)	East (ug/m3)	Error Factor
Ammonium Sulfate	0.12	0.23	2
Ammonium nitrate	0.10	0.10	2
Organic carbon mass	0.47	1.40	2
Elemental carbon	0.02	0.02	2 - 3
Soil	0.50	0.50	1 ½ - 2
Coarse mass	3.0	3.0	1 ½ - 2

2.1. Natural Sources of Ozone, PM and Precursors

Natural emissions can include sources that are either of biogenic or geogenic origin. There are several natural emissions sources of $PM_{2.5}$ precursors including NOx, SOx, NH_3 and VOC. Oxidation of these species by ozone, H_2O_2 and aqueous chemistry leads to the production of secondary $PM_{2.5}$. Because of the role of oxidants in converting natural precursors to secondary $PM_{2.5}$, it is also necessary to use air quality models to simulate the amount of natural oxidants in the atmosphere to estimate the secondary production of natural $PM_{2.5}$. A comprehensive evaluation of natural $PM_{2.5}$ requires the use of photochemical air quality models that simulates all natural emissions sources, the total oxidant concentration and the formation of secondary $PM_{2.5}$ in an atmosphere that excludes all anthropogenic emissions sources. Although natural oxidants also convert some anthropogenic precursors to secondary $PM_{2.5}$, this mass is typically excluded from estimates of natural $PM_{2.5}$ because the precursor emissions are of anthropogenic origin.

2.1.1. Lightning

Two key issues in the emissions of lightning NOx are the total emission rates and the vertical distribution of the emissions. We first review recent literature on lightning NOx emissions, and then make recommendations for low and high end emissions estimates for use in model simulations bounding the uncertainty range. We then consider vertical distributions of lightning NOx emissions.

Lightning NOx emissions can be estimated either directly using emissions factors per lightning flash or indirectly by inferring the lightning NOx emissions required to fit NOy observations in local or global scale chemistry models. Lightning NOx emissions can be estimated directly based on the number of lightning flashes, the intensity of each flash, the lightning type (cloud to ground versus cloud to cloud), and the emissions factor per flash. While the number of lightning flashes and flash intensity can be estimated from the National Lightning Detection Network (NLDN), there is uncertainty in the estimates of emissions factors per flash. As a result, there remains at least a factor of ten uncertainty in estimates of lightning NOx emissions, with estimates typically ranging from about 1-20 TgN/yr globally (Schumann and Huntrieser, 2007; Zhang et al., 2003a,b; Lee et al., 1997).

The European Lightning Nitrogen Oxides Project (EULINOX, see Holler and Schumann, 2000; also see www.pa.op.dlr.de/eulinox) was designed to estimate the emissions of NOx from lightning. The field campaign was conducted in Europe during summer 1998 and measured concentrations of NOx, CO_2, O_3 and CO in association with thunderstorm anvils. Schumann and Huntrieser (2007) describe key findings of EULINOX including 15 (2-40)$\times10^{25}$ molecules NO per flash (i.e., 250 moles or 3.5 KgN per flash). Using a global flash rate of 44±5 flashes per second, they estimated global lightning NOx emissions of 5 TgN/yr. Given the uncertainty in the flash rate and emissions per flash, global NOx emissions could range from about 0.6 to 7.2 TgN/yr.

Beirle et al. (2004) use Global Ozone Monitoring Experiment (GOME) satellite data to estimate that globally lightning produces 2.8 TgN/yr with an uncertainty range of 0.8-14 TgN/yr. This is substantially lower than the 5 TgN/yr estimated in EULINOX. The Beirle et al. estimate was calculated using lightning frequency data and GOME total column NO2 measurements for Central Australia where other NOx emissions sources are small.

Ott et al. (2007) used the three-dimensional Goddard Cumulus Ensemble (GCE) model to simulate a 21 July 1998 thunderstorm that occurred during the EULINOX project. They then used the CGE output to drive an offline cloud-scale chemical transport model which calculates tracer transport and includes a parameterization of lightning NOx production which uses observed flash rates as input. An emissions factor of 360 moles of NO per flash for both inter-cloud and cloud to ground flashes compared most favorably with NOx column mass and probability distribution functions calculated from their observations. The NOx production per flash calculated in their study corresponds to a global annual lightning NOx source of 7 TgN/yr. Other studies cited in the reference section estimate global lightning NOx emissions in the range of 1 to 20 TgN/yr, however, we believe that the more recent estimates discussed above and based on EULINOX are the best current estimates available.

Given the large uncertainties in estimated lightning NOx emissions, modeling studies to evaluate their effects should be performed as a bounding exercise using probable lower and upper estimates. Based on results of EULINOX, we recommend using the upper and lower estimated emissions rates of 1.5 and 30 Kg NOx per flash (i.e., 0.46 and 9.3 KgN per flash).

Lightning flash data in the United States are available from the National Lightning Detection Network (NLDN) which consists of over 100 remote, ground-based sensing stations that instantaneously detect the electromagnetic signals given off when lightning strikes the earth's surface. These remote sensors send the raw data via a satellite-based communications network to the Network Control Center operated by Vaisala Inc. in Tucson, Arizona. The Visalia webpage is https://thunderstorm.vaisala.com, and a NASA webpage also provides a summary description of the NLDN: http://gcmd.nasa.gov/records/GCMD_NLDN.html.

Visalia sells the lightning data to insurance companies and other industries. The cost for a complete 2002 dataset that includes latitude, longitude, time, and intensity for all lightning flashes in the US would be approximately $22,000. However, Visalia sometimes provides discounts or research grants.

Lightning flash counts have also been estimated from satellite data including the EOS Optical Transient Detector (OTD) and the Lightning Imaging Sensor (LIS) that was launched in November 1997 aboard the Tropical Rainfall Measuring Mission (TRMM). These satellite data provide global lightning counts with high spatial resolution, detection efficiency, coverage beginning in 1997 through the present, and daily lightning count summaries are available at http://thunder.nsstc.nasa.gov/data/lisbrowse.html.

2.1.2. Vertical Distribution of Lightning NOx

The vertical distribution of lightning NOx will affect the degree to which it participates in photochemical formation of ozone and the speed at which it is transported away from the source region. If lightning NOx is formed in planetary boundary layer (PBL) or if it is transported to the surface by downward convective activity, it may contribute to the formation of ozone and HNO_3 within the PBL near the source region and caused increased concentrations of these species locally. Alternatively, if lightning NOx emissions are primarily in the free troposphere, it will be transported more rapidly, will have a smaller effect on surface concentrations, and will undergo chemical reactions under the chemical environment of the free troposphere. In this case, lightning NOx emissions would still be expected to have an effect on global chemistry models and would affect the US domain indirectly through global scale transport. This would best be represented in CMAQ simulations through the use of boundary condition (BC) influx, where the BC would be determined from a global chemistry model such as GEOS-CHEM (Liu et al., 2006) or MOZART (Brasseur et al., 1998).

Pickering et al. (1998) developed vertical profiles for lightning NOx emissions for mid-latitude continental, tropical continental, and tropical marine regimes based on profiles computed for individual storms in each regime. They found that for all 3 regimes there was a maximum of lightning NOx in the upper troposphere, usually within 2-4 km of the tropopause, and that this had a substantial effect on upper tropospheric NOx and O_3 concentrations in global simulation models. They also found that downdrafts were strongest in mid-latitude continental systems, up to 23% of the lightning NOx mass in the lowest kilometer, and minima in the vertical profile from 2 to 5 km, creating a “C-shaped” vertical profile.

Zhang et al. (2003a,b) performed 3-dimensional modeling with chemistry of NOx for storms with lightning activity and compared results of their modeled concentrations to observed NO and NO_2 concentrations. Their case study only included inter-cloud lightning (cloud to ground was not implemented in the model), however, they found that some NO reached the ground even in the case of inter-cloud lightning. Their storm system was less intense than that of Pickering et al. (1998), but Zhang et al. still found that some NOx from the lightning reached the stratosphere. In contrast to the results of Pickering et al. (1998), Zhang et al. did not find a “C-shaped” vertical profile for NOx, instead, they found a NOx maximum at mid-levels of the storm from 3.4 to 6 km.

The USEPA is currently conducting model sensitivity studies of the effects of lightning NOx emissions in the eastern US (Pinder, 2008). Preliminary CMAQ model results showed that lightning NOx had only small effects on ozone production because the emissions occurred in areas with low VOC/NOx ratios, and the NOx was rapidly converted to HNO_3. However, there are large uncertainties in these preliminary results, and EPA plans to perform additional modeling studies using new vertical distribution profiles of lightning NOx to be developed by Pickering. This new research is beginning in 2008 and will not be available for use in the time frame of the CRC project.

It is difficult to recommend a vertical profile for NOx emissions, given conflicting results of the Pickering and Zhang studies. It is possible that vertical profiles may depend on storm intensity. The Zhang study did not include cloud to ground lightning, but most lightning is inter-cloud. Although there are large uncertainties, for this study we propose to use the mid-latitude, continental vertical profiles developed by Pickering et al. (1998). A second option would be to use a uniform vertical profile.

An additional concern is the extent to which the convective activity in the MM5 simulated data is inconsistent with convective activity in locations where lightning flashes occur in the NLDN data. To the extent that MM5 does not correctly simulate thunderstorm activity, it is possible that lightning NOx emissions will be introduced into the air quality model for incorrect meteorology conditions. For example, if NLDN has strong lightning activity at times and location for which MM5 does not have thunderstorm activity, the lightning NOx emissions may be introduced into the model for inappropriate advection and photochemical conditions. The new research study by Pickering is being designed to address this issue and may be available for future studies. Possible methods to address this in the CRC study would be to parameterize lightning NOx emissions based on convective activity in MM5.

2.1.3. Wildfires

Fire emissions can be classified as: (1) natural wildfires; (2) prescribed burning; and (3) agricultural burning. Furthermore, prescribed fires can be considered either biogenic or anthropogenic depending on the conditions under which the burning takes place. The Western Regional Air Partnership (WRAP) has extensively analyzed fire emissions in the western US (Randall, 2006) because fire emissions are one of the largest sources of $PM_{2.5}$ and its precursors in the western USA, both because of the large mass of fire emissions and the relatively small source of anthropogenic emissions in sparsely populated regions of the west. Although other RPOs have included fire emissions in their evaluations of $PM_{2.5}$, they represent a smaller component of $PM_{2.5}$ in other regions of the USA because of the smaller mass emissions from fires and the relatively larger sources of anthropogenic emissions in the more densely populated central and eastern US.

2.1.4. Geogenic Sources

Geogenic sources of SO_2 primarily include emissions of SO_2 from volcanic activity. Unfortunately measurements of geogenic emissions are not routinely made and such measurement are highly variable and episodic. For example, measurements of SO_2 emissions from Mount St. Helens in Washington were zero most of the time. But in November 2004, three measurements of SO_2 emissions produced values of 65, 110 and 140 tons per day (McGee, 2006). Given that such measurements are not routinely available this source category is difficult to characterize.

2.1.5. Natural Sources from the Oceans

Important species emitted from oceans include sea salt (NaCl) aerosols and dimethyl sulfide (DMS).

CMAQ version 4.5 was the first release to include sea salt aerosols which were implemented in version AERO4 of the aerosol module, and it includes calculations of sea-salt in the thermodynamics module, whereas previous version of CMAQ did not. In AERO4, emissions of sea salt from the open ocean are calculated as a function of wind speed and relative humidity. These emissions are speciated into sodium, chloride, and sulfate, and are distributed by size to the fine and coarse modes. Thermodynamic equilibrium between the accumulation-mode (which now includes sodium and chloride) and the gas phase (which now includes hydrochloric acid) is treated within the ISORROPIA equilibrium module. Sea-salt species in the coarse mode are treated as inert tracers. All sea-salt emission calculations are done within the CMAQ model and do not require any pre-processing in SMOKE. However, a new input file called the “OCEANfile” is needed to run CMAQ with the AERO4 module. The OCEANfile is a time-invariant I/O API file that has 1 vertical layer and the same columns and rows as the CMAQ domain. The OCEANfile contains a variable named "OPEN" which represents the fraction of each grid cell that is covered by open ocean and a variable “SURF” that represents the surf zone.

Oceanic dimethyl sulfide (DMS) is a major natural source of sulfur to the atmosphere and contributes to sulfate aerosol formation and growth in the atmosphere. Global DMS emissions are believed to account for 15% of the total global sulfur emissions of 3.2 TgS/year (Bates et al., 1992). CMAQ version 4.5 also includes sulfate emissions from the oceans to account for the effects of DMS emissions. This is treated in the CMAQ as a direct emissions rate of sulfate because the conversion of DMS to sulfate is rapid. The default CMAQ emissions rates of DMS are 50 micromole/m^2/day for oceans and 1 micromole/m^2/day for land. This is equivalent to 1.75 g/m^2/year for oceans and 0.035 g/m^2/year for land.

DMS is also emitted in biomass burning (Meinardi et al., 2003), however, the fire emissions inventories discussed above include sulfur as direct emissions of sulfate. Because DMS is treated as direct sulfate emissions for all emissions source categories, the air quality model and chemical mechanisms do not need to be modified to represent DMS chemical transformations. Furthermore, because the large majority of oceanic DMS emissions occur outside of the USA modeling domain, its effects on sulfate within the USA will be represented primarily by the boundary condition sulfate concentrations derived from the global GEOS-CHEM simulations. However, we will use the default CMAQ emissions rates of DMS for the areas of oceans that are included within our CMAQ domain.

2.1.6. Natural Ammonia Sources

Natural sources of ammonia emissions include microbial activity in soils and urea from wild animals. Natural emissions of ammonia have very large uncertainty (Chitjian and Mansell, 2003a,b). For both anthropogenic and biogenic sources, ammonia emission inventories are determined by land use/land cover (LULC) characteristics, environmental factors, and tabulated emissions factors for each activity type. ENVIRON has developed a GIS-based (ArcINFO 7.2) ammonia emission modeling system for California (ENVIRON, 2001) and has recently enhanced and expanded the model to include the entire conterminous U.S. for the WRAP visibility modeling study (Mansell, 2005). Emissions factors and land use data for this model were based on Chitjian and Mansell (2003a,b). The model was designed to include five major source categories of ammonia emissions: livestock, fertilizer usage, domestic sources, native soils, and wild animals. Of these source categories, only native soils and wild animals are considered natural sources of ammonia emissions. Each of these is reviewed next.

Natural soils can be both a source and a sink of ammonia emissions depending on the ambient NH3 concentrations, climatic conditions and the conditions of the soils. While there are a number of researchers investigating this issue, ammonia emissions from natural soils remain highly uncertain. For the WRAP inventory, ammonia emission from natural soils were estimated based on emission factors developed or recommended by Battye et al. (2003) and Chinkin et al. (2003). Land use data used for the inventory were developed from the National Land Cover Database (http://edcwww.cr.usgs.gov/pub/edcuser/vogel/states/), as discussed below. Emissions from agricultural lands were considered anthropogenic and are not included here. The total area of each land use type from the LULC data used for the project provides the activity data for estimating soil emissions. A complete listing of each land use type by county is presented in Appendix C of Mansell (2005). Temporal allocation of native soil ammonia emissions was calculated using temporally resolved temperature, soil moisture and pH data derived from MM5. Table 2-2 list the emission factors used in the updated ENVIRON model. Derivation of these emissions factors is discussed by Mansell (2005), and Figure 2-1 shows the 2002 WRAP gridded emissions inventory from native soils.

Table 2-2. Emission factors for native soils.

Land type	Emission Factor (kg/km^2-yr)
Urban	10
Barren/Desert land	10
Deciduous Forest	174
Evergreen Forest	54
Mixed Forest	114
Shrubland	400
Grasslands	400
Fallow	205
Urban/Recreational Grasses	400
Wetlands	400

Wild animal ammonia emissions were based on activity data from CMU that included deer, elk and bears. Other wild animals were not included, and there are gaps in the CMU data, e.g., the CMU data did not include any deer in CA. Figure 2-2 shows the gridded ammonia emissions for wild animals in the ENVIRON 2002 inventory.

Table 2-3 (from Mansell, 2005) lists total ammonia emissions calculated using the ENVIRON ammonia model for calendar year 2002 for each state for both anthropogenic and natural source categories.

These emissions were calculated using an emissions factor set at the midpoint between the high and low estimates. However, in a WRAP CMAQ model performance evaluation using these estimates (Tonnesen et al., 2006), it was concluded that they were implausibly large in comparison to other ammonia emissions sources, and they were excluded from subsequent WRAP modeling studies. For future modeling studies we recommend that native soil ammonia emissions should be set to zero or that a low end estimate be used for the native soil ammonia emissions factor.

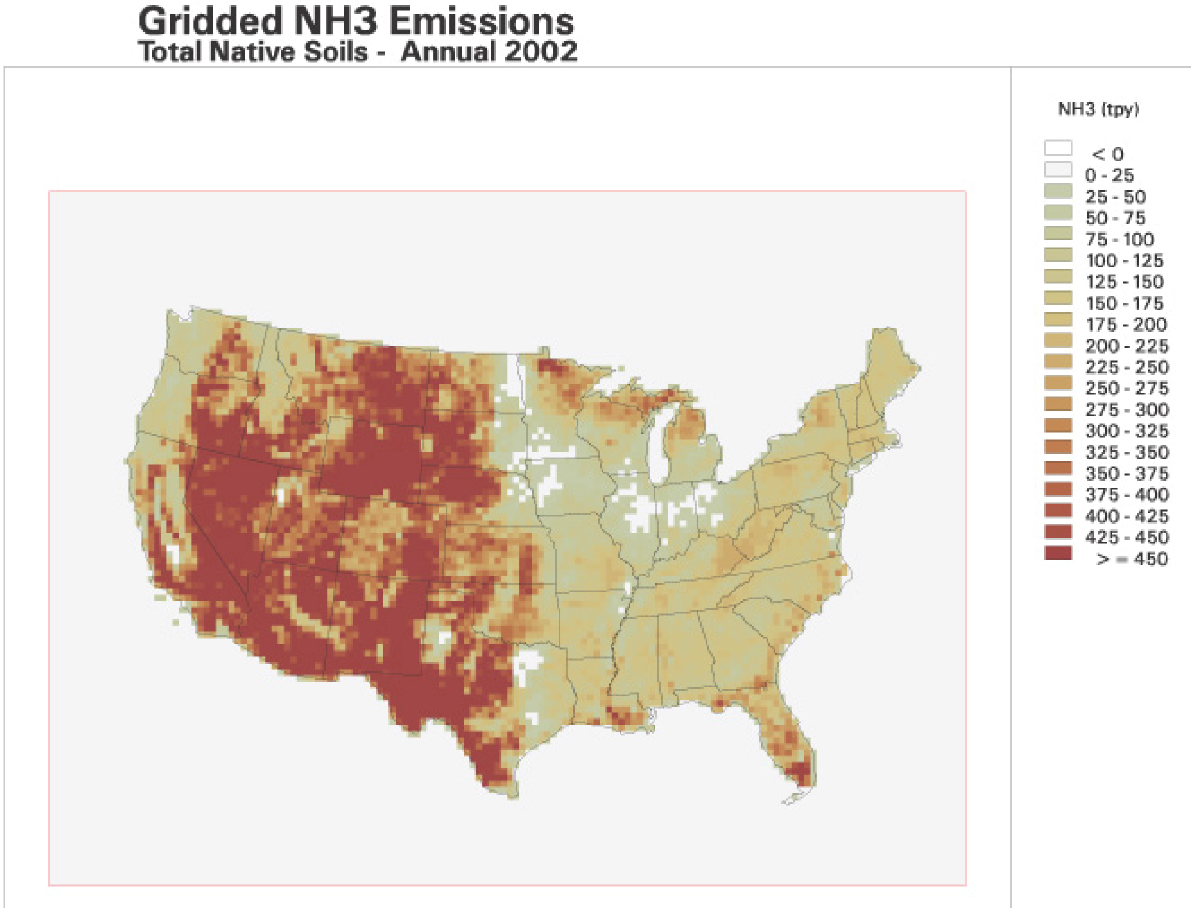

Figure 2-1. 2002 native soil NH3 emissions for the 36-km gridded RPO domain (from Mansell, 2005).

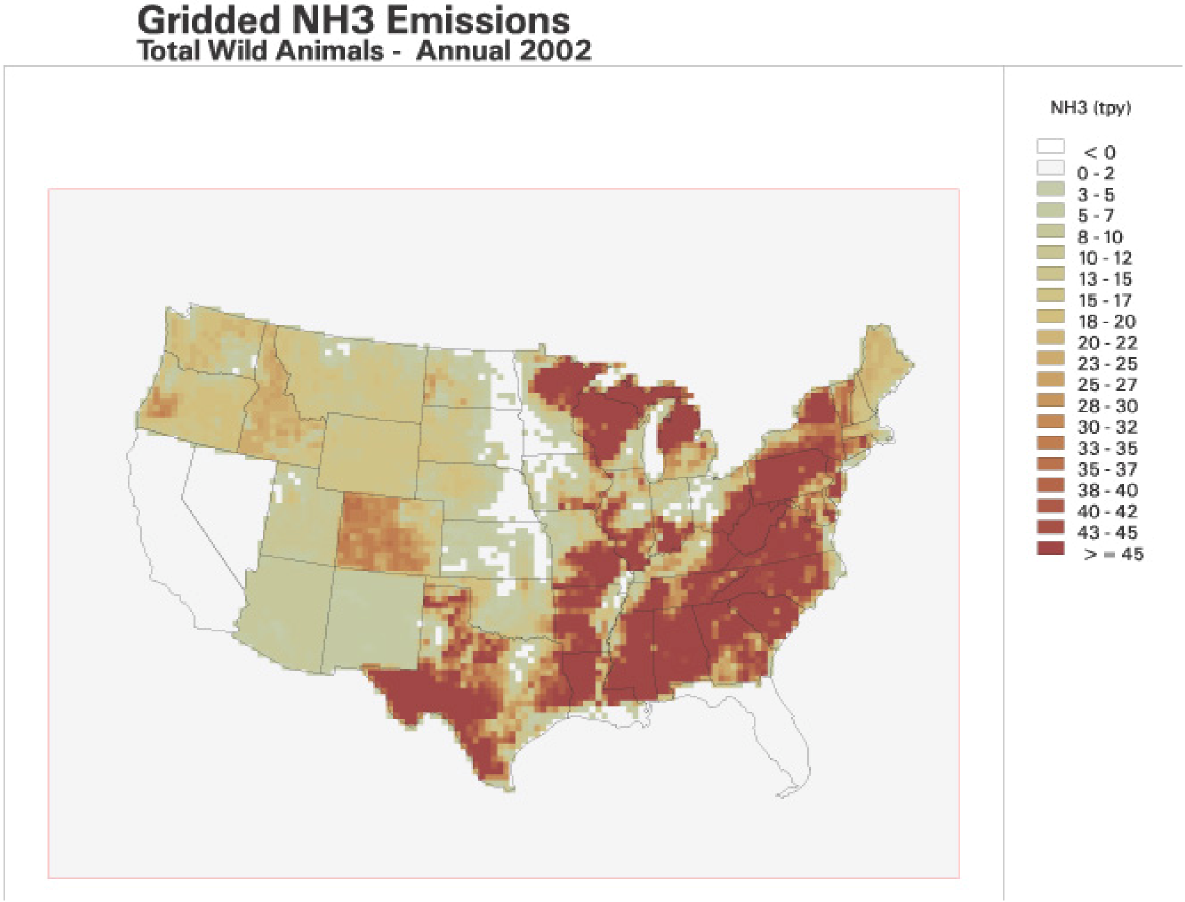

Figure 2-2. 2002 annual wild animal NH3 emissions for the 36-km gridded RPO domain (from Mansell, 2005).

Table 2-3. Annual 2002 NH_3 emissions by state (tons), from Mansell (2005).

State	Fertilizer	Livestock	Domestic	Wild Animals	Native Soils	TOTAL
AL	5,562	34,306	2,259	7,500	15,793	65,419
AZ	12,109	10,331	2,553	1,798	102,837	129,628
AR	38,744	45,396	1,365	4,023	14,578	104,107
CA	78,052	97,721	16,704	302	102,447	295,225
CO	18,848	34,133	2,127	5,586	74,967	135,661
CT	796	1,802	1,668	375	1,937	6,577
DE	888	4,607	387	110	531	6,523
DC	0	0	272	0	9	281
FL	3,300	20,562	6,632	6	28,667	59,167
GA	6,468	38,408	4,132	5,203	18,229	72,440
ID	31,442	30,082	660	3,425	51,230	116,839
IL	120,817	48,391	6,137	3,699	6,361	185,405
IN	46,642	38,690	3,055	2,123	4,418	94,928
IA	120,694	159,638	1,472	1,500	6,729	290,032
KS	100,340	69,753	1,351	748	44,151	216,344
KY	26,858	34,476	2,049	2,184	12,066	77,633
LA	15,273	9,326	2,246	5,001	18,973	50,820
ME	924	2,321	645	1,299	10,449	15,638
MD	4,294	11,049	2,604	974	2,753	21,673
MA	405	1,487	3,079	304	3,059	8,334
MI	26,409	25,964	4,954	8,874	22,820	89,021
MN	114,864	86,787	2,460	4,587	26,827	235,525
MS	14,228	26,361	1,469	7,498	13,630	63,186
MO	61,084	62,834	2,798	3,820	16,543	147,079
MT	31,376	24,926	454	4,024	102,946	163,727
NE	91,584	80,050	859	1,255	48,356	222,105
NV	1,395	4,415	988	92	106,982	113,872
NH	56	967	619	335	3,150	5,128
NJ	808	1,268	4,101	931	2,425	9,532
NM	5,599	21,397	913	1,414	112,468	141,791
NY	4,471	33,157	9,289	3,673	14,724	65,315
NC	6,771	101,463	4,071	5,517	17,005	134,827
ND	95,026	21,540	323	1,141	32,021	150,051
OH	55,453	34,443	5,632	2,049	7,192	104,769
OK	37,626	72,221	1,740	1,652	35,297	148,535
OR	22,988	17,325	1,691	3,361	55,624	100,989
PA	8,924	46,840	6,014	5,894	13,934	81,605
RI	56	112	507	52	450	1,176
SC	3,864	10,754	2,025	4,249	10,081	30,973
SD	66,051	50,786	386	1,316	43,705	162,244
TN	14,680	29,369	2,861	3,704	12,330	62,944
TX	83,349	146,410	10,502	18,012	175,959	434,233
UT	2,091	17,458	1,150	1,623	62,973	85,295
VT	624	6,529	309	635	3,087	11,183
VA	8,352	26,787	3,501	4,021	12,851	55,512
WA	17,300	18,349	2,911	2,186	28,024	68,771
WV	1,331	6,449	911	3,790	9,465	21,947
WI	28,807	73,031	2,674	6,932	16,352	127,795
WY	11,037	15,159	246	2,944	93,013	122,400
TOTAL	1,448,659	1,755,633	137,752	151,744	1,620,414	5,114,202

2.1.7. Wind Blown Dust

Wind blown fugitive dust can be considered either anthropogenic or natural in origin. The majority of fugitive dust emissions occur in association with human activities that disturb surfaces such as agriculture, construction sites, unpaved roads and recreational activities. Undisturbed surfaces typically have lower emissions of fugitive dust, especially in the central and eastern U.S. in regions with plant cover and high soil moisture. In arid ecosystems in the western U.S. natural emissions can be an import source of course particulate matter. Mansell et al. (2006) reviewed recent literature on wind blown fugitive dust and developed a wind blown dust model for use in the WRAP visibility modeling.

A number of windblown dust studies have recently been identified in the literature and are summarized with respect to the algorithms and physical parameters considered. Draxler et al. (2001) constructed a regional model for estimating PM_{10} from wind blown dust using the concept of threshold friction velocity which is dependent on the aerodynamic roughness length of the surface, Z_o. PM_{10} vertical mass flux was calculated using the Marticorena et al. (1997) algorithm. The flux is a function of wind velocity, threshold wind velocity, and a coefficient that relates the surface soil texture to PM_{10} emissions. Emissions start when the friction velocity is greater than the threshold friction velocity at that height. Friction velocity was calculated as a function of the aerodynamic roughness length. Threshold friction velocity was calculated as the ratio of the threshold velocity for smooth surface (U_{*ts}) to f_{eff}, the efficient friction velocity. f_{eff} is defined by Marticorena and Bergamette (1995) as the ratio of friction velocity for a smooth surface to actual friction velocity. To determine this ratio, the aerodynamic roughness length for a smooth surface (Z_{os}), which is defined as the mean soil particle diameter (D_p) divided by 30 (Greeley and Iversen, 1985), and the actual aerodynamic roughness length are needed. Soil samples were collected from the modeled area to determine Dp. Z_{os} was calculated using the measured D_p. Using a mean value of 22 cm/s for U_{*ts}, the actual threshold friction velocity was calculated for different values of aerodynamic roughness lengths.

Using images of the area, a map of surface conditions and geomorphology, the U_{*t} data from the Mojave Desert (Gillette et al., 1980; 1982), the authors estimated the threshold friction velocity and surface roughness length for each surface classification. The coefficient that relates the surface soil texture to PM_{10} emissions was estimated using data for several soils from semi-arid areas (Gillette et al., 1997) showing the ratio of vertical flux of PM_{10} to total horizontal mass flux as function of friction velocity. In their work, Draxler et al. (2001) considered a special case of wind blown dust. Land with vegetative cover has a relatively high threshold velocity and was not considered as an emission source. Two types of soil surface conditions were considered: loose undisturbed soil and disturbed soil. All the area was considered dry and therefore the effect of rain and snow was not considered.

Zender et al. (2003) developed a Dust Entrainment And Deposition (DEAD) model for studying dust related processes at both local and global scales. They considered three major factors that affect the dust flux: wind friction velocity, vegetation cover and surface soil moisture content. The approach developed by Marticorena and Bergamette (1995) was used to develop the model. For computing the threshold friction velocity they used a semi-empirical equation developed by Iversen and White (1982). In this equation, the friction velocity is a function of soil density and particle size, and air density and kinematic viscosity. The constant surface roughness length of 0.01 cm was assumed for the entire domain.

The change in threshold friction velocity was calculated using the equation developed by Marticorena and Bergamette (1995), similar to what as Draxler et al. (2001) used in their model. Zender used one global value of 0.0033 cm for the roughness length for a smooth surface. The effect of moisture content of the surface soil was considered in the Zender model. A threshold moisture content was calculated as a function of the mass fraction of clay as adopted from Fécan et al. (1999). Land covered by vegetation was not considered as dust emitting source.

The vertical mass flux was calculated as a function of the horizontal mass flux, a global tuning factor, a source erodibility factor, the fraction of bare soil, and the fraction of clay mass. The horizontal mass flux was calculated as a function of friction velocity and threshold friction velocity.

Shao (2001) developed an emission flux model as a function of the horizontal mass flux, threshold friction velocity and an empirical function of the diameters of saltating and emitted particles. In his work, Shao emphasized the micro-scale forces working on saltating particles and the impact of these particles on dust emissions. In this model a particle size distribution of the soil is required.

In Mansell et al. (2004), refinements to the WBD model were primarily focused on improving the determination of surface friction velocities and threshold friction velocities, as well as the calculation of dust emission fluxes. The characterization of the disturbance level of vacant land parcels was also considered. Land use datasets to more accurately characterize vacant lands were identified for use in the revised dust emission model developed under Phase II of the Wind Blown Dust project. The dust model was applied with these revisions for the WRAP regional modeling domains at 36- and 12-km resolution. A model performance evaluation was also presented in Mansell et al. (2004).

2.2. Natural Background Concentrations of Ozone, PM and Precursors

Natural background concentrations can defined as those concentrations of ozone, PM and their precursors that would occur as a result of only natural (i.e., biogenic and geogenic) emissions. Contributions to background ozone include both photochemical production from natural precursors and stratospheric intrusion of ozone into the troposphere, while background contributions to secondary PM include photochemical production from natural emissions and direct emissions of primary PM.

“Background” can be defined in several different ways. A related concept is policy relevant background (PRB) which is defined by the EPA (2006) as those concentrations that would occur in the United States in the absence of anthropogenic emissions in continental North America, including the United States, Canada and Mexico. The USEPA adopts this definition of PRB because it identifies the effects of pollution that can be controlled by US regulations and international agreements with neighboring countries. However, this definition of PRB is problematic because there is no certainty that international agreements will effectively reduce emissions in Mexico and Canada, and it is also possible that international agreements could reduce some emissions in countries other than Mexico and Canada. A plausible alternate definition of PRB would be those concentrations that would occur in the United States in the absence of anthropogenic emissions in the United States.

A further complication arises in the estimation of natural emissions because they can be calculated either for a pristine environment with no human effects on land use or for the present day environment in which human activity has significantly altered natural ecosystems. For example, natural emissions are likely to be substantially different in the present compared to historical conditions because emissions from agricultural operations and urban and residential areas are now considered anthropogenic. Thus, large land areas are excluded from the calculation of present day biogenic emissions. We can define pristine natural background as those concentrations occurring under pristine conditions with limited human effects on land use, versus present day natural background as those concentrations occurring from natural emissions given the substantially modified land use activity in the present. Table 2-4 summarizes four possible classifications of "background" concentrations.

Table 2-4. Definitions of background concentrations.

Background Type	Description
Pristine natural background	Concentrations occurring under pristine conditions with limited human effects on land use.
Present day natural background	Concentrations occurring from natural emissions given the substantially human modified land use activity in the present.
North America Policy Relevant Background	Concentrations that would occur in the United States in the absence of anthropogenic emissions in continental North America.
U.S. Policy Relevant Background	Concentrations that would occur in the United States in the absence of anthropogenic emissions in the United States.

Two approaches can be used to estimate background concentrations. One approach uses historical data and air quality models, and the second approach uses an analysis of observed concentrations at clean, relatively remote monitoring sites. Both of these approaches have significant limitations. Historical data is very limited, and modeled natural emissions have large uncertainty. Moreover, historic monitoring data can not be directly compared to model simulations of present day background because the historic monitoring data is from a time period during which land use activity was different from the present. In the second approach, it is not possible to fully exclude the contribution of anthropogenic emissions at relatively remote monitoring sites which can result in over estimates of natural background. Alternatively, if high concentrations events of natural origin were excluded from the analysis of the relatively remote sites, this analysis would under estimate natural background concentrations. While both approaches for estimating background concentrations have uncertainty, a combination of the two approaches should be useful for estimating upper and lower bounds the contributions of natural background to ozone and PM. We review previous evaluation using both approaches for ozone and PM next.

2.2.1. Previous estimates of background ozone

The ozone criteria document (EPA, 2006) reviews ambient ozone data from four clean, relatively remote monitoring sites. The USEPA review is limited to sites in the western US because no site in the eastern US was considered relatively remote. The western US sites included Theodore Roosevelt National Park (NP), Yellowstone NP, Glacier NP, and Olympic NP for the period from 1995 to 2004. Mean 8-hour average ozone concentrations ranged from 20 to 40 ppb, and there was no observed trend in ozone over the 10 year period at these sites.

Other observation based methods have been used to estimate background ozone using theoretical considerations of the amount of ozone produced per molecule of NOx emissions. There is uncertainty in this approach because of uncertainty in natural NOx emissions and uncertainty in the fate and deposition rates of odd nitrogen (NOy) species. In this approach, background ozone is estimated from the y-intercept of a plot of the concentrations of ozone versus either NOy or NOy minus NOx. Using this approach, background ozone has been estimated to range from 25 to 45 ppb (Trainer et al., 1993; Hirsch et al., 1996; Altschuller and Lefohn, 1996).

2.2.2. Previous estimates of background PM

Natural background concentrations of PM have been reviewed by the USEPA in both the PM criteria documents (EPA, 2004) and in "Guidance for Estimating Natural Visibility Conditions under the Regional Haze Rule" (EPA, 2003), referred to as RHR below. The background concentrations in RHR were based on the 1990 National Acid and Precipitation Program study (NAPAP, 1991) and are summarized in Table 2-1.

2.3. Previous Modeling Studies

Modeling studies for natural ozone and PM have been completed at both the global and regional scale. Global scale simulations are necessary even when the focus is on local or regional conditions because international transport is rapid, with a time constant of several days to weeks. Global scale models, however, typically have coarse spatial resolution which limits their usefulness for evaluating local scale variability in pollutant concentrations. Global scale model simulations of background ozone and PM have been performed with the GEOS-CHEM model (Fiore et al., 2003; Park et al., 2004). Global scale model simulations of international transport have been performed with both the GEOS-CHEM model (Heald et al., 2006) and the MOZART model (Liu and Mauzerall, 2007). Heald et al. (2006) found enhancement of sulfate in North America caused by transport from Asia, with average enhancement of sulfate of 0.16 $\mu g/m^3$ during spring 2001. This was 33% greater than the 0.12 $\mu g/m^3$ sulfate concentration used to represent total background sulfate in the western US. In global scale studies of background ozone using GEOS-CHEM, Fiore et al. (2003) found that natural ozone levels were typically between 10 to 25 ppb and never exceeded 40 ppb. When including international transport, they found that background ozone in the US was between 15 to 30 ppb with some incidences between 40 to 50 ppb in the western US. They also concluded that stratospheric intrusion of ozone was always less than 20 ppb and that it represented a minor contribution to background ozone.

WRAP has performed model sensitivity simulations designed to evaluate $PM_{2.5}$ and visibility in the absence of anthropogenic emissions (Tonnesen et al., 2006). This study is significant because it used a high resolution 36-km CMAQ simulation for most of North America nested within the global-scale GEOS-CHEM model. The higher resolution CMAQ model is expected to more accurately simulate photochemical production of ozone and secondary PM and to better resolve local variability in terrain, meteorology and ozone and PM concentrations compared to the relatively coarse resolution global scale models. The WRAP study also included a much more detailed and higher resolution emissions inventory for North America compared to the global scale models. However, as discussed next, the WRAP study also has some limitations compared to the global scale models.

Tonnesen et al. (2006) described the WRAP CMAQ simulation as a “clean conditions” scenario rather than a “natural conditions” scenario because it did not include all known source of biogenic emissions. For example, lightning NOx, sea salt and DMS emissions were not included in this model simulation. Rather than representing natural background, the WRAP study was designed to investigate the “model floor” for $PM_{2.5}$, i.e., the extent to which visibility could be improved if all anthropogenic emissions were removed. Although this model simulation did not represent true natural conditions, it did include the following emissions sources:

- *Biogenic VOC:* Generated in the WRAP 2002 base case version A (Base02a) by BEIS3.12 using SMOKE.
- *WRAP Ammonia:* The Base02a ammonia emissions for the WRAP region were developed with a GIS by ENVIRON. The five emissions category modeled included three anthropogenic sources (domestic animals, livestock, and fertilizer application) and two natural sources (soils and wildlife). The clean simulation included only the two natural sources.
- *CENRAP Ammonia:* To create ammonia inventory files for only natural sources, a list of SCCs representing natural sources was used to extract the emissions records of these sources from the monthly inventory files that were used in Base02a. There were no natural ammonia sources in the MRPO monthly inventory files.
- *Natural Area Sources:* The Base02a area-source inventory files included natural sources, such as wildfires and wild animals. These records were extracted from the stationary-area-source inventories. Note that the WRAP area-source files did not include any natural sources.
- *Natural Fires:* Of the five fire categories modeled in Base02a—wildfires, wildland fire use, non-Federal rangeland prescribed fires, prescribed fires (which were split into natural and anthropogenic prescribed for the purpose of this sensitivity), and agricultural fires—the categories that represent natural fires were used: wildfires, wildland fire use, and natural prescribed fires.
- *Windblown Dust:* A windblown dust inventory that ENVIRON and the RMC developed for use in case Base02a was used. Additional details on this dust inventory are available at http://www.cert.ucr.edu/aqm/308/wb_dust2002/wb_dust_ii_36k.shtml.

Figure 2-3 shows the annual average model simulated ozone concentration for the WRAP study. Ozone concentration were greatest in the western US because of the large contribution of fires to NOx emissions in the west. If lightning NOx emissions had been included, there would be expected increases in ozone throughout the model domain with larger increases in the eastern US and especially in the southeastern US where lightning activity is greatest. The WRAP modeled background ozone concentration in the eastern US was between 20 to 25 pbb, which is at the low end compared to previous studies. Annual average ozone concentration in the inland western US varied from 30 to 42 ppb which is slightly greater than previous studies.

Figure 2-4 shows the model-reconstructed light extinction in the clean emissions model simulation. Because the natural fire emissions in the WRAP states were a major component of the clean emissions, the largest visibility impairment was in the regions with natural fire emissions. Contributions to light extinction from natural sources were small in regions without large fire emissions, as evidenced in the eastern US, where the extinction was only slightly larger (about 2 Mm^{-1}) than perfectly clean Rayleigh conditions of 10 Mm^{-1}.

Although there were large uncertainties in the natural emissions and the emissions data did not include certain types of natural emissions, the components of the natural inventory used in this sensitivity simulation contributed to relatively large visibility impairment in regions where there were large wildfires. Extinction coefficients as large as 90 Mm^{-1} were simulated in the southern Oregon and northern California regions; this was most likely a result of the large Biscuit fire in Oregon, plus contributions from smaller fires and other natural emissions. These visibility impairment levels exceed the natural visibility levels specified in the EPA regional haze natural visibility guidance document. It will thus be more difficult for the modeling to demonstrate attainment of progress goals in areas of the country subject to wildfires because of their large contribution to visibility impairment that is not controllable. In other regions of the country for which the inventories lacked large natural fire emissions, the modeled clean visibility was only slightly greater than clean Rayleigh conditions. The model results for clean conditions in the eastern US were not reliable because of the lack of natural emissions inventory.

These results are very tentative because of the large uncertainties in natural emissions. Considerable effort would be needed to more fully investigate natural conditions in future modeling studies. It will always be difficult to determine and quantify “clean conditions” based on observations because of the pervasive influence of anthropogenic emissions.

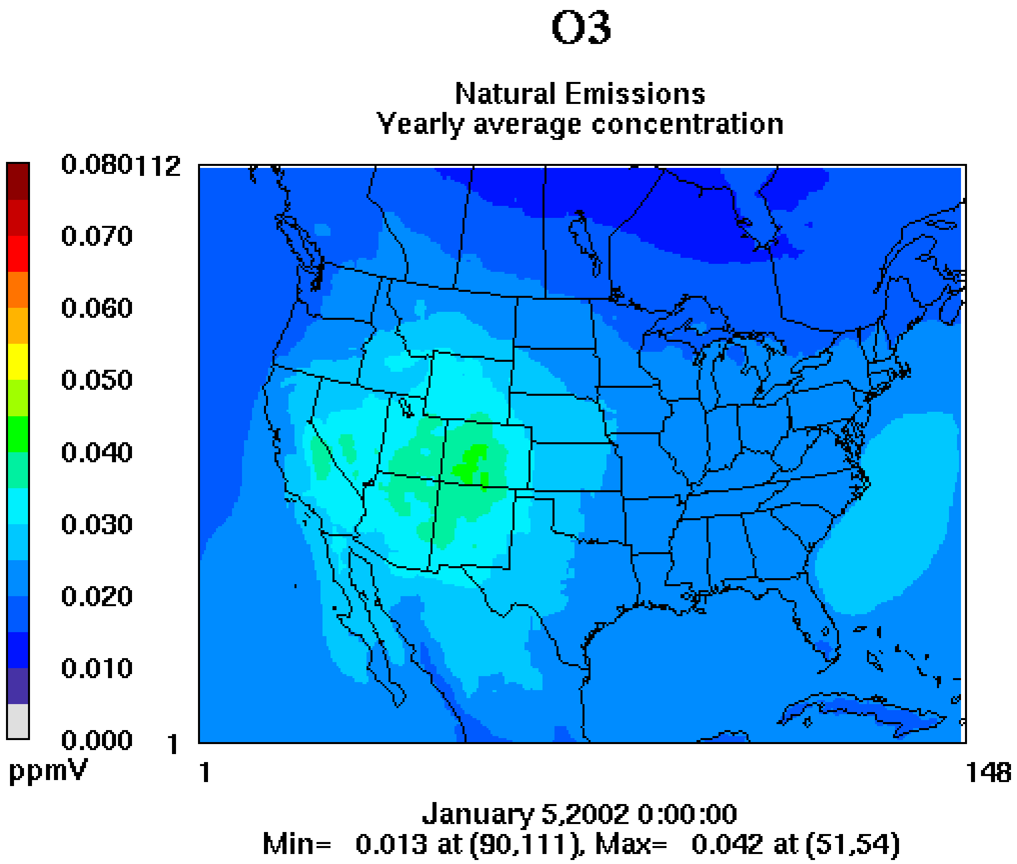

Figure 2-3. Annual average CMAQ model simulated ozone concentration for “clean conditions”, excluding lightning NOx emissions (from Tonnesen et al., 2006).

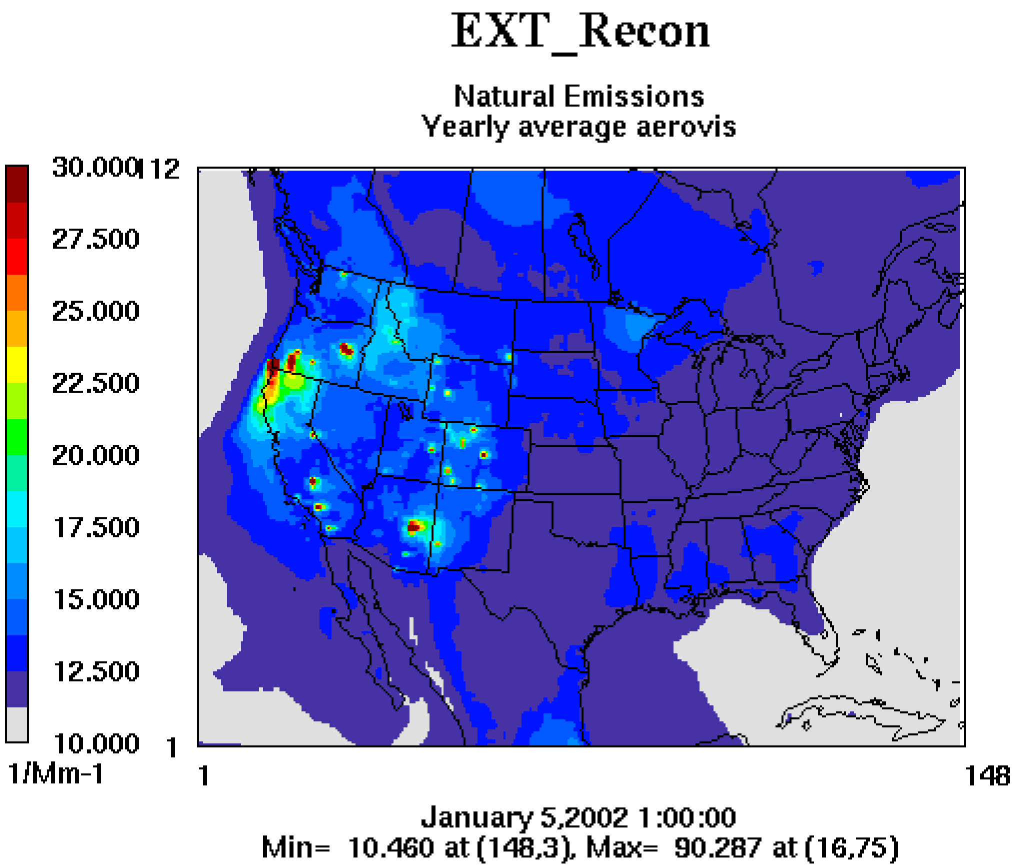

Figure 2-4. Annual average model-reconstructed "clean conditions" visibility as extinction coefficient (from Figure 7-1 in Tonnesen et al., 2006).

3. MODELING PLAN

3.1. Modeling Setup

The WRAP 2002 36 km continental US modeling database will be used for the natural conditions modeling analysis. The national RPO 36 km modeling grid used for the WRAP modeling is shown in Figure 3-1. The original WRAP simulation was performed using version 4.5.1 of the Community Multiscale Air Quality (CMAQ) modeling system with AE3 aerosol scheme which does not have active sea salt. The following four modeling configurations will be set up:

1. Current Standard Simulation

This represents the current regulatory modeling practice, and will use the current WRAP 2002 Base Case modeling database. The following updates will be made to the original WRAP 2002 Base Case simulation:

- AE4 aerosol scheme instead of AE3 will be used for sea salt emissions;
- Gas-phase chemistry will be updated from the CB-IV mechanism to the CB05 mechanism;
- The 2002 GEOS-CHEM global model outputs will be re-mapped to the CB05 species for the CMAQ boundary conditions (BCs).

Species mapping between GEOS-CHEM and CMAQ CB05 species is discussed in Section 3.3.

2. Current Natural Simulation

The WRAP 2002 “clean condition” modeling database will be used for this setup. The clean condition emissions are described in more detail in Section 2.3. Similarly, the following updates will be made to the original setup:

- AE4 aerosol scheme;
- CB05 gas-phase chemistry mechanism;
- CB05 BCs will be generated from the 2002 “no global anthropogenic” GEOS-CHEM modeling outputs.

3. Revised Natural Simulation

Based on the review performed and described in the previous Section, the current WRAP 2002 clean condition emissions will be revised. The proposed “revisions” are discussed in Section 3.2.2. These revisions will be applied incrementally so that the impact of each revision can be evaluated separately.

4. Revised Standard Simulation

The same revisions as above will be applied to the natural components of the “Current Standard” setup.

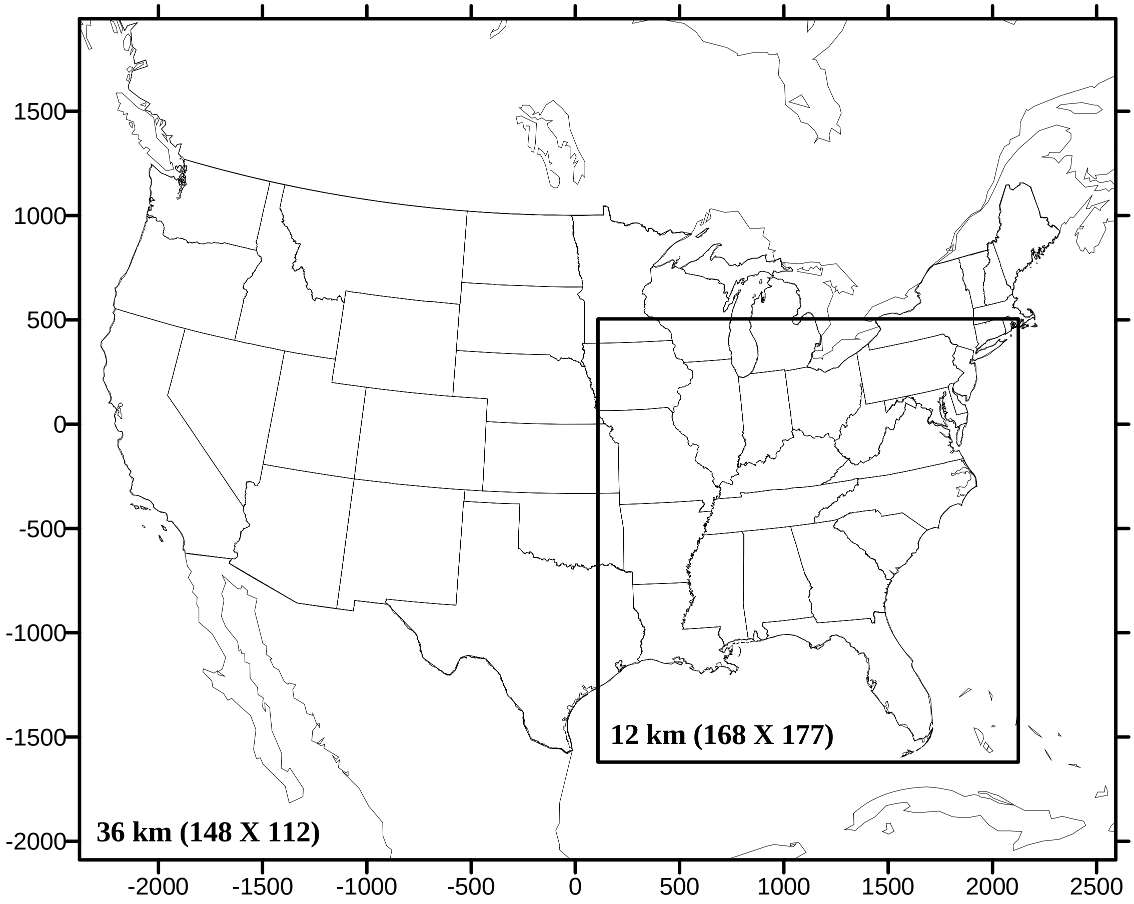

Figure 3-1. National RPO 36 km modeling domain used by the WRAP and VISTAS and 12 km nested grid for VISTAS.

The 2002 annual simulation will be performed for these setups and the results will be evaluated. The results of the two "Standard" simulations will be compared against 2002 observations while the two "Natural" simulations will be compared against estimates of natural background identified in Section 2.

3.2. Emissions

3.2.1. Current Natural Emissions

The WRAP 2002 "clean condition" emissions are used for the Current Natural simulation. Although the "clean condition" simulation eliminated anthropogenic emission sources, it is missing some of the important natural sources, for example, lightning NOx, sea salt, etc. The "clean" emissions include:

- SMOKE BEIS3 biogenic emissions (including soil NO emissions);
- Natural component of fire emissions;
- Windblown fugitive PM dust emissions from WRAP Windblown Dust model;
- Natural component of NH_3 emissions from WRAP Ammonia model;

Also, “no global anthropogenic” GEOS-CHEM results provided BCs for this simulation. More details on the emissions of this simulation are found in Section 2.3.

3.2.2. Revised Natural Emissions

Based on the literature review and previous WRAP clean condition study, we will consider the following list of new natural sources for the revised natural background simulations:

Sea Salt

It has been reported from the previous WRAP and VISTAS modeling studies that the internally generated sea salt emissions with the CMAQ AE4 scheme generally underestimate chlorine (Cl) measurement at IMPROVE monitoring sites. However, the IMPROVE data may include chlorine sources other than sea salt. It may also be due to the fact that the current AE4 scheme does not treat the sea salt emissions from the surf zone, thus underestimate the sea salt generated in the spray zone. We will generate sea salt emissions using an external sea salt generation algorithm to optimize the chlorine model performance at the coastal monitoring sites where the chlorine measurements are representative of sea salt.

Sulfur Emissions from Ocean

Dimethyl sulfide (DMS) and methyl sulfonic acid (MSA) are the main sulfur-carrying chemicals from ocean. For the ocean area inside our US modeling domain, CMAQ will internally generate sulfate emissions from ocean. The DMS and MSA emissions from outside of the modeling domain will interact with sulfur dioxide and sulfate within the modeling domain through the boundary conditions. DMS and MSA from the GEOS-CHEM simulations were not originally mapped to the CMAQ BCs. We will include these sulfur species in the revised species mapping for the GEOS2CMAQ BC converter.

Background Methane

The background methane concentration is set to 1.85 ppm in the current version of CMAQ, which could be adjusted to pre-industrial level of 0.70 ppm (Blunier et al., 1993).

Updated Biogenic Emissions

New biogenic emissions generated from the latest Model of Emissions of Gases and Aerosols from Nature (MEGAN) biogenic emissions model instead of the SMOKE-BEIS3 will be used. The MEGAN provides more biogenic species from updated land use data with higher resolution.

Updated Biogenic SOA Formation

We will modify the CMAQ V4.5.1 SOA module to include biogenic SOA formation from isoprene and sesquiterpenes as done for the VISTAS regional haze modeling (Morris et al., 2006). SOA from isoprene and sesquiterpenes is not included in the standard version of CMAQ.

Lightning NOx Emissions

Orville et al. (2002) estimated about 30 million flashes per year for North America cloud-to-ground lightning. Using a multiplier of 2.8 to get intracloud flashes (Boccippio et al., 2001), we estimate a total of 114 million flashes per year. This represents 8.2% of total estimated global flash rate of 44 flashes per second (1.39 billion flashes per year). Using the high and low NOx emissions per flash estimates from the EULINOX study (Holler and Schumann, 2000) which estimate emissions rates lower and upper bounds of 0.46 and 9.3 KgN per flash, we get upper and lower bounds of 0.052 and 1.06 TgN per year for North America.

These low- and high-end estimates of annual total lightning NOx emissions will be spatially and temporally allocated to the modeling grid cells based on the amount of convective precipitation activity in each cell. We do not recommend to using the MCIP (MM5) precipitation data directly because CMAQ uses its own internal diagnosis of sub-grid convective activity. We will be using MM5CAMx instead of MCIP since MM5CAMx has been updated to better address the vertical distribution of convective activity. The hourly and gridded 3-D lightning NOx emissions will be then merged into the other CMAQ emissions inputs.

3.3. Boundary Conditions

3.3.1. GEOS-CHEM Simulation

The GEOS-CHEM model is a cooperative global chemical transport model used by 21 institutions in North America and Europe, and centrally managed by Dr. Daniel Jacob's group at Harvard University (http://www-as.harvard.edu/chemistry/trop/geos). It is driven by assimilated meteorological observations from the Global Earth Observation System (GEOS) of the NASA Global Modeling and Assimilation Office (GMAO).

In 2005, the Harvard group performed GEOS-CHEM simulations to provide chemical boundary conditions for the VISTAS 2002 CMAQ 36 km modeling. GEOS meteorological observations for the year 2002 were used for assimilation. The data through August 2002 are from the GEOS-3 assimilation, with horizontal resolution of 1^ox1^o and 55 vertical layers. The data after August 2002 are from the updated GEOS-4 assimilation, with horizontal resolution of 1^ox1.25^o and 48 vertical layers. The GEOS-CHEM simulations used coarser 4^ox5^o horizontal resolution and 20 vertical layers. Three full-year simulations for 2002 were conducted:

- A baseline simulation with best estimates of 2002 emissions;
- A background simulation modified from the baseline by shutting off U.S. anthropogenic emissions;
- A natural simulation modified from the baseline by shutting off global anthropogenic emissions.

The outputs were produced for 3-D concentration fields with 3-hour temporal resolution. More details about these simulations can be found elsewhere (Jacob et al., 2005).

The BCs for the VISTAS CMAQ run were extracted from the outputs and mapped to CMAQ CB-IV species using GEOS2CMAQ BC converter developed by Dr. Daewon Byun's group at

University of Houston (Moon and Byun, 2004). Later, these BCs were also used for the WRAP 2002 base case and clean condition simulations.

3.3.2. CB05 Species Mapping

For the simulations in this study, we have updated the GEOS2CMAQ code to add species mapping for CB05 chemistry mechanism. The new CB05 species mapping is shown in Table 3-1.

Table 3-1. Species mapping for GEOS-CHEM and CMAQ CB05 AE4 species.

CMAQ (CB05; AE4)	GEOS-CHEM (NOx-Ox-Hydrocarbon)
NO2	NOx
O3	Ox - NOx
CO	CO
N2O5	N2O5
HNO3	HNO3
PNA	HNO4
H2O2	H2O2
NTR	R4N2
FORM	CH2O
ALD2	0.5 ALD2
ALDX	RCHO
PAR	0.333 PRPE + ALK4 +0.5 C3H8 + ACET + MEK + RCHO
OLE	0.333 PRPE
ETHA	0.5 C2H6
MEPX	MP
PAN	PAN
PANX	PPN + PMN
ISOP	0.2 ISOP
ISPD	MACR + MVK
TERP	ALPH + LIMO + ALCO
SO2	SO2 + DMS
NH3	NH3
SGTOT_TRP_1	0.2 SOG1 +0.2 SOA1 +0.2 SOG2 +0.2 SOA2 +0.2 SOG3 +0.2 SOA3
SGTOT_TRP_2	0.8 SOG1 +0.8 SOA1 +0.8 SOG2 +0.8 SOA2 +0.8 SOG3 +0.8 SOA3
ASO4J	SO4 + MSA
ANO3J	NIT
ANH4J	NH4
AORGBJ	0.847 SOA1 +0.904 SOA2 +1.24 SOA3
AORGPAJ	0.0545 OCPI +0.0545 OCPO
AECJ	BCPI + BCPO
A25J	0.145 DST1 +0.145 DST2
ANAJ	1.03 SALA
ANAK	1.03 SALC
ACLJ	1.03 SALA
ACLK	1.03 SALC
ASOIL	0.29 DST3 +0.29 DST4

3.4. Sensitivity Simulations

The primary goal of the CRC Project A-65 is to assess ozone and PM responses to emissions reductions under current and revised natural background emissions. For the sensitivity simulations, we will use the VISTAS 2002 36 and 12 km CMAQ modeling database. VISTAS uses the same national RPO 36 km domain as used by WRAP and a 12 km grid that covers the eastern US, from Houston and Minneapolis in the west to all of Florida and New York City in the east (Figure 3-1). The 36 and 12 km modeling will have different focus:

36 km simulation:

- Runs for the full year of 2002;
- Focuses on ozone and $PM_{2.5}$.

12 km simulation:

- Runs only for the third quarter (Q3) of 2002;
- Focuses on ozone; could be used for checking consistency of the PM results with the 36 km annual run.

We will conduct a future year (2018) base case simulation using the 36 km (annual) and 12 km (Q3) grids with two sets of natural background conditions: with the “current” and the “revised” natural background sources. Then, the future year sensitivity runs will be performed with various anthropogenic emissions controls for each of the two natural background conditions (Table 3-2).

The EPA Model Attainment Test Software (MATS) will process the base and control case runs to obtain the 2018 projected 8-hr ozone and $PM_{2.5}$ Design Values and regional haze metrics at Class I areas (The $PM_{2.5}$ projection component of MATS tool is now available). We will also look at other types of plots including spatial difference plots and time-series plots to help understand the impacts of natural sources on the model responses of ozone and PM to the anthropogenic emissions controls.

Table 3-2. Level of anthropogenic emission reductions selected for the future year sensitivity runs.

	NO_x	**VOC**	**SO_2**	**NH_3**	**$PM_{2.5}$**
$PM_{2.5}$ 36 km (Annual)	30%	-	-	-	-
	-	30%	-	-	-
	-	-	30%	-	-
	-	-	-	30%	-
	-	-	-	-	30%
Ozone 36/12 km (Q3)	30%	-	-	-	-
	-	30%	-	-	-
	30%	30%	-	-	-

4. REFERENCES

Altshuller, A. P. and A. S. Lefohn (1996) Background ozone in the planetary boundary layer over the United States, J. Air Waste Management, 46, 134-141.

Bates, T. S., B. K. Lamb, A. Guenther, J. Dignon and R. E. Stoiber (1992). “Sulfur emissions to the atmosphere from natural sources.” J. Atmos. Chem., 14:315-337.

Battye, William, Aneja, Viney P., Roelle, Paul A. (2003) Evaluation and Improvement of Ammonia Emission Inventories, Atmospheric Environment, 37, 3873-3883.

Beirle, S., U. Platt, M. Wenig and T. Wagner (2004) NOx production by lightning estimated with GOME, Advances in Space Research 34(4): 793.

Blunier, T., J. A. Chappellaz, J. Schwander, J.-M. Barnola, T. Desperts, B. Stauffer, and D. Raynaud (1993) Atmospheric methane, record from a Greenland ice core over the last 1000 year, Geophys. Res. Lett., 20(20), 2219.

Boccippio, D. J., K. L. Cummins, H. J. Christian, and S. J. Goodman (2001) Combined Satellite- and Surface-Based Estimation of the Intracloud-Cloud-to-Ground Lightning Ratio over the Continental United States, Mon. Wea. Rev., 129, 108-122.

Bond, D. W., S. Steiger, R. Zhang, X. Tie and R. E. Orville (2002). "The importance of NOx production by lightning in the tropics." Atmospheric Environment 36(9): 1509.

Brasseur, G.P., Hauglustaine, D.A., Walters, S., Rasch, P.J., Mueller,J.F., Granier C., and . Tie X.X. (1998). "MOZART, a global chemical transport model for ozone and related chemical tracers 1. Model description." J. Geophys. Res. 103: 28265-28289.

Chinkin, L.R., P.A. Ryan, and D.L. Coe (2003) Recommended Imporvements to the CMU Ammonia Emission Inventory Model for Use by LADCO, Prepared for Lake Michigan Air Directors Consortium.

Chitjian, M. and Mansell, G. (2003a) An Improved Ammonia Inventory for the WRAP Domain – Literature Review, Prepared for the WRAP Emissions Forum. October.

Chitjian, M. and Mansell, G. (2003b) An Improved Ammonia Inventory for the WRAP Domain – Technical Description of the Modeling System, Prepared for the WRAP Emissions Forum. November.

DeCaria, A., K. Pickering, G. Stenchikov, J. Scala, J. Stith, J. Dye, B. Ridley and P. Laroche (2000) A cloud-scale model study of lightning-generated NO x in an individual thunderstorm during STERAO-A, J. Geophys. Res., 105(D9), 11601-11616.

DeCaria, A. J., K. E. Pickering, G. L. Stenchikov and L. E. Ott (2005) Lightning-generated NO X and its impact on tropospheric ozone production: A three-dimensional modeling study of a Stratosphere-Troposphere Experiment: Radiation, Aerosols and Ozone (STERAO-A) thunderstorm, J. Geophys. Res., 110(D14), 1-13.

Derwent, R. G., D. S. Stevenson, W. J. Collins and C. E. Johnson (2004) Intercontinental transport and the origins of the ozone observed at surface sites in Europe, Atmospheric Environment, 38(13), 1891.

Dore, A. J., M. Vieno, Y. S. Tang, U. Dragosits, A. Dosio, K. J. Weston and M. A. Sutton (2007) Modelling the atmospheric transport and deposition of sulphur and nitrogen over the United Kingdom and assessment of the influence of SO2 emissions from international shipping, Atmospheric Environment, 41(11), 2355.

Draxler, R. R., Gillette, D. A., Kirkpatrick, J. S., and Heller J. (2001) Estimating PM_{10} air concentration from dust storms in Iraq, Kuwait, and Saudi Arabia, J. Atmospheric Envir., 35, 4315-4330.

Duncan Fairlie, T., D. J. Jacob and R. J. Park (2007) The impact of transpacific transport of mineral dust in the United States, Atmospheric Environment, 41(6), 1251.

Egorova, T., V. Zubov, S. Jagovkina and E. Rozanov (1999) Lightning production of NOX and ozone, Physics and Chemistry of the Earth, Part C: Solar, Terrestrial & Planetary Science, 24(5), 473.

EPA (2003) Guidance for Estimating Natural Visibility Conditions Under the Regional Haze Rule, U.S. Environmental Protection Agency, Research Triangle Park, NC. EPA-454/B-03-005. September.

EPA (2004) Air Quality Criteria for Particulate Matter, U.S. Environmental Protection Agency, Research Triangle Park, NC. EPA/600/P-99/002aF. October.

EPA (2006) Air Quality Criteria for Ozone and Related Photochemical Oxidants, U.S. Environmental Protection Agency, Research Triangle Park, NC. EPA 600/R-05/004aF. February.

EPA (2007) Guidance on the Use of Models and Other Analyses for Demonstrating Attainment of Air Quality Goals for Ozone, PM2.5 and Regional Haze, U.S. Environmental Protection Agency, Research Triangle Park, NC. EPA-454/B-07-002. April.

Fécan, F., B. Marticorena, and G. Bergametti (1999) Parameterization of the increase of the aeolian erosion threshold wind friction velocity due to soil moisture for arid and semi-arid areas, Ann. Geophys., 17, 149-157.

Fiore, A., D. J. Jacob, H. Liu, R. M. Yantosca, T. D. Fairlie and Q. Li (2003) Variability in surface ozone background over the United States: Implications for air quality policy, J. Geophys. Res., 108, ACH 19-1 - ACH 19-12.

Fiore, A. M., D. J. Jacob, I. Bey, R. M. Yantosca, B. D. Field, A. C. Fusco and J. G. Wilkinson (2002) Background ozone over the United States in summer: Origin, trend, and contribution to pollution episodes, J. Geophys. Res., 107.

Gillette, D.A., Adams, J., Muhs, D. and Kihl, R. (1982) Threshold friction velocities and rupture moduli for crusted desert soils for the input of soil particles into the air, Journal of Geophysical Research, 87(C10), 9003-9015.

Gillette, D.A., Fryrear, W. D., Gill, T. E., Ley, T., Cahill, T. A., and Gearhart, E. A. (1997) Relation of vertical flux of PM_{10} to total Aeolian horizontal mass flux at Owens Lake, J. Geophysical. Research, 102, 26009-26015.

Greely, R., and Iversen, J. D. (1985) Wind as a geological process, No. 4 in Cambridge Planetary Science Series, Cambridge Univ. Press, New York, NY.

Gillette, D.A., Adams, J., Endo, E. and Smith, D. (1980) Threshold velocities for input of soil particles into the air by desert soils, Journal of Geophysical Research, 85(C10), 5621- 5630.

Grewe, V., D. T. Shindell and V. Eyring (2004) The impact of horizontal transport on the chemical composition in the tropopause region: lightning NOx and streamers, Advances in Space Research, 33(7), 1058.

Grewe, V. (2007) Impact of climate variability on tropospheric ozone, Science of The Total Environment, 374(1), 167.

Heald, C. L., D. J. Jacob, R. J. Park, B. Alexander, T. D. Fairlie, R. M. Yantosca and D. A. Chu (2006) Transpacific transport of Asian anthropogenic aerosols and its impact on surface air quality in the United States, J. Geophys. Res., 111(D14), 1-13.

Hirsch, A.I., Munger, J.W., Jacob, D.J., Horowitz, L.W., and Goldstein, A.H. (1996) Seasonal variation of the ozone production efficiency per unit NO_x at Harvard Forest, Massachusetts, J. Geophys. Res., 101, 12659-12 666.

Holler, H. and Schumann, U. (2000) EULINOX – The European Lightning Nitrogen Oxides Project, 240pp, Deutsches Zentrum fur Luft- und Raumfahrt, Koln, Germany, DLR-FB 2000-28.

Horowitz, L. W., S. Walters, D. L. Mauzerall, L. K. Emmons, P. J. Rasch, C. Granier, X. Tie, J. F. Lamarque, M. G. Schultz, G. S. Tyndall, J. J. Orlando and G. P. Brasseur (2003) A global simulation of tropospheric ozone and related tracers: Description and evaluation of MOZART, version 2, J. Geophys. Res., 108(D24), ACH 16-1 - ACH 16-25.

Hudman, R. C., D. J. Jacob, S. Turquety, E. M. Leibensperger, L. T. Murray, S. Wu, A. B. Gilliland, M. Avery, T. H. Bertram, W. Brune, R. C. Cohen, J. E. Dibb, F. M. Flocke, A. Fried, J. Holloway, J. A. Neuman, R. Orville, A. Perring, X. Ren, G. W. Sachse, H. B. Singh, A. Swanson and P. J. Wooldridge (2007) Surface and lightning sources of nitrogen oxides over the United States: Magnitudes, chemical evolution, and outflow Inventory of boreal fire emissions for North America in 2004: Importance of peat burning and pyroconvective injection, J. Geophys. Res., 112(D12), 1-14.

Iversen, J.D. and White, B. R. (1982) Saltation threshold on Earth, Mars, and Venus, Sedimentology, 29, 111-119.

Jacob, D. J., R. Park, and J. A. Logan (2005) Documentation and Evaluation of the GEOS-CHEM Simulation for 2002 Provided to the VISTAS Group, Final Report submitted for VISTAS, June.

Jaffe, D., I. McKendry, T. Anderson and H. Price (2003) Six 'new' episodes of trans-Pacific transport of air pollutants, Atmospheric Environment, 37(3), 391.

Jaffe, D. and J. Ray (2007) Increase in surface ozone at rural sites in the western US, Atmospheric Environment, 41(26), 5452.

Jourdain, L. and D. A. Hauglustaine (2001) The global distribution of lightning NOx simulated on-line in a general circulation model, Physics and Chemistry of the Earth,Part C: Solar,Terrestrial & Planetary Science, 26(8), 585.

Lee, D. S., I. Kohler, E. Grobler, F. Rohrer, R. Sausen, L. Gallardo-Klenner, J. G. J. Olivier, F. J. Dentener and A. F. Bouwman (1997) Estimations of global no, emissions and their uncertainties, Atmospheric Environment, 31(12), 1735.

Liu, H., J. H. Crawford, R. B. Pierce, P. Norris, S. E. Platnick, G. Chen, J. A. Logan, R. M. Yantosca, M. J. Evans, C. Kittaka, Y. Feng and X. Tie (2006) Radiative effect of clouds on tropospheric chemistry in a global three-dimensional chemical transport model, J. Geophys. Res., 111(D20), 1-18.

Liu, J. and D. L. Mauzerall (2007) Potential influence of inter-continental transport of sulfate aerosols on air quality, Environ. Res. Lett., 2(4), 045029.

Luo, C., C. S. Zender, H. Bian and S. Metzger (2007) Role of ammonia chemistry and coarse mode aerosols in global climatological inorganic aerosol distributions, Atmospheric Environment, 41(12), 2510.

Mansell, G.E., R. Morris and M. Omary (2004) Recommendations and model performance evaluation for the Phase II Windblown Fugitive Dust Emission Project, Technical Memorandum prepared for the WRAP Dust Emission Joint Forum, July.

Mansell, G.E. (2005) An Improved Ammonia Inventory for the WRAP Domain, Final Report Prepared for the Western Governors' Association, 1515 Cleveland Place, Suite 200, Denver, CO 80202.

Mansell, G.E., Lau, S., Russell, J. Omary, M. (2006) Fugitive Wind Blown Dust Emissions and Model Performance Evaluation Phase II., Final Report prepared for the Western Governors' Association, 1515 Cleveland Place, Suite 200, Denver, CO 80202.

Marticorena, B., and Bergametti, G. (1995) Modeling the atmospheric dust cycle,1. Design of an a soil-derived dust emissions scheme, J. Geophysics. Research., 100, 16415-16430.

Marticorena, B., Bergametti, G., Gillette, D., and Belnap, J. (1997) Factors controlling threshold friction velocity in semiarid and arid areas of the United States, J. Geophysics Research, 102 (D19), 23277-23287.

McGee K. (2006) Mt. St. Helens SO_2 and other emissions. Via email August 4.

McKenzie, D., S. M. O'Neill, N. K. Larkin and R. A. Norheim (2006) Integrating models to predict regional haze from wildland fire, Ecological Modelling, 199(3), 278.

Meinardi, S., I. J. Simpson, N. J. Blake, D. R. Blake, and F. S. Rowland (2003) Dimethyl disulfide (DMDS) and dimethyl sulfide (DMS) emissions from biomass burning in Australia, *Geophys. Res. Lett.*, 30(9), 1454, doi:10.1029/2003GL016967.

Moon, N. and D. W. Byun (2004) A Simple User's Guide for "geos2cmaq" Code: Linking CMAQ with GEOS-CHEM, August. (http://pah.cert.ucr.edu/vistas/vistas2/BC_files/geos2cmaq_uguide_aug22_2004.pdf)

Morris, R. E., B. Koo, A. Guenther, G. Yarwood, D. McNally, T. W. Tesche, G. Tonnesen, J. Boylan and P. Brewer (2006) Model Sensitivity Evaluation for Organic Carbon using Two Multi-Pollutant Air Quality Models that Simulate Regional Haze in the Southeastern United States, *Atmos. Environ.*, 40, 4960-4972.

National Acid and Precipitation Program (1991) Acid Deposition: State of Science and Technology Report 24. Visibility: Existing Historical Conditions – Causes and Effects. Table 24-6, Washington D.C.

Ott, L. E., K. E. Pickering, G. L. Stenchikov, H. Huntrieser and U. Schumann (2007) Effects of lightning NO x production during the 21 July European Lightning Nitrogen Oxides Project storm studied with a three-dimensional cloud-scale chemical transport model, J. Geophys. Res., 112(D5), 1-18.

Orville, R. E., G. R. Huffines, W. R. Burrows, R. L. Holle, and K. L. Cummins (2002) The North American Lightning Detection Network (NALDN)-First Results: 1998-2000, Mon. Wea. Rev., 130, 2098-2109.

Park, R.J., D.J. Jacob, B.D. Field, R.M. Yantosca, and M. Chin (2004) Natural and transboundary pollution influences on sulfate-nitrate-ammonium aerosols in the United States: Implications for policy, J. Geo-phys Res., 109, D15204, doi:10.1029/2003JD004473.

Park, R. J., D. J. Jacob, N. Kumar and R. M. Yantosca (2006) Regional visibility statistics in the United States: Natural and transboundary pollution influences, and implications for the Regional Haze Rule, Atmospheric Environment, 40(28), 5405.

Park, R. J., D. J. Jacob and J. A. Logan (2007) Fire and biofuel contributions to annual mean aerosol mass concentrations in the United States, Atmospheric Environment, 41(35), 7389.

Penner, J., D. Bergmann, J. Walton, D. Kinnison, M. Prather, D. Rotman, C. Price, K. Pickering and S. Baughcum (1998) An evaluation of upper troposphere NO x with two models, J. Geophys. Res., 103(D17), 22097-22113.

Pickering, K., Y. Wang, W. K. Tao, C. Price and J. F. Müller (1998) Vertical distributions of lightning NO x for use in regional and global chemical transport models, J. Geophys. Res., 103(D23), 31203-31216.

Pinder, R. (2008) Personal communication.

Randall, D. (2006) Technical Memorandum: Fire Emissions Inventory – Phase III Base-Control Case, Prepared for Western Regional Air Partnership Fire Emissions Joint Forum by Dave Randall, *Air Sciences, Inc*., April 28, 2006.

Schumann, U. and H. Huntrieser (2007) The global lightning-induced nitrogen oxides source, Atmos. Chem. Phys. Discuss, 7, 2623-2818.

Shao, Y. (2001) A model for mineral dust emission, J. Geophysics Research, 106, 20239-20254.

Stockwell, D. Z., C. Giannakopoulos, P. H. Plantevin, G. D. Carver, M. P. Chipperfield, K. S. Law, J. A. Pyle, D. E. Shallcross and K. Y. Wang (1999) Modelling NOx from lightning and its impact on global chemical fields, Atmospheric Environment, 33(27), 4477.

Tonnesen, G., M. Omary, Z. Wang, C-J, Jung, R. Morris, G. Mansell, Y. Jia, B. Wang and Z. Adelman (2006) Report for the Western Regional Air Partnership Regional Modeling Center, University of California Riverside, Riverside, California, November. (http://pah.cert.ucr.edu/aqm/308/reports/final/2006/WRAP-RMC_2006_report_FINAL.pdf)

Trainer, M., and 19 others (1993) Correlation of ozone with NOγ in photochemically aged air, J. Geophys. Res., 98, 2917-2925.

Tsigaridis, K. and M. Kanakidou (2007) Secondary organic aerosol importance in the future atmosphere, Atmospheric Environment, 41(22), 4682.

van Donkelaar, A., R. V. Martin, R. J. Park, C. L. Heald, T.-M. Fu, H. Liao and A. Guenther (2007) Model evidence for a significant source of secondary organic aerosol from isoprene, Atmospheric Environment, 41(6), 1267.

Vingarzan, R. (2004) A review of surface ozone background levels and trends, Atmospheric Environment, 38(21), 3431.

West, J. J., A. M. Fiore, V. Naik, L. W. Horowitz, M. D. Schwarzkopf and D. L. Mauzerall (2007) Ozone air quality and radiative forcing consequences of changes in ozone precursor emissions, Geophys. Res. Lett., 34, 1-5.

Wu, S., L. J. Mickley, D. J. Jacob, J. A. Logan, R. M. Yantosca and D. Rind (2007) Why are there large differences between models in global budgets of tropospheric ozone? J. Geophys. Res., 112(D5), 1-18.

Wuebbles, D. J., H. Lei and J. Lin (2007) Intercontinental transport of aerosols and photochemical oxidants from Asia and its consequences, Environmental Pollution, 150(1), 65.

Zender, C. S., Bian, H., and Newman, D. (2003) The mineral dust entrainment and deposition (DEAD) model: Description and 1990's dust climatology, J. Geophysics Research, 108, 4416-4437.

Zhang, X., J. J. H. Helsdon and R. D. Farley (2003a) Numerical modeling of lightning-produced NOx using an explicit lightning scheme: 1. Two-dimensional simulation as a 'proof of concept', J. Geophys. Res., 108(D18), ACH 5-1 - ACH 5-20.

Zhang, X., J. J. H. Helsdon and R. D. Farley (2003b) Numerical modeling of lightning-produced NOx using an explicit lightning scheme: 2. Three-dimensional simulation and expanded chemistry, J. Geophys. Res., 108(D18), ACH 6-1 - ACH 6-17.

Zhou, Y., S. Soula, V. Pont and X. Qie (2005) NOx ground concentration at a station at high altitude in relation to cloud-to-ground lightning flashes, Atmospheric Research, 75(1-2), 47.

APPENDIX B

Progress Report #2

Progress Report

CRC Project No. A-65

Accuracy of Regional Simulations of Background Ozone and Particulate Matter

Prepared for

Coordinating Research Council
3650 Mansell Road, Suite 140
Alpharetta, GA 30022

Prepared by

Bonyoung Koo
Greg Yarwood
Ralph Morris
ENVIRON International Corporation
773 San Marin Drive, Suite 2115
Novato, CA 94998

And

Gail Tonnesen
Chao-Jung Chien
University of California at Riverside
1084 Columbia Avenue
Riverside, CA 92507

March 10, 2009

1. INTRODUCTION

1.1. Background

Air quality modeling for atmospheric ozone and particulate matter (PM) requires emission inventories from both anthropogenic and natural sources. While extensive efforts have been given to investigate and quantify emissions from these sources for the purpose of air quality management, there still exist significant uncertainties, especially in the natural sources. There are many natural sources of ozone precursors and PM, including both direct emissions of primary PM (such as windblown dust) and emissions of gaseous species that undergo photochemical transformation or condensation to form secondary PM. These natural sources are of concern because they represent background levels of ozone and PM that cannot be controlled in National Ambient Air Quality Standard (NAAQS) attainment strategies. Current standard modeling practice for the State Implementation Plans (SIPs) either neglects (e.g., lightning NOx) or simplifies (e.g., biogenics) many natural sources of ozone and PM. Natural contribution to atmospheric ozone and PM formation will become more important as the national standards for the pollutants recently revised and tightened. Also, as the control measures adopted will reduce emissions from the anthropogenic sources, the impact of the natural sources will become more significant in the future years.

There are four issues related to natural sources and background conditions that are important in air quality management planning:

1. Are natural sources alone able to result in exceedances of the ozone and/or PM NAAQS?
2. Are non-U.S. anthropogenic sources sufficient to cause exceedances of the NAAQS?
3. What are the levels of background ozone and PM concentrations in the absence of anthropogenic sources (or U.S. anthropogenic sources)?
4. What effects do natural sources and background concentrations have on the development of ozone and PM attainment emission control strategies?

The focus of the current CRC project (Project A-65) is on the fourth issue.

In the first task of the project, we focused on improving and refining the current natural source emissions. We have reviewed the available literature to identify potentially important sources of natural background ozone, PM and precursors that are usually missing in the regulatory modeling, and obtained estimates of their natural background concentrations. Findings from the literature review have been summarized in the previous Progress Report.

1.2. Modeling Configurations

To assess impacts of the natural sources identified in the review task, we conducted a series of regional scale simulations using the Western Regional Air Partnership (WRAP) 2002 annual modeling database. The details of the WRAP modeling database are described elsewhere (Tonnesen et al., 2006a). The modeling domain used is the Regional Planning Organization (RPO) Unified Continental 36 km modeling grid that covers the contiguous 48 US states, southern Canada and northern Mexico (Figure 1-1). The vertical grid consists of 19 layers that extend to the lower stratosphere (~15 km). Two sets of boundary conditions (BCs) for the modeling domain were obtained from the GEOS-CHEM global model simulations with and without global anthropogenic emissions. It has been later discovered that the model predicts unrealistically high ozone concentrations over some of the western states (Colorado, New Mexico, etc.). Further investigation revealed that the problem was caused by very high concentrations of ozone in the top layer of the lateral BCs (from the stratospheric ozone) which was transported to the surface layer over the high terrain region due to incorrectly diagnosed vertical velocity profiles by the model. We modified the lateral BCs in the uppermost model layers to avoid the problem. This issue is explained with more details in Appendix.

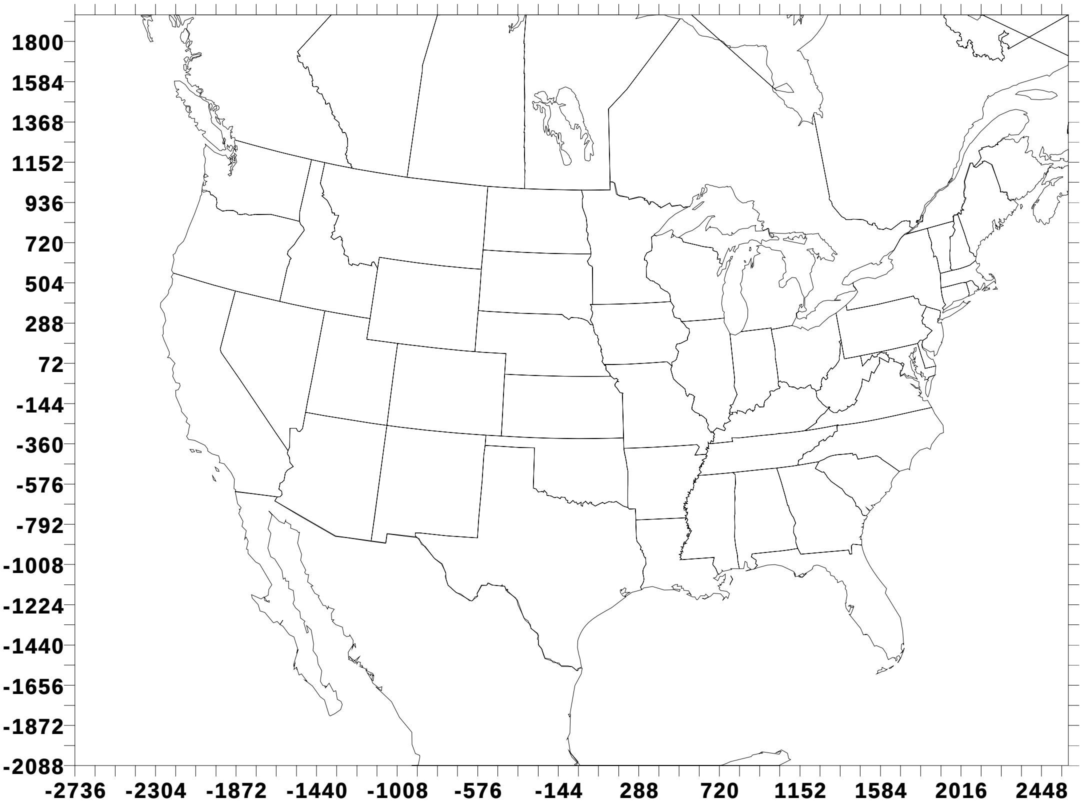

Figure 1-1. RPO Unified Continental 36 km modeling grid

The following four modeling configurations were set up:

<u>1. Current Standard Simulation</u>

This represents the current regulatory modeling practice. The WRAP 2002 base case (base02b) simulation had originally been performed using version 4.5.1 of the Community Multiscale Air Quality (CMAQ) modeling system with CB-IV gas-phase chemistry mechanism and AERO3 aerosol module which does not have active sea salt. The following updates were made for our "Current Standard" simulation:

- AERO4 aerosol module was used for sea salt emissions;
- Gas-phase chemistry was updated from the CB-IV mechanism to the CB05 mechanism;
- The 2002 GEOS-CHEM global model outputs were re-mapped to the CB05 species for the CMAQ BCs.

Table 1-1 lists the science options selected for the CMAQ simulations performed in this study.

Table 1-1. Model configurations for the CMAQ simulations.

Model Option	CMAQ version 4.6
Horizontal advection	Piecewise Parabolic Method (PPM)
Vertical advection	Global mass-conserving scheme (Yamartino scheme)
Horizontal diffusion	Multiscale
Vertical diffusion	Eddy diffusion (K_v)
Minimum vertical diffusivity	1.0 m^2/s
MM5 configuration	Pleim-Xiu/ACM
MM5 processing	MCIP v2.3 pass-through
Gas-phase chemistry	CB05
Gas-phase chemistry solver	EBI
Secondary organic aerosol	SORGAM
Aqueous-phase chemistry	RADM
Aerosol chemistry	AERO4
Dry deposition	Revised Pleim-Xiu
Cloud process	Asymmetric convective model (ACM)
Plume-in-grid	Off
Initial conditions	CENRAP 36-km spin-up
Boundary conditions	2002 3-hourly modified GEOS-CHEM

2. Current Natural Simulation

The Western Regional Air Partnership (WRAP) has performed a model sensitivity simulation designed to evaluate $PM_{2.5}$ and visibility in the absence of anthropogenic emissions (Tonnesen et al., 2006b). Note that this WRAP "Clean Condition" scenario does not represent true natural conditions for it is missing some important sources of biogenic emissions (e.g., lightning NOx, sea salt). We used this modeling as our base case for the natural simulations ("Current Natural"). The same updates as above were also applied for this simulation: AERO4 aerosol module; CB05 chemistry mechanism; and updated GEOS-CHEM BCs mapped for CB05 species. The BCs were generated from the 2002 "no global anthropogenic" GEOS-CHEM modeling outputs.

3. Revised Natural Simulation

Based on the literature review and previous WRAP clean condition study, we considered the following updates to the current representation of natural sources:

- Sulfur emissions from ocean – Dimethyl sulfide (DMS) and Methyl sulfonic acid (MSA)
- NOx emissions from lightning
- Alternative sea salt emissions
- Updated biogenic secondary organic aerosol (SOA) formation with emissions from the Model of Emissions of Gases and Aerosols from Nature (MEGAN)
- Pre-industrial level of methane

These revisions were applied incrementally so that the impact of each revision could be evaluated separately.

4. Revised Standard Simulation

The revised natural components listed above were applied to the "Current Standard" simulation. The results from the standard and revised simulations were compared and evaluated against 2002 observations.

2. EVALUATION OF REVISED NATURAL COMPONENTS

2.1. Dimethyl Sulfide (DMS) and Methyl Sulfonic Acid (MSA) from Ocean

Oceanic dimethyl sulfide (DMS) and Methyl sulfonic acid (MSA) are important natural sources of sulfur to the atmosphere and contributes to sulfate aerosol formation and growth in the atmosphere. In the CMAQ model, their emissions are treated as sulfate and are speciated from sea salt emissions. CMAQ version 4.5 was the first release to include sea salt aerosols which were implemented in the AERO4 aerosol module. The emissions of sea salt aerosols from the open ocean are calculated based on wind speed and relative humidity (Shankar et al., 2005). In the AERO4 module, sulfate is speciated from the sea salt aerosols using a mass ratio of 0.0755.

For the emissions of DMS and MSA outside of the US modeling domain, their effects need to be represented by the boundary conditions (BCs). However, the GEOS-CHEM BCs used for the previous WRAP CMAQ modeling did not include DMS and MSA from the GEOS-CHEM outputs. For the revised simulations, we mapped the GEOS-CHEM DMS and MSA to sulfur dioxide (SO_2) and sulfate (SO_4) in the CMAQ BCs, respectively.

Figure 2-1 shows changes in annual and quarterly averages of ozone concentrations due to added sulfur in the BCs. An increase in SO_2 can lead to higher ozone because SO_2 reacts with hydroxyl radical ($OH\cdot$) to produce hydroperoxy radical ($HO_2\cdot$) in the atmosphere (similar to CO). This effect can be seen in summer when oxidant concentrations are higher. In winter, ozone is decreased because SO_2 reacts with ozone in the aqueous phase to form sulfate. However, the magnitudes of the ozone changes are very small (less than 0.1 ppb).

Increases in sulfate due to DMS/MSA are less than 0.1 $\mu g/m^3$ in most inland area (Figure 2-2). The largest increase is seen in the northwestern corner of the modeling domain in summer, but little is transported inland. In winter months, sulfate concentrations in the Eastern US increase slightly.

Figure 2-3 shows extra chloride due to DMS/MSA. As sulfate increases, particulate chloride decreases because chloride in sea salt (sodium chloride) is replaced by sulfate and evaporates into the gas-phase as hydrogen chloride (HCl). Comparing Figure 2-3 with Figure 2-2, it can be noted that regions of chloride decreases match well with those of sulfate increases. However, it is not clear why the chloride concentrations (and sodium as seen in Figure 2-4) increase in the northeastern part of the modeling domain in winter with the updated BCs.

Inclusion of DMS and MSA in the BCs results in slight increases in the $PM_{2.5}$ concentrations in winter mostly due to increases in sodium and chloride (Figure 2-5).

(a) annual average O_3 (base case)

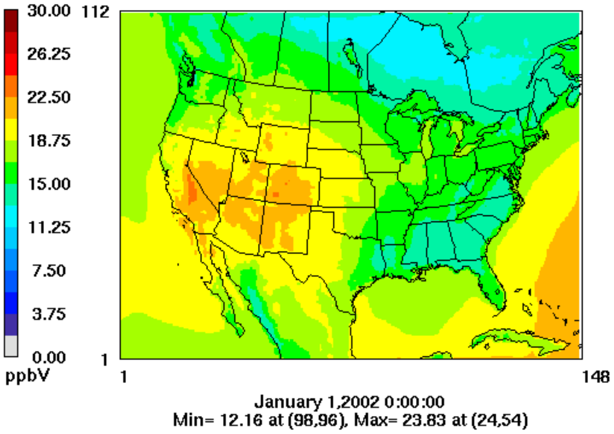

(b) changes in annual average O_3

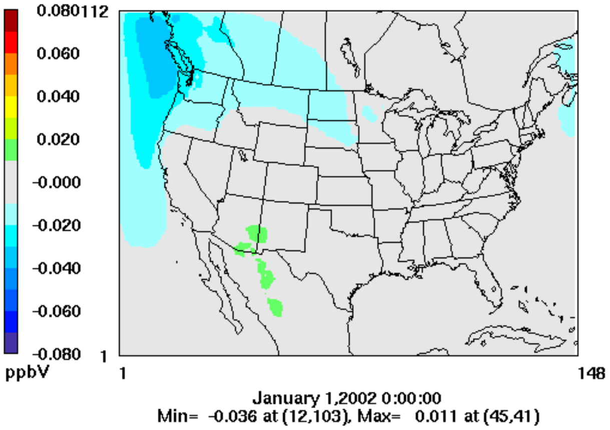

(c) quarterly average O_3 (base – Q1)

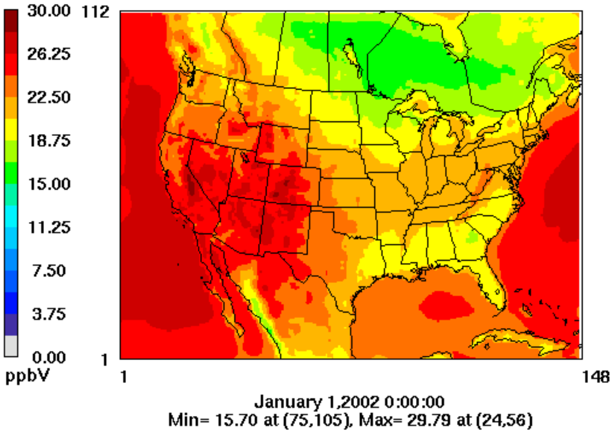

(d) changes in quarterly average O_3 (Q1)

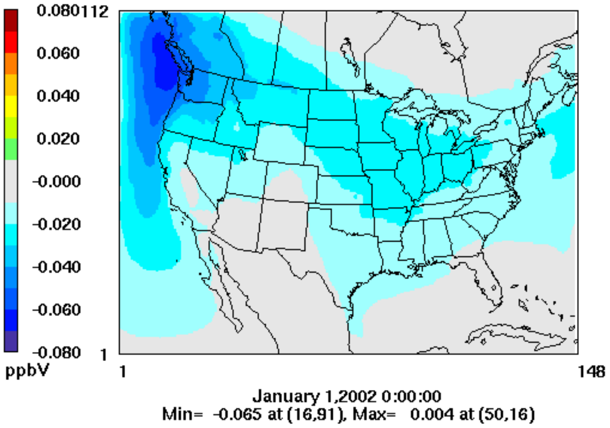

(e) quarterly average O_3 (base – Q2)

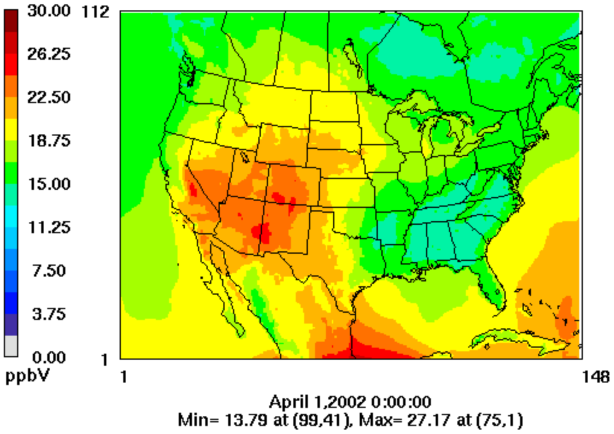

(f) changes in quarterly average O_3 (Q2)

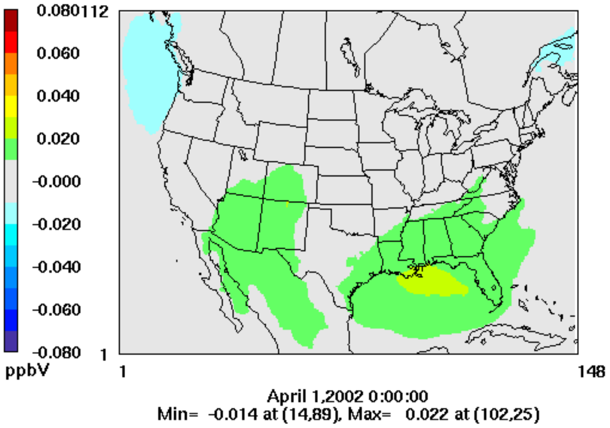

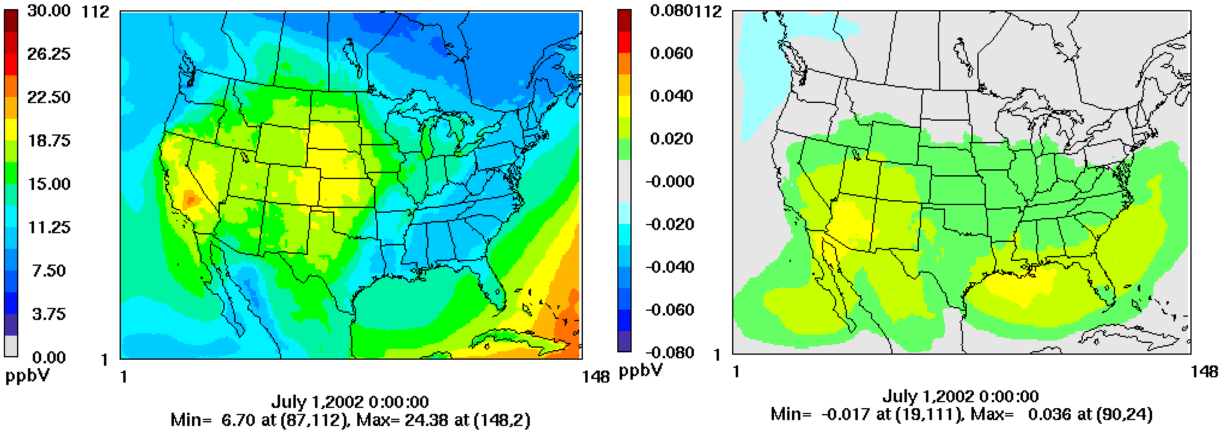

(g) quarterly average O_3 (base – Q3)

(h) changes in quarterly average O_3 (Q3)

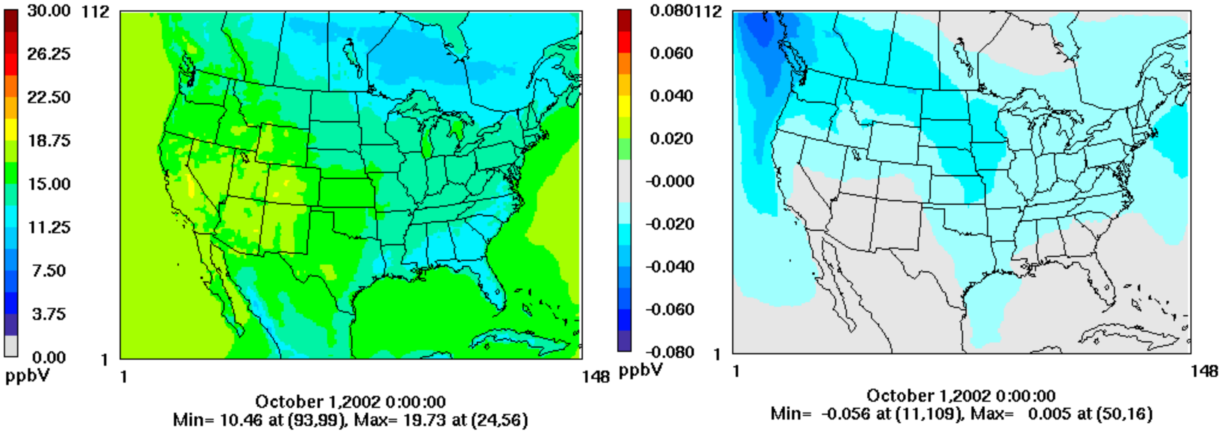

(i) quarterly average O_3 (base – Q4)

(j) changes in quarterly average O_3 (Q4)

Figure 2-1. Impact of oceanic DMS/MSA on ozone. The concentration changes are given as ozone from the new case (simulation with DMS/MSA) minus ozone from the base case (simulation before DMS/MSA is added).

(a) annual average ASO4 (base case)

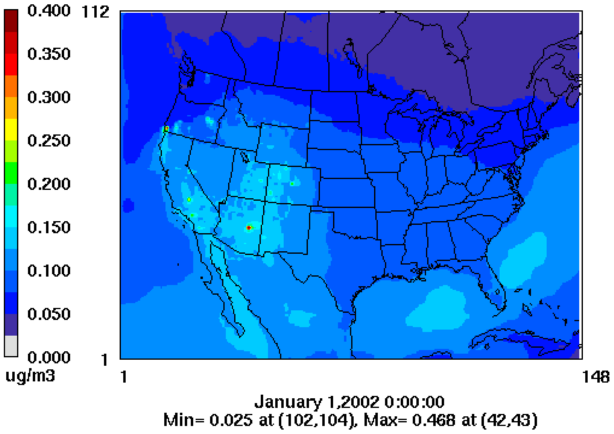

(b) changes in annual average ASO4

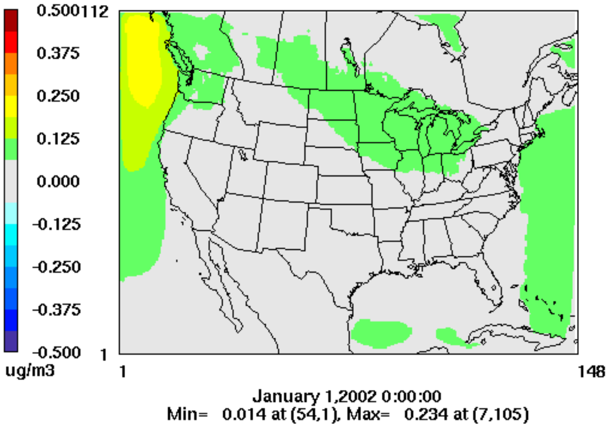

(c) quarterly average ASO4 (base – Q1)

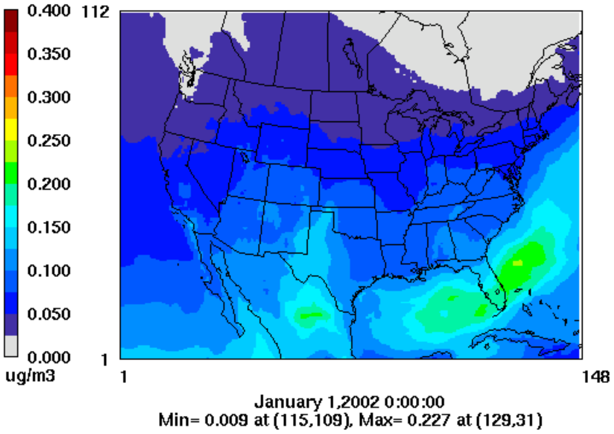

(d) changes in quarterly average ASO4 (Q1)

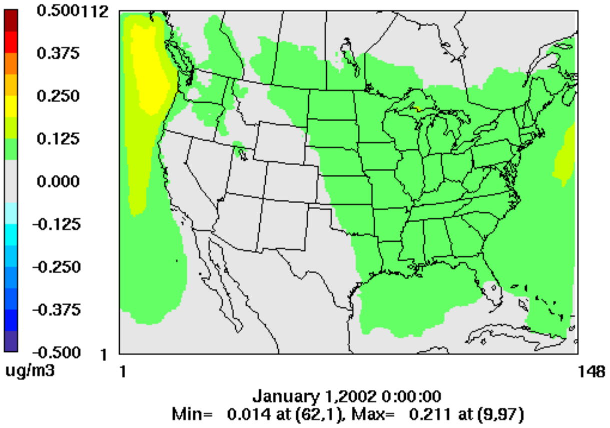

(e) quarterly average ASO4 (base – Q2)

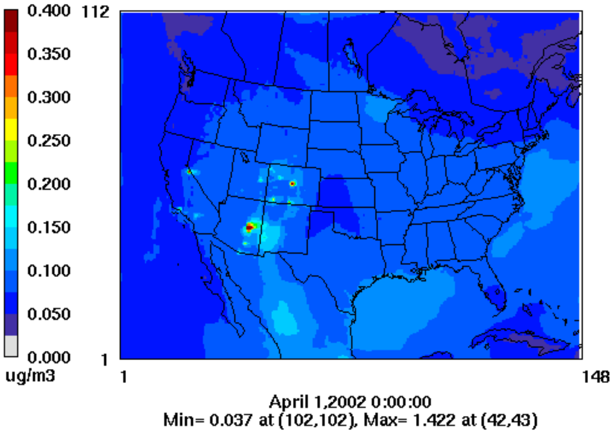

(f) changes in quarterly average ASO4 (Q2)

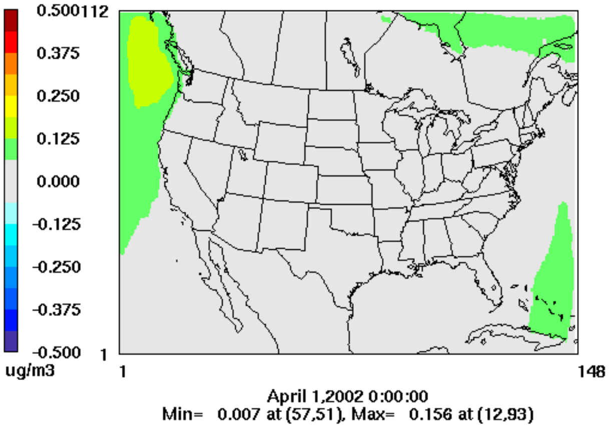

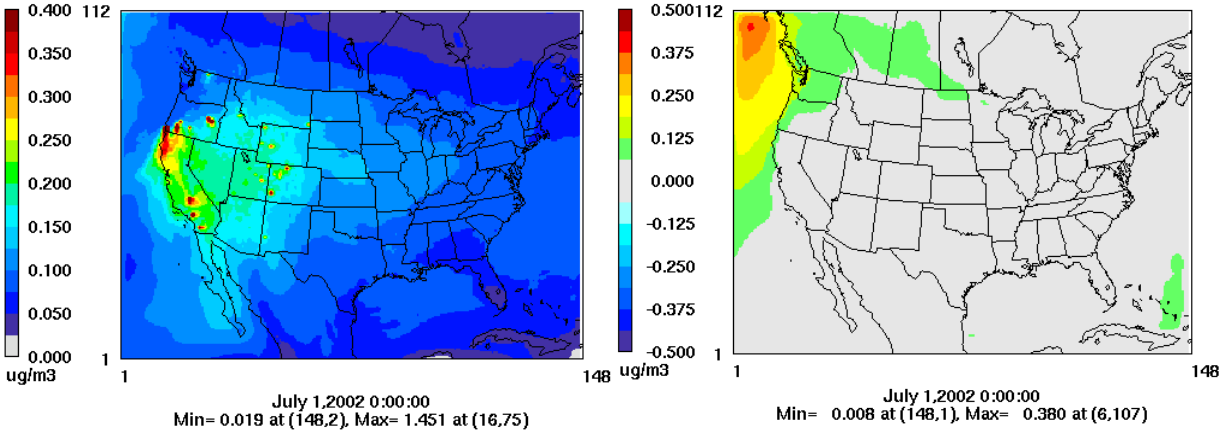

(g) quarterly average ASO4 (base – Q3)

(h) changes in quarterly average ASO4 (Q3)

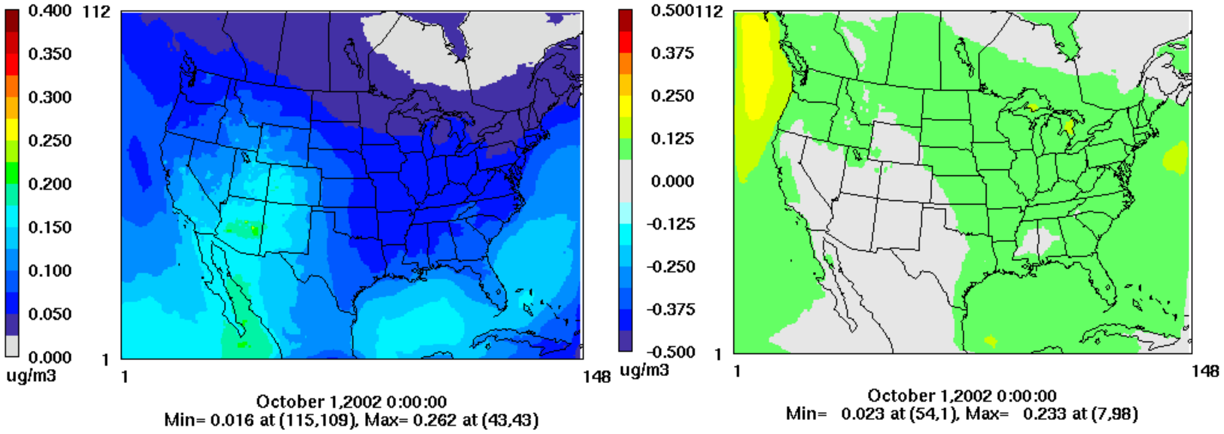

(i) quarterly average ASO4 (base – Q4)

(j) changes in quarterly average ASO4 (Q4)

Figure 2-2. Impact of oceanic DMS/MSA on fine sulfate (ASO4). The concentration changes are given as ASO4 from the new case (simulation with DMS/MSA) minus ASO4 from the base case (simulation before DMS/MSA is added).

(a) annual average ACL (base case)

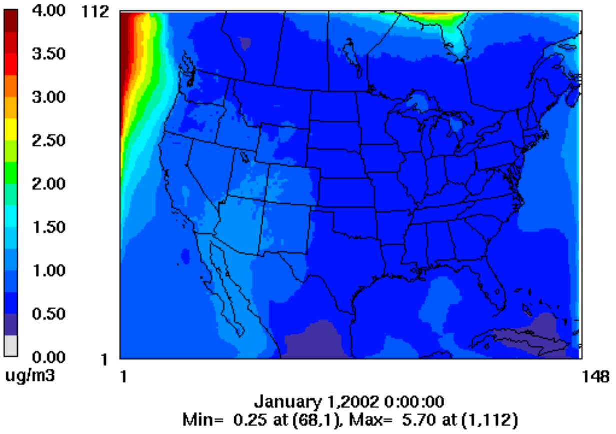

(b) changes in annual average ACL

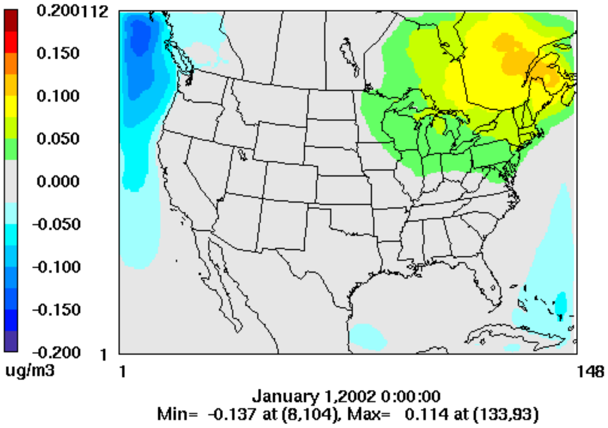

(c) quarterly average ACL (base – Q1)

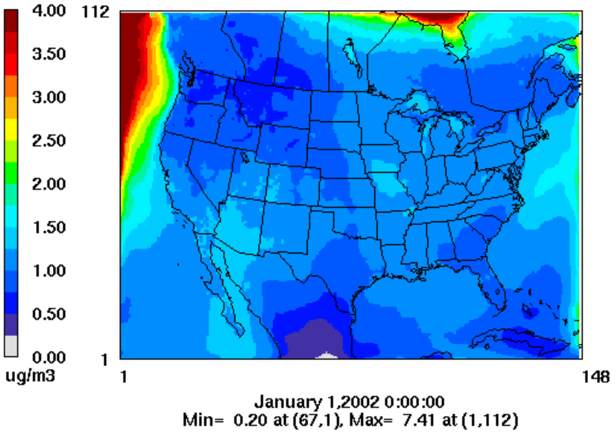

(d) changes in quarterly average ACL (Q1)

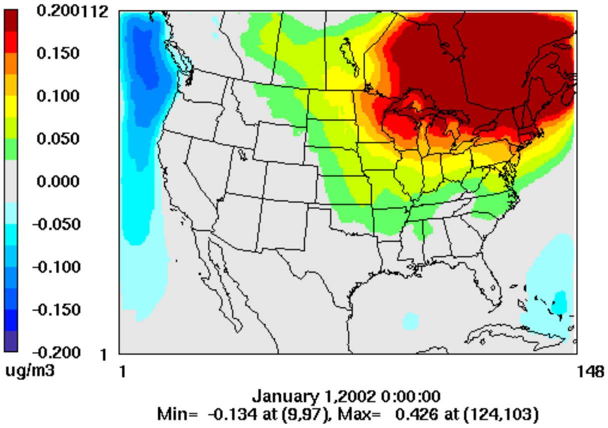

(e) quarterly average ACL (base – Q2)

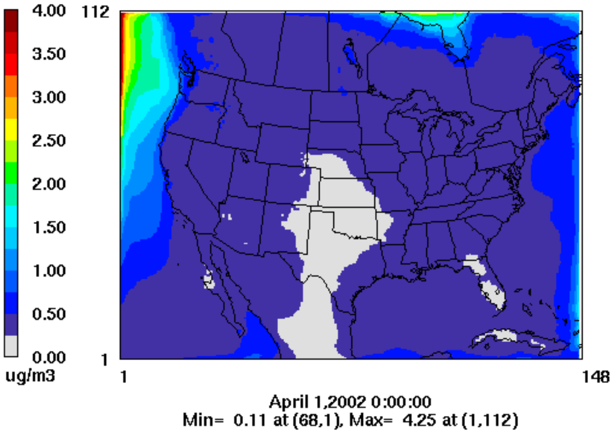

(f) changes in quarterly average ACL (Q2)

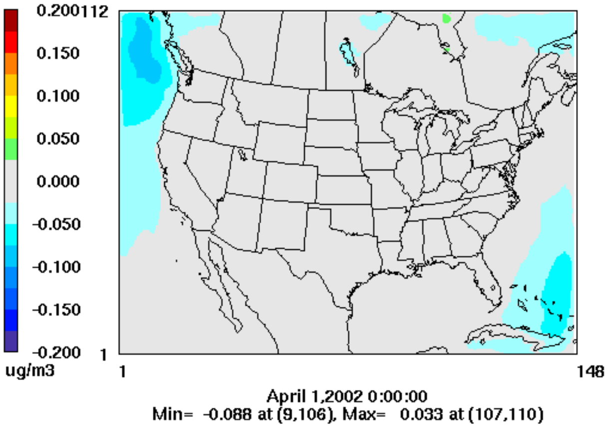

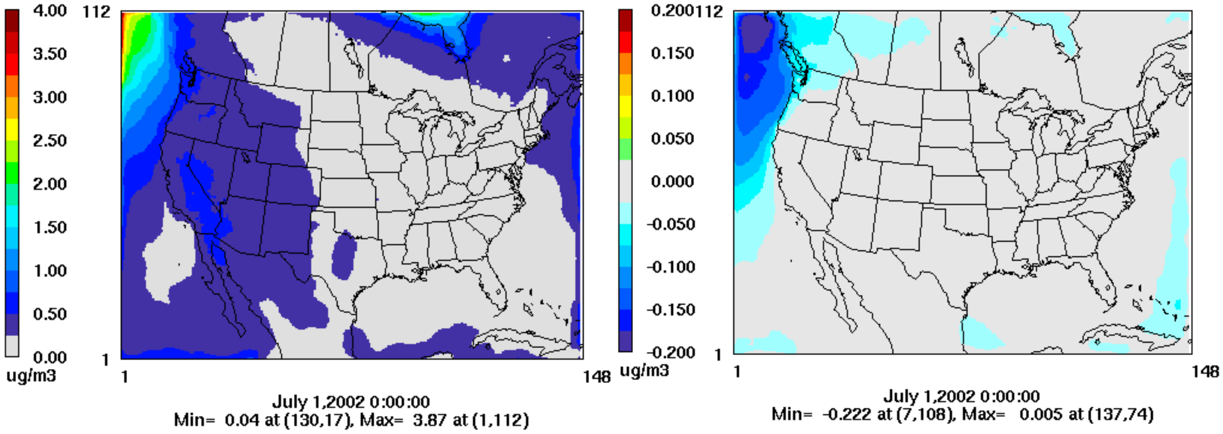
(g) quarterly average ACL (base – Q3)

(h) changes in quarterly average ACL (Q3)

(i) quarterly average ACL (base – Q4)

(j) changes in quarterly average ACL (Q4)

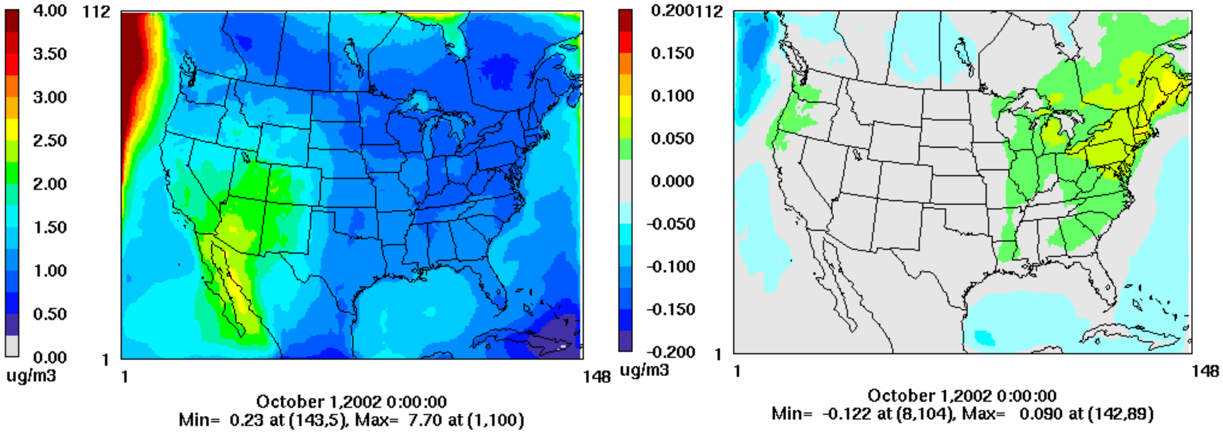

Figure 2-3. Impact of oceanic DMS/MSA on fine chloride (ACL). The concentration changes are given as ACL from the new case (simulation with DMS/MSA) minus ACL from the base case (simulation before DMS/MSA is added).

(a) annual average ANA (base case)

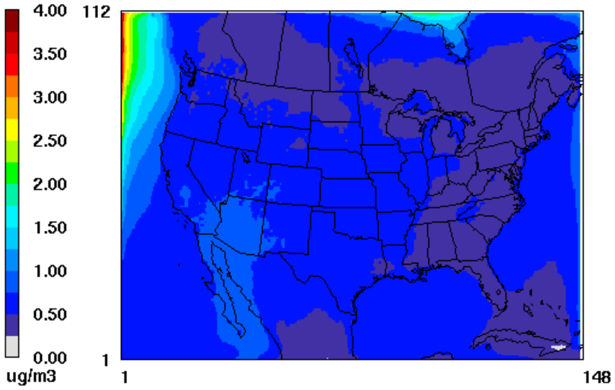

January 1,2002 0:00:00
Min= 0.23 at (142,5), Max= 3.78 at (1,112)

(b) changes in annual average ANA

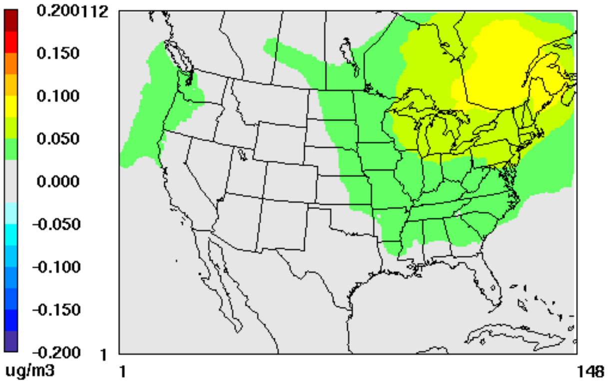

January 1,2002 0:00:00
Min= 0.003 at (148,10), Max= 0.097 at (133,93)

(c) quarterly average ANA (base – Q1)

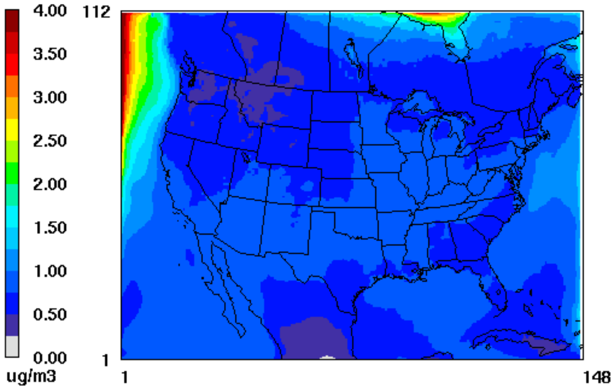

January 1,2002 0:00:00
Min= 0.21 at (67,1), Max= 4.89 at (1,112)

(d) changes in quarterly average ANA (Q1)

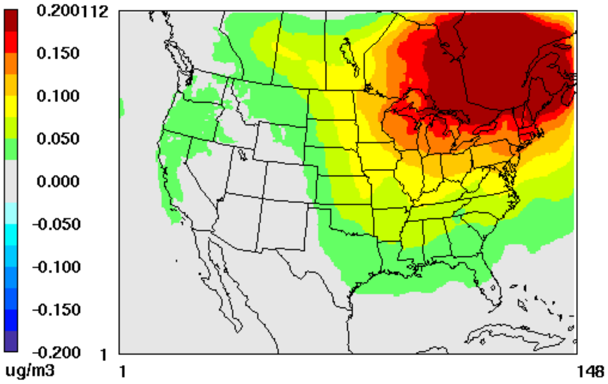

January 1,2002 0:00:00
Min= -0.003 at (1,112), Max= 0.302 at (133,93)

(e) quarterly average ANA (base – Q2)

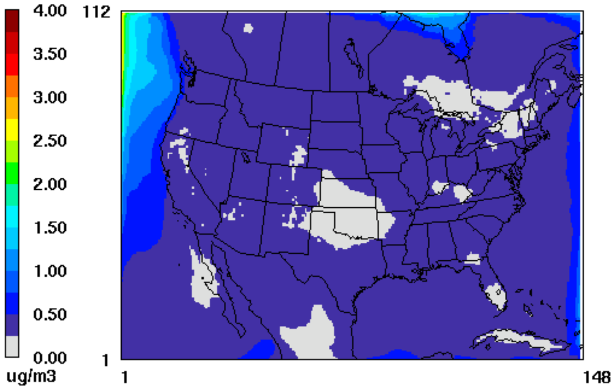

April 1,2002 0:00:00
Min= 0.19 at (64,7), Max= 2.82 at (1,112)

(f) changes in quarterly average ANA (Q2)

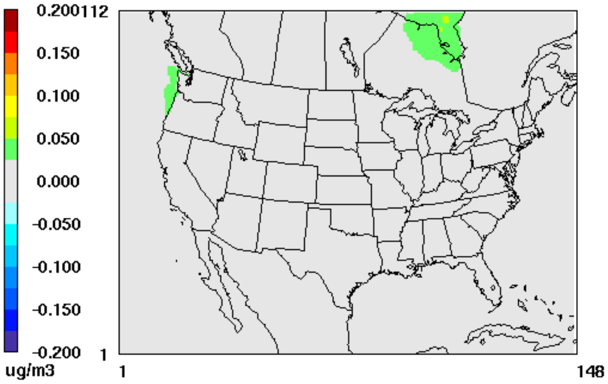

April 1,2002 0:00:00
Min= 0.001 at (57,51), Max= 0.053 at (106,110)

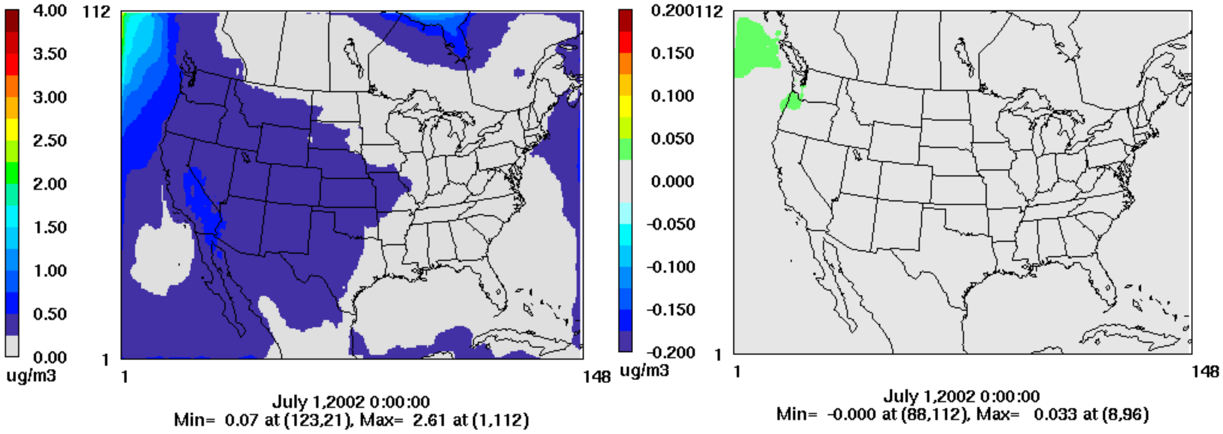

(g) quarterly average ANA (base – Q3)

(h) changes in quarterly average ANA (Q3)

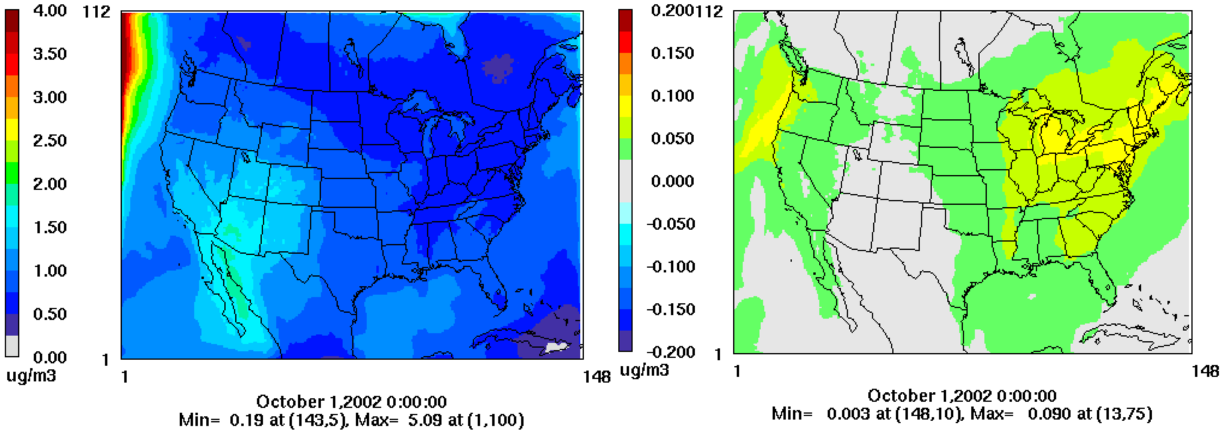

(i) quarterly average ANA (base – Q4)

(j) changes in quarterly average ANA (Q4)

Figure 2-4. Impact of oceanic DMS/MSA on fine sodium (ANA). The concentration changes are given as ANA from the new case (simulation with DMS/MSA) minus ANA from the base case (simulation before DMS/MSA is added).

(a) annual average $PM_{2.5}$ (base case)

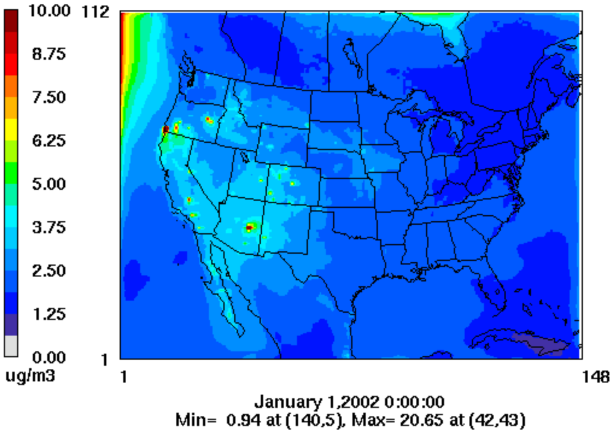

(b) changes in annual average $PM_{2.5}$

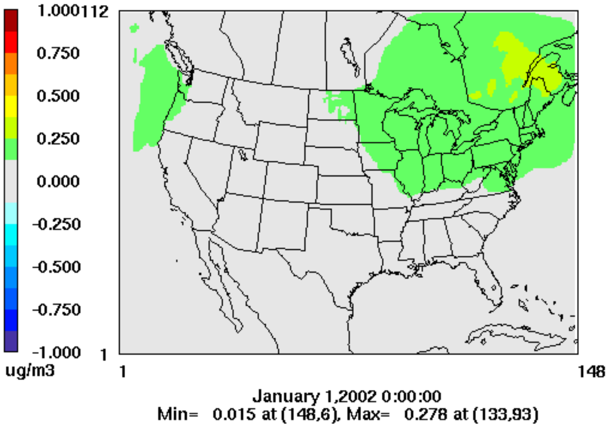

(c) quarterly average $PM_{2.5}$ (base – Q1)

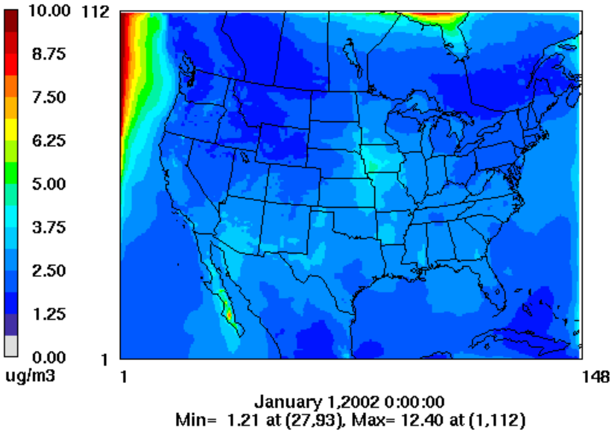

(d) changes in quarterly average $PM_{2.5}$ (Q1)

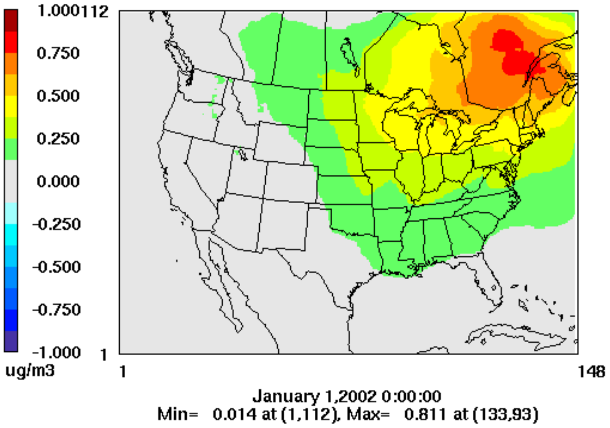

(e) quarterly average $PM_{2.5}$ (base – Q2)

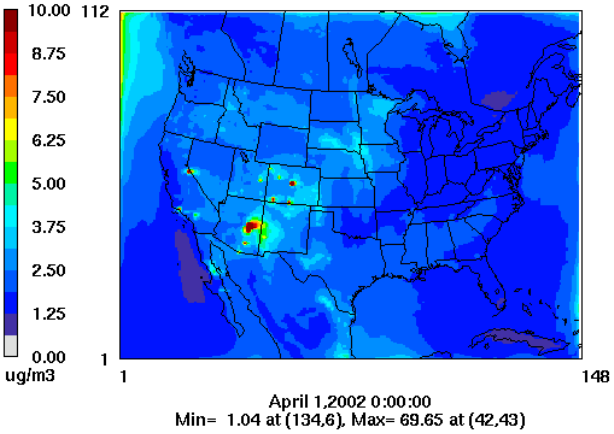

(f) changes in quarterly average $PM_{2.5}$ (Q2)

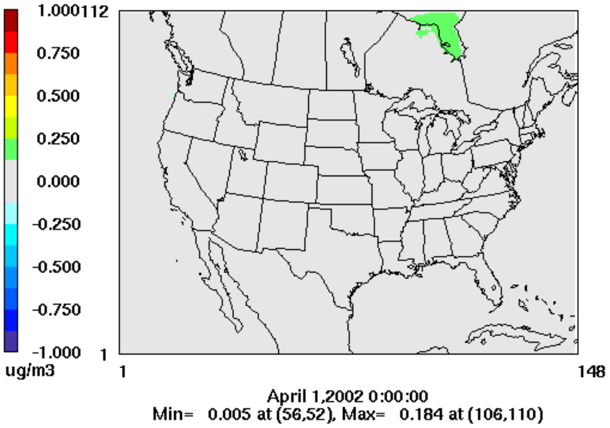

(g) quarterly average $PM_{2.5}$ (base – Q3) (h) changes in quarterly average $PM_{2.5}$ (Q3)

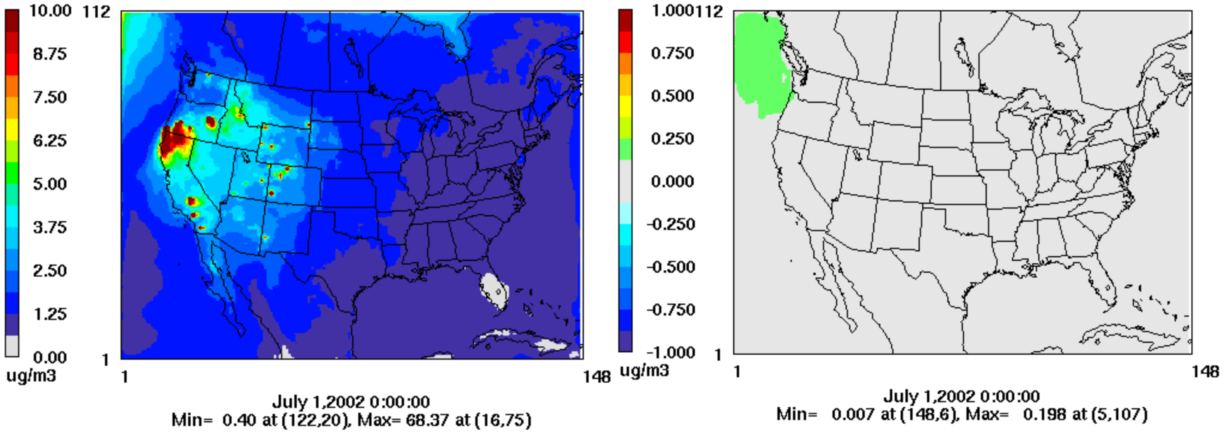

(i) quarterly average $PM_{2.5}$ (base – Q4) (j) changes in quarterly average $PM_{2.5}$ (Q4)

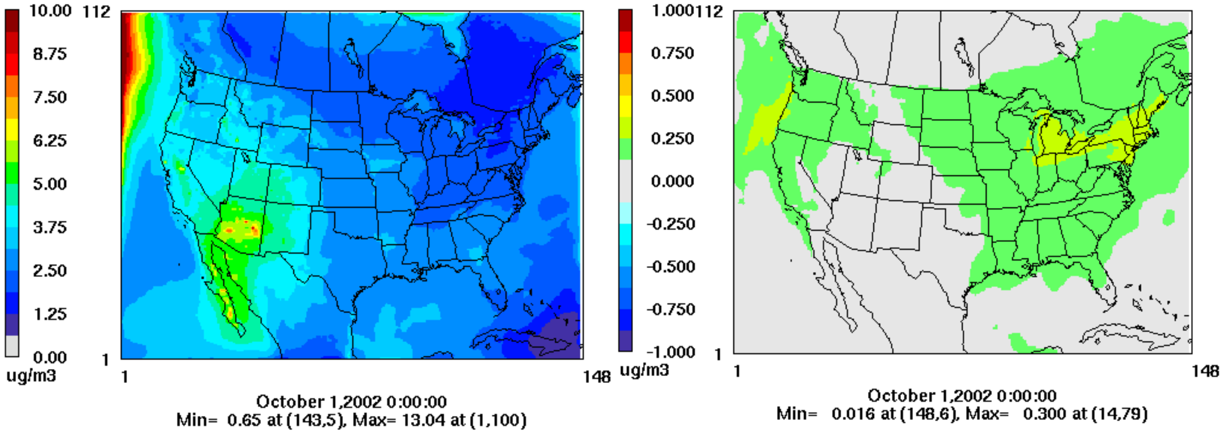

Figure 2-5. Impact of oceanic DMS/MSA on $PM_{2.5}$. The concentration changes are given as $PM_{2.5}$ from the new case (simulation with DMS/MSA) minus $PM_{2.5}$ from the base case (simulation before DMS/MSA is added).

2.2. NOx from Lightning

Orville et al. (2002) estimated about 30 million flashes per year for North America cloud-to-ground lightning. Using a multiplier of 2.8 to get intracloud flashes (Boccippio et al., 2001), we estimate a total of 114 million flashes per year. Using the upper bound NOx emissions per flash estimate of 9.3 Kg N per flash from the EULINOX study (Holler and Schumann, 2000), we obtained 1.06 Tg N per year for North America. This high-end estimate of annual total lightning NOx emissions was then spatially and temporally allocated to the modeling grid cells based on the amount of convective precipitation activity in each cell. We have developed a lightning NOx emissions processor that determines the allocation using MM5 convective precipitation as a proxy for lightning activity. The hourly and gridded 3-D lightning NOx emissions are calculated as follows:

$$E(\bar{x},t) = R_{NO} P_c(\bar{x},t) D(\bar{x},t) p'(\bar{x},t)$$

where:

$E(\bar{x},t)$	NO emission rate (mol hr^{-1}) at time t and grid location $\bar{x}$
R_{NO}	NO resistance factor (s m^{-1})
$P_c(\bar{x},t)$	convective precipitation (m) at time t and grid location $\bar{x}$
$D(\bar{x},t)$	convective cloud depth (m) at time t and grid location $\bar{x}$
$p'(\bar{x},t)$	perturbation pressure (Pa) at time t and grid location $\bar{x}$

Setting $\sum E(\bar{x},t)$ to 1.06 Tg N yr^{-1} returns a value of R_{NO} equal to 3.9 x 10^{-12} s m^{-1}, which was then subsequently used by the processor generate the hourly and gridded lightning NOx emissions for the 2002 year.

Figure 2-6 is a vertical profile plot of the WRAP domain average lightning NOx emissions, averaged hourly over January and July 2002. Lightning NOx emission rates are higher in July due to much stronger and widespread convective activity. Figure 2-7 shows spatial plots of the total vertical column lightning NOx emissions, averaged hourly over January and July 2002.

Adding lightning NOx emissions resulted in significant increases in ozone concentration over southeastern US in summer where biogenic VOC emissions are high and convective activity is strong (Figure 2-8). Increases in the NOx emissions also lead to more nitrate formation (Figure 2-9). However, excess nitrate will replace chloride in sea salt (similar to sulfate replacing chloride) resulting in less chloride in particle phase (Figure 2-10). Figure 2-11 shows that the concentration of total PM$_{2.5}$ is slightly increased with lightning NOx emissions. Note that we have used a high-end estimate of lightning NOx emissions. Therefore, these concentration changes should be regarded as upper bound values.

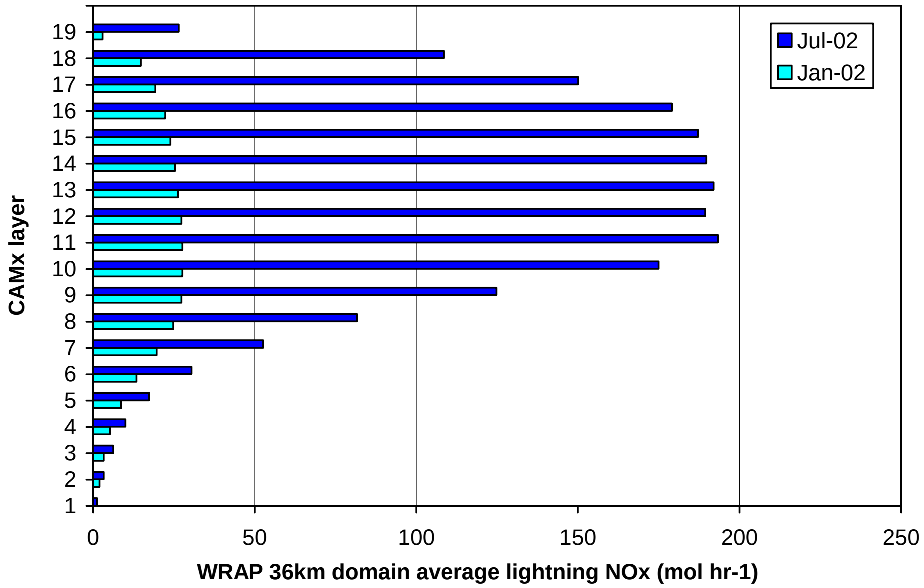

Figure 2-6. Vertical profile of the WRAP domain average lightning NOx emissions, averaged over the months of January and July, 2002.

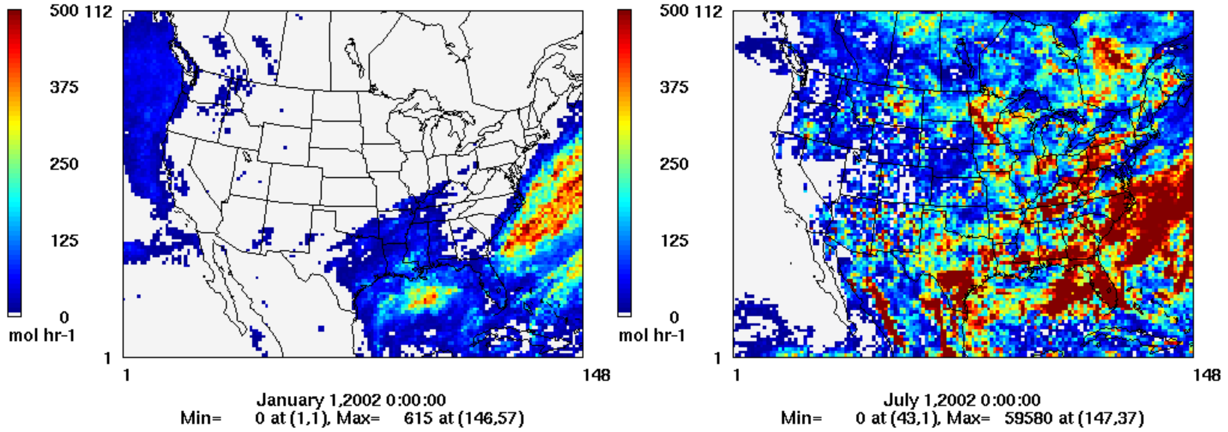
(a) January 2002

(b) July 2002

Figure 2-7. Spatial plots of the total vertical column lightning NOx emissions, averaged over the months of January and July, 2002.

(a) annual average O_3 (base case)

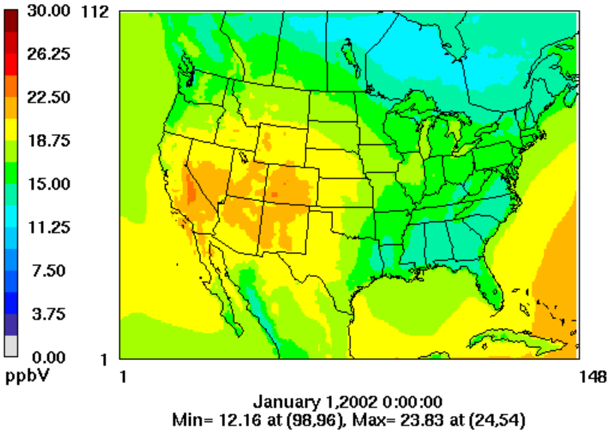

(b) changes in annual average O_3

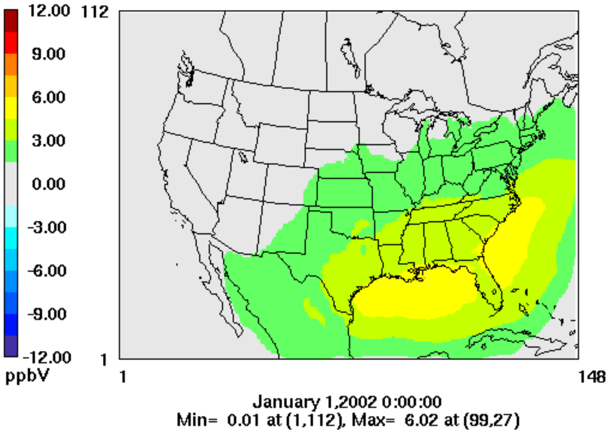

(c) quarterly average O_3 (base – Q1)

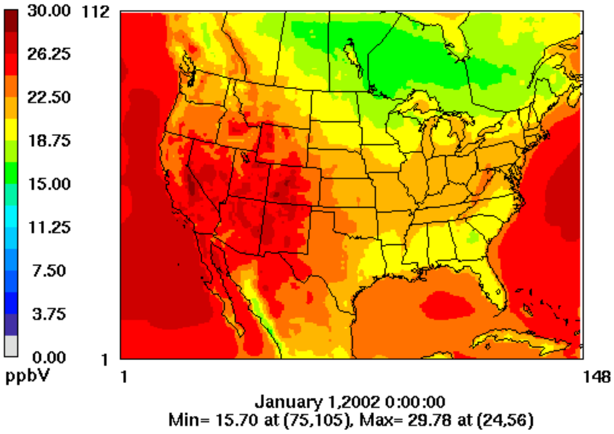

(d) changes in quarterly average O_3 (Q1)

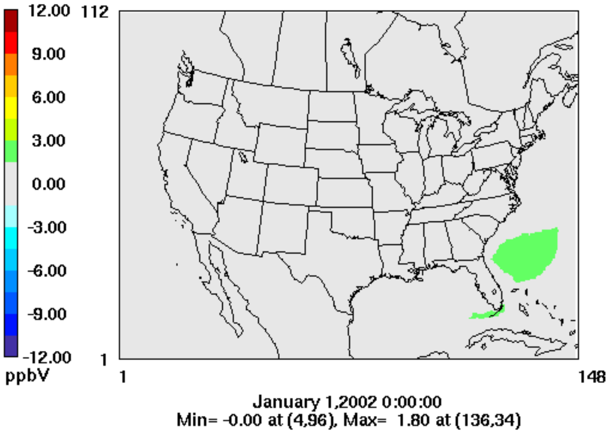

(e) quarterly average O_3 (base – Q2)

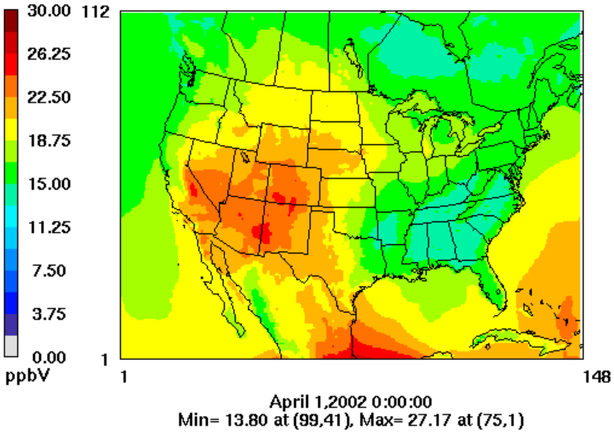

(f) changes in quarterly average O_3 (Q2)

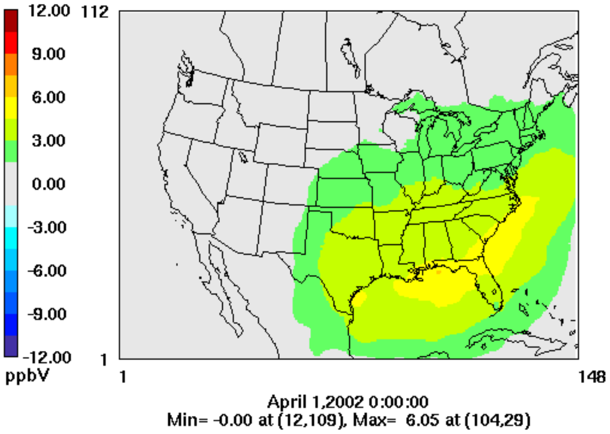

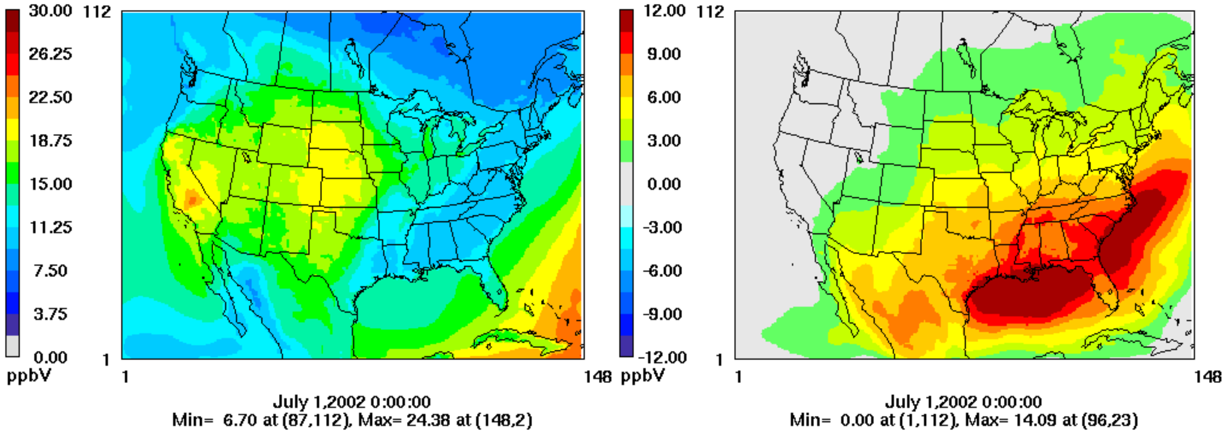
(g) quarterly average O_3 (base – Q3)

(h) changes in quarterly average O_3 (Q3)

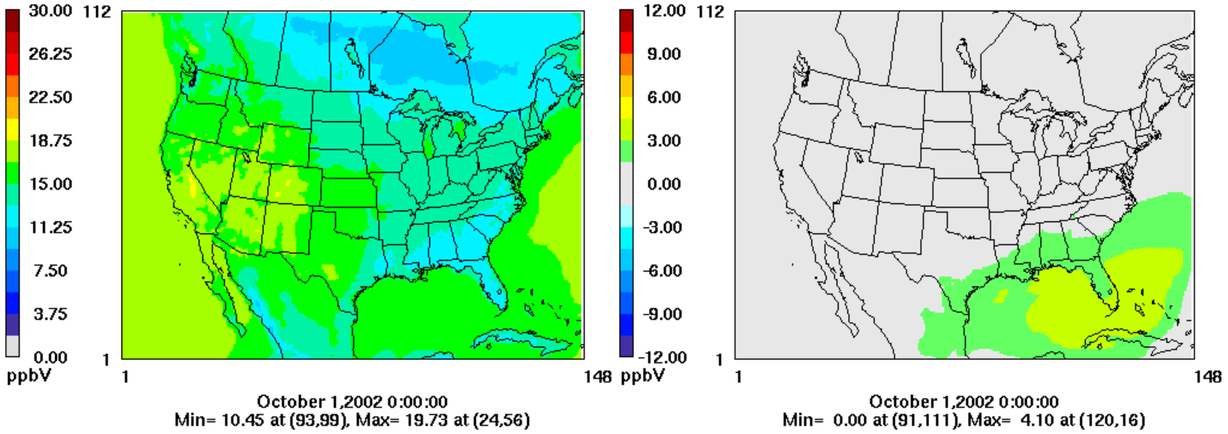
(i) quarterly average O_3 (base – Q4)

(j) changes in quarterly average O_3 (Q4)

Figure 2-8. Impact of lightning NOx emissions on ozone. The concentration changes are given as ozone from the new case (simulation with lightning NOx) minus ozone from the base case (simulation before lightning NOx is added).

(a) annual average ANO3 (base case)

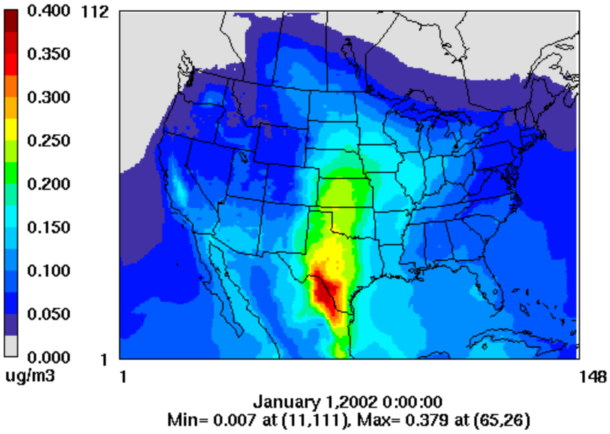

(b) changes in annual average ANO3

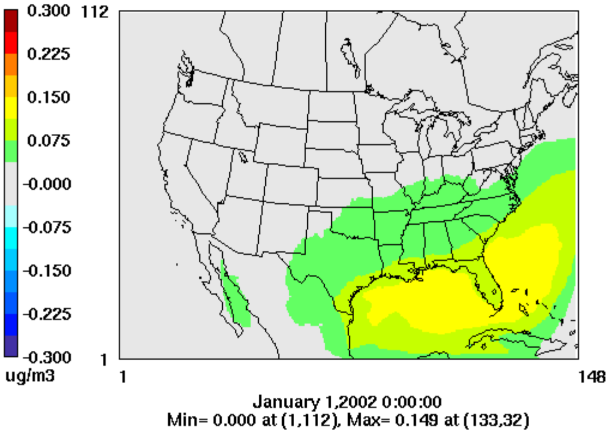

(c) quarterly average ANO3 (base – Q1)

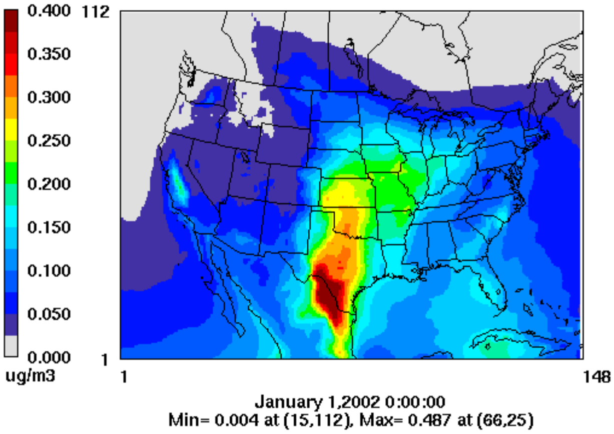

(d) changes in quarterly average ANO3 (Q1)

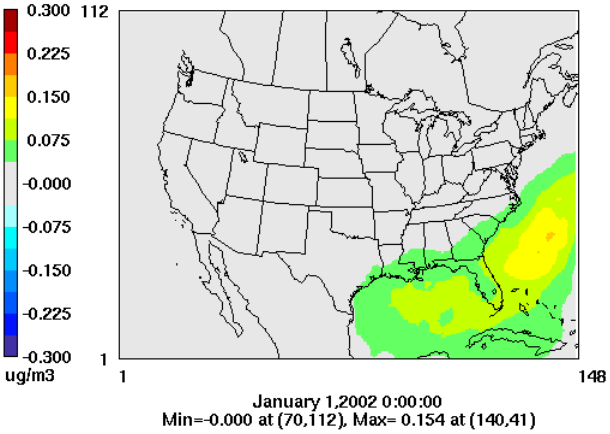

(e) quarterly average ANO3 (base – Q2)

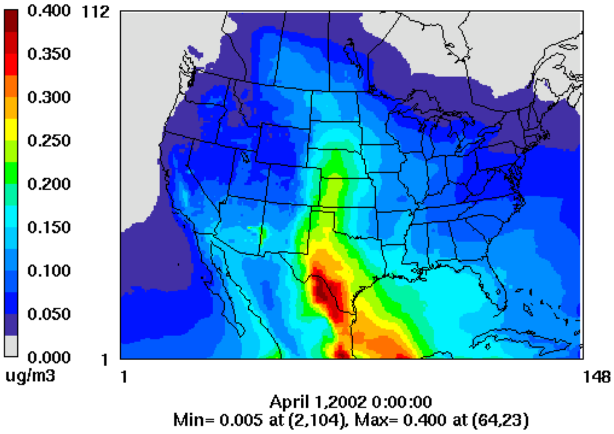

(f) changes in quarterly average ANO3 (Q2)

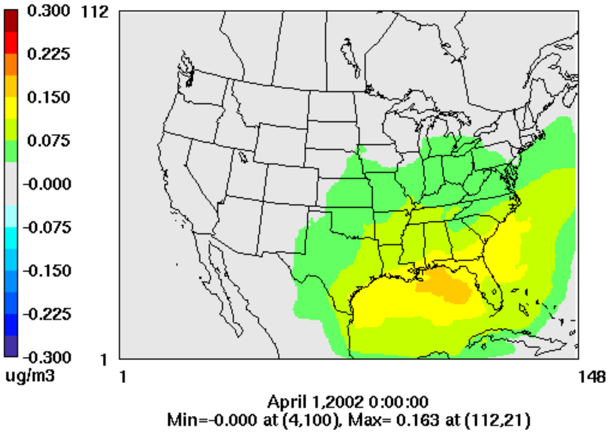

(g) quarterly average ANO3 (base – Q3) (h) changes in quarterly average ANO3 (Q3)

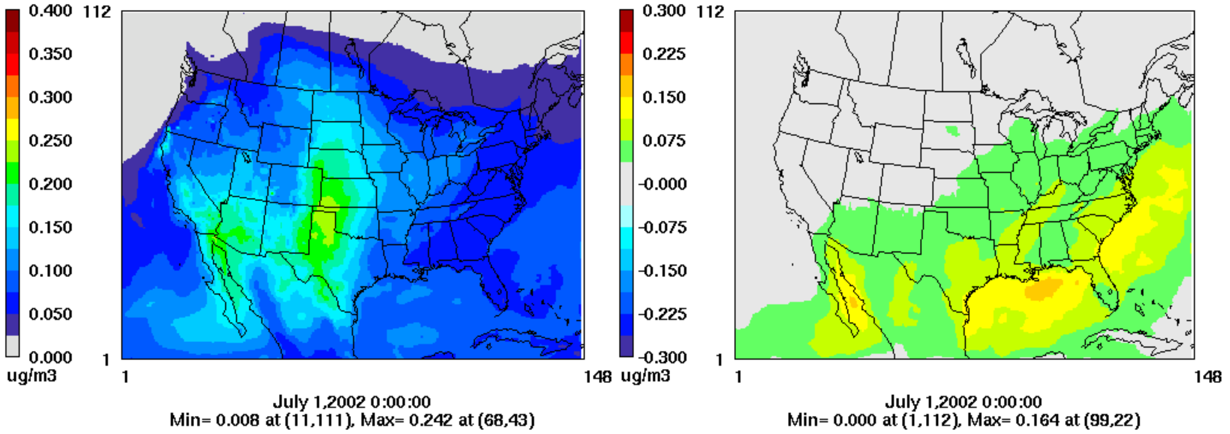

(i) quarterly average ANO3 (base – Q4) (j) changes in quarterly average ANO3 (Q4)

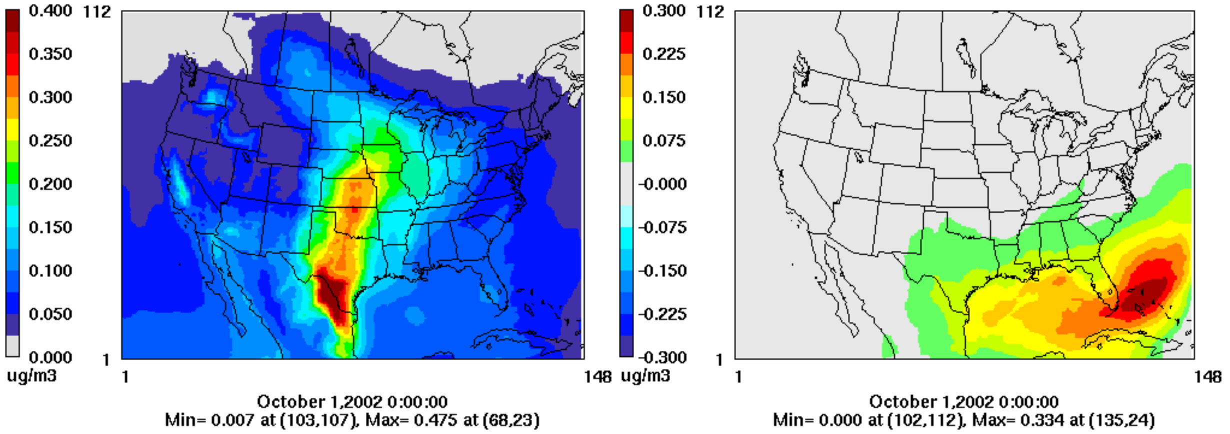

Figure 2-9. Impact of lightning NOx emissions on fine nitrate (ANO3). The concentration changes are given as ANO3 from the new case (simulation with lightning NOx) minus ANO3 from the base case (simulation before lightning NOx is added).

(a) annual average ACL (base case)

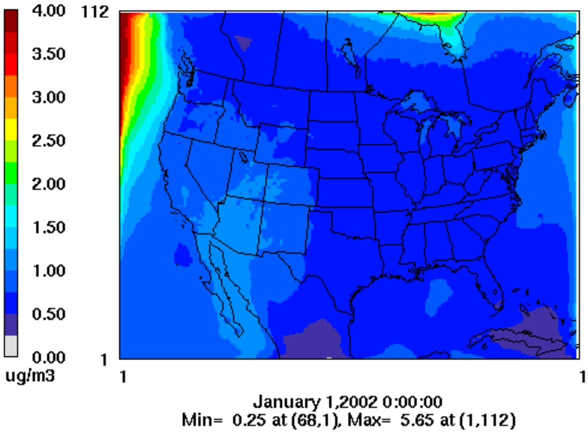

(b) changes in annual average ACL

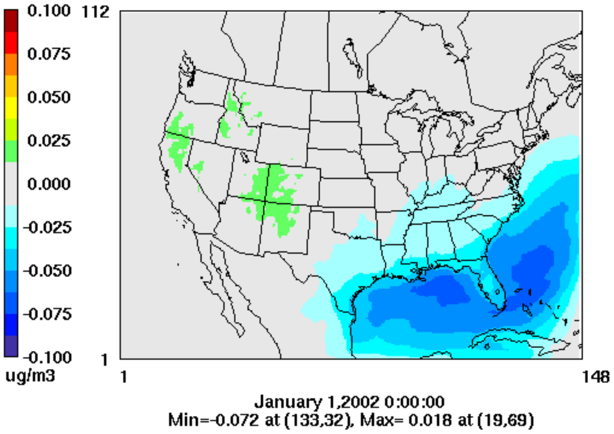

(c) quarterly average ACL (base – Q1)

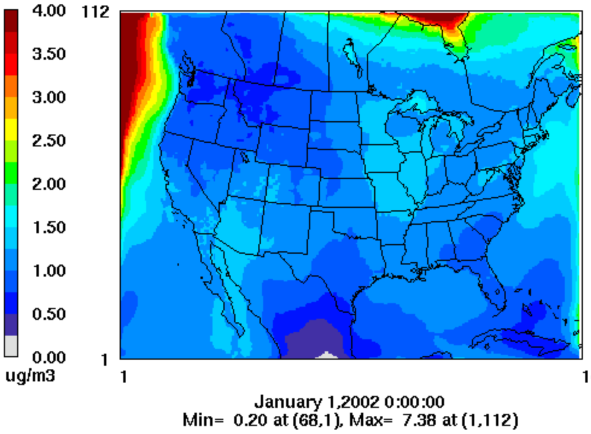

(d) changes in quarterly average ACL (Q1)

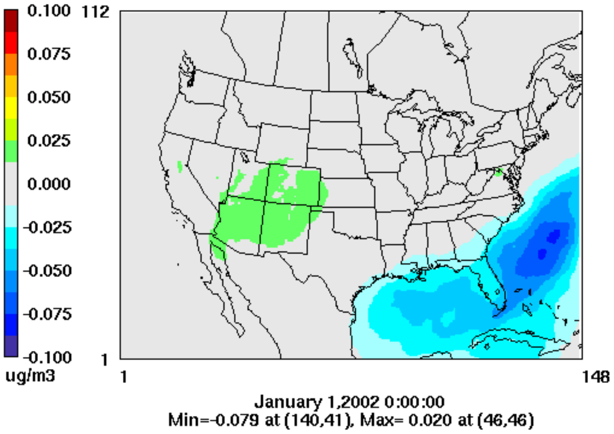

(e) quarterly average ACL (base – Q2)

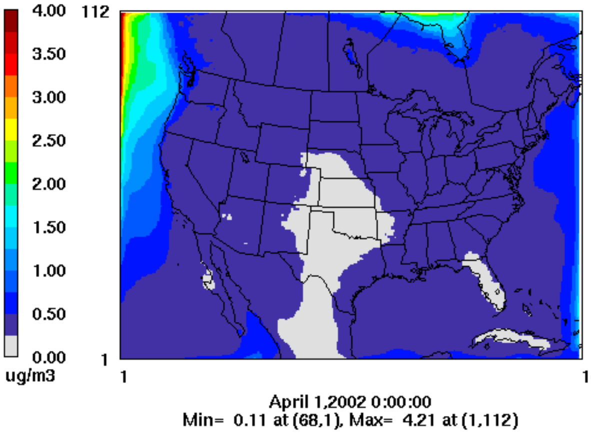

(f) changes in quarterly average ACL (Q2)

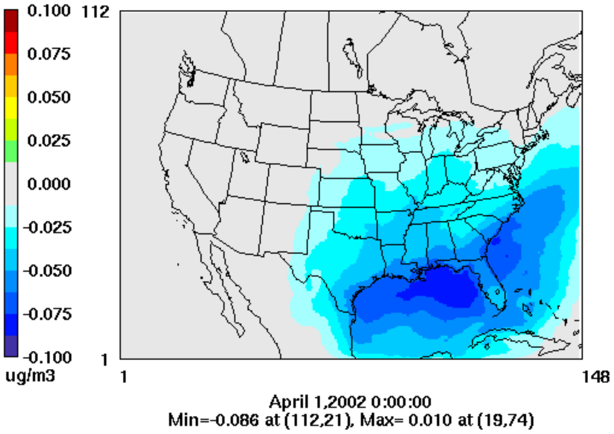

(g) quarterly average ACL (base – Q3) (h) changes in quarterly average ACL (Q3)

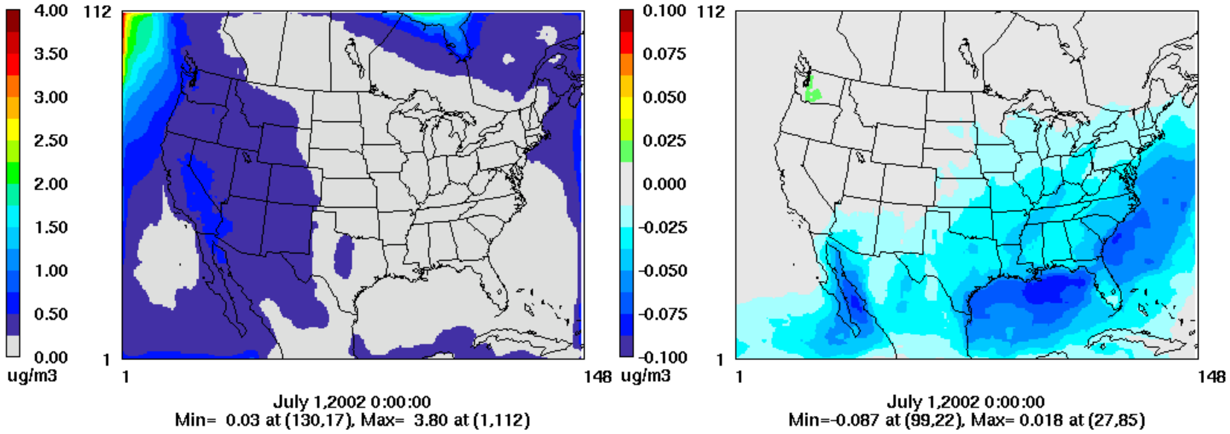

(i) quarterly average ACL (base – Q4) (j) changes in quarterly average ACL (Q4)

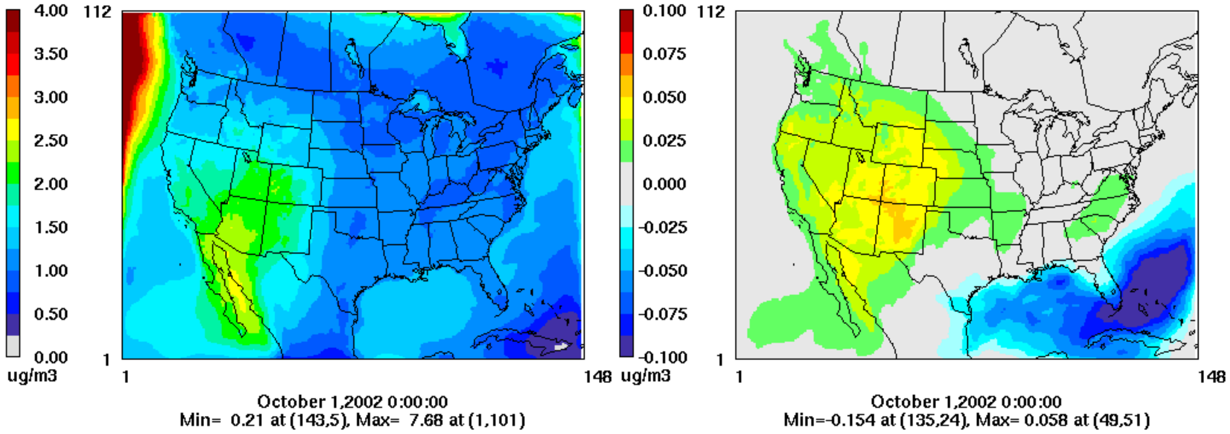

Figure 2-10. Impact of lightning NOx emissions on fine chloride (ACL). The concentration changes are given as ACL from the new case (simulation with lightning NOx) minus ACL from the base case (simulation before lightning NOx is added).

(a) annual average $PM_{2.5}$ (base case) (b) changes in annual average $PM_{2.5}$

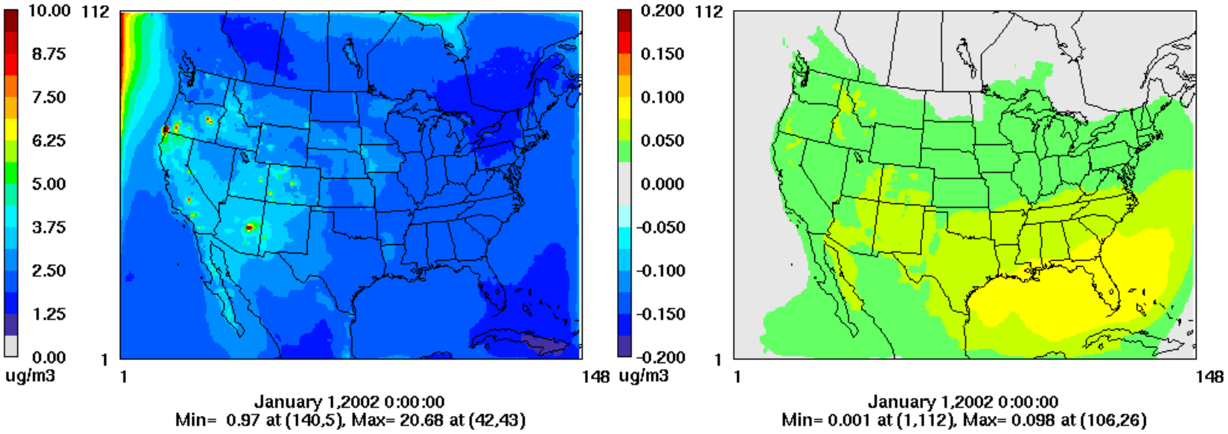

(c) quarterly average $PM_{2.5}$ (base – Q1) (d) changes in quarterly average $PM_{2.5}$ (Q1)

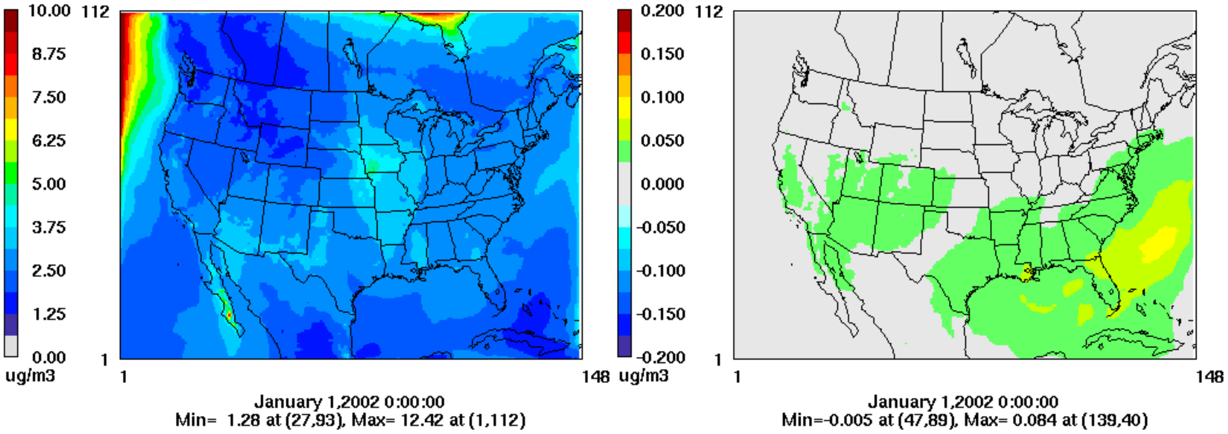

(e) quarterly average $PM_{2.5}$ (base – Q2) (f) changes in quarterly average $PM_{2.5}$ (Q2)

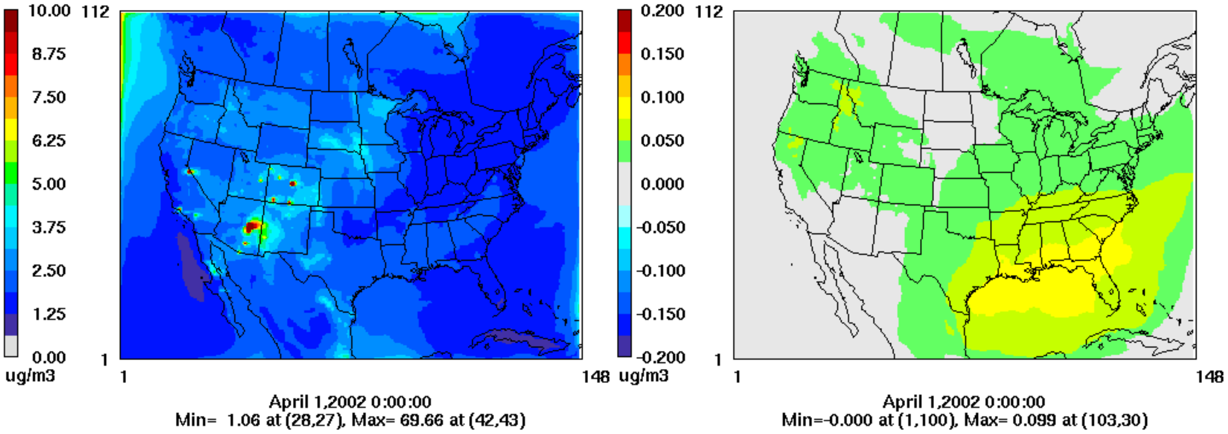

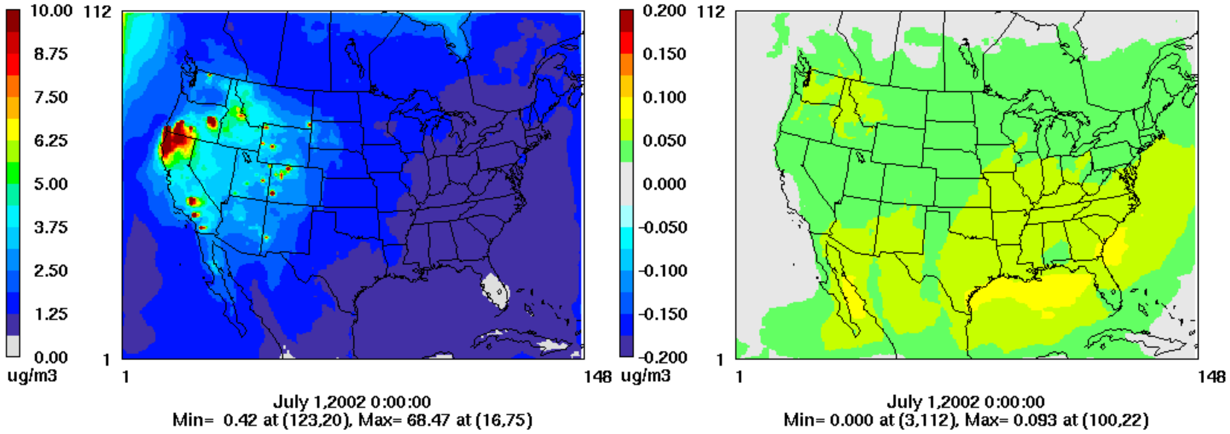

(g) quarterly average $PM_{2.5}$ (base – Q3)

(h) changes in quarterly average $PM_{2.5}$ (Q3)

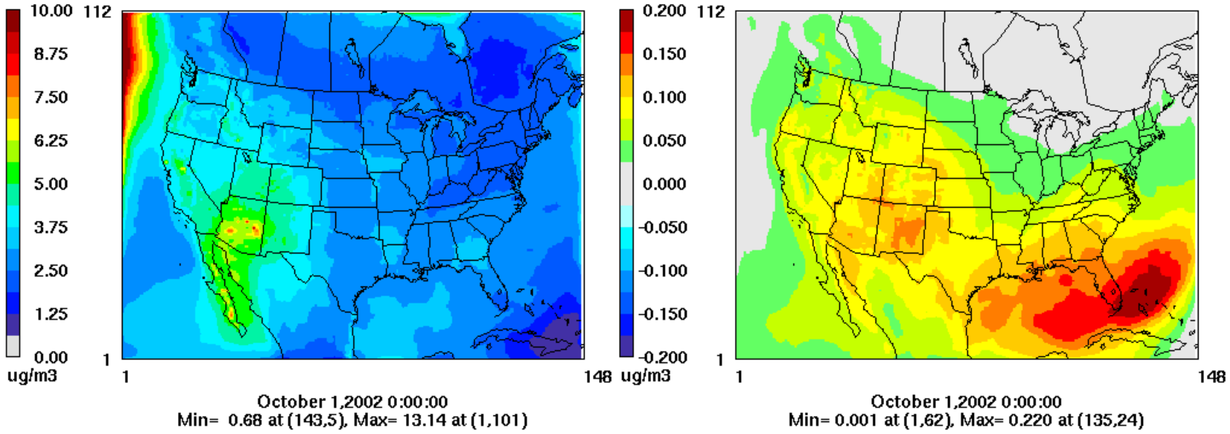

(i) quarterly average $PM_{2.5}$ (base – Q4)

(j) changes in quarterly average $PM_{2.5}$ (Q4)

Figure 2-11. Impact of lightning NOx emissions on $PM_{2.5}$. The concentration changes are given as $PM_{2.5}$ from the new case (simulation with lightning NOx) minus $PM_{2.5}$ from the base case (simulation before lightning NOx is added).

2.3. Alternative Sea Salt Emissions

It has been reported from the previous WRAP and VISTAS modeling studies that the internally generated sea salt emissions with the CMAQ AERO4 module generally underestimate measured chlorine (Cl) concentrations although there may be other chlorine sources contributing to the measurement data. For the revised sea salt emissions, we used the CAMx sea salt emissions preprocessor. The CAMx sea salt emissions preprocessor generates hourly sea salt aerosol emissions using the wind field at the lowest model layer interpolated to a height of 10 meters above sea level. The upper limit for the sea salt aerosol size range was set to 2.5 microns. For particles with dry diameter greater than 8 microns, the flux is calculated using the Smith-Harrison parameterization (Smith and Harrison, 1998). For particles with dry diameter less than 8 microns, either the Gong (2003) or Monaghan et al. (1986) parameterization may be used (in this study, the parameterization by Gong was used). The flux represents the rate of production of marine aerosol droplets per unit area of the sea surface per increment of droplet radius. From the particle flux, the emitted particle mass is calculated assuming spherical particle geometry, and a density of 1150 kg m^{-3} (Grini et al. 2002). Sulfate emissions are added using the sulfate-to-sodium ratio of 0.25. The externally generated sea salt (and sulfate) emissions were then supplied to a modified CMAQ code where the internal sea salt generation code was disabled.

Figure 2-12 shows that ozone concentrations are slightly decreased over the ocean with the alternative sea salt and sulfate emissions. This is because increased sodium chloride with the alternative emissions reduces nitric acid over the ocean, replacing chloride in the sea salt with nitrate. Under a very low NOx condition, ozone is destroyed by OH and HO2 radicals. Over the ocean where there is no NOx sources, however, ozone can still be produced because nitric acid from inland can slowly turn into NOx. There are two pathways curently implemented in the CB05 mechanism that convert nitric acid back to NOx: (1) oxidation with OH radical (OH + HNO3 → H2O + NO3) and (2) photolysis (HNO3 → OH + NO2). In this situation, reduced nitric acid due to increased sea salt will result in less ozone production.

The alternative emissions add slightly more sulfate (Figure 2-13). Sodium and chloride concentrations increased the most over the northern Pacific Ocean while changes in their concentrations on inland areas are much smaller (Figures 2-14 and 2-15). The changes in sulfate, sodium and chloride make up most of $PM_{2.5}$ changes (Figure 2-16).

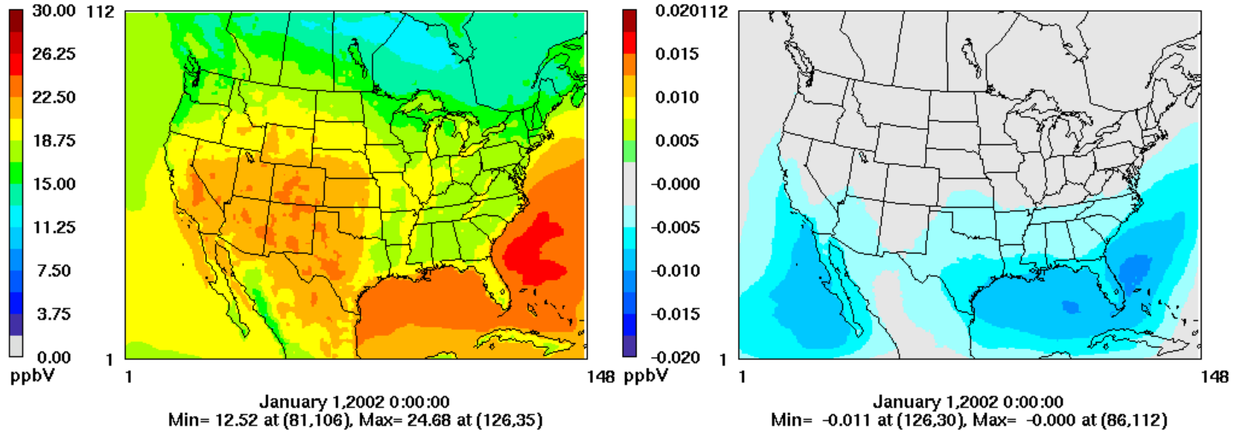
(a) annual average O_3 (base case)

(b) changes in annual average O_3

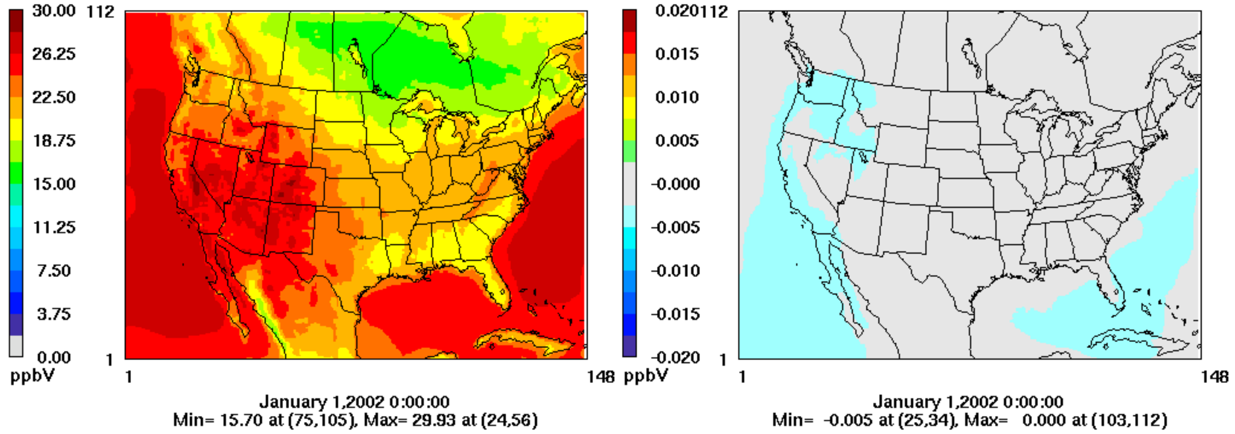
(c) quarterly average O_3 (base – Q1)

(d) changes in quarterly average O_3 (Q1)

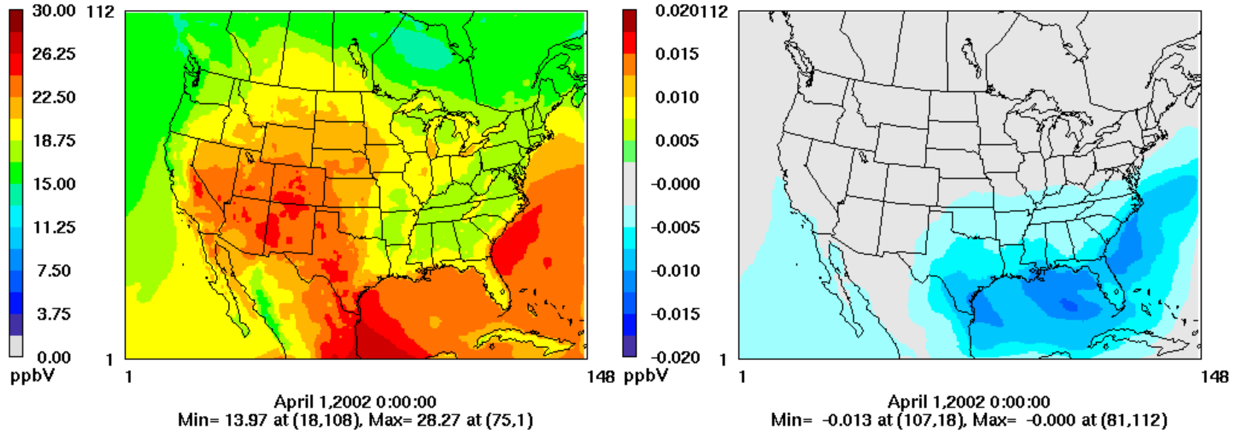
(e) quarterly average O_3 (base – Q2)

(f) changes in quarterly average O_3 (Q2)

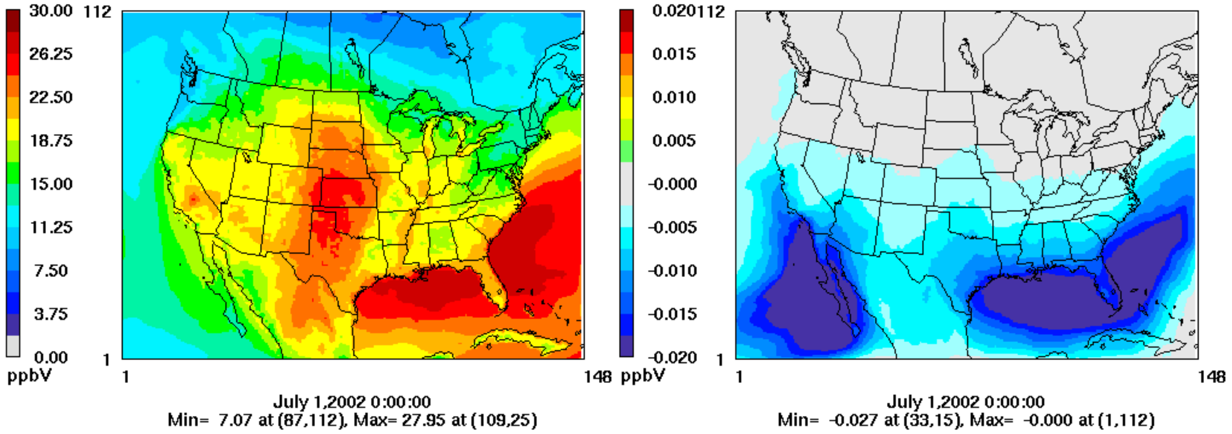

(g) quarterly average O_3 (base – Q3)

(h) changes in quarterly average O_3 (Q3)

(i) quarterly average O_3 (base – Q4)

(j) changes in quarterly average O_3 (Q4)

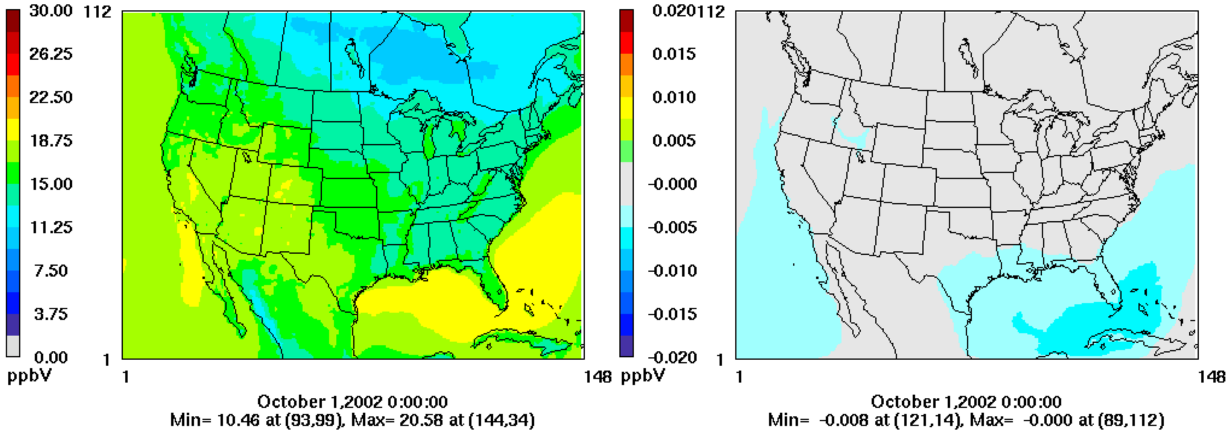

Figure 2-12. Impact of alternative sea salt emissions on ozone. The concentration changes are given as ozone from the new case (simulation with alternative sea salt) minus ozone from the base case (simulation before alternative sea salt is added).

(a) annual average ASO4 (base case)

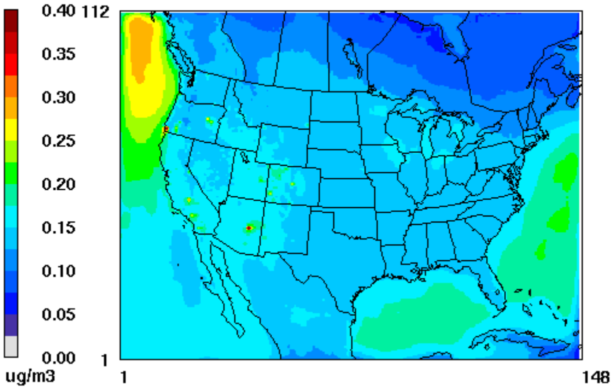

January 1,2002 0:00:00
Min= 0.05 at (148,1), Max= 0.50 at (42,43)

(b) changes in annual average ASO4

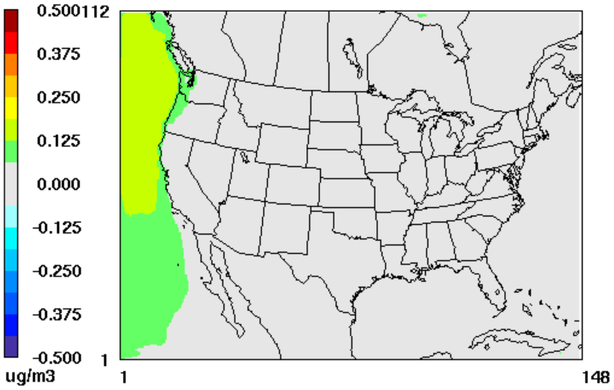

January 1,2002 0:00:00
Min= 0.000 at (74,112), Max= 0.183 at (9,69)

(c) quarterly average ASO4 (base – Q1)

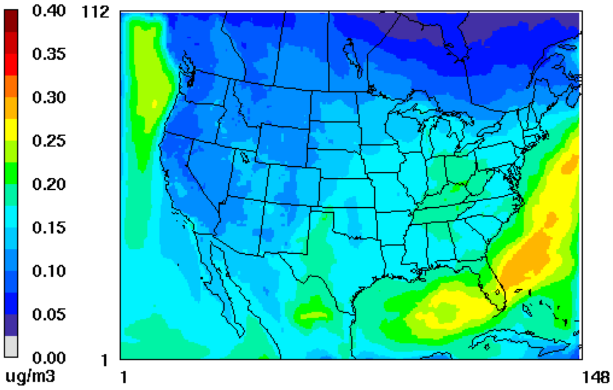

January 1,2002 0:00:00
Min= 0.03 at (91,110), Max= 0.30 at (129,31)

(d) changes in quarterly average ASO4 (Q1)

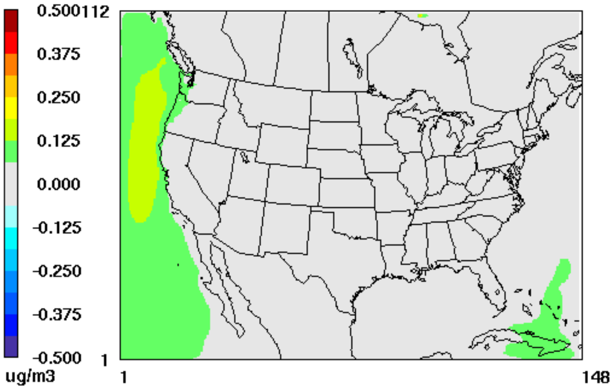

January 1,2002 0:00:00
Min= 0.000 at (75,112), Max= 0.292 at (97,111)

(e) quarterly average ASO4 (base – Q2)

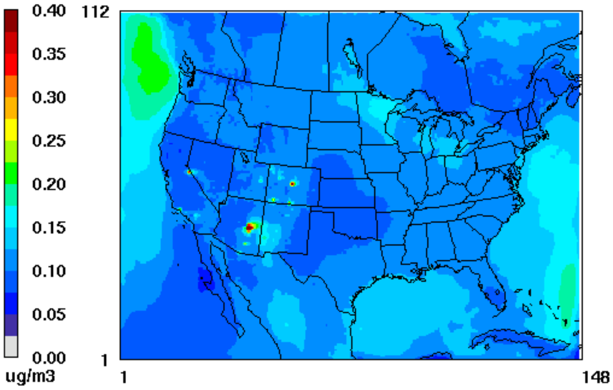

April 1,2002 0:00:00
Min= 0.06 at (148,1), Max= 1.43 at (42,43)

(f) changes in quarterly average ASO4 (Q2)

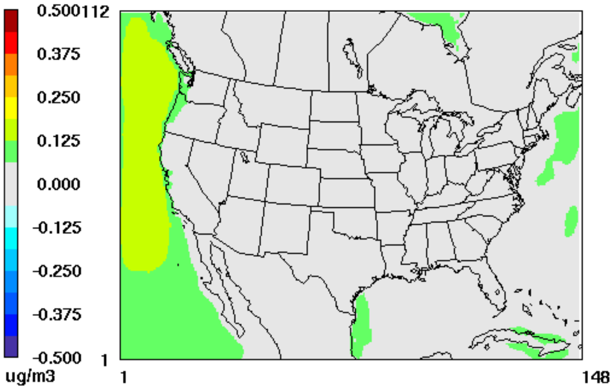

April 1,2002 0:00:00
Min= 0.000 at (74,112), Max= 0.181 at (12,52)

(g) quarterly average ASO4 (base – Q3) (h) changes in quarterly average ASO4 (Q3)

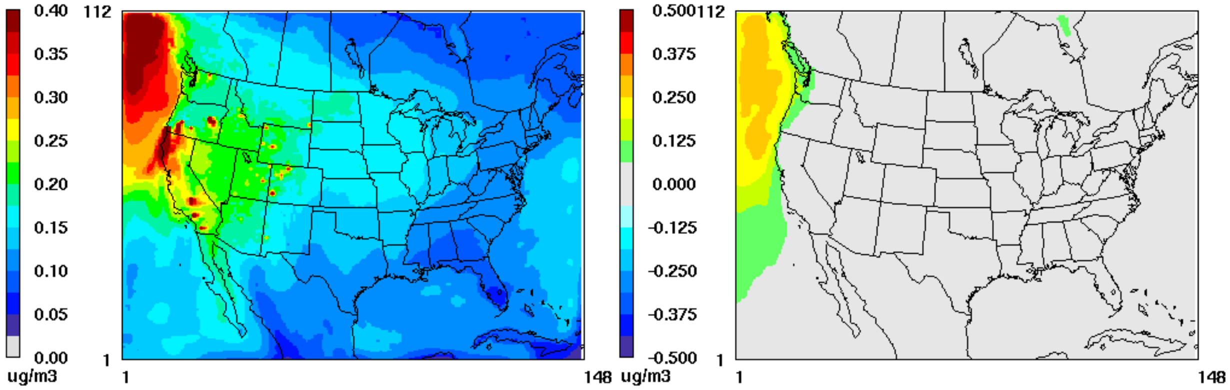

July 1,2002 0:00:00
Min= 0.03 at (148,1), Max= 1.54 at (16,75)

July 1,2002 0:00:00
Min= 0.000 at (74,112), Max= 0.288 at (7,109)

(i) quarterly average ASO4 (base – Q4) (j) changes in quarterly average ASO4 (Q4)

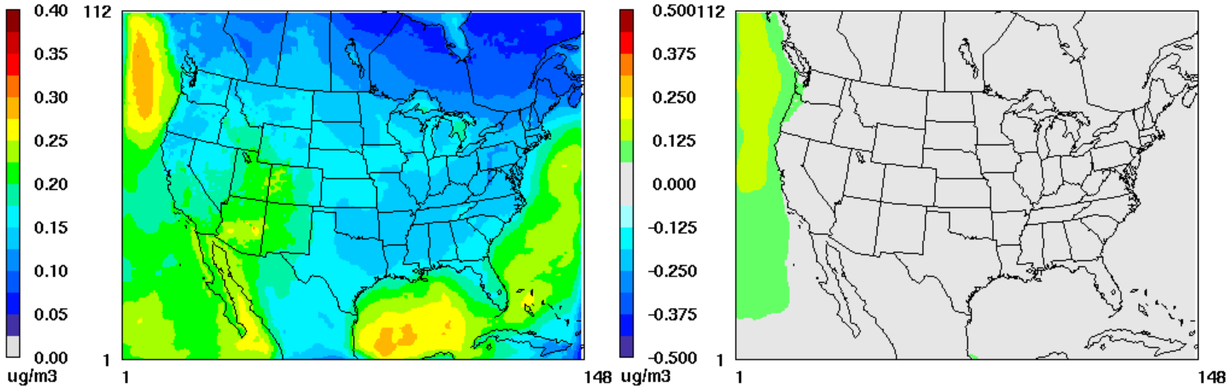

October 1,2002 0:00:00
Min= 0.05 at (89,112), Max= 0.31 at (43,43)

October 1,2002 0:00:00
Min= -0.004 at (91,112), Max= 0.162 at (6,98)

Figure 2-13. Impact of alternative sea salt emissions on fine sulfate (ASO4). The concentration changes are given as ASO4 from the new case (simulation with alternative sea salt) minus ASO4 from the base case (simulation before alternative sea salt is added).

(a) annual average ACL (base case)

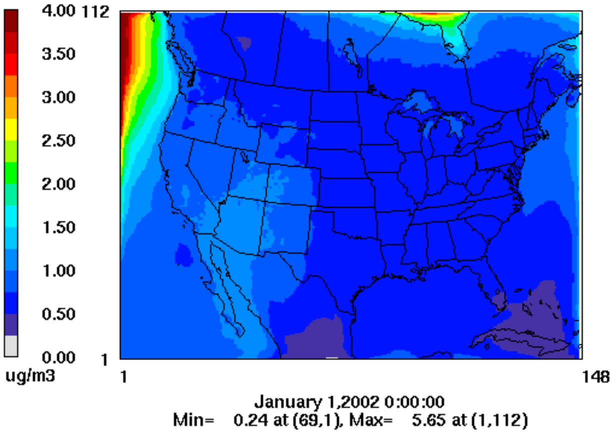

(b) changes in annual average ACL

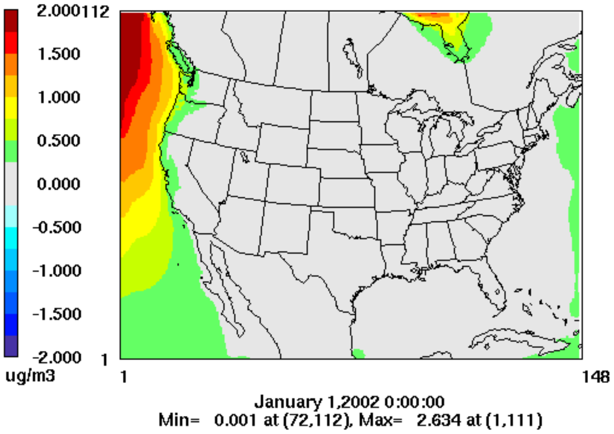

(c) quarterly average ACL (base – Q1)

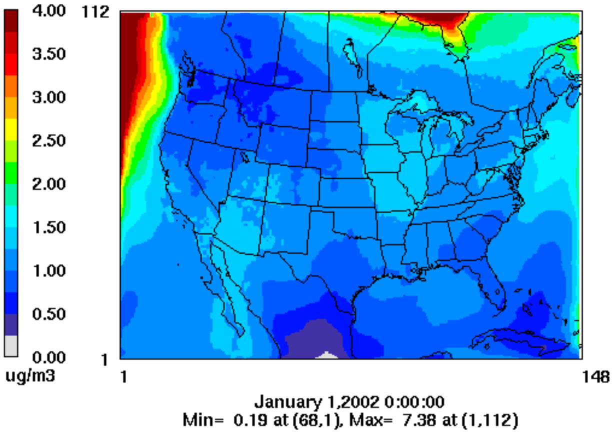

(d) changes in quarterly average ACL (Q1)

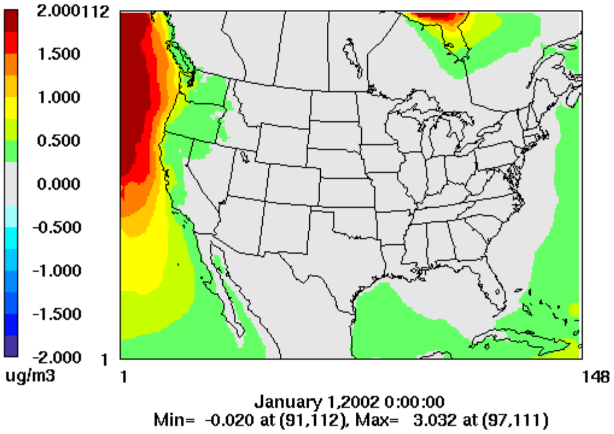

(e) quarterly average ACL (base – Q2)

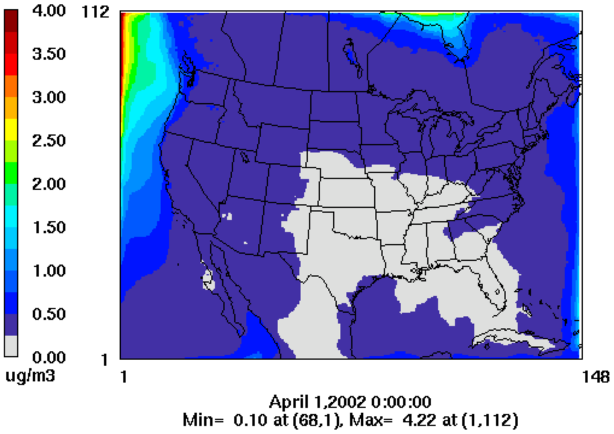

(f) changes in quarterly average ACL (Q2)

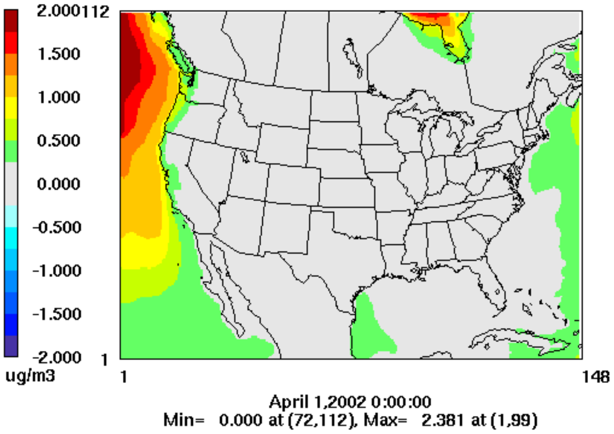

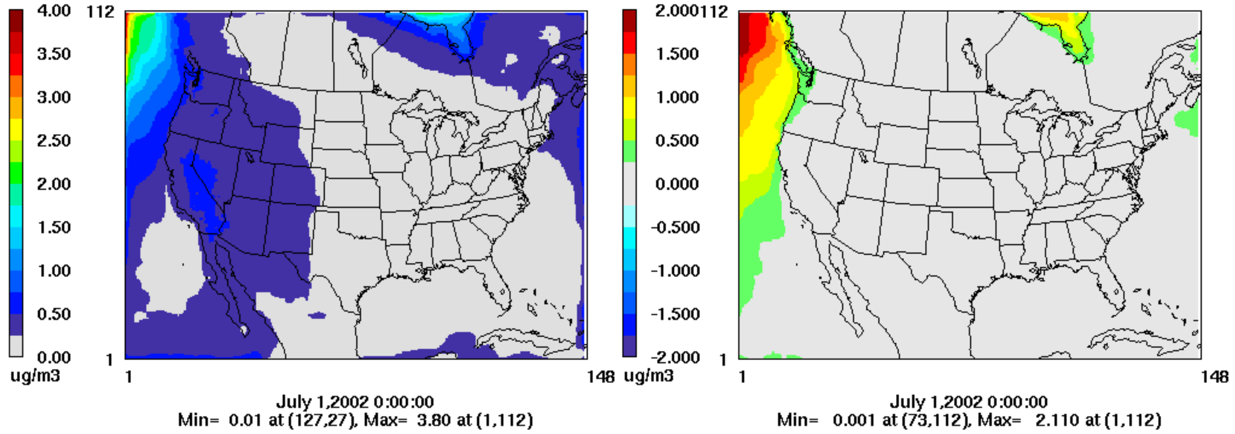
(g) quarterly average ACL (base – Q3)

(h) changes in quarterly average ACL (Q3)

(i) quarterly average ACL (base – Q4)

(j) changes in quarterly average ACL (Q4)

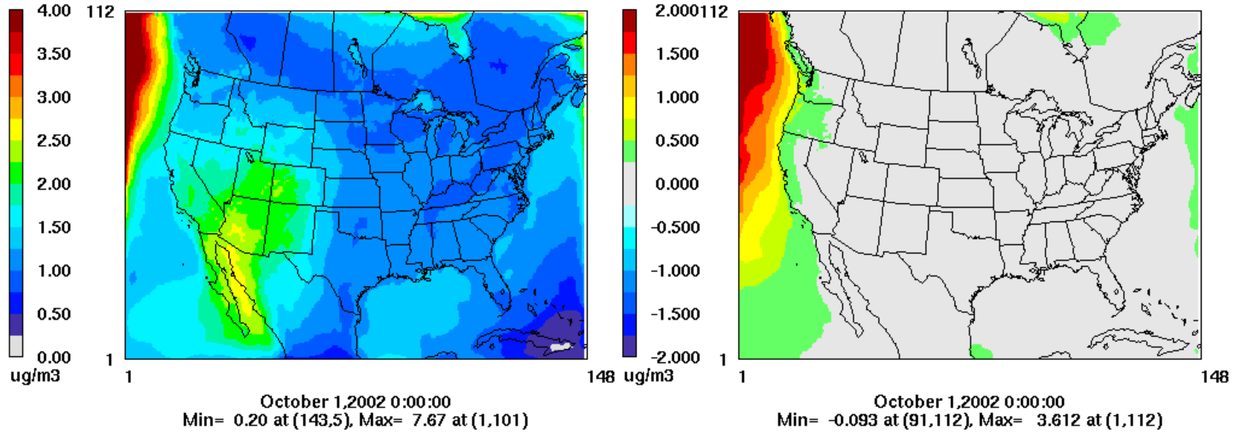

Figure 2-14. Impact of alternative sea salt emissions on fine chloride (ACL). The concentration changes are given as ACL from the new case (simulation with alternative sea salt) minus ACL from the base case (simulation before alternative sea salt is added).

(a) annual average ANA (base case)

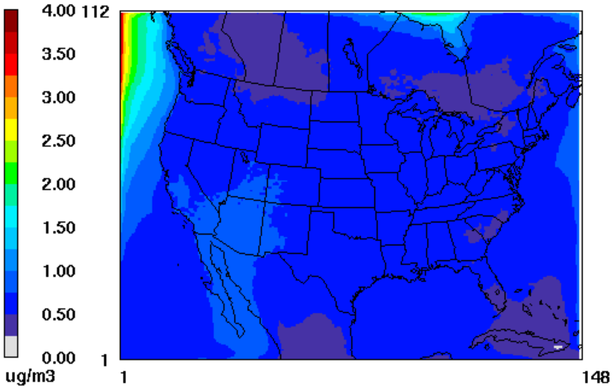

January 1,2002 0:00:00
Min= 0.24 at (142,5), Max= 3.79 at (1,112)

(b) changes in annual average ANA

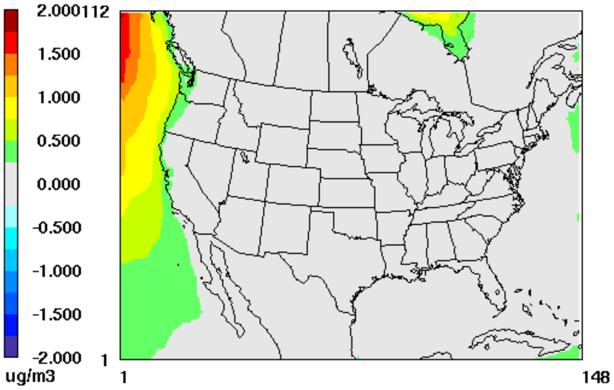

January 1,2002 0:00:00
Min= 0.001 at (72,112), Max= 1.779 at (1,111)

(c) quarterly average ANA (base – Q1)

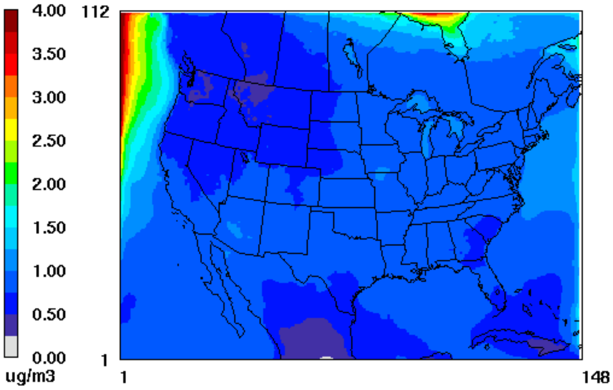

January 1,2002 0:00:00
Min= 0.22 at (67,1), Max= 4.89 at (1,112)

(d) changes in quarterly average ANA (Q1)

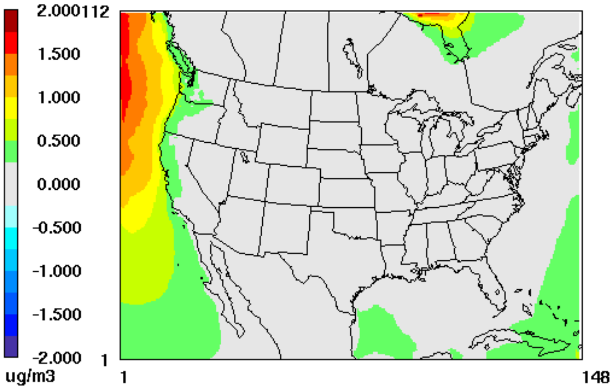

January 1,2002 0:00:00
Min= -0.013 at (91,112), Max= 2.095 at (97,111)

(e) quarterly average ANA (base – Q2)

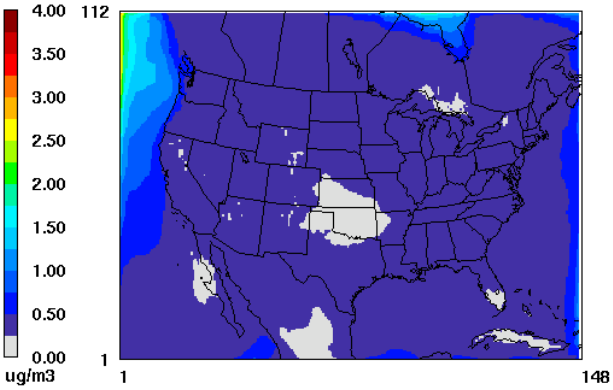

April 1,2002 0:00:00
Min= 0.19 at (64,7), Max= 2.83 at (1,112)

(f) changes in quarterly average ANA (Q2)

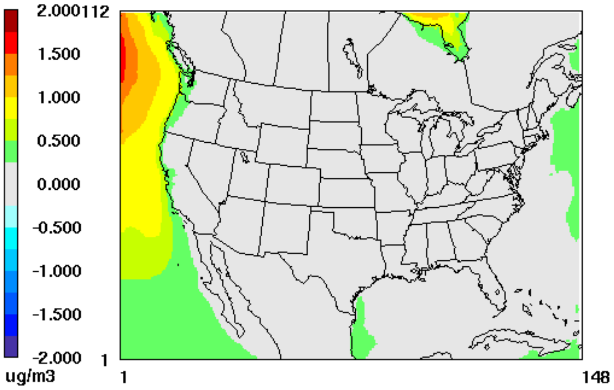

April 1,2002 0:00:00
Min= 0.000 at (72,112), Max= 1.612 at (1,99)

(g) quarterly average ANA (base – Q3) (h) changes in quarterly average ANA (Q3)

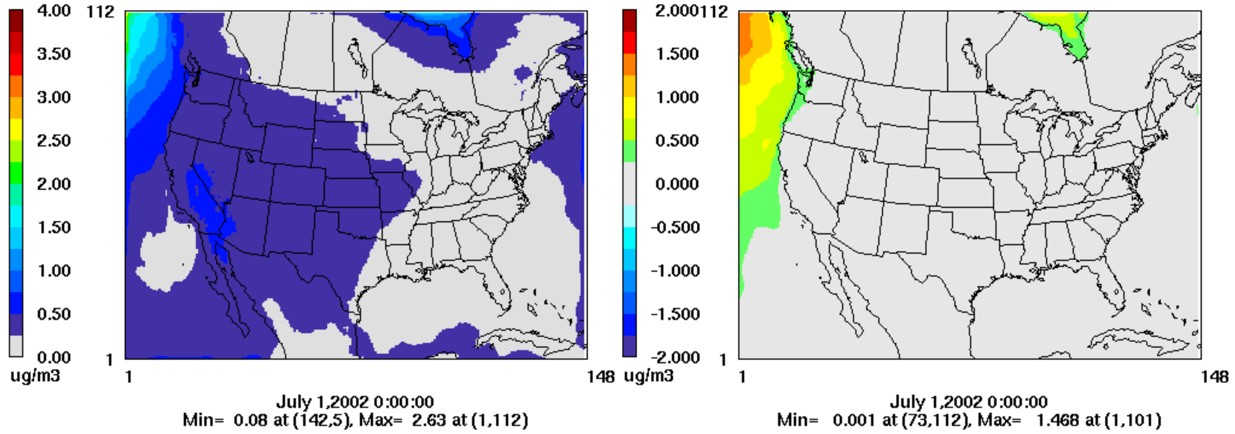

(i) quarterly average ANA (base – Q4) (j) changes in quarterly average ANA (Q4)

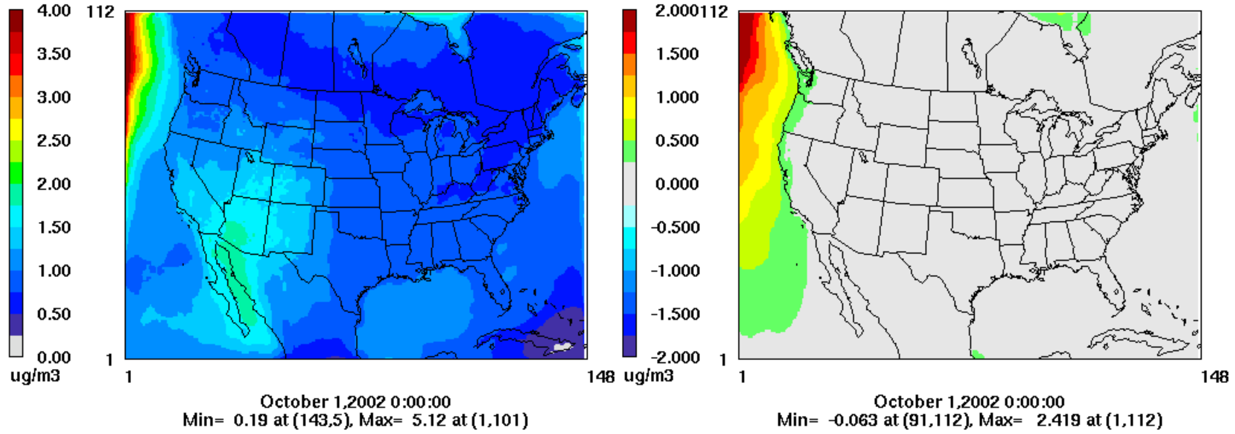

Figure 2-15. Impact of alternative sea salt emissions on fine sodium (ANA). The concentration changes are given as ANA from the new case (simulation with alternative sea salt) minus ANA from the base case (simulation before alternative sea salt is added).

(a) annual average $PM_{2.5}$ (base case)

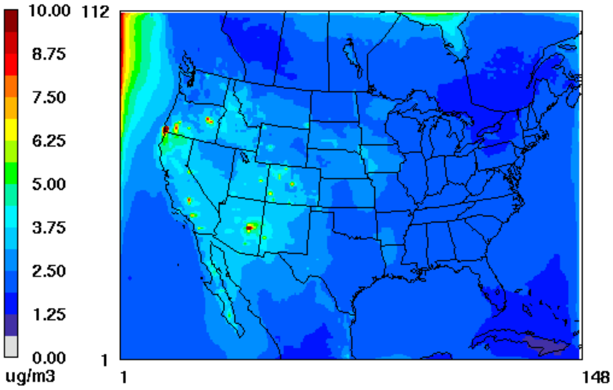

January 1,2002 0:00:00
Min= 0.99 at (140,5), Max= 20.74 at (42,43)

(b) changes in annual average $PM_{2.5}$

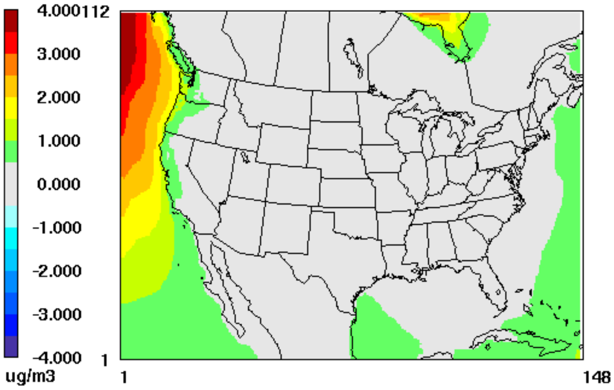

January 1,2002 0:00:00
Min= 0.003 at (72,112), Max= 4.609 at (1,111)

(c) quarterly average $PM_{2.5}$ (base – Q1)

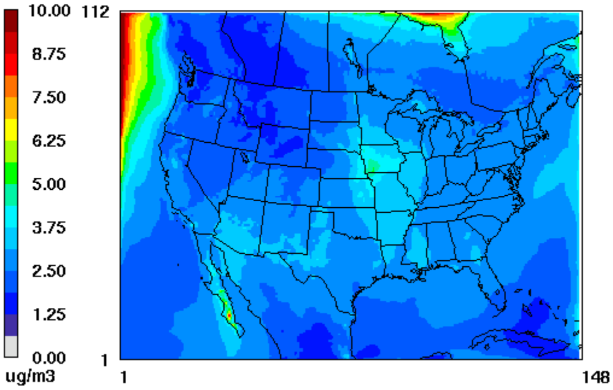

January 1,2002 0:00:00
Min= 1.29 at (27,93), Max= 12.42 at (1,112)

(d) changes in quarterly average $PM_{2.5}$ (Q1)

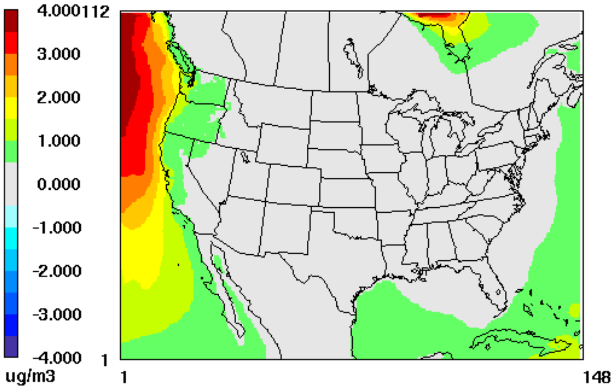

January 1,2002 0:00:00
Min= -0.033 at (91,112), Max= 5.455 at (97,111)

(e) quarterly average $PM_{2.5}$ (base – Q2)

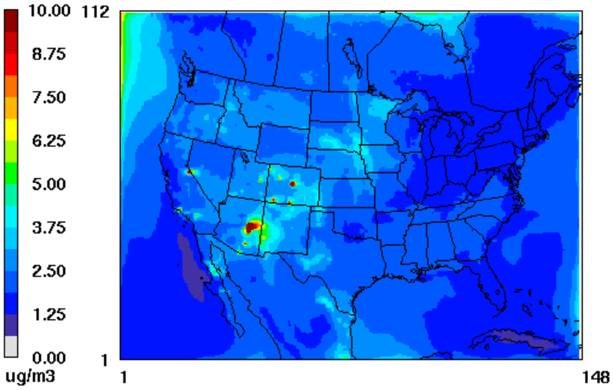

April 1,2002 0:00:00
Min= 1.07 at (28,27), Max= 69.68 at (42,43)

(f) changes in quarterly average $PM_{2.5}$ (Q2)

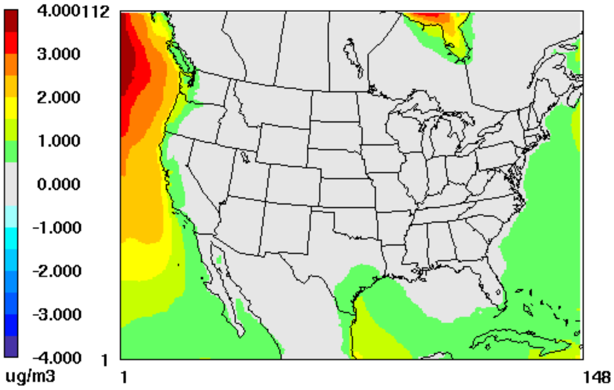

April 1,2002 0:00:00
Min= -0.028 at (97,1), Max= 4.247 at (1,99)

(g) quarterly average $PM_{2.5}$ (base – Q3)

(h) changes in quarterly average $PM_{2.5}$ (Q3)

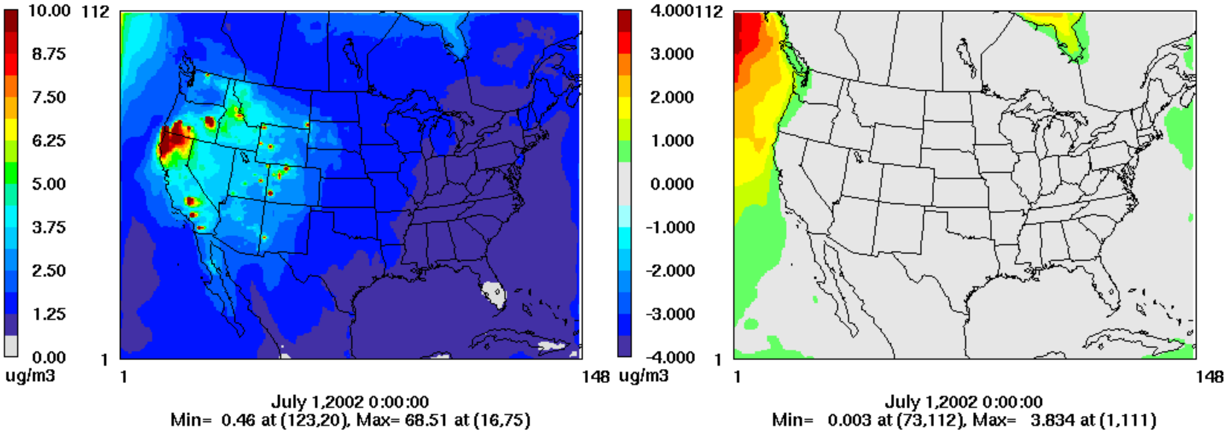

(i) quarterly average $PM_{2.5}$ (base – Q4)

(j) changes in quarterly average $PM_{2.5}$ (Q4)

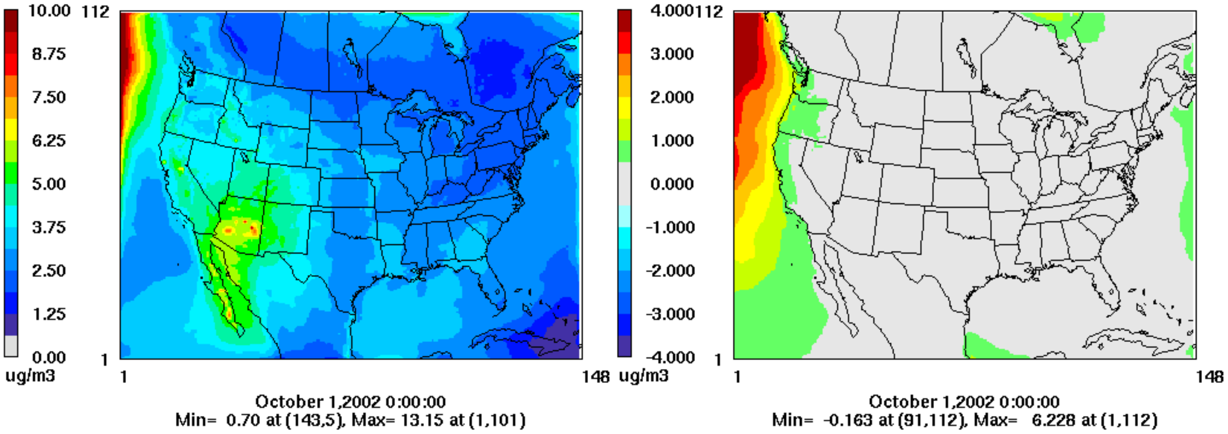

Figure 2-16. Impact of alternative sea salt emissions on $PM_{2.5}$. The concentration changes are given as $PM_{2.5}$ from the new case (simulation with alternative sea salt) minus $PM_{2.5}$ from the base case (simulation before alternative sea salt is added).

2.4. Updated Biogenic SOA Model with MEGAN Emissions

Modeling secondary organic aerosol (SOA) has been subject to high uncertainties. Modeling studies conducted for the Visibility Improvement State and Tribal Association of the Southeast (VISTAS) have shown that air quality models exhibit poor organic PM performance with significant underprediction in southeastern US. To improve the model performance, Morris et al. (2006) modified the SOA scheme in CMAQ to incorporate potentially important SOA forming processes which have been missing in the traditional SOA modeling: (1) SOA formation from isoprene, (2) SOA formation from sesquiterpenes, and (3) Polymerization of SOA. Since sesquiterpenes are not accounted for in the SMOKE BEIS3 model, Morris et al. (2006) used an empirical scaling factor to estimate sesquiterpenes from the BEIS3 monoterpene emissions. For this study, we used the same modified SOA scheme to add the new processes. The biogenic emissions were generated by the latest MEGAN biogenic emissions model which provides more biogenic species (including sesquiterpenes) using updated land use data with higher resolution. However, we used isoprene emissions from SMOKE BEIS3 instead of MEGAN because previous modeling studies showed that the MEGAN isoprene emissions, which is significantly higher than the estimates by the SMOKE BEIS3 in some area (by factor of 2~3), resulted in overestimation of ozone with the current chemistry mechanisms. There have been a few measurement studies that suggest the current chemistry mechanisms significantly underpredict OH radical concentrations under a low NOx condition and thus cause isoprene to accumulate in the boundary layer (Kuhn et al., 2007; Lelieveld et al., 2008). However, a lot of uncertainties still remain as to how the additional OH is produced. Figure 2-17 showed emissions of some biogenic species estimated by SMOKE BEIS3 and MEGAN. Biogenic NO emissions from MEGAN are generally lower than those from SMOKE BEIS3, especially in central US. Monoterpene emissions are higher with MEGAN in southeastern US, but less in western US.

The above changes resulted in decreases in ozone concentrations showing most reduction in central US (Figure 2-18). This is mainly due to reduced biogenic NO emissions by MEGAN. Figure 2-19 shows that SOA from monoterpenes (AORGB) decreases in western US while slightly increasing in southeastern US in summer. Note that while AORGB of the base case represents total SOA mass formed from monoterpenes, AORGB of the new run does not include polymerized fraction, thus representing only part of the monoterpene SOA. Contribution of isoprene to SOA formation is relatively minor considering its huge emissions (Figure 2-20). The yield and partitioning ratio for oxidation products of isoprene used in this study (Morris et al., 2006) are based on a field study and highly uncertain. Note that different parameters have been reported based on smog chamber experiments (Kroll et al., 2005, 2006; Henze and Seinfeld, 2006). Figure 2-21 shows SOA from sesquiterpenes (SOA2) predicted by the updated SOA model with the MEGAN biogenic emissions. Although MEGAN estimates sesquiterpene emissions much smaller than monoterpenes, SOA2 concentrations are predicted slightly higher than AORGB (of the new run; not shown) in the southeastern US because we assumed that oxidation products of sesquiterpenes stay mostly in the particle phase due to their low vapor pressures. Also, as explained above, AORGB excludes polymerized portion. Among the new SOA forming pathways, polymerization into non-volatile particles is shown to have the largest impact (Figure 2-22). It should be noted, however, that there exists significant uncertainty in the estimated polymerization rate. Overall, the new SOA scheme with the MEGAN emissions increased total SOA concentrations in eastern US, but decreased over the northwestern states (Figure 2-23). Some inorganic PM species are also affected. Nitrate concentrations decrease because MEGAN estimates less biogenic NO emissions than SMOKE BEIS3 (Figure 2-24). It is not clear, however, why chloride (Figure 2-25) and sodium (not shown) increase slightly.

Increases in chloride concentrations may be partly explained by less nitrate replacing chloride in sea salt. Figure 2-26 shows overall impact on total $PM_{2.5}$ concentrations with significant increases over southeastern US in summer.

(a) NO (SMOKE BEIS3)

(b) NO (MEGAN)

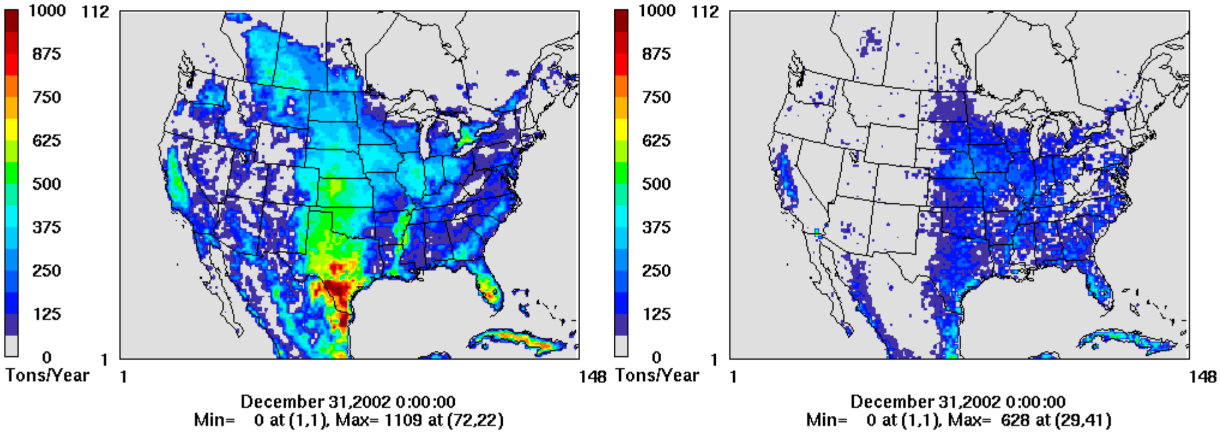

(c) Monoterpenes (SMOKE BEIS3)

(d) Monoterpenes (MEGAN)

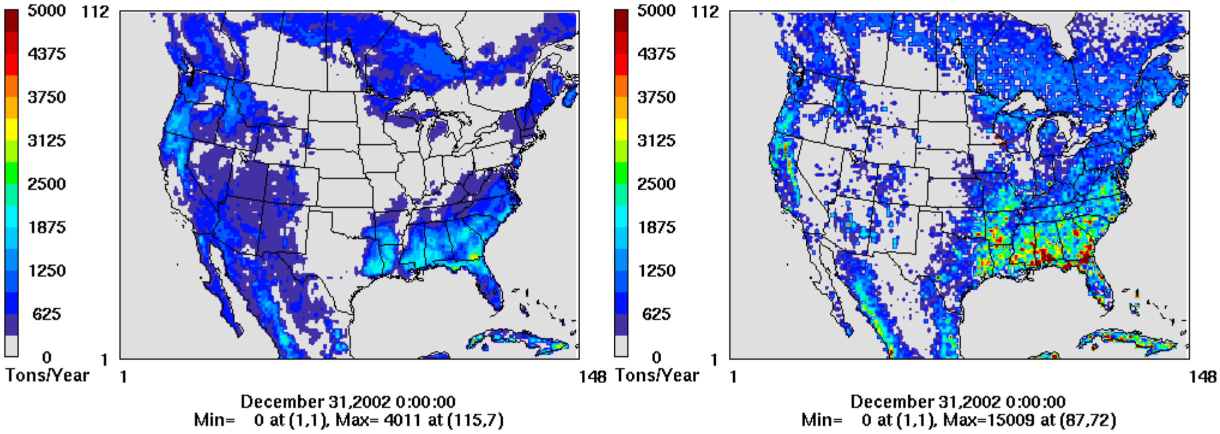

(e) Isoprene (SMOKE BEIS3)

(f) Sesquiterpenes (MEGAN)

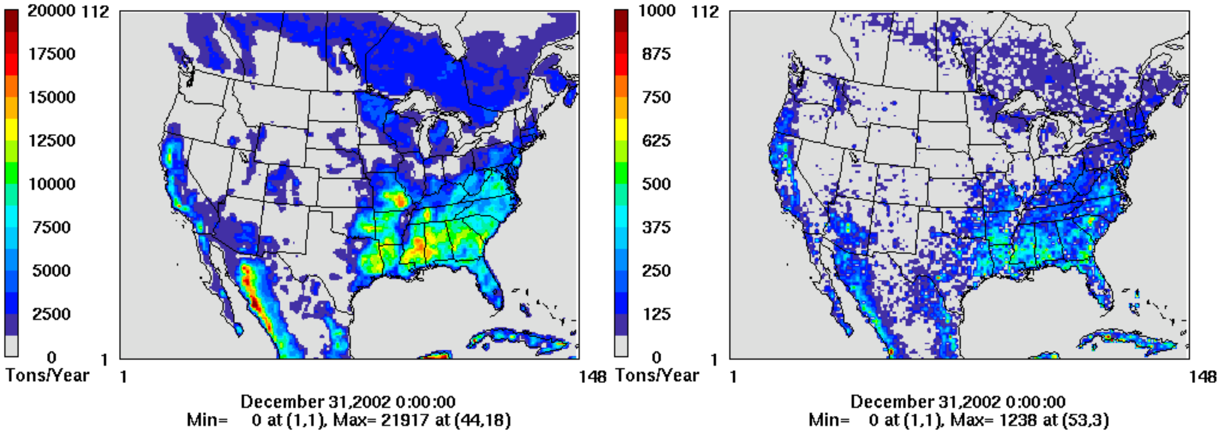

Figure 2-17. Annual total biogenic emissions by SMOKE BEIS3 and MEGAN emission models.

(a) annual average O_3 (base case)

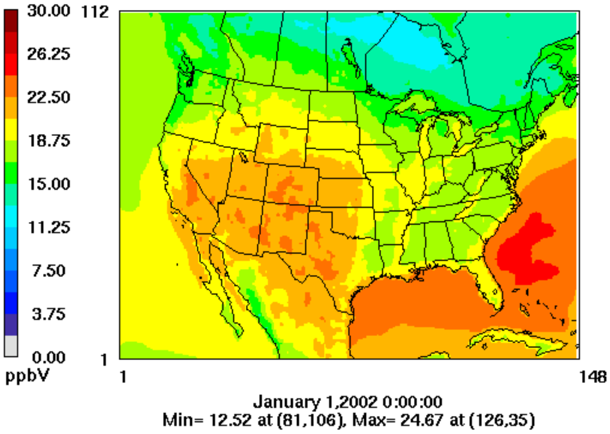

(b) changes in annual average O_3

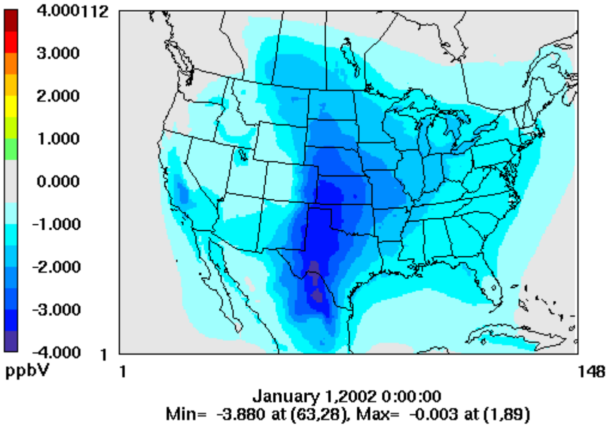

(c) quarterly average O_3 (base – Q1)

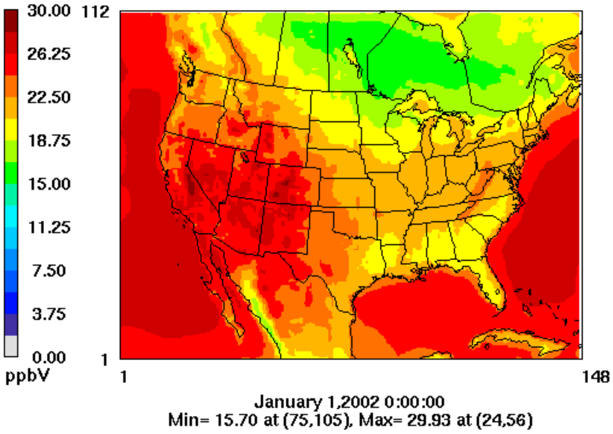

(d) changes in quarterly average O_3 (Q1)

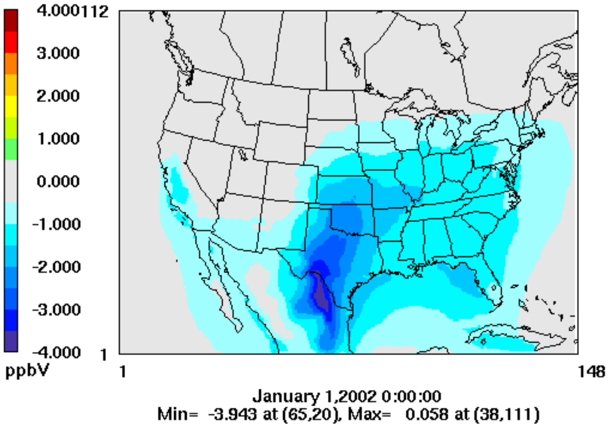

(e) quarterly average O_3 (base – Q2)

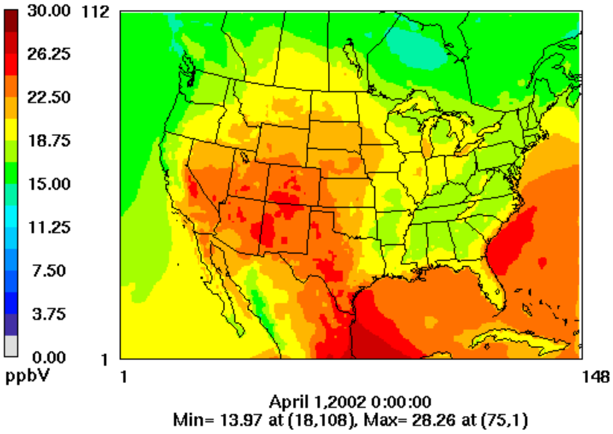

(f) changes in quarterly average O_3 (Q2)

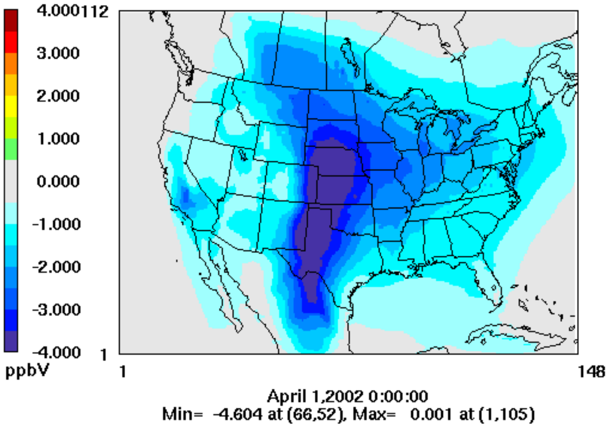

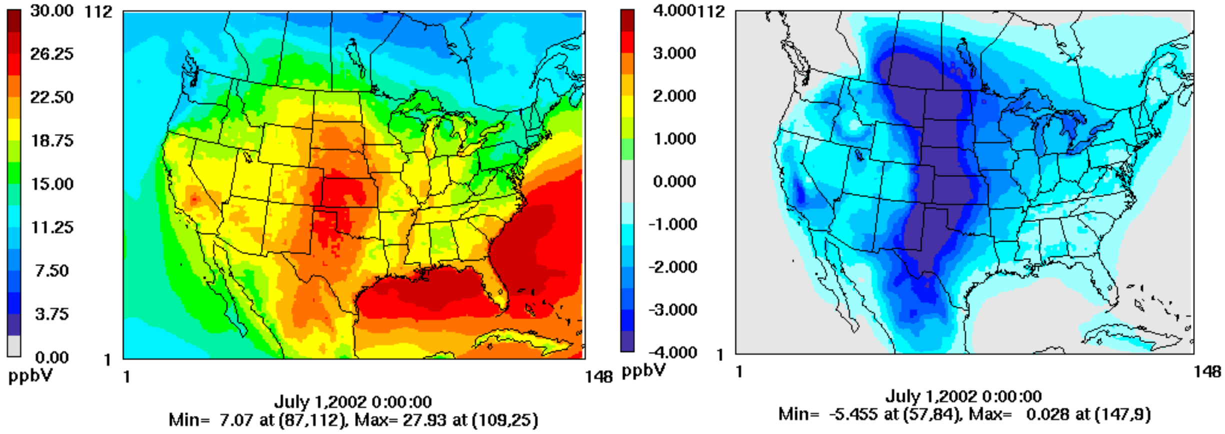

(g) quarterly average O_3 (base – Q3)

(h) changes in quarterly average O_3 (Q3)

(i) quarterly average O_3 (base – Q4)

(j) changes in quarterly average O_3 (Q4)

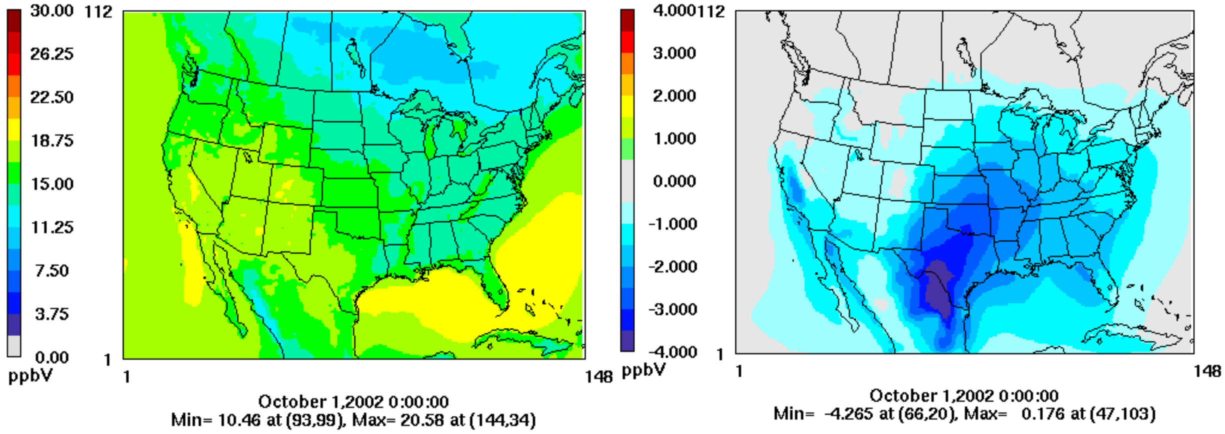

Figure 2-18. Impact of the updated SOA model with MEGAN emissions on ozone. The concentration changes are given as ozone from the new case (simulation with the updated SOA model) minus ozone from the base case (simulation before the updated SOA model is adopted).

(a) annual average AORGB (base case)

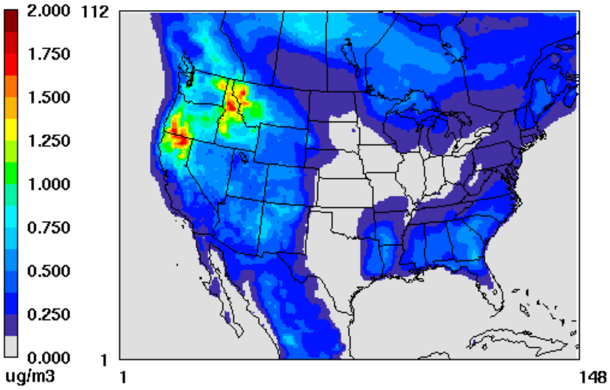

January 1,2002 0:00:00
Min= 0.000 at (148,17), Max= 1.870 at (21,70)

(b) changes in annual average AORGB

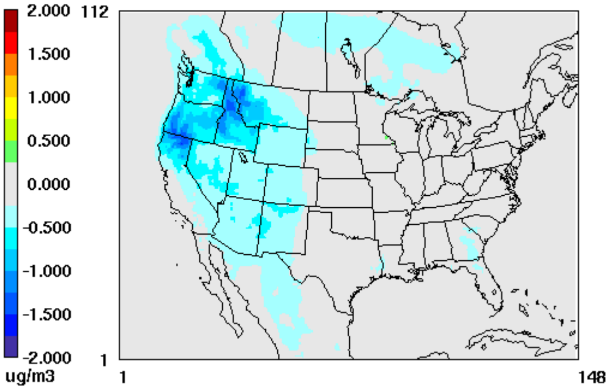

January 1,2002 0:00:00
Min=-1.530 at (21,70), Max= 0.408 at (89,70)

(c) quarterly average AORGB (base – Q1)

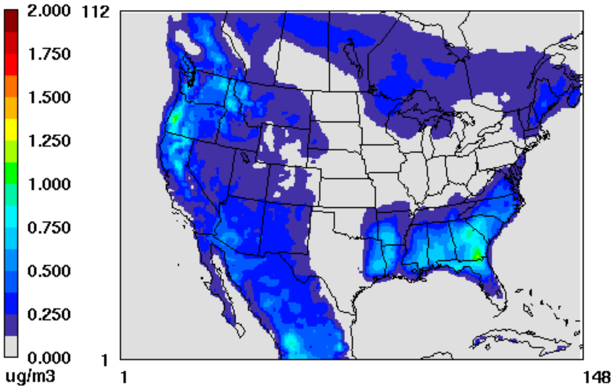

January 1,2002 0:00:00
Min= 0.000 at (1,22), Max= 1.164 at (115,34)

(d) changes in quarterly average AORGB (Q1)

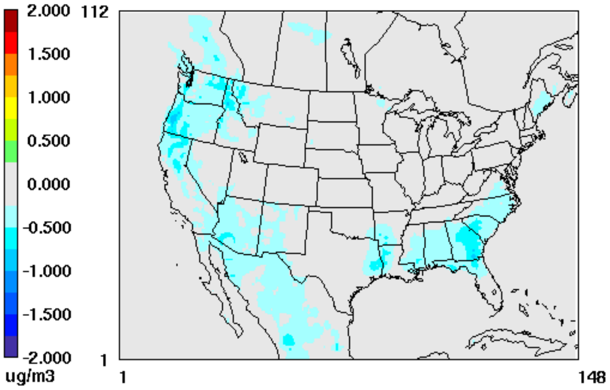

January 1,2002 0:00:00
Min=-0.995 at (18,78), Max= 0.093 at (71,1)

(e) quarterly average AORGB (base – Q2)

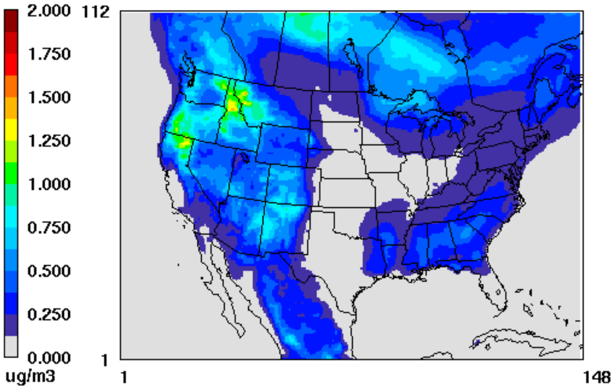

April 1,2002 0:00:00
Min= 0.000 at (148,17), Max= 1.399 at (37,81)

(f) changes in quarterly average AORGB (Q2)

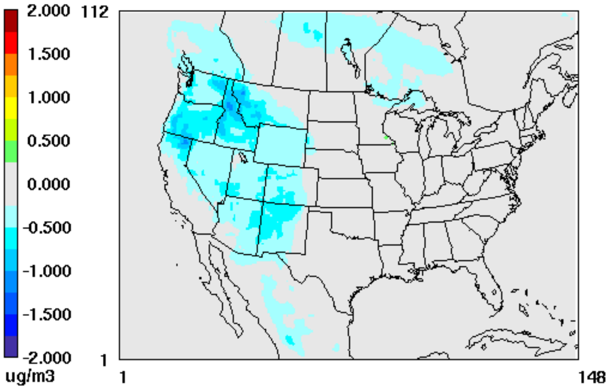

April 1,2002 0:00:00
Min=-1.146 at (41,86), Max= 0.473 at (87,72)

(g) quarterly average AORGB (base – Q3) (h) changes in quarterly average AORGB (Q3)

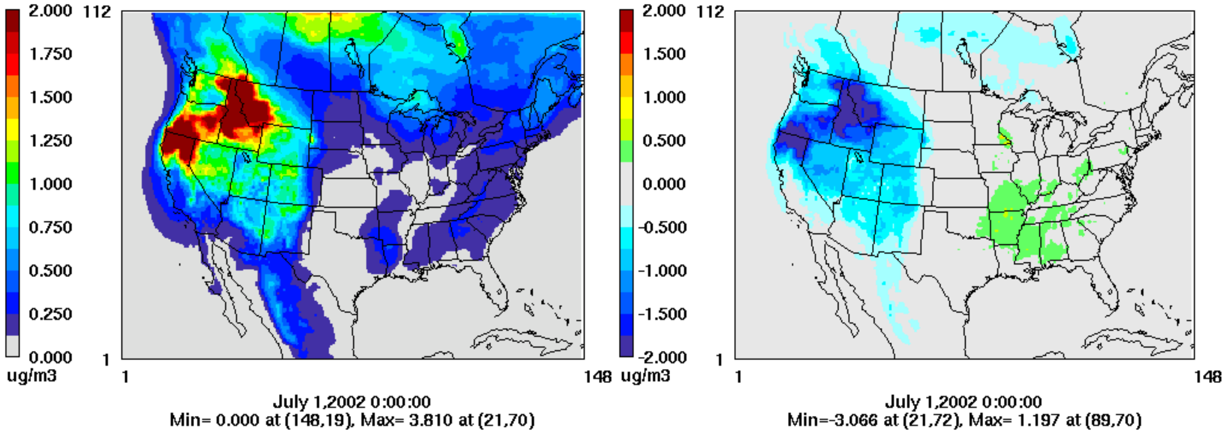

(i) quarterly average AORGB (base – Q4) (j) changes in quarterly average AORGB (Q4)

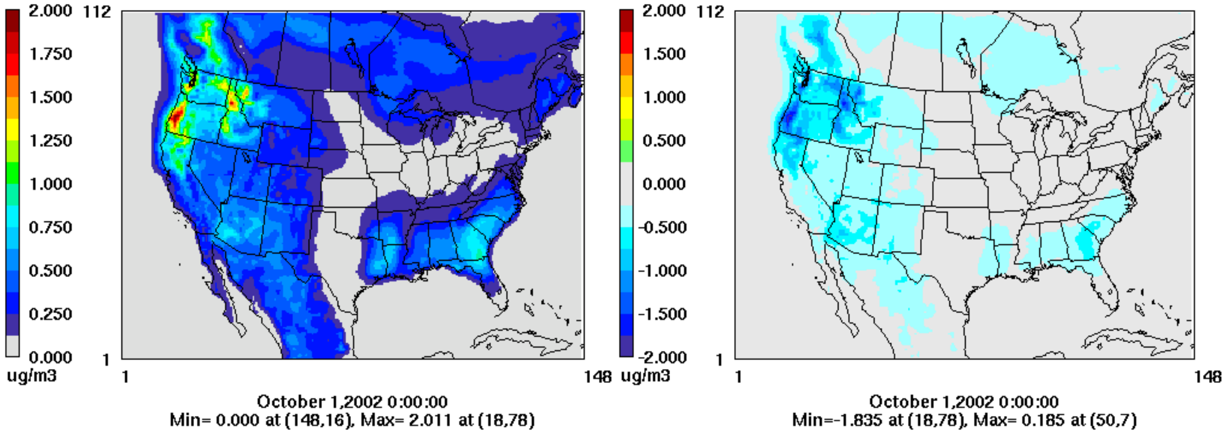

Figure 2-19. Impact of the updated SOA model with MEGAN emissions on SOA from monoterpenes (AORGB). The concentration changes are given as AORGB from the new case (simulation with the updated SOA model) minus AORGB from the base case (simulation before the updated SOA model is adopted).

(a) annual average SOA3

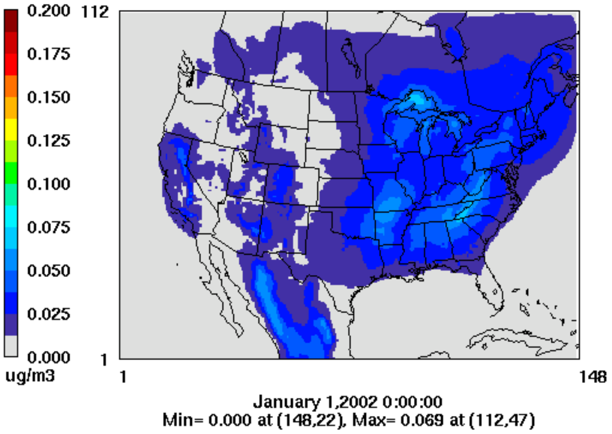

(b) quarterly average SOA3 (Q1)

(c) quarterly average SOA3 (Q2)

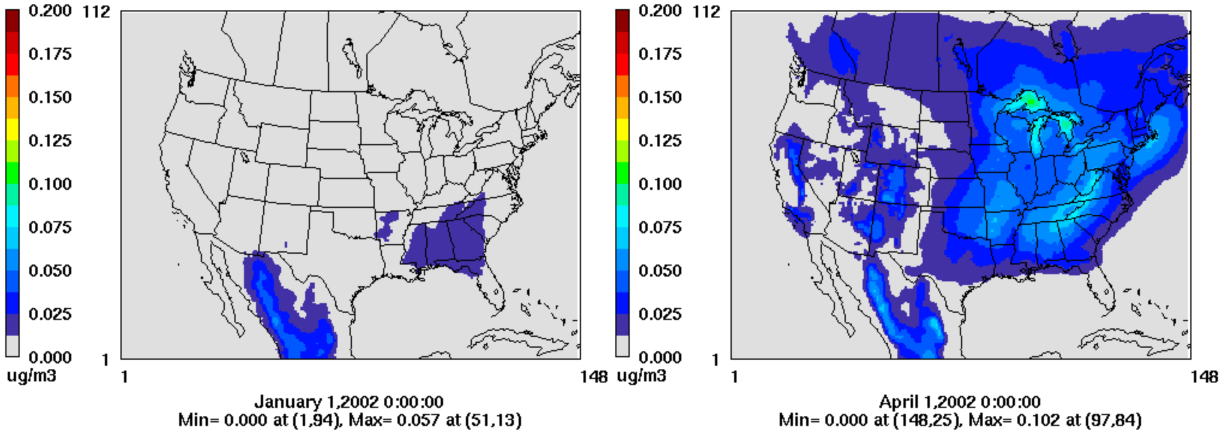

(d) quarterly average SOA3 (Q3)

(e) quarterly average SOA3 (Q4)

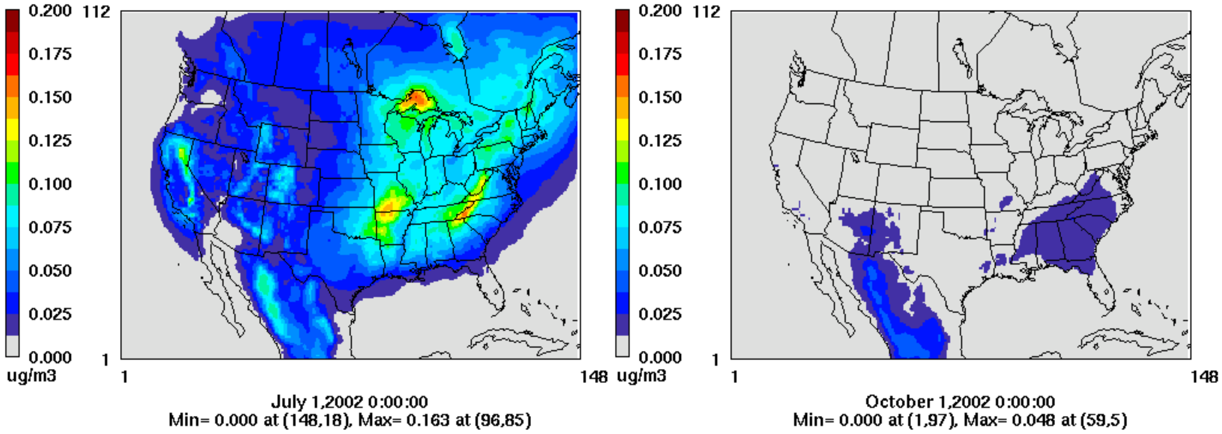

Figure 2-20. SOA from isoprene (SOA3) predicted by the updated SOA model with MEGAN emissions.

(a) annual average SOA2 (base case)

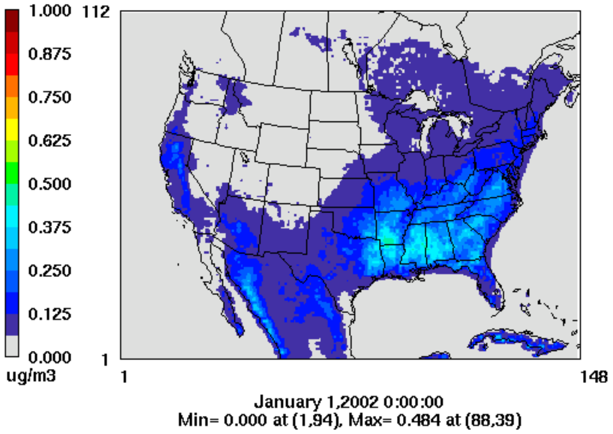

(b) quarterly average SOA2 (Q1)

(c) quarterly average SOA2 (Q2)

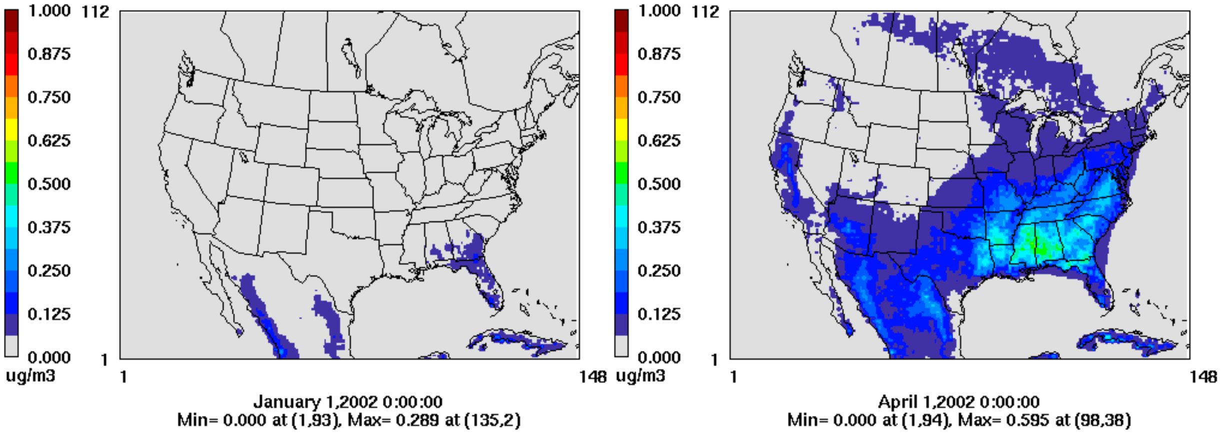

(d) quarterly average SOA2 (Q3)

(e) quarterly average SOA2 (Q4)

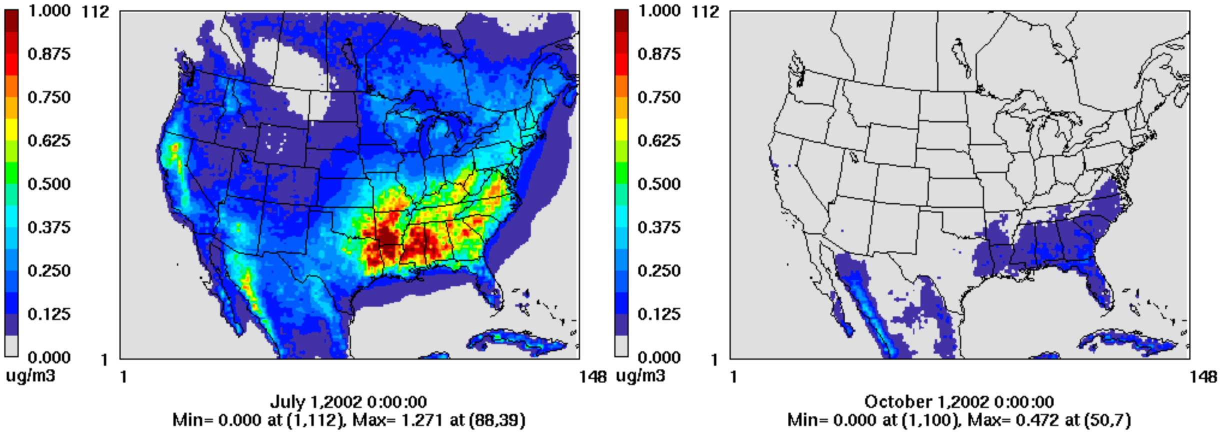

Figure 2-21. SOA from sesquiterpenes (SOA2) predicted by the updated SOA model with MEGAN emissions.

(a) annual average SOA1 (base case)

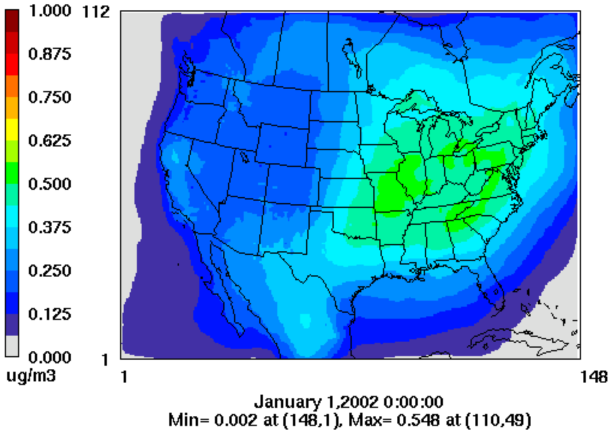

January 1,2002 0:00:00
Min= 0.002 at (148,1), Max= 0.548 at (110,49)

(b) quarterly average SOA1 (Q1)

(c) quarterly average SOA1 (Q2)

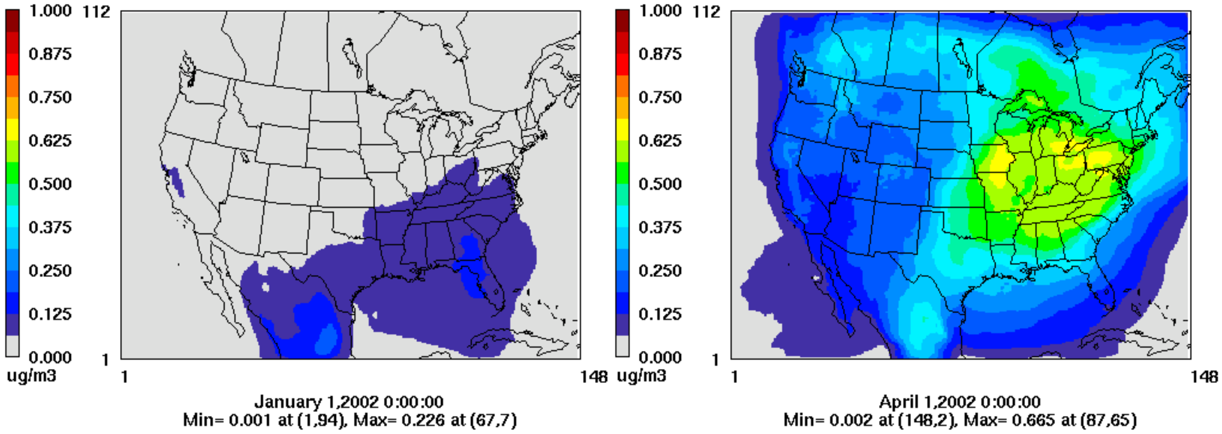

January 1,2002 0:00:00
Min= 0.001 at (1,94), Max= 0.226 at (67,7)

April 1,2002 0:00:00
Min= 0.002 at (148,2), Max= 0.665 at (87,65)

(d) quarterly average SOA1 (Q3)

(e) quarterly average SOA1 (Q4)

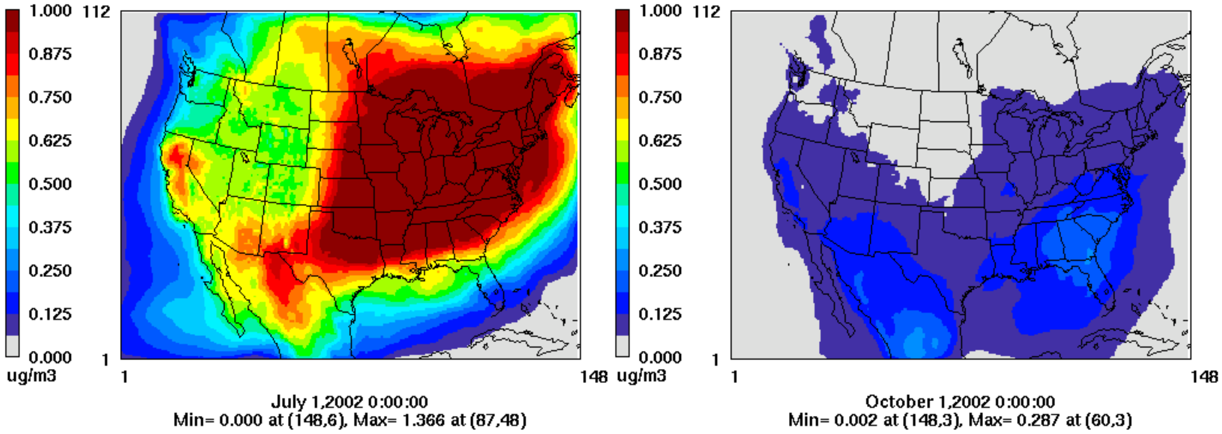

July 1,2002 0:00:00
Min= 0.000 at (148,6), Max= 1.366 at (87,48)

October 1,2002 0:00:00
Min= 0.002 at (148,3), Max= 0.287 at (60,3)

Figure 2-22. SOA from polymerization (SOA1) predicted by the updated SOA model with MEGAN emissions.

(a) annual average TSOA (base case)

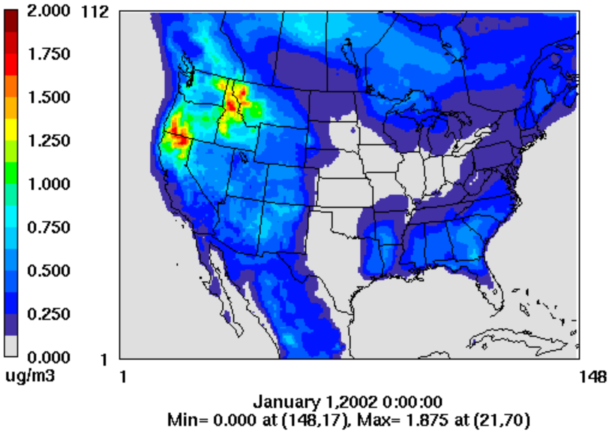

(b) changes in annual average TSOA

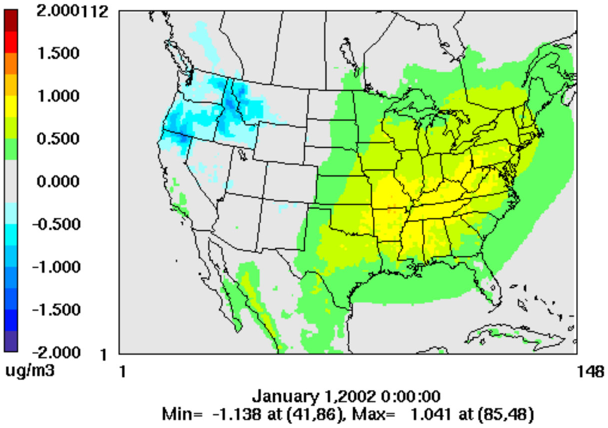

(c) quarterly average TSOA (base – Q1)

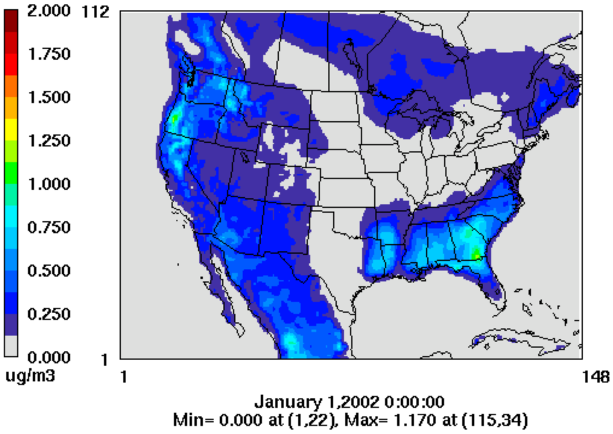

(d) changes in quarterly average TSOA (Q1)

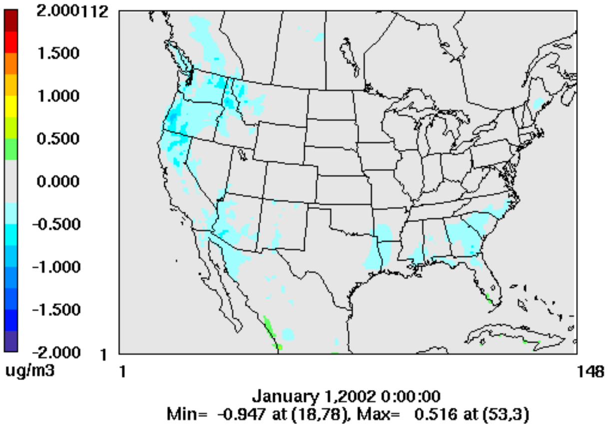

(e) quarterly average TSOA (base – Q2)

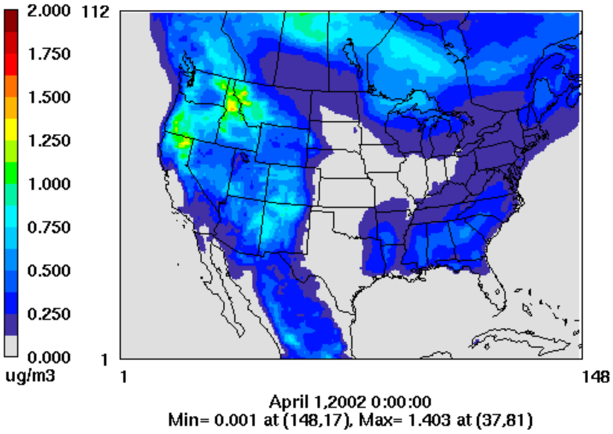

(f) changes in quarterly average TSOA (Q2)

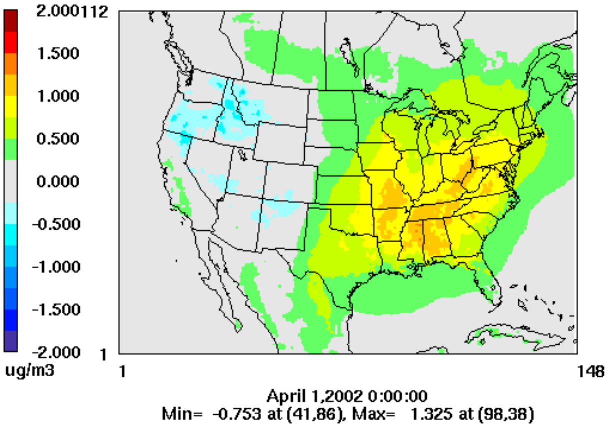

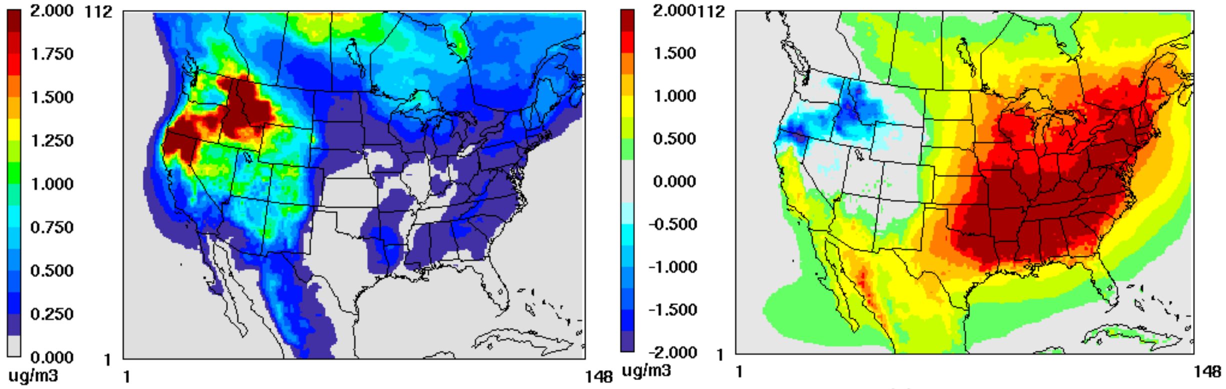
(g) quarterly average TSOA (base – Q3)

(h) changes in quarterly average TSOA (Q3)

July 1,2002 0:00:00
Min= 0.000 at (148,19), Max= 3.823 at (21,70)

July 1,2002 0:00:00
Min= -2.168 at (21,72), Max= 2.949 at (88,39)

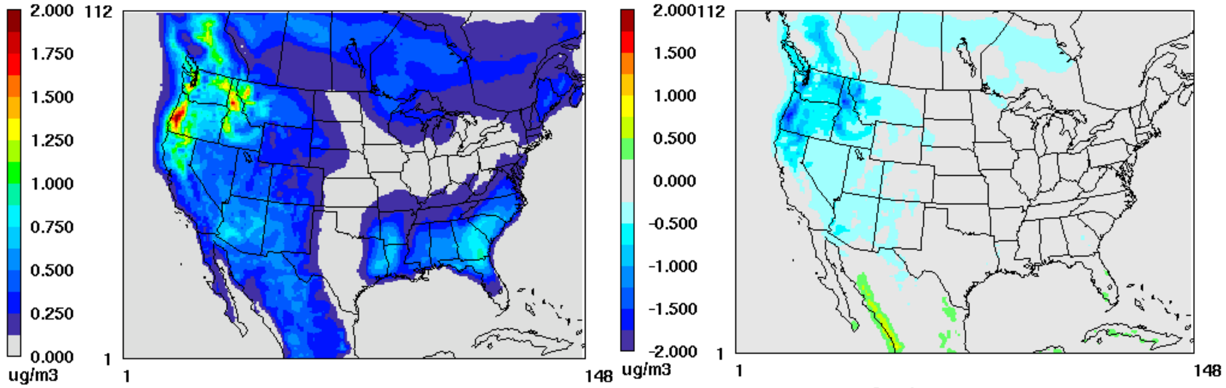
(i) quarterly average TSOA (base – Q4)

(j) changes in quarterly average TSOA (Q4)

October 1,2002 0:00:00
Min= 0.000 at (148,16), Max= 2.014 at (18,78)

October 1,2002 0:00:00
Min= -1.710 at (18,78), Max= 0.868 at (50,7)

Figure 2-23. Impact of the updated SOA model with MEGAN emissions on total SOA (TSOA). The concentration changes are given as TSOA from the new case (simulation with the updated SOA model) minus TSOA from the base case (simulation before the updated SOA model is adopted).

(a) annual average ANO3 (base case)

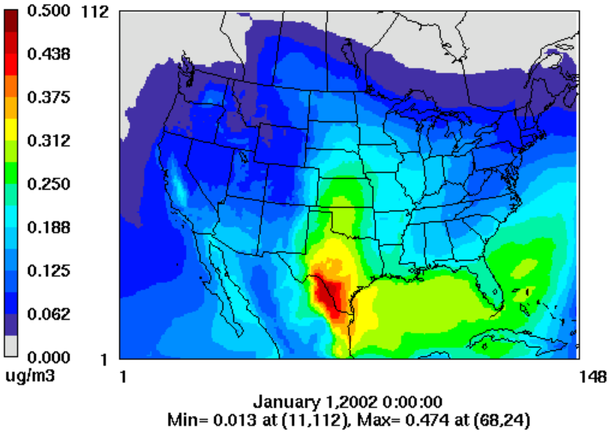

(b) changes in annual average ANO3

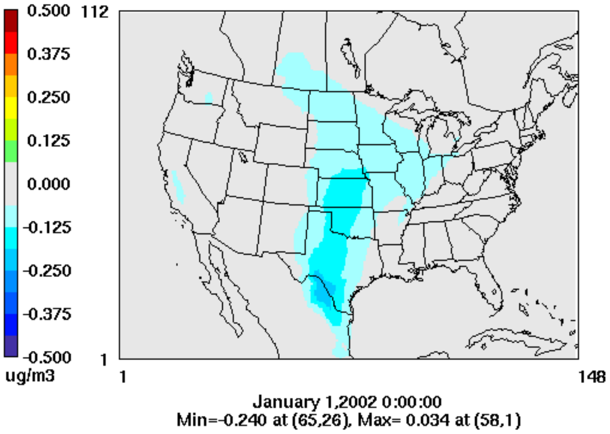

(c) quarterly average ANO3 (base – Q1)

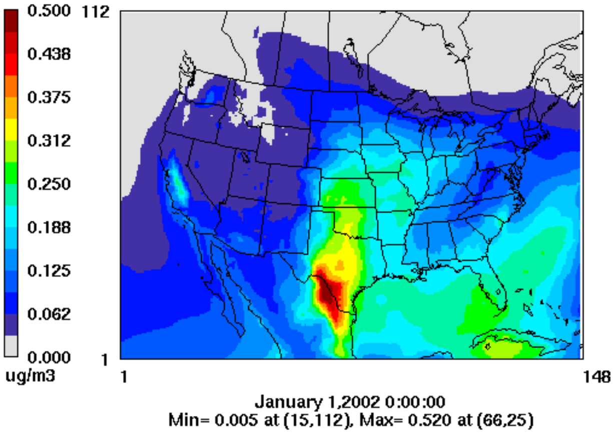

(d) changes in quarterly average ANO3 (Q1)

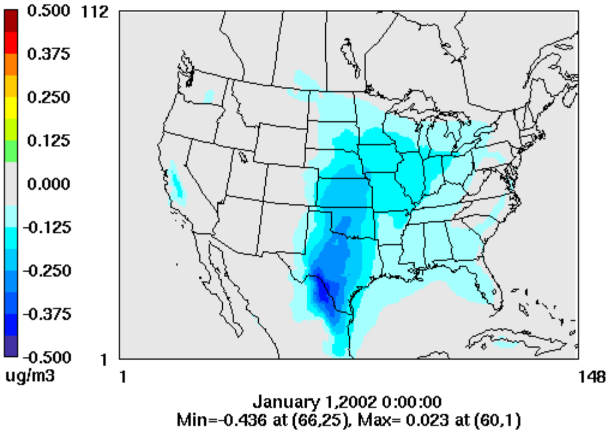

(e) quarterly average ANO3 (base – Q2)

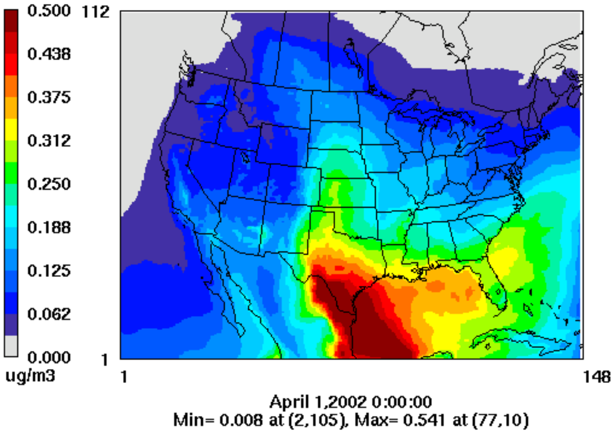

(f) changes in quarterly average ANO3 (Q2)

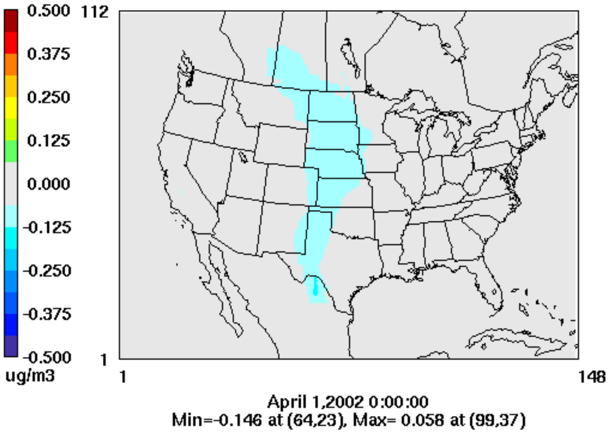

(g) quarterly average ANO3 (base – Q3)

(h) changes in quarterly average ANO3 (Q3)

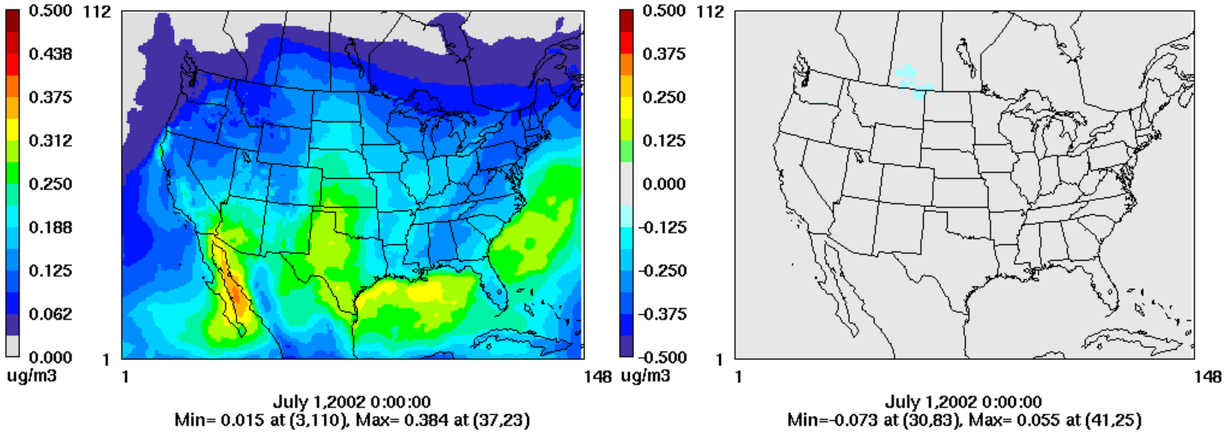

(i) quarterly average ANO3 (base – Q4)

(j) changes in quarterly average ANO3 (Q4)

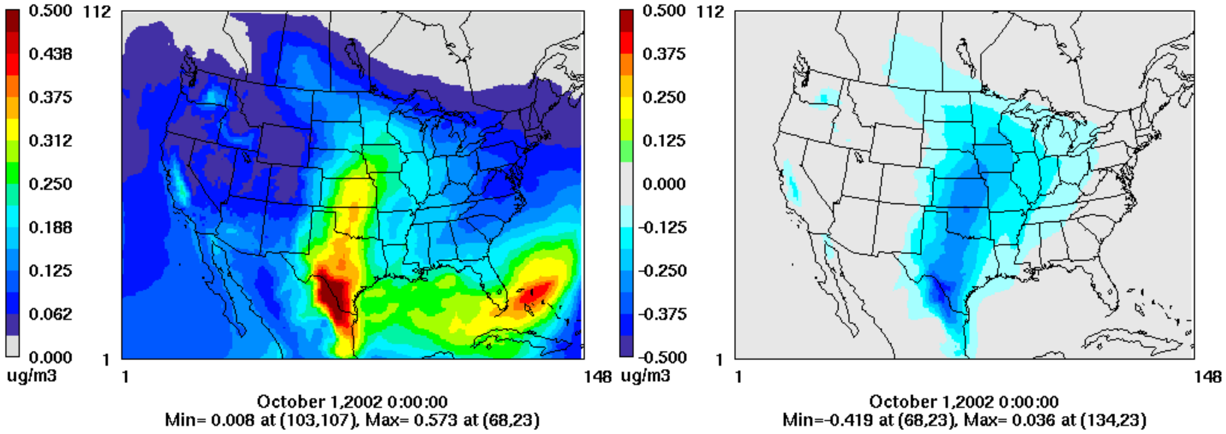

Figure 2-24. Impact of the updated SOA model with MEGAN emissions on fine nitrate (ANO3). The concentration changes are given as ANO3 from the new case (simulation with the updated SOA model) minus ANO3 from the base case (simulation before the updated SOA model is adopted).

(a) annual average ACL (base case)

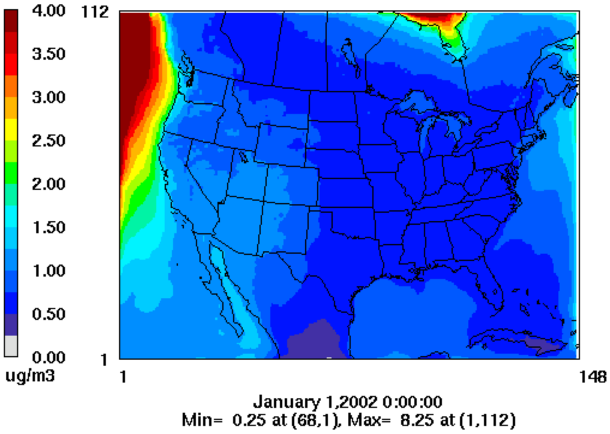

(b) changes in annual average ACL

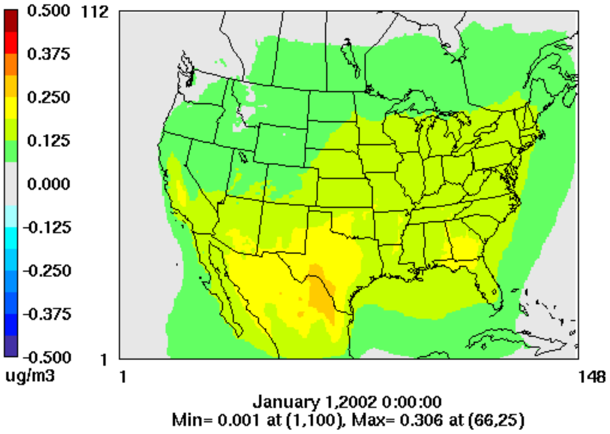

(c) quarterly average ACL (base – Q1)

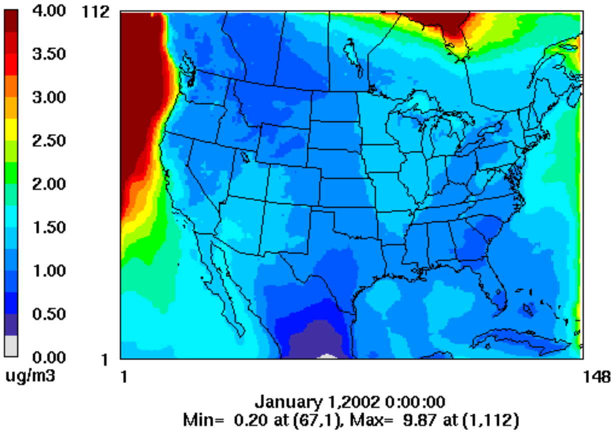

(d) changes in quarterly average ACL (Q1)

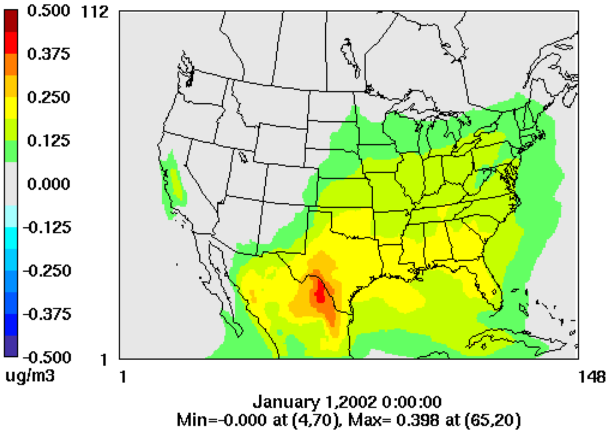

(e) quarterly average ACL (base – Q2)

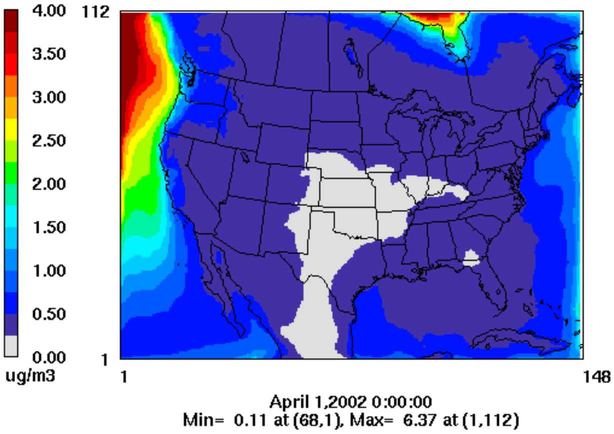

(f) changes in quarterly average ACL (Q2)

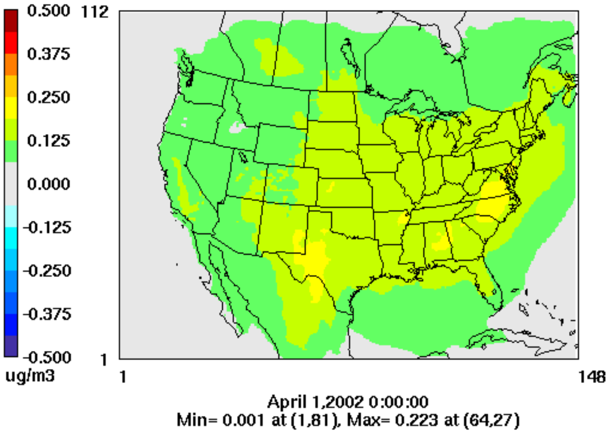

(g) quarterly average ACL (base – Q3) (h) changes in quarterly average ACL (Q3)

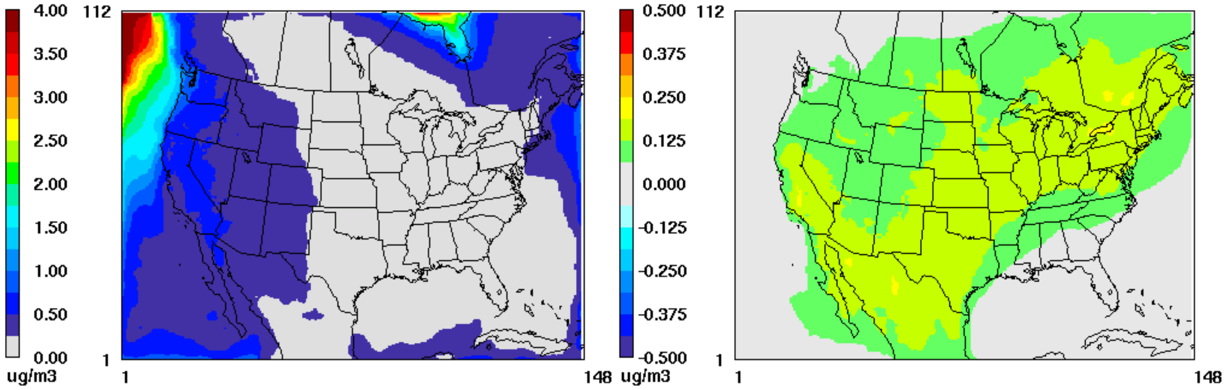

July 1,2002 0:00:00
Min= 0.03 at (127,26), Max= 5.91 at (1,112)

July 1,2002 0:00:00
Min=-0.000 at (146,13), Max= 0.201 at (22,51)

(i) quarterly average ACL (base – Q4) (j) changes in quarterly average ACL (Q4)

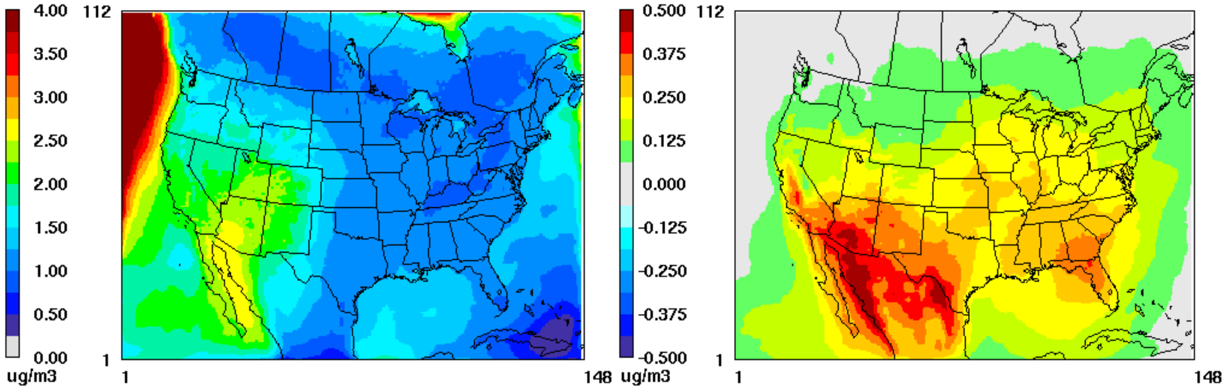

October 1,2002 0:00:00
Min= 0.31 at (143,5), Max= 11.06 at (1,102)

October 1,2002 0:00:00
Min=-0.000 at (2,89), Max= 0.514 at (41,25)

Figure 2-25. Impact of the updated SOA model with MEGAN emissions on fine chloride (ACL). The concentration changes are given as ACL from the new case (simulation with the updated SOA model) minus ACL from the base case (simulation before the updated SOA model is adopted).

(a) annual average $PM_{2.5}$ (base case)

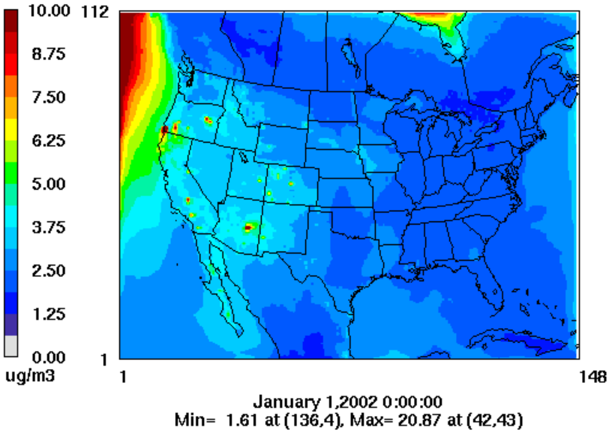

(b) changes in annual average $PM_{2.5}$

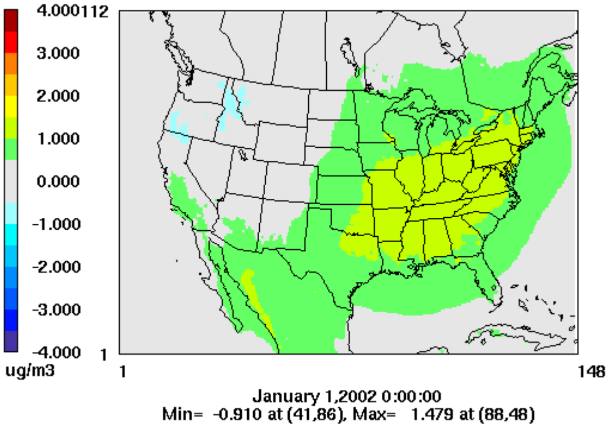

(c) quarterly average $PM_{2.5}$ (base – Q1)

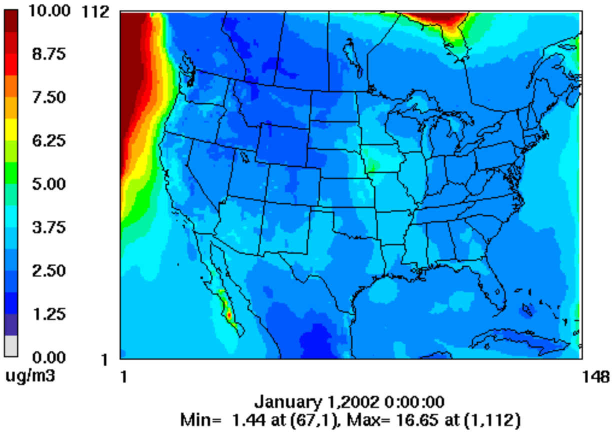

(d) changes in quarterly average $PM_{2.5}$ (Q1)

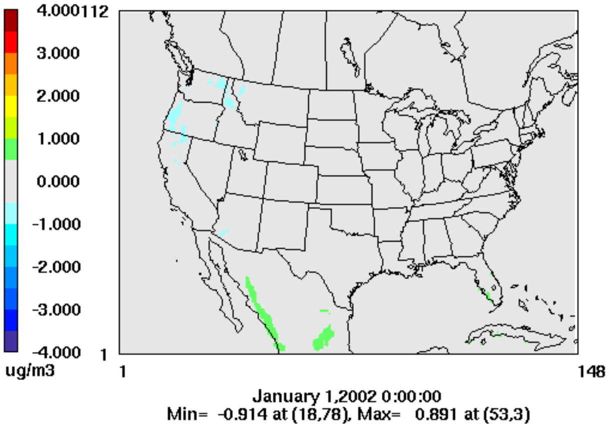

(e) quarterly average $PM_{2.5}$ (base – Q2)

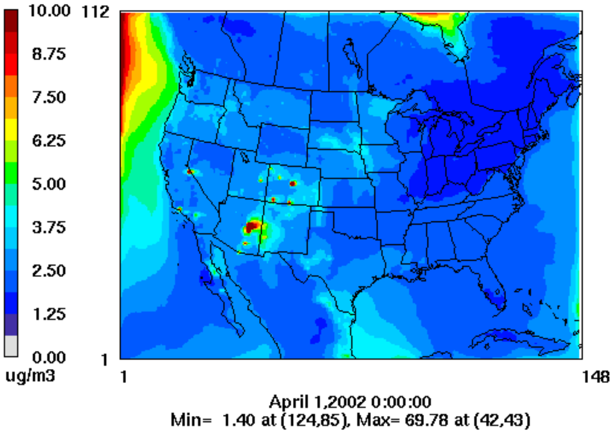

(f) changes in quarterly average $PM_{2.5}$ (Q2)

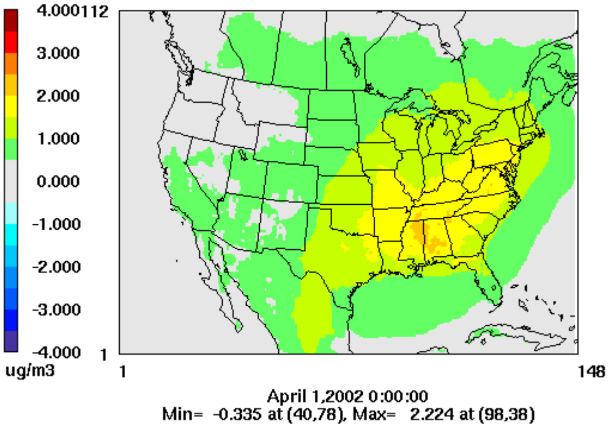

(g) quarterly average $PM_{2.5}$ (base – Q3) (h) changes in quarterly average $PM_{2.5}$ (Q3)

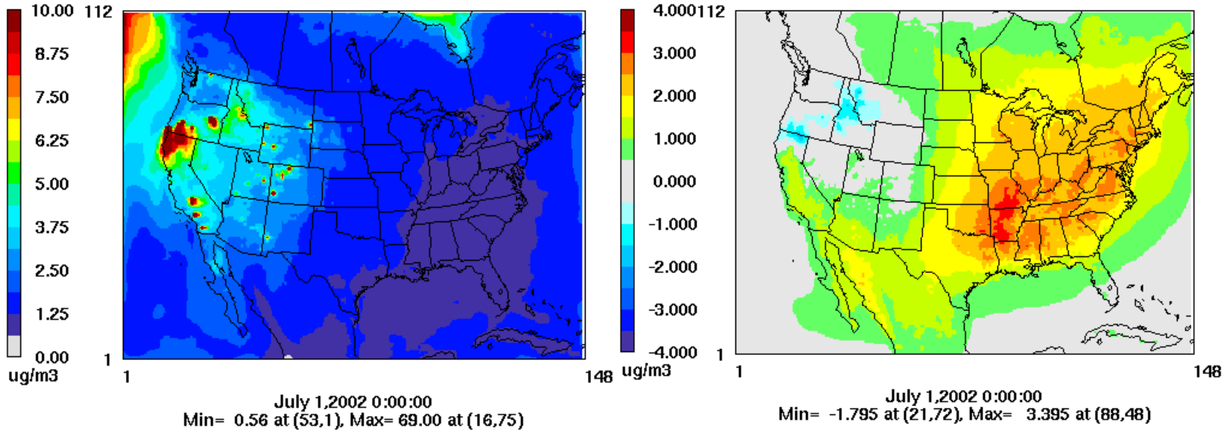

(i) quarterly average $PM_{2.5}$ (base – Q4) (j) changes in quarterly average $PM_{2.5}$ (Q4)

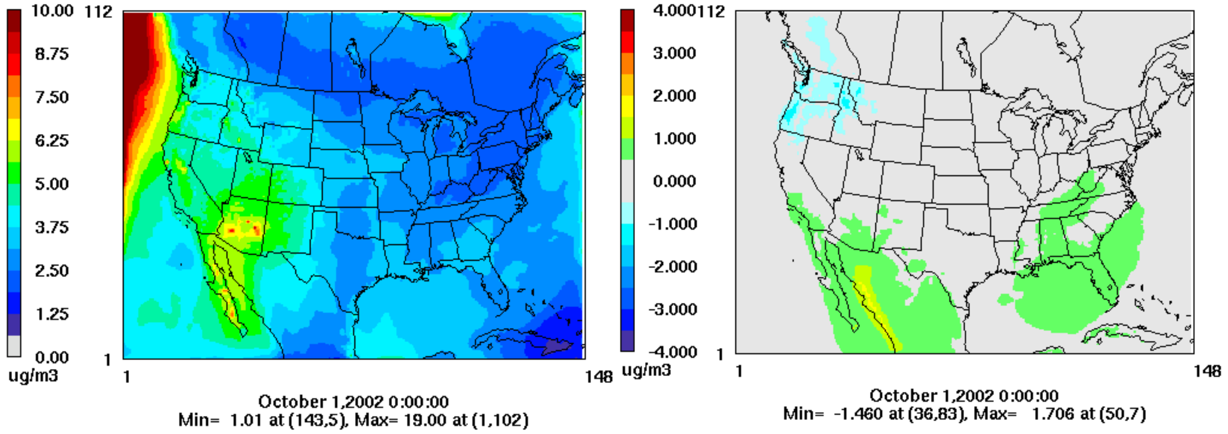

Figure 2-26. Impact of the updated SOA model with MEGAN emissions on $PM_{2.5}$. The concentration changes are given as $PM_{2.5}$ from the new case (simulation with the updated SOA model) minus $PM_{2.5}$ from the base case (simulation before the updated SOA model is adopted).

2.5. Pre-industrial Methane Level

Current version of CMAQ uses a constant background methane concentration of 1.85 ppm. We changed it to 0.70 ppm to reflect pre-industrial level estimated by Blunier et al. (1993).

Methane reacts with hydroxyl radical to form methyl peroxy radical ($CH_3O_2\cdot$). Reaction of $CH_3O_2\cdot$ with NO produces methoxy radical ($CH_3O\cdot$), whose oxidation yields formaldehyde and hydroperoxy radical ($HO_2\cdot$). Under sufficiently high NOx conditions, $CH_3O_2\cdot$ and $HO_2\cdot$ react predominantly with NO, which leads to ozone formation. Therefore, reducing methane concentration means less ozone formation (Figure 2-27). Ozone decreases due to reduced methane and ozone increases due to lightning NOx emissions show similar spatial patterns while magnitude of the former is much smaller than that of the latter. Total $PM_{2.5}$ concentrations slightly increase due to lowered methane (Figure 2-28). The increases in $PM_{2.5}$ mostly come from increases in sodium and chloride (not shown). While it is not clear how reduced background methane affects sodium and chloride concentrations, their changes are very small.

(a) annual average O_3 (base case)

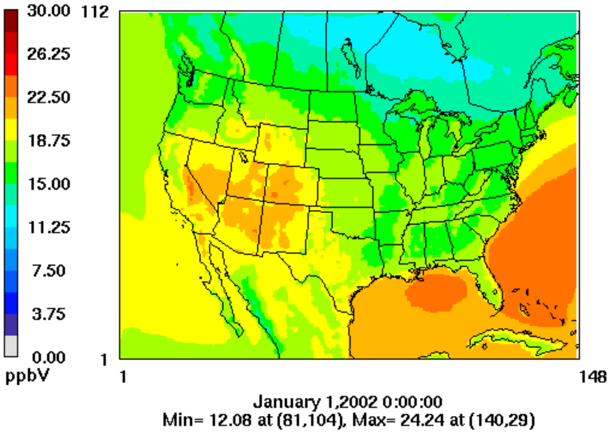

(b) changes in annual average O_3

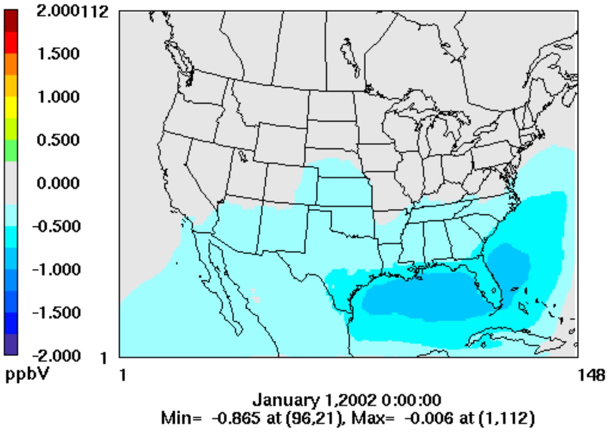

(c) quarterly average O_3 (base – Q1)

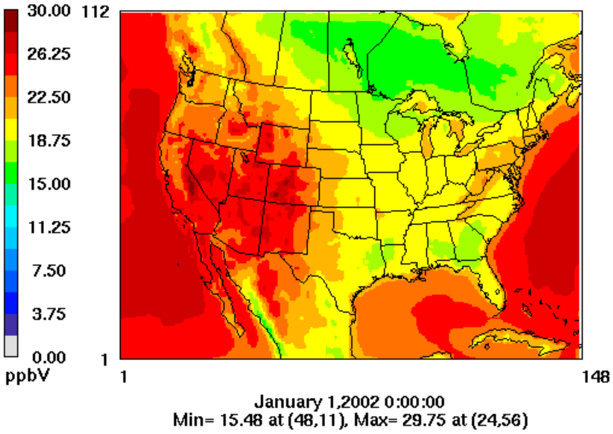

(d) changes in quarterly average O_3 (Q1)

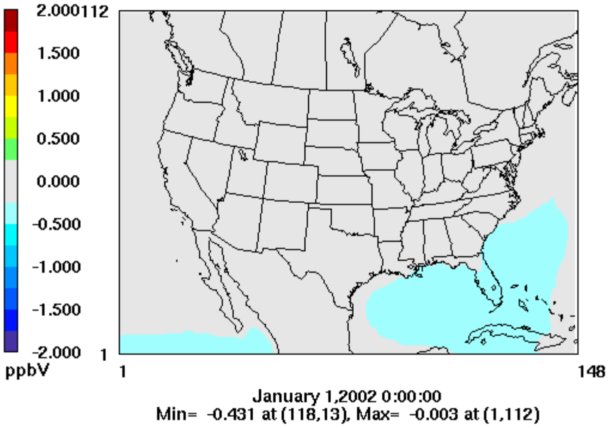

(e) quarterly average O_3 (base – Q2)

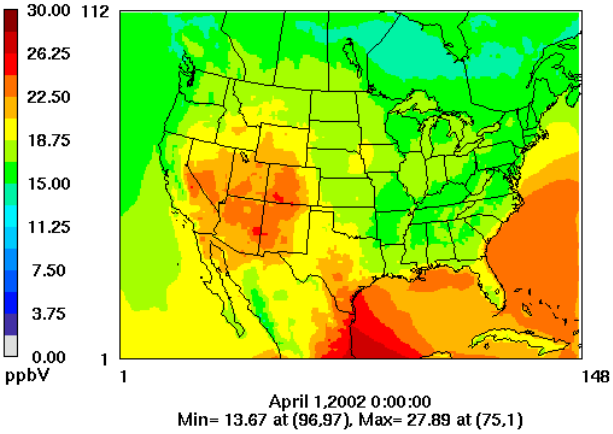

(f) changes in quarterly average O_3 (Q2)

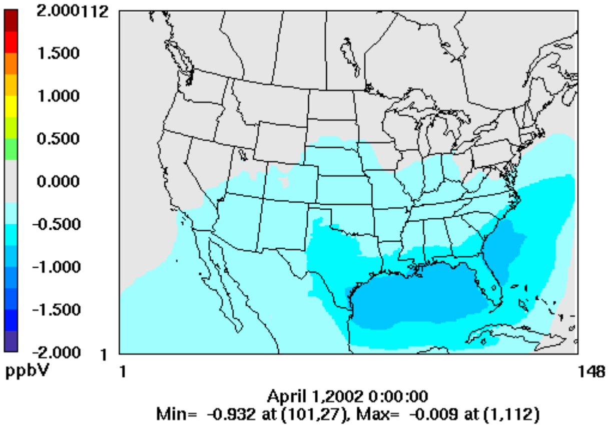

(g) quarterly average O_3 (base – Q3)   (h) changes in quarterly average O_3 (Q3)

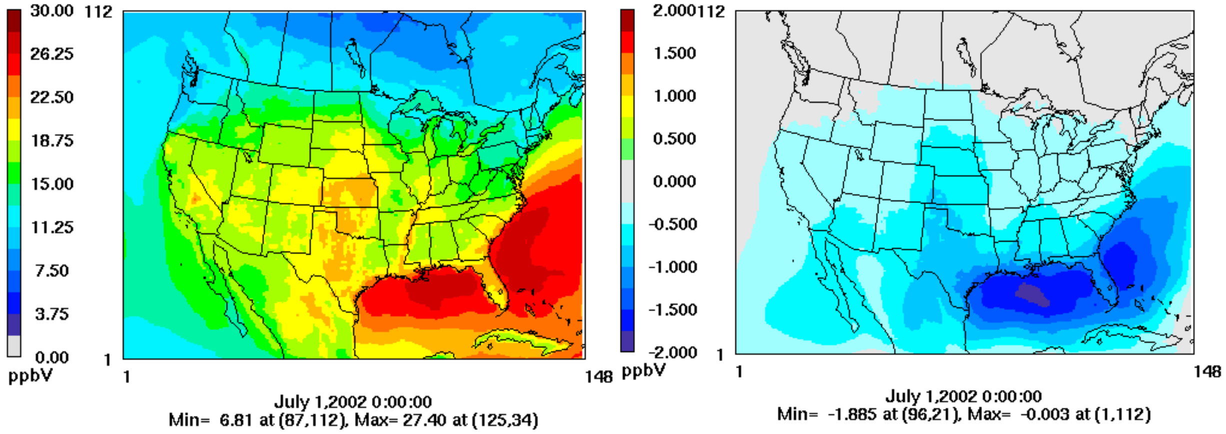

(i) quarterly average O_3 (base – Q4)   (j) changes in quarterly average O_3 (Q4)

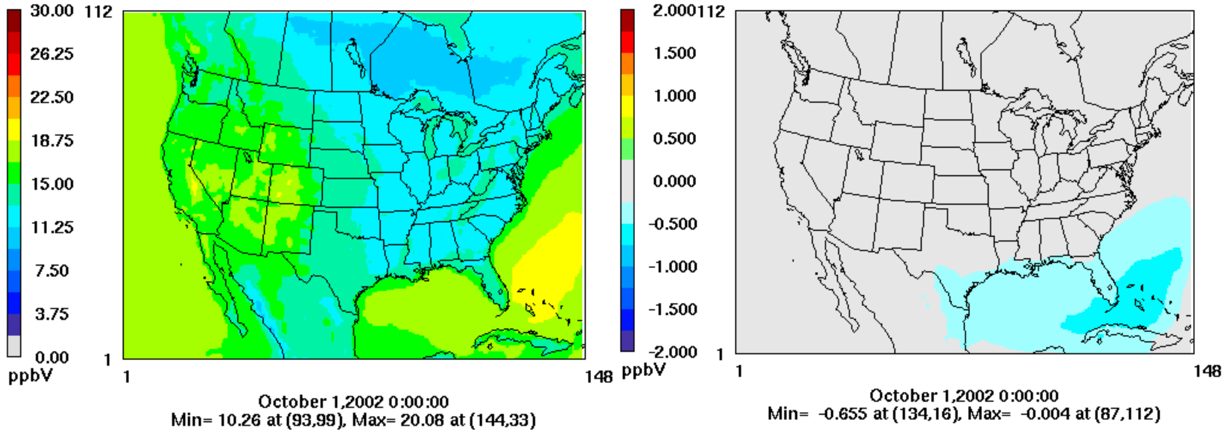

Figure 2-27. Impact of background methane adjusted to pre-industrial level on ozone. The concentration changes are given as ozone from the new case (simulation with the pre-industrial level of methane) minus ozone from the base case (simulation with the original background methane concentration).

(a) annual average $PM_{2.5}$ (base case)

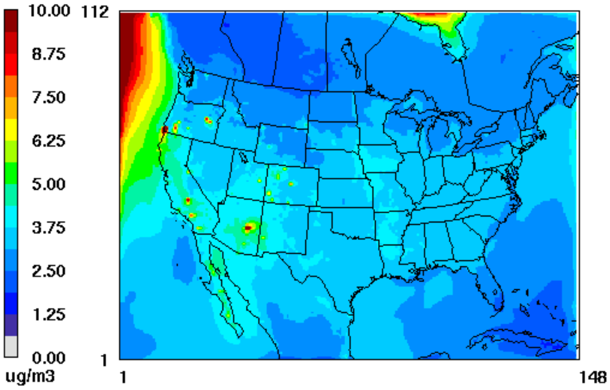

January 1,2002 0:00:00
Min= 1.81 at (141,5), Max= 21.28 at (42,43)

(b) changes in annual average $PM_{2.5}$

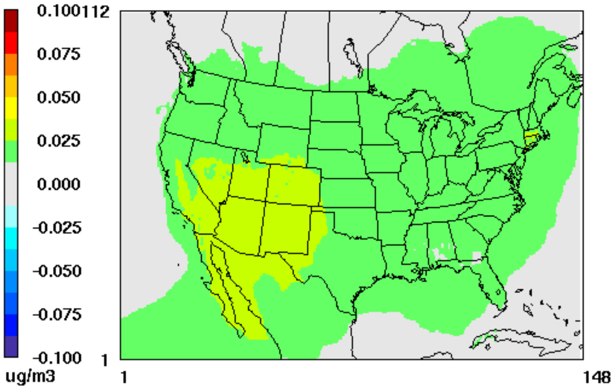

January 1,2002 0:00:00
Min= 0.001 at (1,112), Max= 0.037 at (53,38)

(c) quarterly average $PM_{2.5}$ (base – Q1)

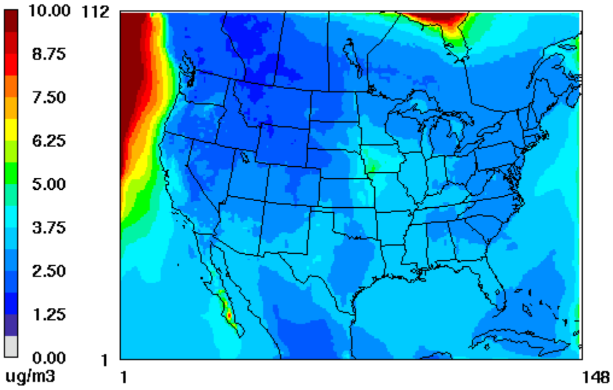

January 1,2002 0:00:00
Min= 1.51 at (27,93), Max= 16.65 at (1,112)

(d) changes in quarterly average $PM_{2.5}$ (Q1)

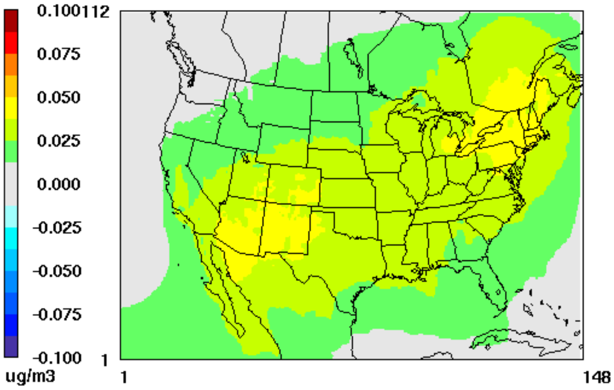

January 1,2002 0:00:00
Min= 0.000 at (1,112), Max= 0.047 at (39,40)

(e) quarterly average $PM_{2.5}$ (base – Q2)

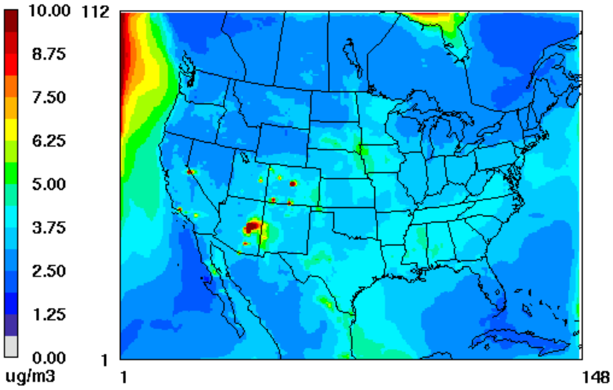

April 1,2002 0:00:00
Min= 1.80 at (28,27), Max= 70.20 at (42,43)

(f) changes in quarterly average $PM_{2.5}$ (Q2)

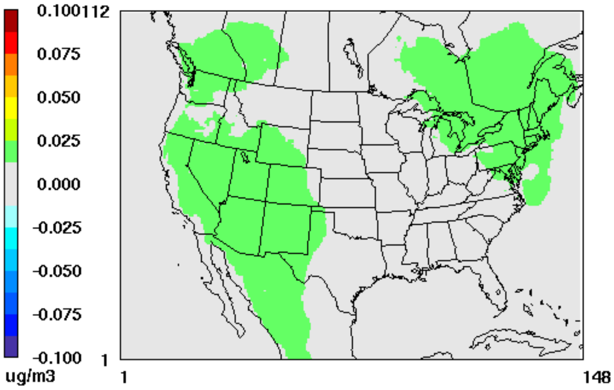

April 1,2002 0:00:00
Min= -0.003 at (104,34), Max= 0.021 at (53,33)

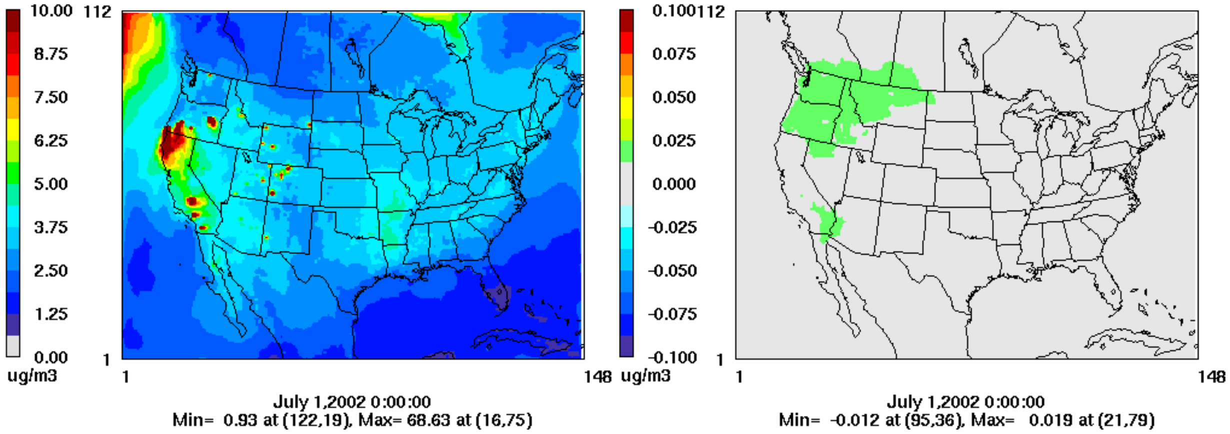
(g) quarterly average $PM_{2.5}$ (base – Q3) (h) changes in quarterly average $PM_{2.5}$ (Q3)

(i) quarterly average $PM_{2.5}$ (base – Q4) (j) changes in quarterly average $PM_{2.5}$ (Q4)

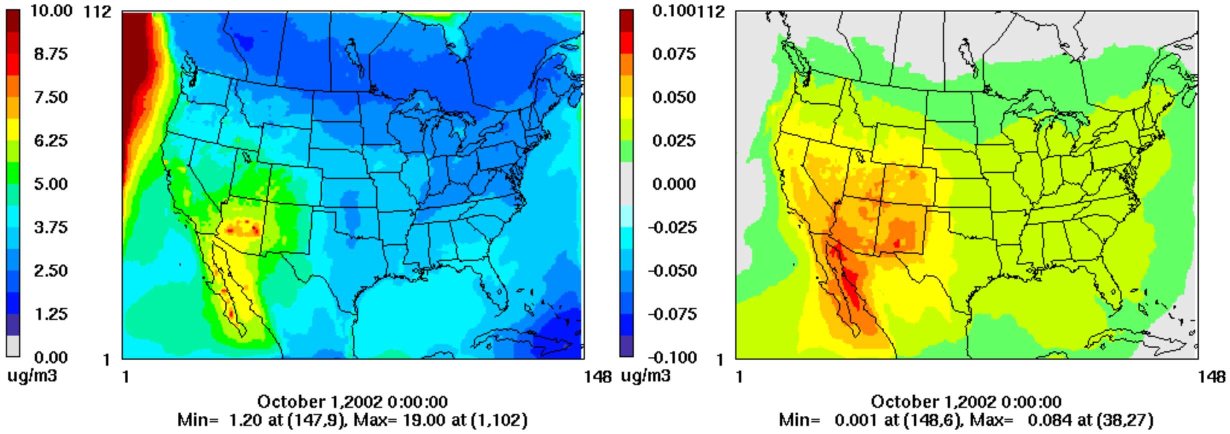

Figure 2-28. Impact of background methane adjusted to pre-industrial level on $PM_{2.5}$. The concentration changes are given as $PM_{2.5}$ from the new case (simulation with the pre-industrial level of methane) minus $PM_{2.5}$ from the base case (simulation with the original background methane concentration).

2.6. Combined Impacts of Revised Natural Components

Figure 2-29 shows overall impacts of the revised natural components on annual and quarterly averages of ozone concentrations. Impact of lightning NOx emissions is dominating the ozone increases with the biggest increases shown over the Gulf of Mexico. The ozone decreases over the central US are mainly due to reduced NO emissions by MEGAN. The $PM_{2.5}$ concentrations are generally increasing with the revised natural sources (Figure 2-30) with major contributions coming from the alternative sea salt emissions and the updated SOA scheme. However, impacts of the alternative sea salt emissions are mostly seen over the northern Pacific Ocean and relatively minor increases are shown inland. Increases in $PM_{2.5}$ over southeastern US are primarily due to additional SOA formation from sesquiterpenes and polymerization.

(a) annual average O_3 (revised case)

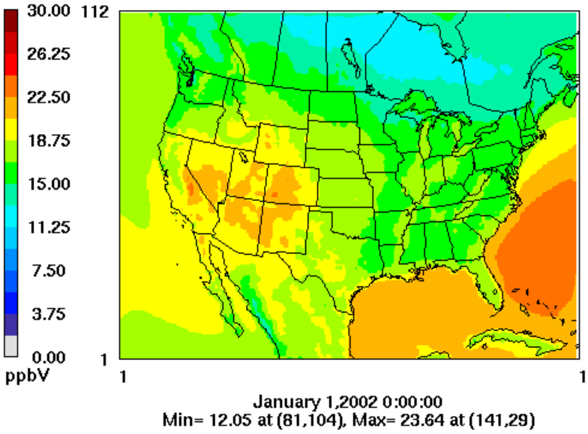

(b) changes in annual average O_3

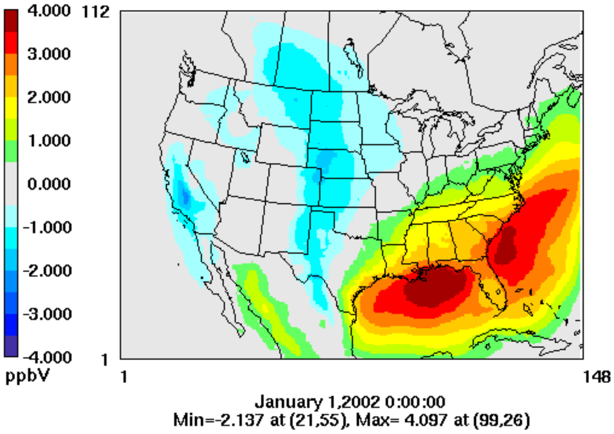

(c) quarterly average O_3 (revised – Q1)

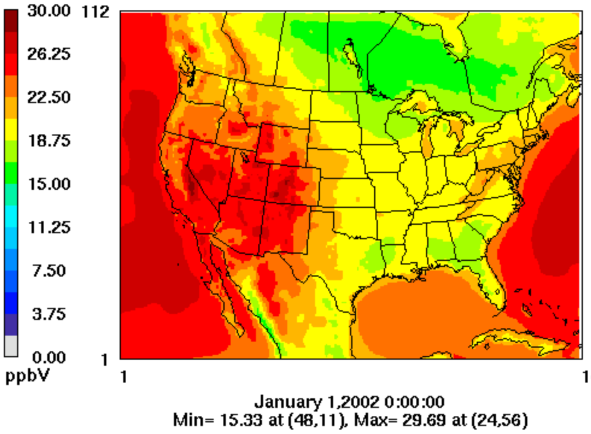

(d) changes in quarterly average O_3 (Q1)

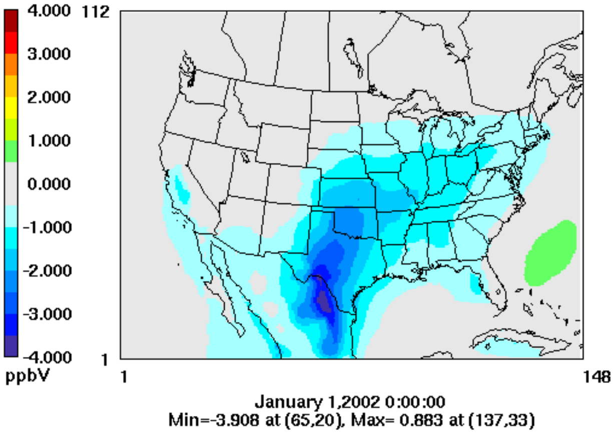

(e) quarterly average O_3 (revised – Q2)

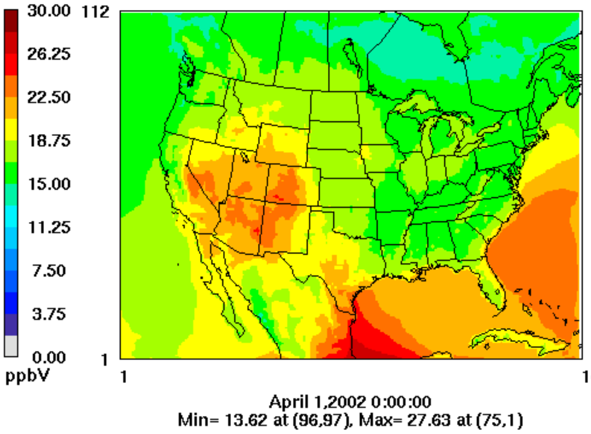

(f) changes in quarterly average O_3 (Q2)

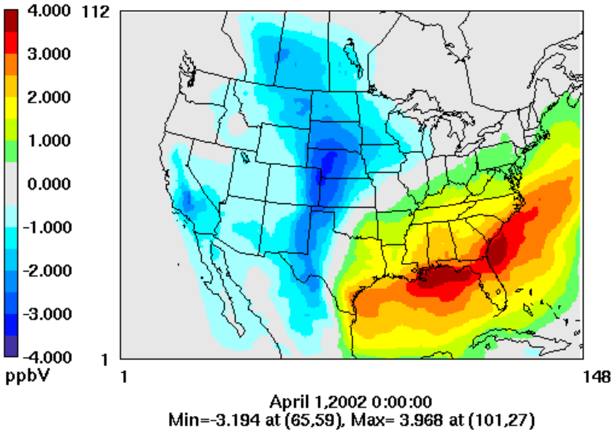

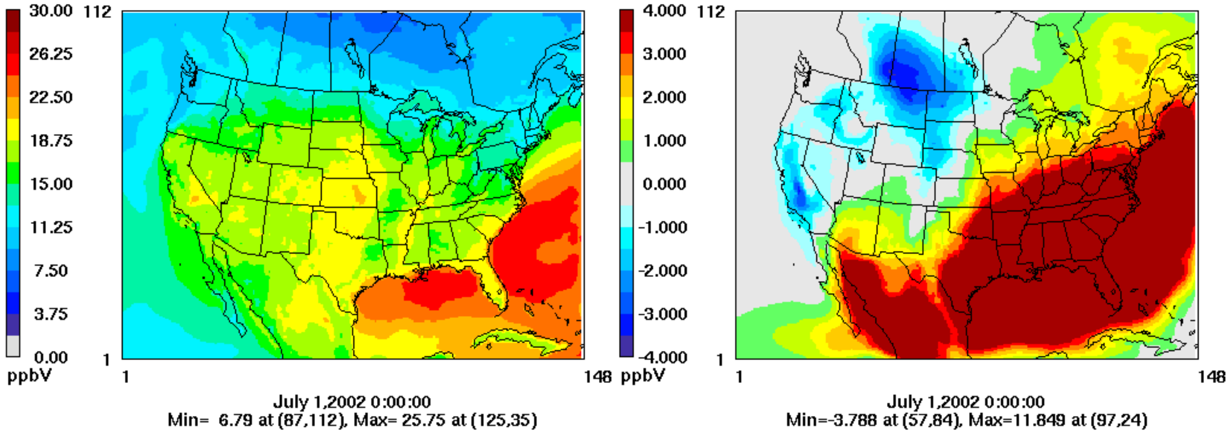

(g) quarterly average O_3 (revised – Q3)

(h) changes in quarterly average O_3 (Q3)

July 1,2002 0:00:00
Min= 6.79 at (87,112), Max= 25.75 at (125,35)

July 1,2002 0:00:00
Min=-3.788 at (57,84), Max=11.849 at (97,24)

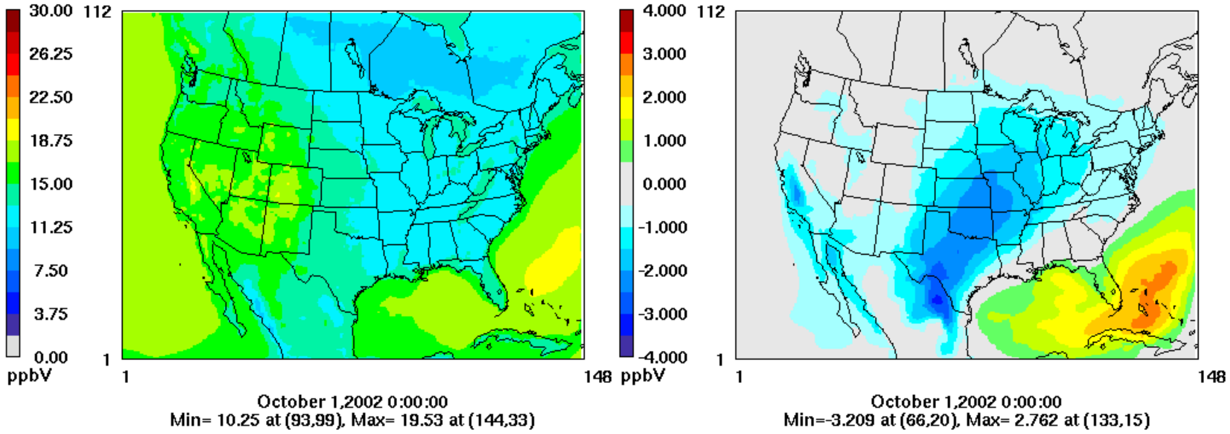

(i) quarterly average O_3 (revised – Q4)

(j) changes in quarterly average O_3 (Q4)

October 1,2002 0:00:00
Min= 10.25 at (93,99), Max= 19.53 at (144,33)

October 1,2002 0:00:00
Min=-3.209 at (66,20), Max= 2.762 at (133,15)

Figure 2-29. Combined impact of the revised natural components on ozone. The concentration changes are given as ozone from the revised case (simulation with all the revised natural components) minus ozone from the base case (simulation with original natural components).

(a) annual average $PM_{2.5}$ (revised case)

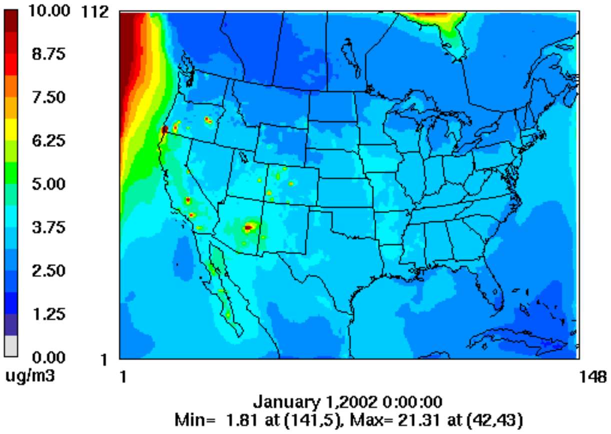

(b) changes in annual average $PM_{2.5}$

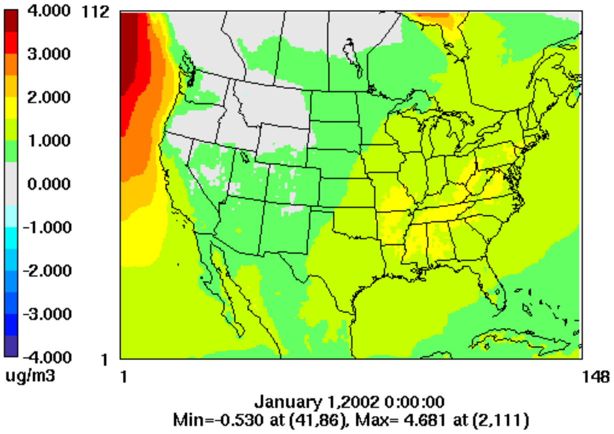

(c) quarterly average $PM_{2.5}$ (revised – Q1)

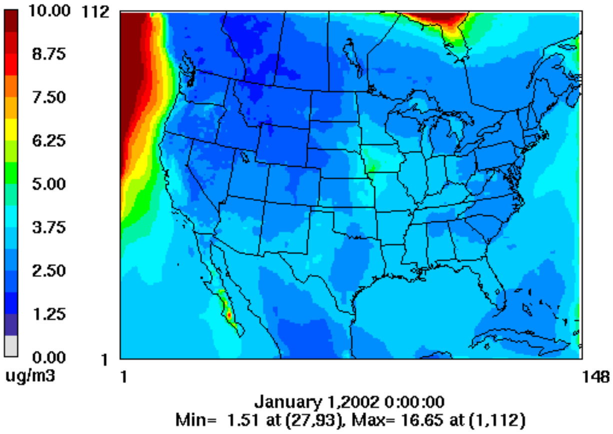

(d) changes in quarterly average $PM_{2.5}$ (Q1)

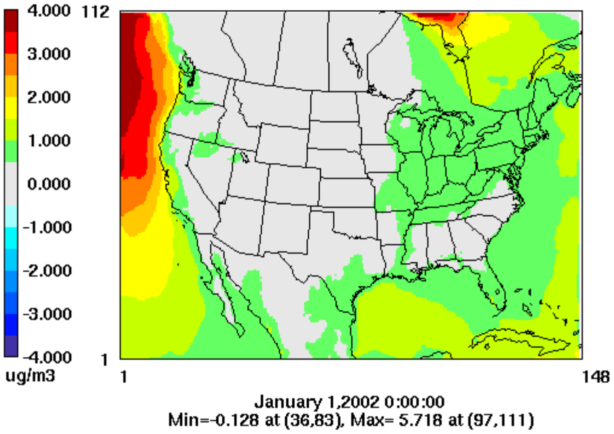

(e) quarterly average $PM_{2.5}$ (revised – Q2)

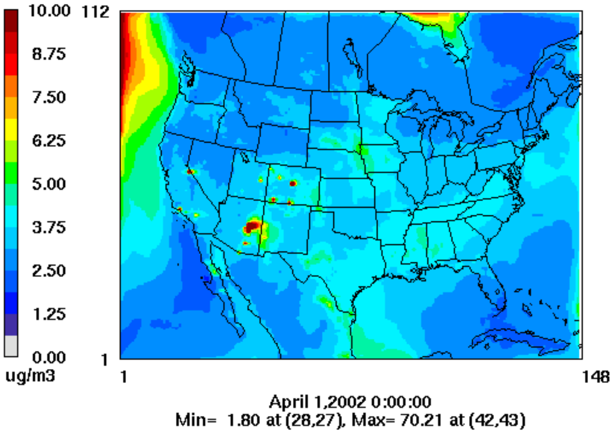

(f) changes in quarterly average $PM_{2.5}$ (Q2)

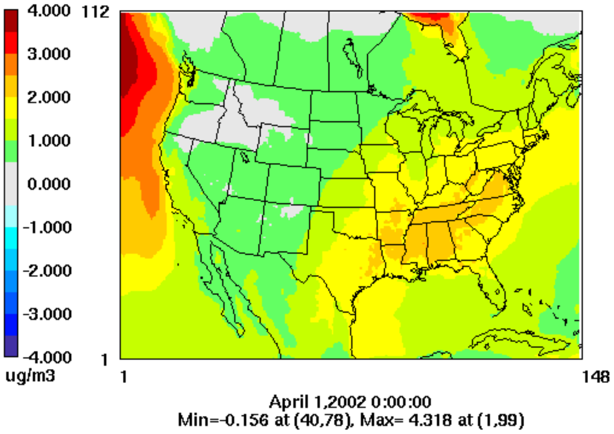

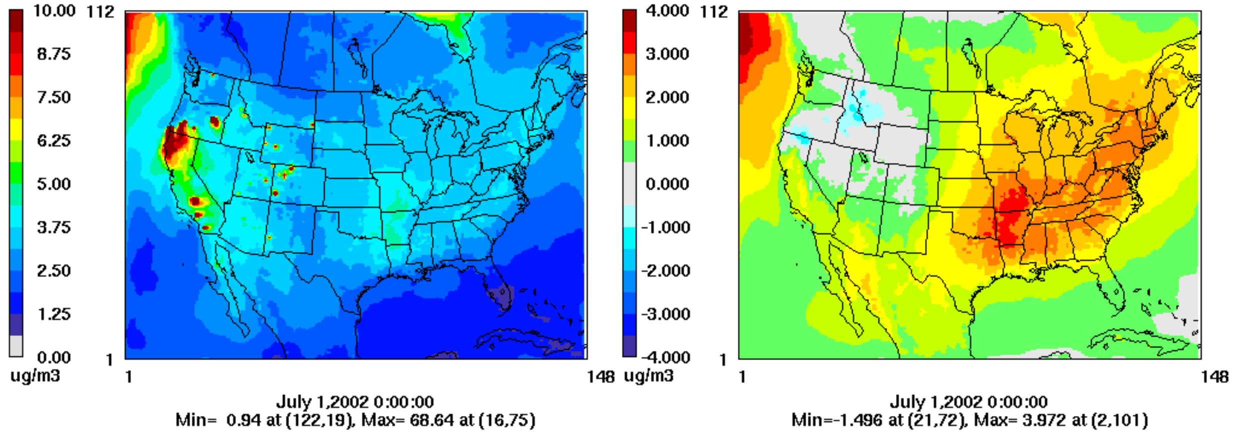

(g) quarterly average $PM_{2.5}$ (revised – Q3)

(h) changes in quarterly average $PM_{2.5}$ (Q3)

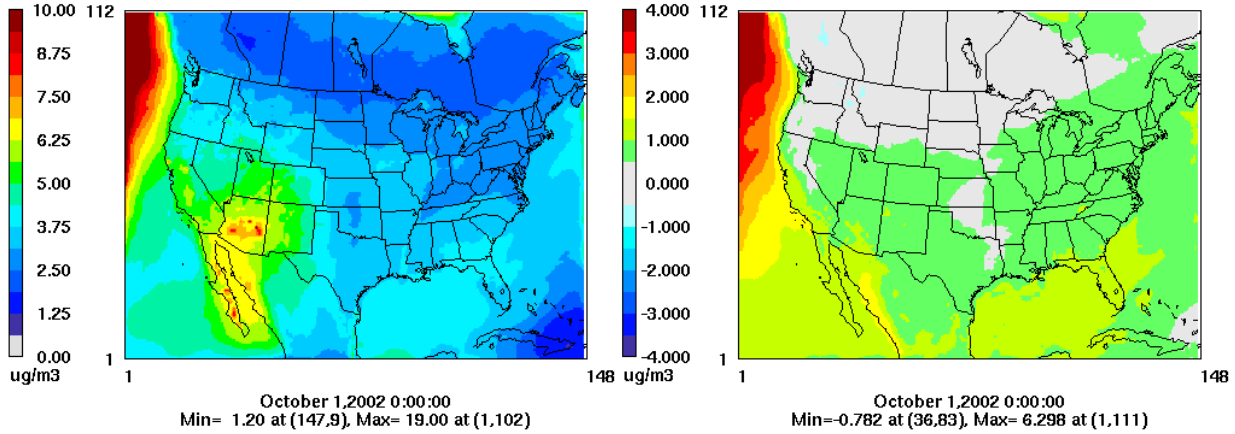

(i) quarterly average $PM_{2.5}$ (revised – Q4)

(j) changes in quarterly average $PM_{2.5}$ (Q4)

Figure 2-30. Combined impact of the revised natural components on $PM_{2.5}$. The concentration changes are given as $PM_{2.5}$ from the revised case (simulation with all the revised natural components) minus $PM_{2.5}$ from the base case (simulation with original natural components).

2.7. Comparison with Best Estimates of Natural Background Ozone and $PM_{2.5}$

Natural sources of ozone include photochemical production from biogenic VOC and NOx precursors and intrusion of ozone from the stratosphere. Although there is large uncertainty in the natural ozone levels, estimates of pre-industrial ozone levels typically range from 20 to 30 ppb. For air quality planning purposes, a more useful metric is the Policy-Relevant Background (PRB) ozone concentration which is defined as that which would occur in the United States in the absence of anthropogenic emissions of VOC and NOx in continental North America (EPA, 2007). The PRB is especially useful for ozone planning using air quality models because it defines the minimum level of ozone that can be simulated in the model when all anthropogenic emissions of VOC and NOx are controlled 100% in North America. PRB ozone levels can be estimated using model simulations. It may also be possible to estimate PRB ozone levels using empirical data at remote sites. In this study, our natural emissions simulations also exclude anthropogenic VOC and NOx emissions outside North America because we use boundary conditions derived from a natural emissions simulation of GEOS-CHEM. Therefore, the ozone results presented here should be less than the PRB ozone levels. Model simulations of natural ozone levels have previously been completed using GEOS-CHEM, however, the poor grid resolution and temporal resolution (i.e., three hour time steps) raises uncertainty in the GEOS-CHEM results. Previous model simulations of natural ozone completed by WRAP did not include lightning NOx emissions, thus, the results presented here are the best available estimate of present day natural ozone levels in North America.

Natural levels of ambient ozone and $PM_{2.5}$ can be considered in two different ways: (1) the historical ambient levels prior to the industrial revolution, when anthropogenic activity began to extensively alter the natural environment; and (2) ambient concentrations of ozone and $PM_{2.5}$ from natural sources in the present day environment. It is not possible to empirically determine the ambient ozone and $PM_{2.5}$ in the historical environment; however, it is possible to perform model simulations of pre-industrial emissions and ambient ozone and $PM_{2.5}$ concentrations. For the purpose of this study, and for developing NAAQS attainment strategies, it is more useful to assess the ambient concentrations from natural sources in the present day environment. Thus, in the natural emissions simulations described here, we used only the biogenic emissions from the emissions data developed for 2002.

Estimates of natural haze levels have been developed by the US EPA for visibility planning purposes and are described in *Guidance for Estimating Natural Visibility Conditions under the Regional Haze Rule* (EPA, 2003). The Regional Haze Rule requires that natural haze levels be attained in Class I areas by the year 2064, and the natural haze levels are used in calculating progress toward that goal for intermediate years. The natural haze levels developed by EPA for reasonable progress calculations were based on ambient data analysis for days with good visibility. It is probable that the results of data analysis for clean days will differ from the results of model simulations of natural visibility, especially when natural wild fire emissions are included in the model simulation. This creates the possibility that modeled levels of natural haze might be inconsistent with the values estimated by EPA for visibility planning. If natural haze levels calculated by the model are greater than the levels used in the EPA guidance for reasonable progress calculation, this would make it difficult for modeling studies to demonstrate progress in attaining visibility goals because the model would predict haze levels that exceeded EPA's natural haze levels even if all anthropogenic sources of $PM_{2.5}$ were removed from the modeling.

The EPA guidance does make provision for refined estimates of site specific background haze that differ from the default values using either data analysis or model simulations.

To compare the results of the natural simulations in this study to the EPA guidance values, we calculated the $PM_{2.5}$ concentrations for the average of the 20% of the best visibility days, shown in Table 2-2, for each IMPROVE site. From Table 2-1, the sum of the $PM_{2.5}$ species for the EPA guidance values is 1.21 $\mu g/m^3$. From Table 2-2, the modeled $PM_{2.5}$ on the best visibility days ranges from about 0.2 to 1.9 $\mu g/m^3$, and at a majority of the IMPROVE sites the modeled values less than the clean values in the EPA guidance document. The model results could be used as part of the process of refining the estimates of natural background haze, and these results indicate that natural visibility conditions would be better than the default values used in the EPA guidance. However, these model simulations were completed using the boundary concentrations from the natural GEOS-CHEM simulation. If boundary concentrations were used from a GEOS-CHEM simulation with anthropogenic emissions outside North America, the $PM_{2.5}$ concentrations for the best visibility days would be greater than the values in Table 2-2.

Table 2-1. Average natural levels of aerosol components from Table 2-1 of *Guidance for Estimating Natural Visibility Conditions under the Regional Haze Rule* (EPA, 2003).

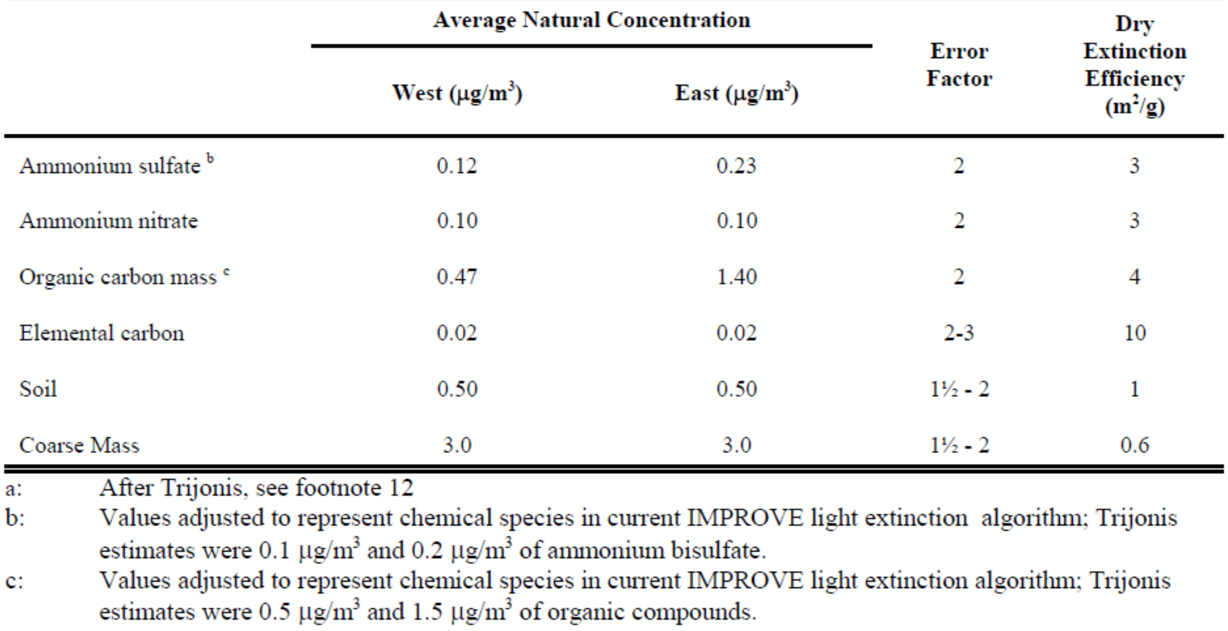

	Average Natural Concentration		**Error Factor**	**Dry Extinction Efficiency (m^2/g)**
	West ($\mu g/m^3$)	**East ($\mu g/m^3$)**		
Ammonium sulfate [b]	0.12	0.23	2	3
Ammonium nitrate	0.10	0.10	2	3
Organic carbon mass [c]	0.47	1.40	2	4
Elemental carbon	0.02	0.02	2-3	10
Soil	0.50	0.50	1½ - 2	1
Coarse Mass	3.0	3.0	1½ - 2	0.6

a: After Trijonis, see footnote 12

b: Values adjusted to represent chemical species in current IMPROVE light extinction algorithm; Trijonis estimates were 0.1 $\mu g/m^3$ and 0.2 $\mu g/m^3$ of ammonium bisulfate.

c: Values adjusted to represent chemical species in current IMPROVE light extinction algorithm; Trijonis estimates were 0.5 $\mu g/m^3$ and 1.5 $\mu g/m^3$ of organic compounds.

Table 2-2. CMAQ model simulated PM2.5 concentration on the best 20% modeled visibility days at each IMPROVE site.

Station	Ammonium Sulfate (μg/m^3)		Ammonium Nitrate (μg/m^3)		Organic Carbon Mass (μg/m^3)		Elemental Carbon (μg/m^3)		Soil (μg/m^3)		PM25 (μg/m^3)	
	current	**revised**	**current**	**revised**	**current**	**revised**	**current**	**revised**	**current**	**revised**	**current**	**revised**
AGTI1	0.25	**0.31**	0.09	**0.09**	0.26	**0.15**	0.01	**0.01**	0.31	**0.40**	0.83	**0.86**
BADL1	0.19	**0.22**	0.11	**0.05**	0.25	**0.04**	0.00	**0.00**	0.82	**0.85**	1.31	**1.11**
BAND1	0.13	**0.16**	0.06	**0.09**	0.34	**0.19**	0.01	**0.01**	0.23	**0.32**	0.73	**0.71**
BIBE1	0.18	**0.23**	0.15	**0.10**	0.32	**0.18**	0.00	**0.00**	0.29	**0.35**	0.86	**0.78**
BLIS1	0.10	**0.13**	0.03	**0.04**	0.13	**0.06**	0.00	**0.00**	0.18	**0.24**	0.41	**0.42**
BOAP1	0.17	**0.23**	0.07	**0.10**	0.30	**0.22**	0.01	**0.01**	0.24	**0.33**	0.73	**0.79**
BOWA1	0.15	**0.20**	0.02	**0.02**	0.67	**0.79**	0.05	**0.05**	0.32	**0.35**	1.18	**1.36**
BRCA1	0.20	**0.25**	0.04	**0.05**	0.22	**0.04**	0.00	**0.00**	0.15	**0.19**	0.57	**0.48**
BRET1	0.12	**0.16**	0.12	**0.28**	0.07	**0.21**	0.01	**0.01**	0.21	**0.27**	0.47	**0.82**
BRID1	0.20	**0.23**	0.04	**0.05**	0.11	**0.05**	0.00	**0.00**	0.22	**0.24**	0.53	**0.52**
BRIG1	0.14	**0.22**	0.04	**0.09**	0.15	**0.40**	0.01	**0.01**	0.22	**0.31**	0.52	**0.95**
BRLA1	0.17	**0.20**	0.04	**0.05**	0.08	**0.04**	0.00	**0.00**	0.15	**0.17**	0.42	**0.43**
CABI1	0.10	**0.15**	0.02	**0.03**	0.43	**0.11**	0.00	**0.00**	0.10	**0.11**	0.63	**0.37**
CACR1	0.15	**0.18**	0.17	**0.06**	0.34	**0.31**	0.00	**0.00**	0.50	**0.53**	1.09	**1.02**
CADI1	0.17	**0.21**	0.12	**0.09**	0.16	**0.46**	0.00	**0.01**	0.43	**0.51**	0.81	**1.20**
CANY1	0.26	**0.32**	0.04	**0.07**	0.25	**0.08**	0.00	**0.00**	0.28	**0.36**	0.77	**0.76**
CHAS1	0.12	**0.18**	0.09	**0.27**	0.07	**0.27**	0.00	**0.01**	0.23	**0.34**	0.46	**0.95**
CHIR1	0.23	**0.28**	0.11	**0.12**	0.46	**0.36**	0.04	**0.04**	0.43	**0.51**	1.19	**1.21**
COGO1	0.11	**0.18**	0.02	**0.03**	0.25	**0.10**	0.00	**0.00**	0.12	**0.17**	0.47	**0.43**
COHU1	0.12	**0.16**	0.07	**0.10**	0.21	**0.42**	0.00	**0.00**	0.48	**0.58**	0.84	**1.21**
CRLA1	0.08	**0.12**	0.02	**0.03**	0.25	**0.05**	0.00	**0.00**	0.07	**0.10**	0.40	**0.26**
CRMO1	0.13	**0.18**	0.04	**0.05**	0.32	**0.14**	0.00	**0.00**	0.32	**0.39**	0.78	**0.72**
DEVA1	0.20	**0.27**	0.08	**0.06**	0.36	**0.08**	0.00	**0.00**	0.29	**0.37**	0.86	**0.70**
DOME1	0.18	**0.21**	0.08	**0.06**	0.34	**0.09**	0.00	**0.00**	0.19	**0.22**	0.73	**0.52**
DOSO1	0.12	**0.14**	0.06	**0.07**	0.08	**0.16**	0.00	**0.00**	0.16	**0.19**	0.38	**0.51**
EVER1	0.13	**0.19**	0.10	**0.27**	0.04	**0.20**	0.00	**0.01**	0.17	**0.26**	0.39	**0.81**
GAMO1	0.12	**0.17**	0.03	**0.04**	0.46	**0.06**	0.00	**0.00**	0.20	**0.22**	0.78	**0.46**
GICL1	0.19	**0.22**	0.06	**0.06**	0.22	**0.11**	0.00	**0.00**	0.22	**0.26**	0.63	**0.59**
GRBA1	0.21	**0.27**	0.04	**0.05**	0.30	**0.08**	0.00	**0.00**	0.19	**0.23**	0.70	**0.57**
GRCA2	0.17	**0.19**	0.05	**0.06**	0.38	**0.20**	0.03	**0.03**	0.14	**0.16**	0.71	**0.59**
GRSA1	0.19	**0.22**	0.05	**0.07**	0.21	**0.10**	0.00	**0.00**	0.22	**0.27**	0.62	**0.62**
GRSM1	0.15	**0.19**	0.07	**0.10**	0.16	**0.20**	0.00	**0.00**	0.26	**0.30**	0.59	**0.71**
GUMO1	0.20	**0.25**	0.12	**0.10**	0.29	**0.20**	0.00	**0.01**	0.33	**0.42**	0.86	**0.89**

Table 2-2. Continued.

Station	Ammonium Sulfate ($\mu g/m^3$)		Ammonium Nitrate ($\mu g/m^3$)		Organic Carbon Mass ($\mu g/m^3$)		Elemental Carbon ($\mu g/m^3$)		Soil ($\mu g/m^3$)		PM25 ($\mu g/m^3$)	
	current	revised	current	revised	current	revised	current	revised	current	revised	current	revised
HECA1	0.14	**0.19**	0.04	**0.05**	0.47	**0.16**	0.00	**0.00**	0.32	**0.38**	0.93	**0.72**
HEGL1	0.16	**0.20**	0.15	**0.07**	0.21	**0.39**	0.01	**0.01**	0.62	**0.72**	1.08	**1.32**
HILL1	0.19	**0.22**	0.05	**0.06**	0.19	**0.07**	0.00	**0.00**	0.18	**0.21**	0.55	**0.48**
HOOV1	0.14	**0.17**	0.05	**0.05**	0.12	**0.04**	0.00	**0.00**	0.15	**0.18**	0.41	**0.39**
IKBA1	0.18	**0.21**	0.07	**0.08**	0.27	**0.30**	0.02	**0.02**	0.16	**0.19**	0.63	**0.73**
ISLE1	0.15	**0.20**	0.02	**0.02**	0.22	**0.32**	0.00	**0.00**	0.17	**0.23**	0.52	**0.72**
JARB1	0.16	**0.22**	0.04	**0.06**	0.16	**0.04**	0.00	**0.00**	0.19	**0.23**	0.51	**0.49**
JARI1	0.16	**0.19**	0.06	**0.08**	0.16	**0.24**	0.00	**0.01**	0.30	**0.40**	0.61	**0.84**
JOSH1	0.21	**0.25**	0.07	**0.07**	0.26	**0.10**	0.01	**0.01**	0.17	**0.20**	0.64	**0.54**
KALM1	0.10	**0.17**	0.02	**0.03**	0.17	**0.05**	0.00	**0.00**	0.04	**0.06**	0.30	**0.27**
LABE1	0.09	**0.12**	0.02	**0.03**	0.29	**0.08**	0.00	**0.00**	0.07	**0.09**	0.45	**0.29**
LAVO1	0.09	**0.12**	0.03	**0.04**	0.14	**0.06**	0.00	**0.00**	0.09	**0.12**	0.32	**0.30**
LIGO1	0.13	**0.15**	0.07	**0.07**	0.16	**0.17**	0.00	**0.00**	0.37	**0.44**	0.67	**0.78**
LOST1	0.23	**0.27**	0.14	**0.04**	0.21	**0.29**	0.00	**0.00**	0.54	**0.57**	1.07	**1.11**
MACA1	0.17	**0.21**	0.11	**0.07**	0.12	**0.23**	0.00	**0.00**	0.45	**0.51**	0.79	**0.95**
MELA1	0.24	**0.29**	0.12	**0.04**	0.26	**0.29**	0.00	**0.00**	0.75	**0.79**	1.31	**1.34**
MEVE1	0.20	**0.24**	0.05	**0.09**	0.20	**0.08**	0.00	**0.00**	0.32	**0.41**	0.73	**0.76**
MING1	0.19	**0.24**	0.12	**0.10**	0.19	**0.69**	0.00	**0.01**	0.55	**0.69**	0.97	**1.65**
MOHO1	0.11	**0.18**	0.01	**0.02**	0.17	**0.07**	0.00	**0.00**	0.05	**0.08**	0.31	**0.31**
MONT1	0.13	**0.17**	0.02	**0.03**	0.44	**0.08**	0.00	**0.00**	0.10	**0.11**	0.67	**0.36**
MORA1	0.08	**0.14**	0.01	**0.02**	0.17	**0.03**	0.00	**0.00**	0.03	**0.05**	0.27	**0.21**
MOZI1	0.19	**0.23**	0.04	**0.05**	0.15	**0.07**	0.00	**0.00**	0.17	**0.19**	0.52	**0.51**
NOAB1	0.13	**0.15**	0.03	**0.04**	0.14	**0.08**	0.01	**0.01**	0.15	**0.17**	0.43	**0.42**
NOCA1	0.08	**0.12**	0.01	**0.02**	0.21	**0.04**	0.00	**0.00**	0.04	**0.06**	0.32	**0.21**
OKEF1	0.13	**0.18**	0.08	**0.20**	0.38	**0.49**	0.00	**0.00**	0.16	**0.24**	0.71	**1.02**
OLYM1	0.09	**0.19**	0.01	**0.02**	0.24	**0.09**	0.00	**0.00**	0.03	**0.05**	0.35	**0.29**
PASA1	0.12	**0.18**	0.04	**0.02**	0.58	**0.08**	0.00	**0.00**	0.09	**0.12**	0.80	**0.36**
PEFO1	0.18	**0.22**	0.06	**0.08**	0.31	**0.10**	0.00	**0.00**	0.20	**0.23**	0.70	**0.57**
PHOE1	0.18	**0.25**	0.14	**0.24**	0.22	**0.56**	0.01	**0.02**	0.51	**0.64**	0.99	**1.58**
PINN1	0.17	**0.27**	0.08	**0.10**	0.08	**0.14**	0.00	**0.00**	0.16	**0.23**	0.43	**0.66**
PORE1	0.20	**0.31**	0.05	**0.06**	0.72	**0.80**	0.07	**0.07**	0.15	**0.21**	1.14	**1.36**
PUSO1	0.17	**0.31**	0.02	**0.04**	0.29	**0.17**	0.00	**0.00**	0.12	**0.20**	0.56	**0.63**
QUVA1	0.24	**0.28**	0.11	**0.15**	0.54	**0.48**	0.05	**0.05**	0.39	**0.45**	1.25	**1.31**
REDW1	0.14	**0.25**	0.02	**0.05**	0.42	**0.33**	0.02	**0.02**	0.06	**0.11**	0.62	**0.68**
ROMA1	0.12	**0.18**	0.08	**0.35**	0.10	**0.27**	0.00	**0.01**	0.14	**0.20**	0.40	**0.87**

Table 2-2. Continued.

Station	Ammonium Sulfate ($\mu g/m^3$)		Ammonium Nitrate ($\mu g/m^3$)		Organic Carbon Mass ($\mu g/m^3$)		Elemental Carbon ($\mu g/m^3$)		Soil ($\mu g/m^3$)		PM25 ($\mu g/m^3$)	
	current	**revised**	**current**	**revised**	**current**	**revised**	**current**	**revised**	**current**	**revised**	**current**	**revised**
ROMO1	0.16	**0.19**	0.04	**0.05**	0.10	**0.05**	0.00	**0.00**	0.19	**0.22**	0.46	**0.47**
SACR1	0.19	**0.23**	0.10	**0.11**	0.27	**0.20**	0.01	**0.01**	0.27	**0.34**	0.76	**0.80**
SAGA1	0.18	**0.22**	0.08	**0.08**	0.12	**0.16**	0.01	**0.01**	0.24	**0.31**	0.56	**0.70**
SAGO1	0.18	**0.21**	0.06	**0.06**	0.26	**0.07**	0.00	**0.00**	0.19	**0.22**	0.64	**0.50**
SAGU1	0.17	**0.20**	0.12	**0.13**	0.26	**0.33**	0.01	**0.01**	0.35	**0.42**	0.84	**1.02**
SAMA1	0.12	**0.18**	0.09	**0.25**	0.09	**0.42**	0.00	**0.01**	0.13	**0.19**	0.38	**0.94**
SAPE1	0.16	**0.20**	0.04	**0.08**	0.18	**0.09**	0.00	**0.00**	0.13	**0.16**	0.48	**0.48**
SAWE1	0.19	**0.25**	0.12	**0.16**	0.34	**0.30**	0.01	**0.01**	1.12	**1.26**	1.70	**1.87**
SAWT1	0.10	**0.12**	0.03	**0.04**	0.13	**0.04**	0.00	**0.00**	0.12	**0.15**	0.35	**0.33**
SHEN1	0.12	**0.15**	0.06	**0.08**	0.22	**0.42**	0.01	**0.01**	0.13	**0.16**	0.50	**0.76**
SHRO1	0.12	**0.14**	0.05	**0.09**	0.11	**0.15**	0.00	**0.00**	0.11	**0.14**	0.36	**0.46**
SIAN1	0.17	**0.20**	0.06	**0.08**	0.61	**0.51**	0.08	**0.08**	0.19	**0.23**	1.07	**1.05**
SIPS1	0.12	**0.15**	0.10	**0.13**	0.29	**0.56**	0.00	**0.00**	0.37	**0.46**	0.84	**1.24**
SNPA1	0.14	**0.22**	0.02	**0.02**	0.26	**0.07**	0.00	**0.00**	0.07	**0.10**	0.45	**0.35**
SPOK1	0.15	**0.22**	0.04	**0.06**	0.53	**0.30**	0.00	**0.00**	0.48	**0.57**	1.16	**1.09**
STAR1	0.14	**0.18**	0.04	**0.05**	0.41	**0.18**	0.00	**0.00**	0.33	**0.39**	0.88	**0.75**
SULA1	0.13	**0.17**	0.03	**0.04**	0.51	**0.05**	0.00	**0.00**	0.12	**0.14**	0.76	**0.36**
SWAN1	0.15	**0.23**	0.06	**0.16**	0.11	**0.28**	0.00	**0.00**	0.14	**0.19**	0.40	**0.76**
SYCA1	0.17	**0.20**	0.06	**0.06**	0.34	**0.17**	0.01	**0.01**	0.32	**0.36**	0.85	**0.75**
THRO1	0.17	**0.20**	0.11	**0.03**	0.24	**0.10**	0.00	**0.00**	1.24	**1.26**	1.72	**1.55**
THSI1	0.08	**0.12**	0.02	**0.04**	0.26	**0.05**	0.00	**0.00**	0.05	**0.07**	0.39	**0.24**
ULBE1	0.14	**0.18**	0.05	**0.04**	0.30	**0.04**	0.00	**0.00**	0.27	**0.30**	0.72	**0.51**
UPBU1	0.17	**0.19**	0.15	**0.07**	0.24	**0.51**	0.01	**0.01**	0.57	**0.63**	1.06	**1.36**
VOYA2	0.16	**0.20**	0.03	**0.03**	0.61	**0.74**	0.03	**0.03**	0.28	**0.33**	1.07	**1.27**
WEMI1	0.21	**0.24**	0.04	**0.07**	0.12	**0.08**	0.00	**0.00**	0.21	**0.24**	0.53	**0.58**
WHIT1	0.22	**0.26**	0.07	**0.08**	0.27	**0.13**	0.00	**0.00**	0.31	**0.37**	0.80	**0.77**
WHPA1	0.10	**0.16**	0.02	**0.03**	0.21	**0.06**	0.00	**0.00**	0.07	**0.10**	0.38	**0.30**
WHPE1	0.18	**0.20**	0.05	**0.06**	0.12	**0.06**	0.00	**0.00**	0.23	**0.26**	0.53	**0.52**
WHRI1	0.20	**0.23**	0.04	**0.06**	0.08	**0.04**	0.00	**0.00**	0.20	**0.23**	0.49	**0.51**
WICA1	0.15	**0.19**	0.05	**0.05**	0.38	**0.12**	0.01	**0.01**	0.25	**0.29**	0.79	**0.60**
WIMO1	0.18	**0.20**	0.28	**0.06**	0.07	**0.09**	0.00	**0.00**	0.26	**0.29**	0.68	**0.57**
YELL2	0.12	**0.14**	0.02	**0.03**	0.14	**0.06**	0.00	**0.00**	0.10	**0.12**	0.36	**0.32**
YOSE1	0.13	**0.17**	0.06	**0.07**	0.17	**0.08**	0.00	**0.00**	0.13	**0.16**	0.44	**0.42**
ZION1	0.22	**0.26**	0.05	**0.07**	0.35	**0.21**	0.02	**0.02**	0.27	**0.32**	0.85	**0.81**

3. EVALUATION OF REVISED STANDARD SIMULATION

The objective of the model performance evaluation (MPE) is to determine whether the air quality model performs sufficiently well for an historical period to justify using the model for projecting future conditions or for sensitivity studies. For the MPE we used ground-level ambient monitoring data for 2002 from several routine and research-grade ambient monitoring databases. Ambient ozone data were from the EPA's AQS database and the following were used for fine PM data:

- Interagency Monitoring of Protected Visual Environments (IMPROVE)
- Clean Air Status and Trends Network (CASTNet)
- EPA Speciation Trends Network (STN)

The 2002 CMAQ simulations performed for this study were based on the WRAP 2002 data sets, and the WRAP emissions data were used for the "Current Standard Simulation" (see Section 1.2). The WRAP modeling and emissions is described in Tonnesen et al. (2006a) and that reports includes a model performance evaluation for the original 2002 CMAQ simulation. In this study, we updated the WRAP datasets as described in Section 1.2. The "Revised Standard Simulation" includes the revised natural components discussed in Section 2.

In Section 3.1 we compare the MPE for the two cases, and Section 3.2 presents model results for the fourth highest 8-hr average ozone and for the eighth highest 24-hr average $PM_{2.5}$.

3.1. Evaluation against Monitoring Networks

We compared the model simulated concentrations to ozone data from AQS database and $PM_{2.5}$ data from the IMPROVE and CASTNet data. As performance metrics we selected the mean fractional error (MFE) and mean fractional bias (MFB) because these metrics work better for low ambient concentration than do mean normalized bias and error:

$$MFE = \frac{2}{N}\sum_{i=1}^{N}\left|\frac{P_i - O_i}{P_i + O_i}\right| \quad , \qquad MFB = \frac{2}{N}\sum_{i=1}^{N}\left(\frac{P_i - O_i}{P_i + O_i}\right)$$

where P_i and O_i represent predicted and observed pollutant concentrations, respectively, at the i-th monitoring station (N is total number of the stations).

For the ozone comparison, we compiled statistics on the performance metrics for all AQS sites and for individual sites. Figure 3-1 shows the average of the MFE and MFB for all AQS sites broken down into 4 seasons, where winter, spring summer and fall are defined by the Julian days 1-90, 91-181, 182-274, and 275-365, respectively. Because of the coarse 36 km grid resolution used in this study, we do not expect the model to perform well for ozone in or near urban areas, since the model is not able to resolve fine scale variability in precursor emissions. Moreover, the MFB and MFE averaged over all sites are not useful for distinguishing particular sites or regions where the model performed well or poorly. However, the average AQS metrics are useful in a general sense for comparing the relative performance for the two model cases and for identify seasonal variability in the results. Table 3-1 summarizes the seasonal average performance metrics from Figure 3-1, and it shows that for both the Current Standard and Revised Standard cases, the model over-predicted ozone, on average, and the over-predictions were largest in the summer months. The performance was very similar for the two cases, with the Current Standard case having slightly larger positive bias compared to the Revised Standard case. Finally, it should be noted that no data filter was applied in compiling these performance metrics. Typically, in ozone performance evaluations, a data filter is applied to screen out all data for which the monitored ozone is less than 60 ppb. This is because the model is typically unable to resolve the night time boundary layer height and the effects of local NOx emissions on titrating ozone in the surface layer for urban and suburban sites. This typically results in the model over-predicting ozone for the night time and early morning in the surface layer, and it is likely that the over-prediction bias shown in Table 3-1 is a result of this effect. We calculated the model performance metrics without using the ozone filter because we are most interested in the results for the rural and remote sites for which local NOx emissions and night titration of ozone is less common.

Table 3-1. Performance metrics for the comparison of model ozone to the AQS data.

Season	**Current Standard Case**		**Revised Standard Case**	
	MFB (%)	MFE (%)	MFB (%)	MFE (%)
Winter	8	51	6	51
Spring	13	37	10	37
Summer	21	47	19	47
Fall	14	57	10	57

Figure 3-2 shows ozone model performance calculated using more traditional ozone metrics, as normalized mean bias, for both model simulations with the top plot showing the performance metrics when ozone monitoring data less than 60 ppb are excluded from the evaluation. The bottom plot shows the performance when all ozone data are included in the evaluation. When excluding the low ozone concentration data, the model under-predicts ozone, with the largest under-predictions in the winter months. When all ozone data are included, the model over-predicts ozone. As noted above, because of the coarse grid resolution, we expect the model to under-predict daytime ozone near urban areas. We also expect the model to over-predict low ozone values during the nighttime because of the poor model skill in resolving the nighttime boundary layer. Therefore, these results are consistent with our expectations for model performance for the non-remote AQS ozone monitoring sites.

Although we did not expect good model performance for ozone for the urban influenced AQS sites, we do expect the model to perform better for rural and remote sites where precursor emissions are smaller in magnitude and more homogeneous, and where transported ozone is expected to be a larger contributor in addition to local photochemical production of ozone. For this comparison we used time-series plots and MFB and MFE calculated for the ozone data at the IMPROVE sites for which are usually in remote locations. Figures 3-3 through 3-8 show the model and measured ozone time-series plots at six different IMPROVE sites (Grand Canyon, Yosemite, Joshua Tree, Rocky Mountain, Glacier, and Yellowstone National Parks). The time-series plots and the tabulated MPB metrics in Table 3-2 show that both model simulations have large negative bias, with the exception of Glacier, which appears to be influenced by night time titration of ozone at the monitoring site. The model performs best for the winter months and has largest over-prediction in the summer months. It is possible that the large negative bias in the model results caused by inadequate transport of ozone, or under-estimates of emissions of ozone precursors, or other factors related in errors in model meteorology. The reduced ozone concentrations in the top layers of the GEOS-CHEM BCs to avoid the stratospheric ozone impact could also have contributed to the negative bias at some sites.

Figures 3-9 through 3-11 show results of the model performance evaluation for the Current Standard (base02bnew) and Revised Standard (newanthro) simulations for the PM species, calculated as fractional bias, for the IMPROVE, CASTNet and STN monitoring networks. The results are shown for each component species of $PM_{2.5}$ and averaged for each of the 4 quarters of the model year, the quarters roughly correspond to the 4 seasons where Q1 is winter (January-March), Q2 is spring (April-June), Q3 is summer (July-September) and Q4 is fall (October-December).

Figure 3-9 shows sulfate results for each of the networks, and it also includes gas phase SO_2 for the CASTNet sites. The Revised Standard simulation (newanthro) had greater sulfate concentrations compared to the Current Standard case (base02bnew) and slightly larger over-prediction bias in the winter months and less under-prediction bias for the summer months. It is possible that there was greater sulfate formation in the Revised Standard simulation because it also had higher ozone concentrations compared to the Current Standard case, and the greater oxidant levels would increase the conversion rate of SO_2 to sulfate.

Figure 3-10 shows the MPE results for nitrate. The results were similar for both simulations with slightly greater nitrate concentrations in the Revised Standard case compared to the Current Standard. Both simulations showed large over-prediction bias in the winter months for nitrate.

Figure 3-11 (top left plot) shows that the largest changes in model performance were for OCM, for which the Revised Standard simulation showed improved performance in summer while exhibiting greater negative biases than the Current Standard case in the winter months (the IMPROVE OC measurement data was converted to OCM by multiplying the OCM/OC ratio of 1.8). Figure 3-12 shows that the poorer OCM performance by the Revised Standard case in winter was dominated by the large negative biases at the WRAP stations as the number of IMPROVE sites located in the WRAP states are much greater than that of the sites in the other RPO states. The underprediction of OCM by the Revised Standard run is due to the fact that MEGAN estimates much less monoterpene emissions than SMOKE BEIS3 in the western US. However, the model performance in summer is more important because organic mass tend to be higher in summer than in winter. The Revised Standard case showed much better OCM performance in summer, especially in the southeastern US (VISTAS) where biogenic precursor emissions are relatively high.

Figure 3-11 also shows MPE results for EC, fine soil and total $PM_{2.5}$. Both model simulations under-predicted EC, but the Revised Standard case had greater EC concentrations compared to the Current Standard case and reduced negative bias. The results were similar for both simulations for fine soil, with both cases showing positive bias, and slightly greater positive bias for the Revised Standard case. Figure 3-11 (bottom right plot) shows the MPE results for the sum of total $PM_{2.5}$. As a result of increases in sulfate, EC and fine soil, the Revised Standard case showed greater positive bias for total $PM_{2.5}$ for all four seasons compared to the Current Standard case. Although the bias is slightly greater for total $PM_{2.5}$ in the Revised Standard case, it has improved performance for sulfate, EC, and summer OCM, and this indicates that the Revised Standard case performs better than the Current Standard case.

Table 3-2. Mean fractional bias (%) for the comparison of model ozone to the AQS data for selected IMPROVE sites.

Season	Current Standard	Revised Standard
Grand Canyon		
Winter	-19	-21
Spring	-34	-37
Summer	-34	-37
Fall	-22	-25
Yosemite		
Winter	0	-1
Spring	-20	-23
Summer	-48	-53
Fall	-31	-33
Joshua Tree		
Winter	-14	-18
Spring	-25	-33
Summer	-31	-40
Fall	-30	-35
Rocky Mountain		
Winter	-22	-24
Spring	-24	-27
Summer	-31	-34
Fall	-23	-25
Glacier		
Winter	25	23
Spring	28	25
Summer	48	48
Fall	57	56
Yellowstone		
Winter	-29	-30
Spring	-29	-31
Summer	-34	-36
Fall	-19	-21

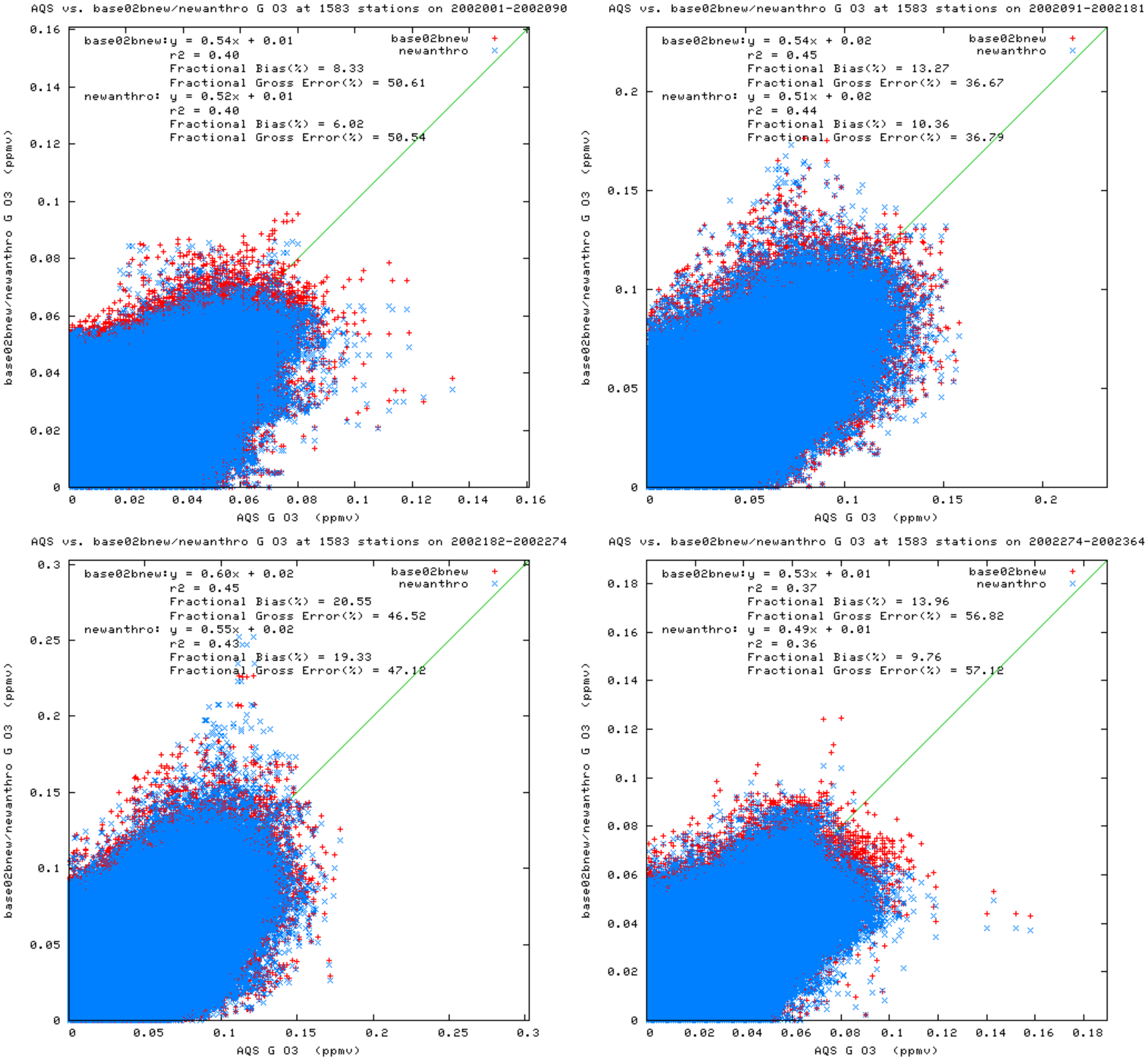

Figure 3-1. CMAQ 2002 36 km Current Standard case (base02bnew in red) vs. Revised Standard case (newanthro in blue) model performances for ozone (O_3) for all AQS monitoring sites in entire US continental in four quarters of the year. 1st quarter (top left), 2nd quarter (top right), 3rd quarter (bottom left) and 4th quarter (bottom right).

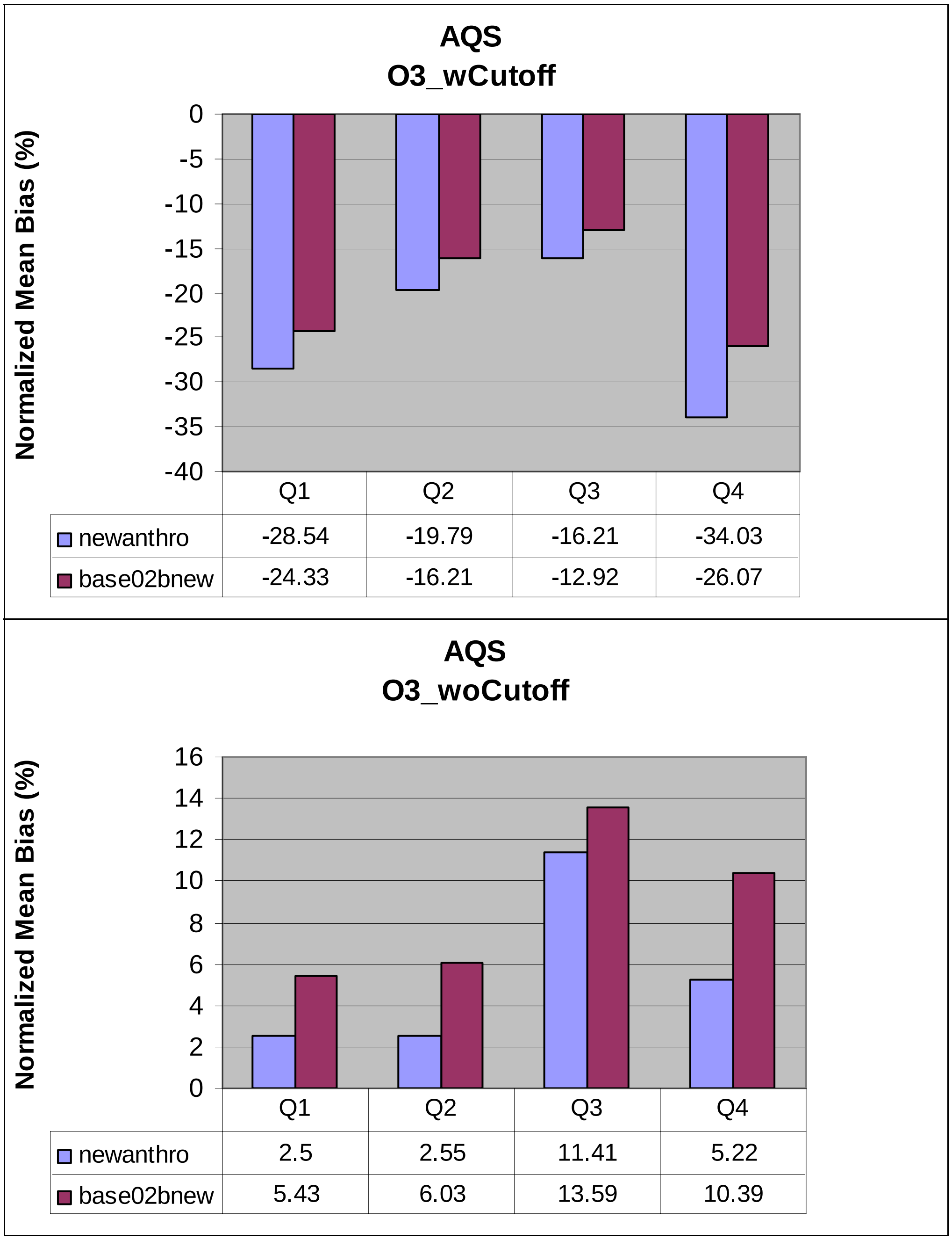

	Q1	Q2	Q3	Q4
▢ newanthro	-28.54	-19.79	-16.21	-34.03
■ base02bnew	-24.33	-16.21	-12.92	-26.07

	Q1	Q2	Q3	Q4
▢ newanthro	2.5	2.55	11.41	5.22
■ base02bnew	5.43	6.03	13.59	10.39

Figure 3-2. Model performance for ozone, calculated as normalized mean bias, with a 60 ppb filter applied to monitoring data (top) and with no data filter (bottom).

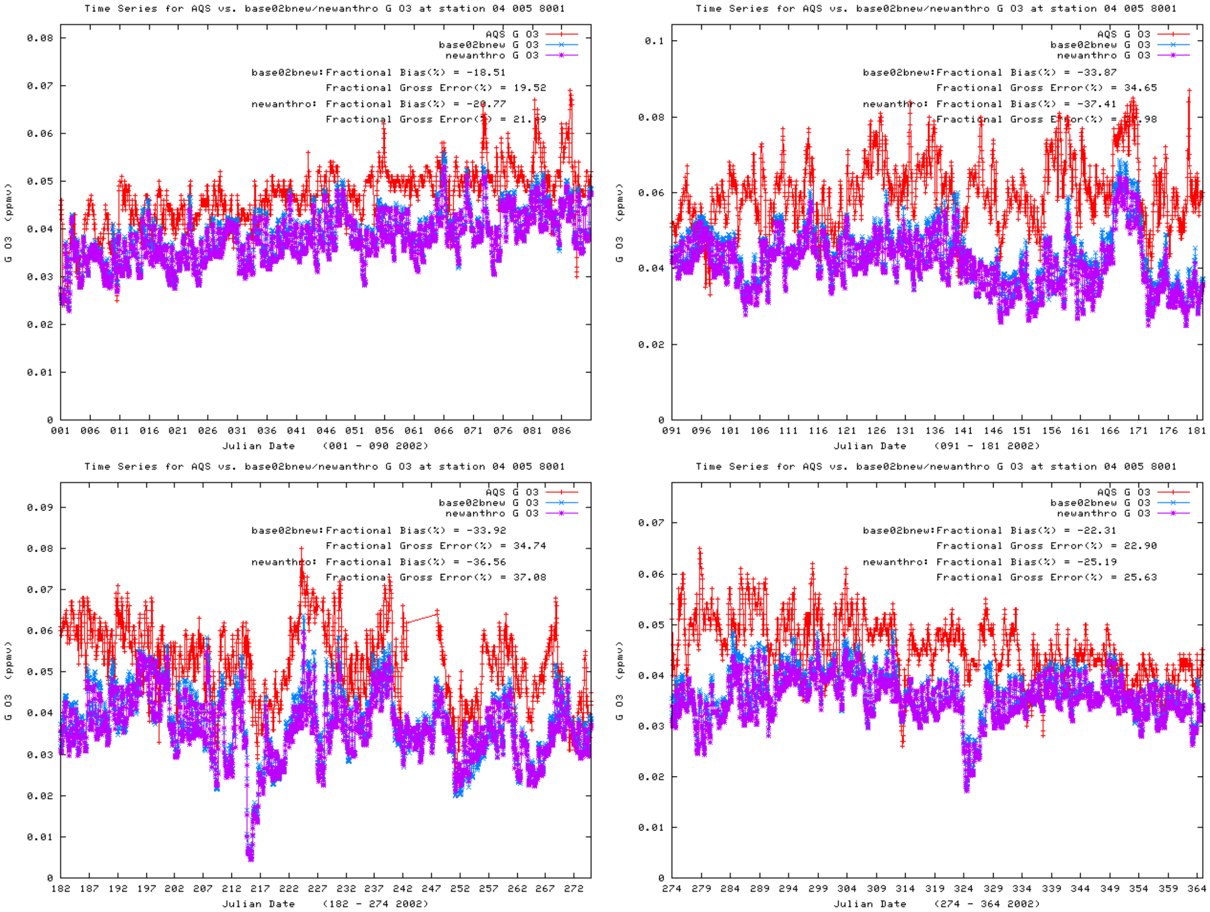

Figure 3-3. Time series of O_3 observed values (in red) vs. modeled values from CMAQ 2002 36 km Current Standard case (base02bnew in blue) and Revised Standard case (newanthro in purple) at the AQS monitoring site, Grand Canyon National Park, AZ. 1st quarter (top left), 2nd quarter (top right), 3rd quarter (bottom left) and 4th quarter (bottom right).

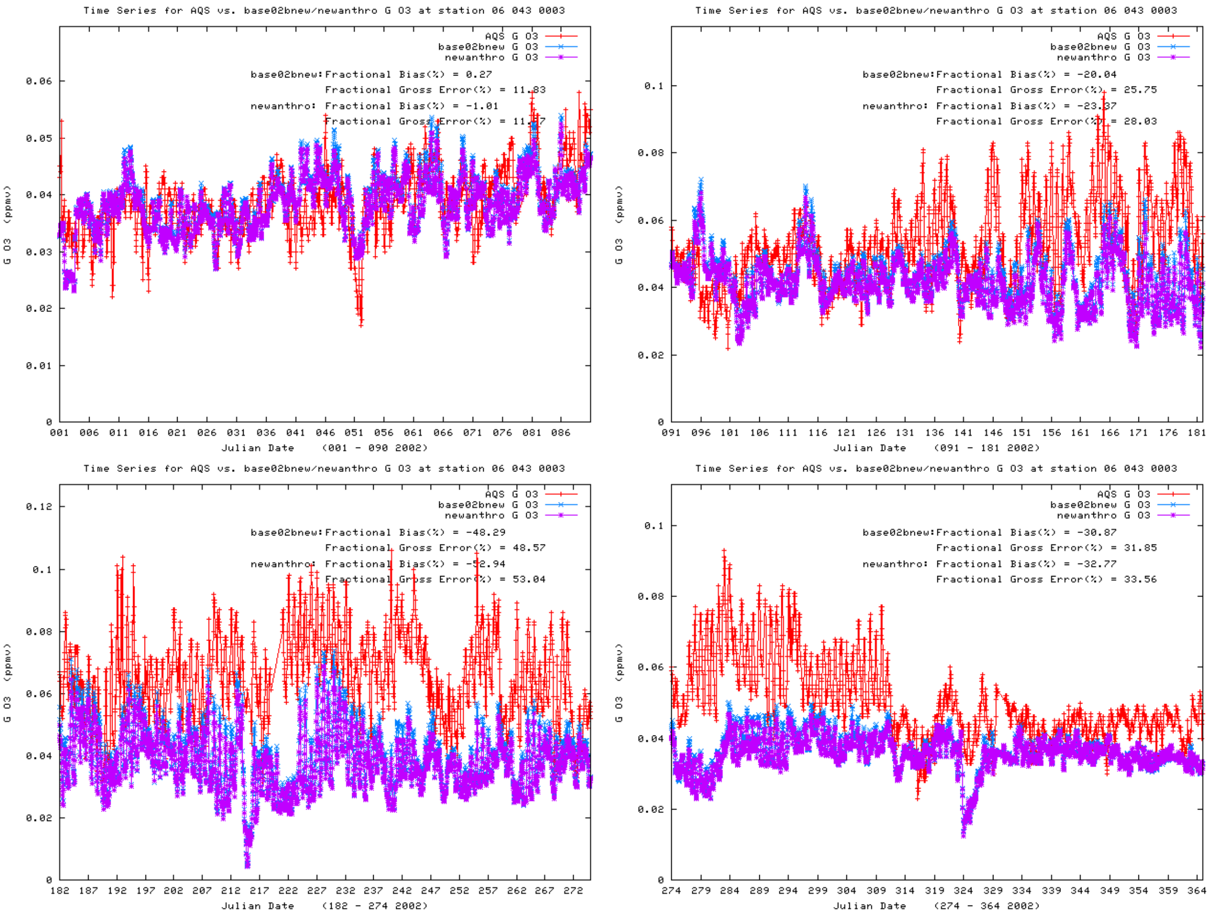

Figure 3-4. Time series of O_3 observed values (in red) vs. modeled values from CMAQ 2002 36 km Current Standard case (base02bnew in blue) and Revised Standard case (newanthro in purple) at the AQS monitoring site, Turtleback Dome, Yosemite National Park, CA. 1st quarter (top left), 2nd quarter (top right), 3rd quarter (bottom left) and 4th quarter (bottom right).

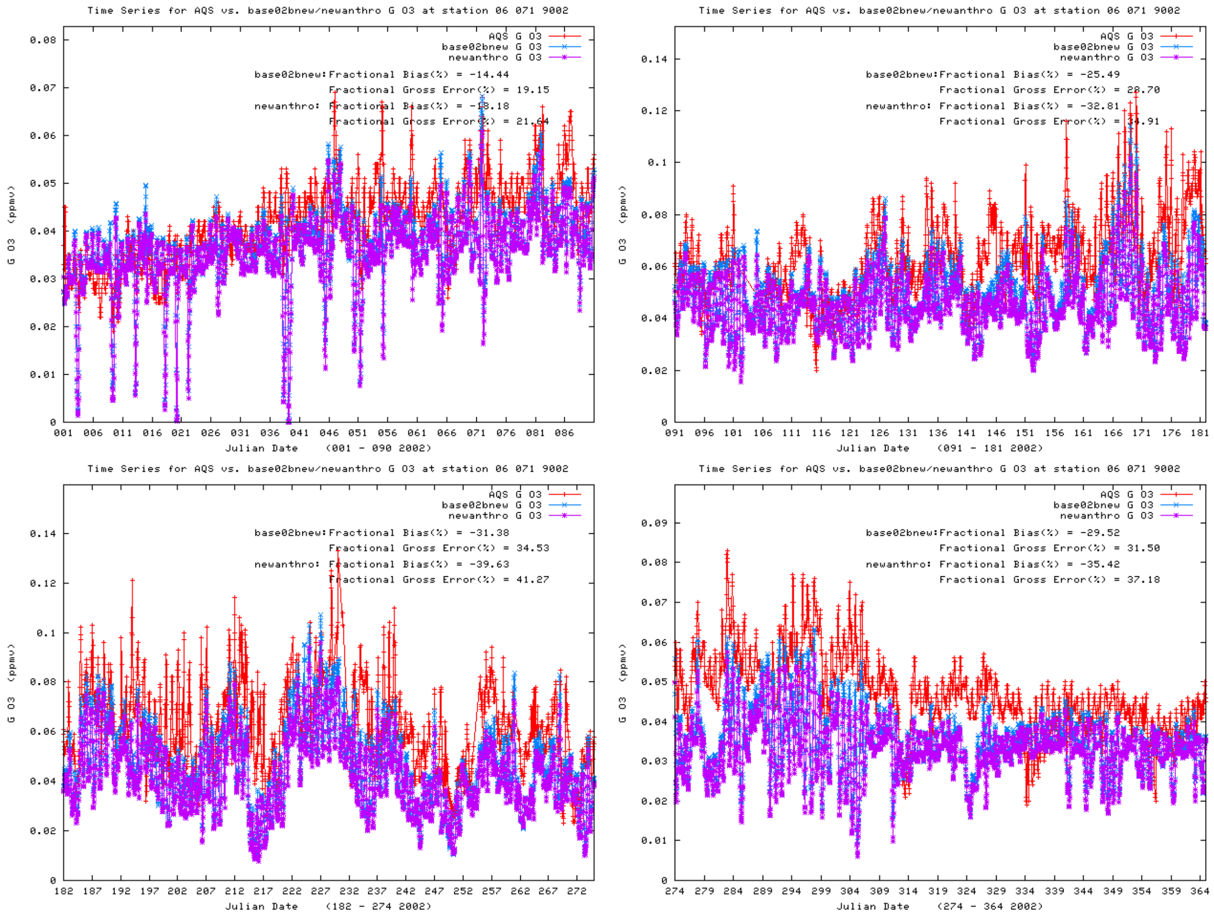

Figure 3-5. Time series of O_3 observed values (in red) vs. modeled values from CMAQ 2002 36 km Current Standard case (base02bnew in blue) and Revised Standard case (newanthro in purple) at the AQS monitoring site, Joshua Tree National Monument, CA. 1st quarter (top left), 2nd quarter (top right), 3rd quarter (bottom left) and 4th quarter (bottom right).

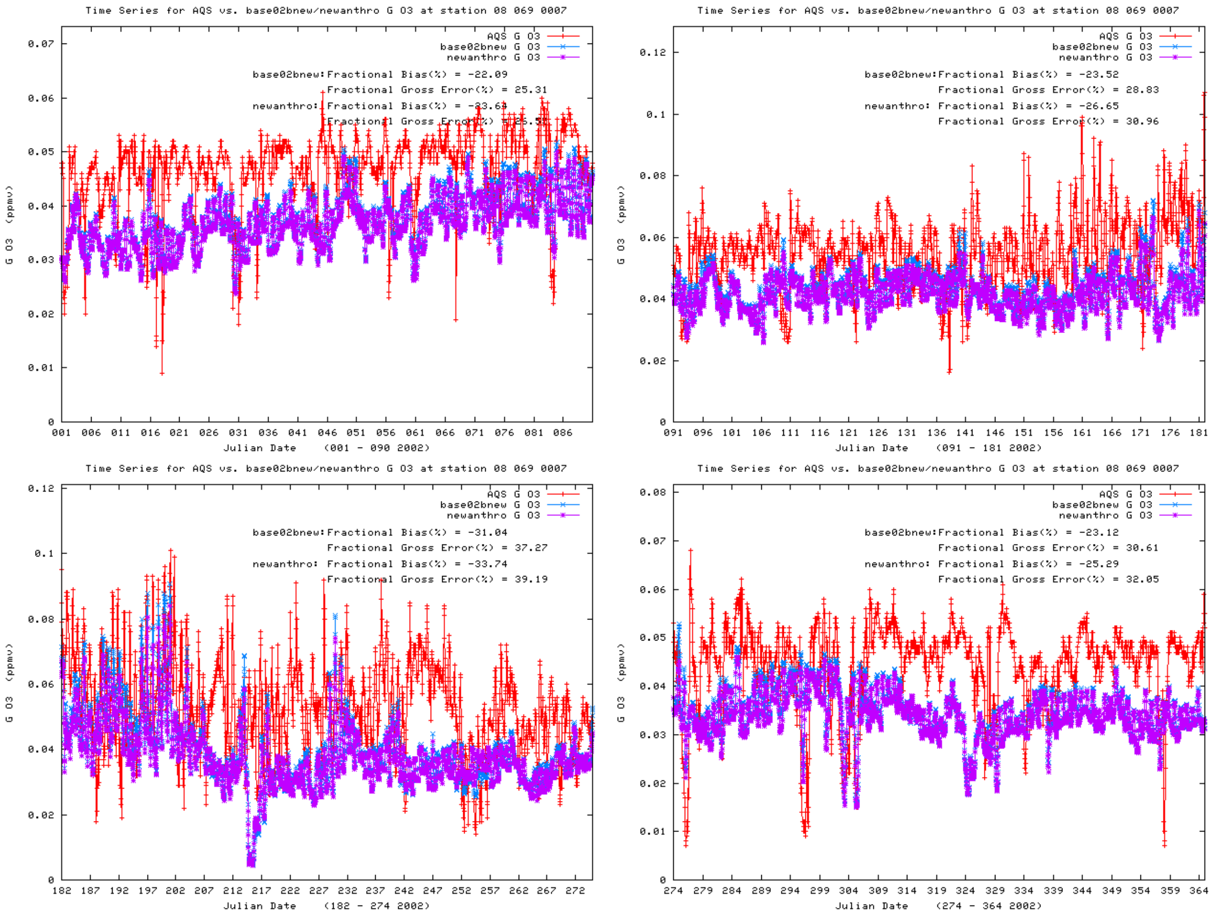

Figure 3-6. Time series of O_3 observed values (in red) vs. modeled values from CMAQ 2002 36 km Current Standard case (base02bnew in blue) and Revised Standard case (newanthro in purple) at the AQS monitoring site, Rocky Mountain National Park, CO. 1st quarter (top left), 2nd quarter (top right), 3rd quarter (bottom left) and 4th quarter (bottom right).

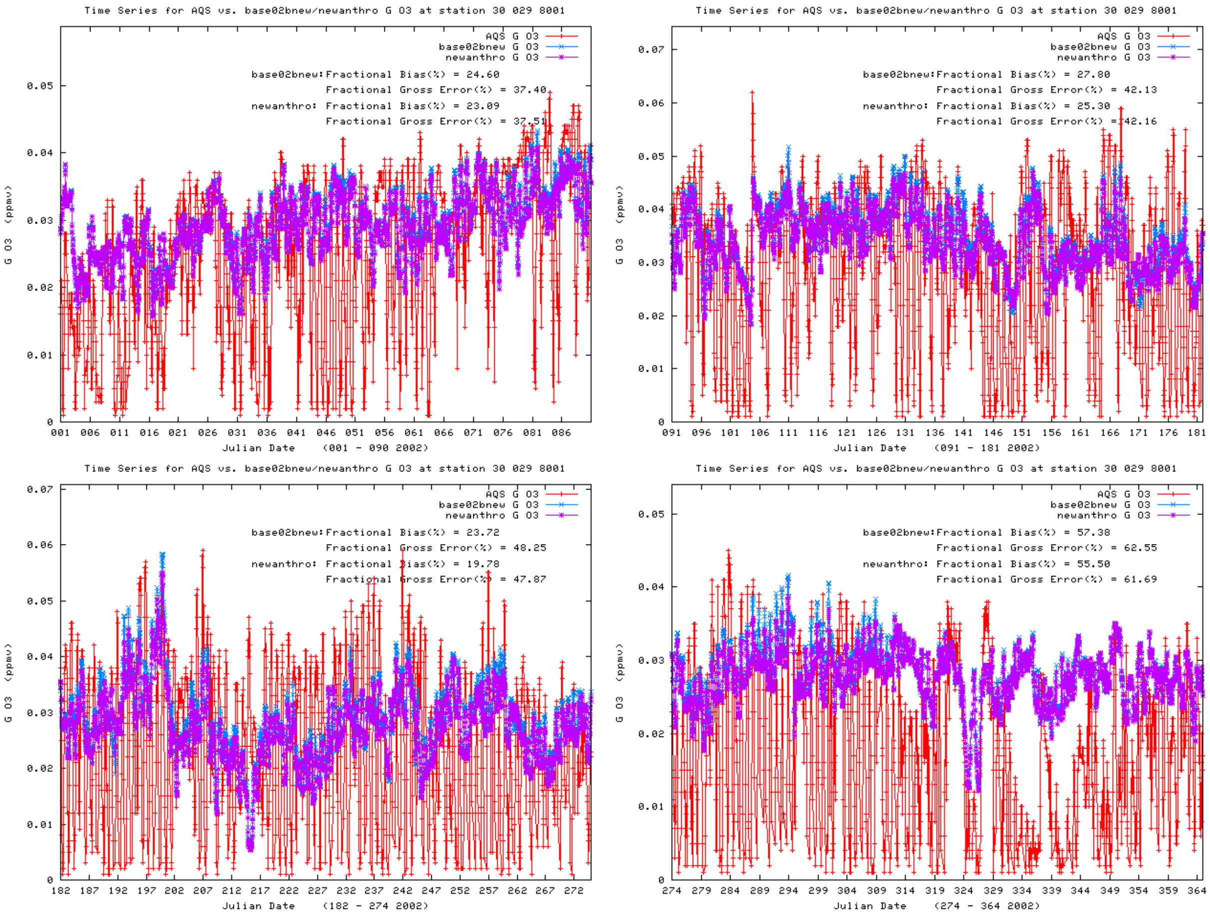

Figure 3-7. Time series of O_3 observed values (in red) vs. modeled values from CMAQ 2002 36 km Current Standard case (base02bnew in blue) and Revised Standard case (newanthro in purple) at the AQS monitoring site, Glacier National Park, MT. 1st quarter (top left), 2nd quarter (top right), 3rd quarter (bottom left) and 4th quarter (bottom right).

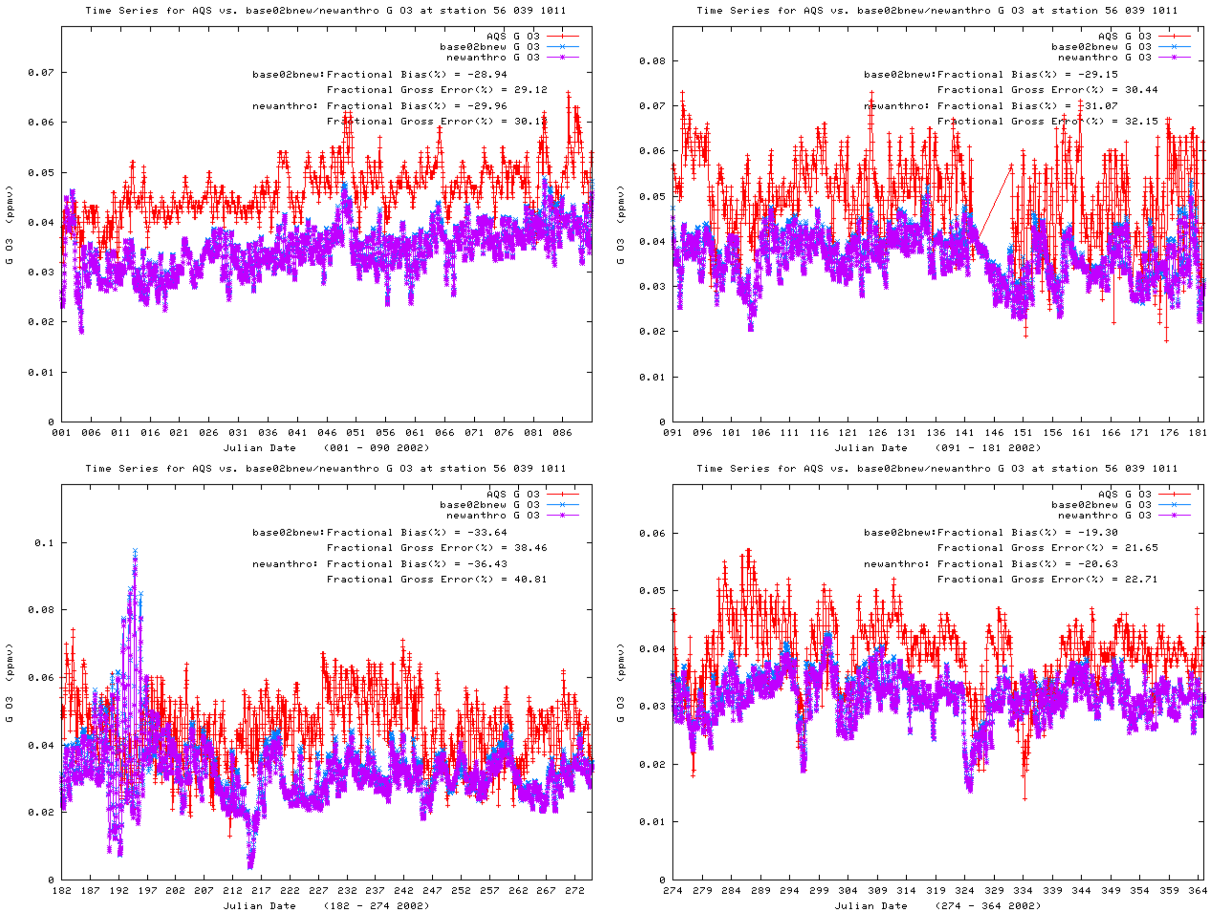

Figure 3-8. Time series of O_3 observed values (in red) vs. modeled values from CMAQ 2002 36 km Current Standard case (base02bnew in blue) and Revised Standard case (newanthro in purple) at the AQS monitoring site, Yellowstone National Park, WY. 1st quarter (top left), 2nd quarter (top right), 3rd quarter (bottom left) and 4th quarter (bottom right).

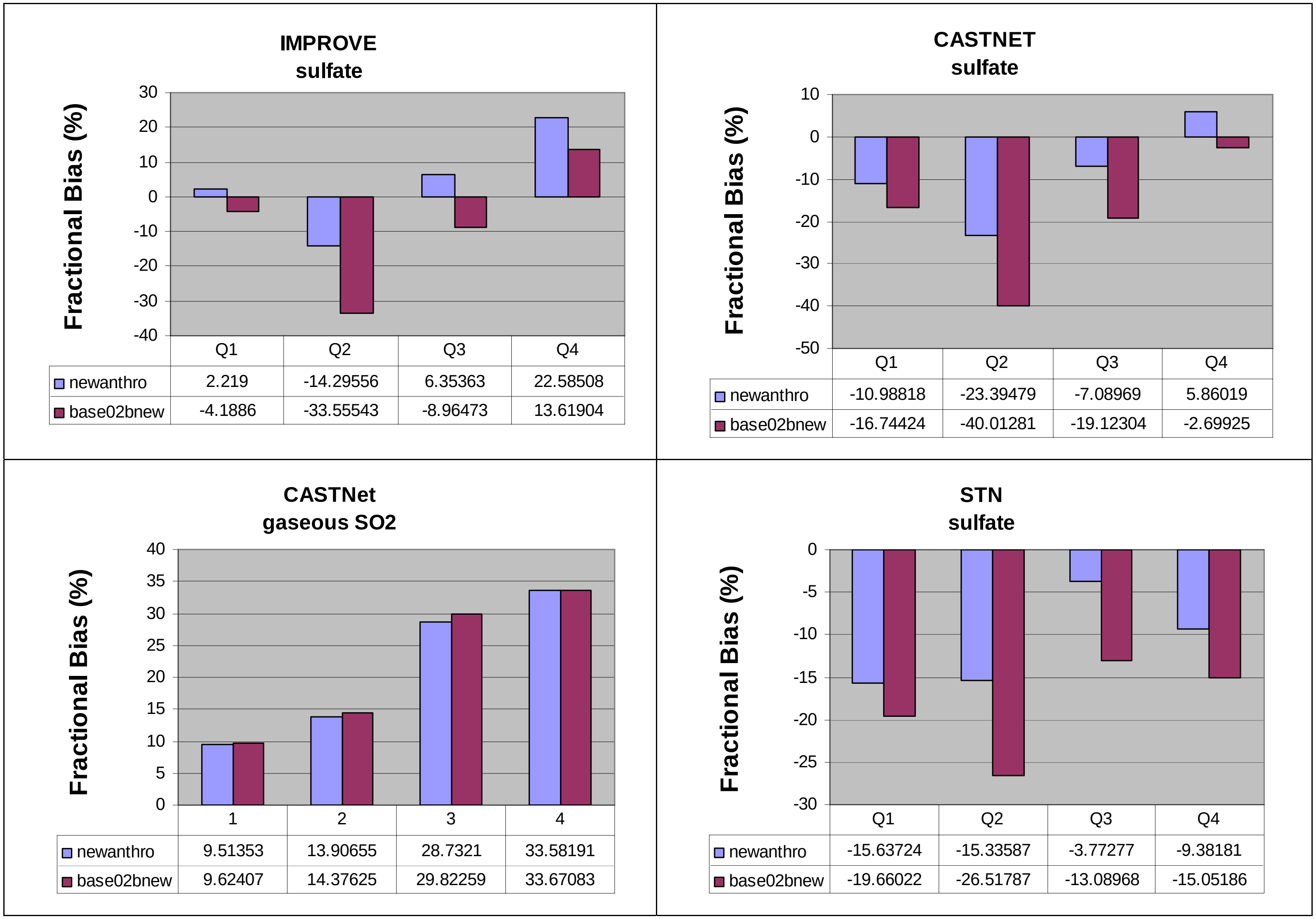

IMPROVE sulfate

	Q1	Q2	Q3	Q4
🟦 newanthro	2.219	-14.29556	6.35363	22.58508
🟪 base02bnew	-4.1886	-33.55543	-8.96473	13.61904

CASTNET sulfate

	Q1	Q2	Q3	Q4
🟦 newanthro	-10.98818	-23.39479	-7.08969	5.86019
🟪 base02bnew	-16.74424	-40.01281	-19.12304	-2.69925

CASTNet gaseous SO2

	1	2	3	4
🟦 newanthro	9.51353	13.90655	28.7321	33.58191
🟪 base02bnew	9.62407	14.37625	29.82259	33.67083

STN sulfate

	Q1	Q2	Q3	Q4
🟦 newanthro	-15.63724	-15.33587	-3.77277	-9.38181
🟪 base02bnew	-19.66022	-26.51787	-13.08968	-15.05186

Figure 3-9. SOx and sulfate performance for both model simulations for the IMPROVE, CASTNet and STN monitoring sites.

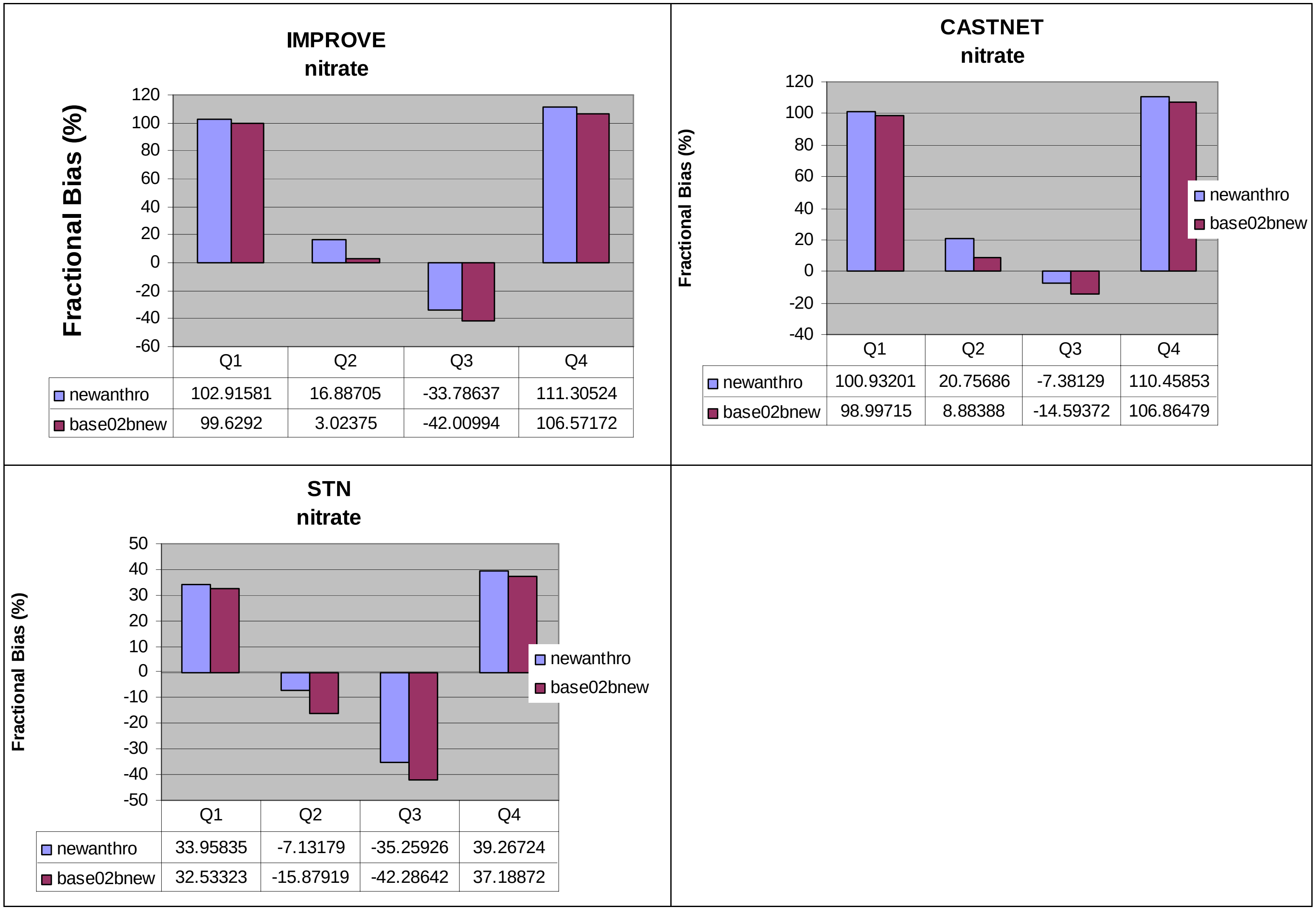

IMPROVE nitrate

	Q1	Q2	Q3	Q4
■ newanthro	102.91581	16.88705	-33.78637	111.30524
■ base02bnew	99.6292	3.02375	-42.00994	106.57172

CASTNET nitrate

	Q1	Q2	Q3	Q4
■ newanthro	100.93201	20.75686	-7.38129	110.45853
■ base02bnew	98.99715	8.88388	-14.59372	106.86479

STN nitrate

	Q1	Q2	Q3	Q4
■ newanthro	33.95835	-7.13179	-35.25926	39.26724
■ base02bnew	32.53323	-15.87919	-42.28642	37.18872

Figure 3-10. Nitrate performance for both model simulations for the IMPROVE, CASTNet and STN monitoring sites.

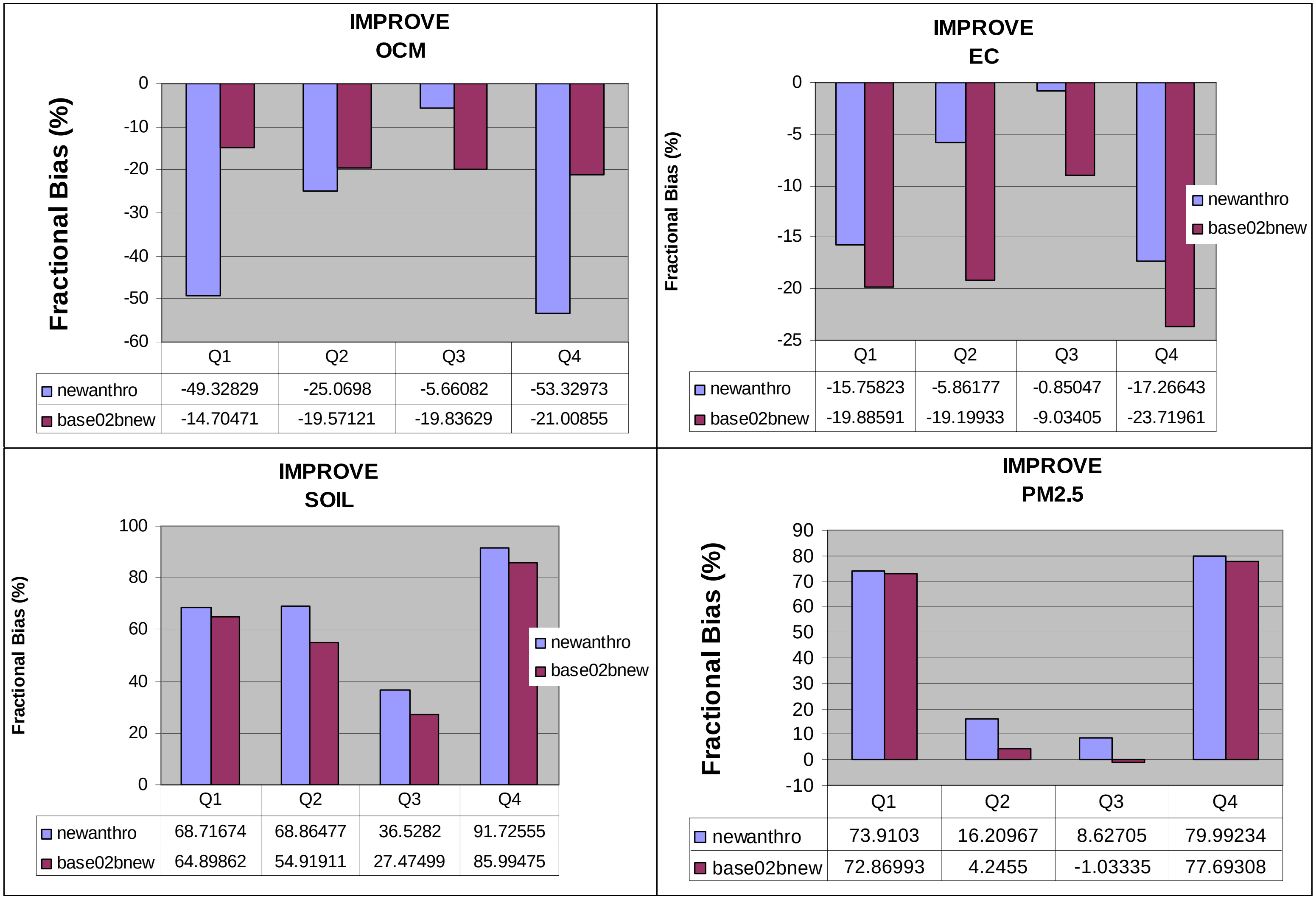

IMPROVE
OCM

	Q1	Q2	Q3	Q4
newanthro	-49.32829	-25.0698	-5.66082	-53.32973
base02bnew	-14.70471	-19.57121	-19.83629	-21.00855

IMPROVE
EC

	Q1	Q2	Q3	Q4
newanthro	-15.75823	-5.86177	-0.85047	-17.26643
base02bnew	-19.88591	-19.19933	-9.03405	-23.71961

IMPROVE
SOIL

	Q1	Q2	Q3	Q4
newanthro	68.71674	68.86477	36.5282	91.72555
base02bnew	64.89862	54.91911	27.47499	85.99475

IMPROVE
PM2.5

	Q1	Q2	Q3	Q4
newanthro	73.9103	16.20967	8.62705	79.99234
base02bnew	72.86993	4.2455	-1.03335	77.69308

Figure 3-11. Model performance for OCM, EC, soil and total $PM_{2.5}$ for the IMPROVE monitoring sites.

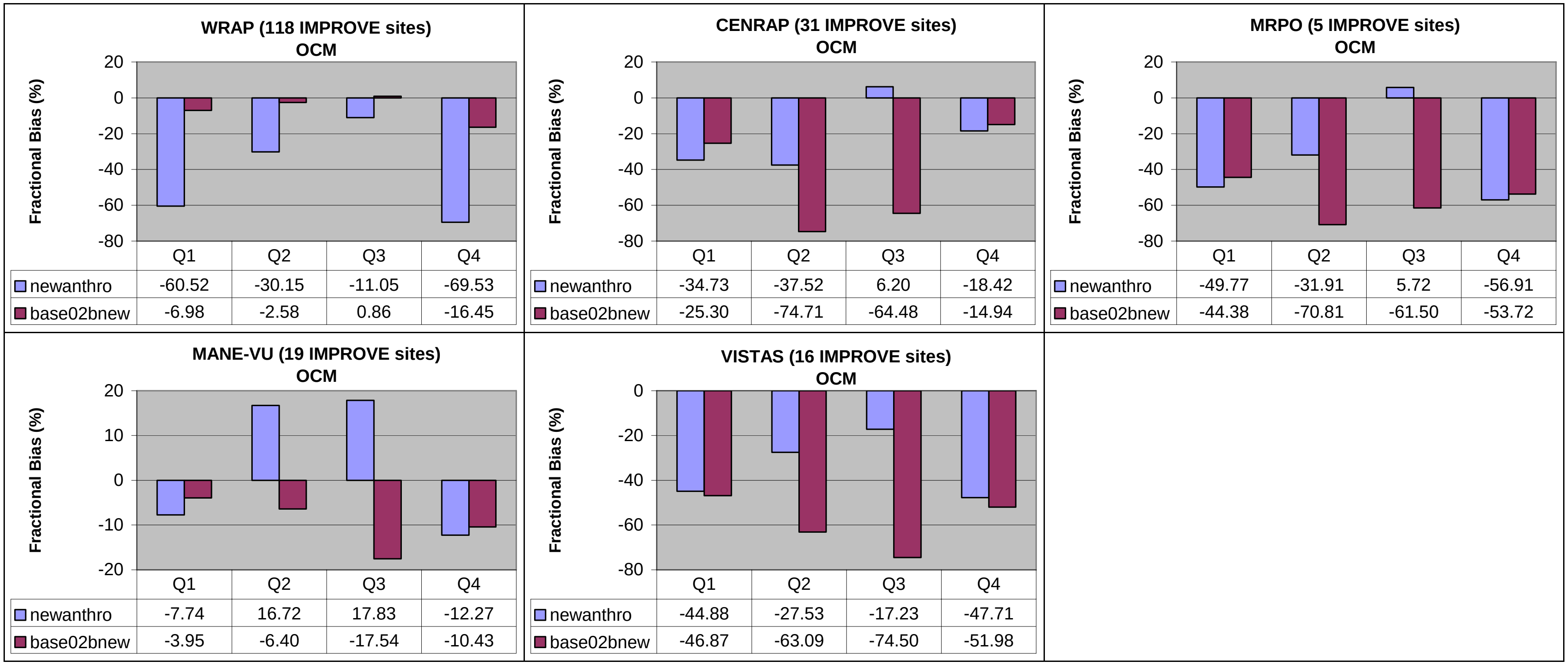

WRAP (118 IMPROVE sites)
OCM

	Q1	Q2	Q3	Q4
newanthro	-60.52	-30.15	-11.05	-69.53
base02bnew	-6.98	-2.58	0.86	-16.45

CENRAP (31 IMPROVE sites)
OCM

	Q1	Q2	Q3	Q4
newanthro	-34.73	-37.52	6.20	-18.42
base02bnew	-25.30	-74.71	-64.48	-14.94

MRPO (5 IMPROVE sites)
OCM

	Q1	Q2	Q3	Q4
newanthro	-49.77	-31.91	5.72	-56.91
base02bnew	-44.38	-70.81	-61.50	-53.72

MANE-VU (19 IMPROVE sites)
OCM

	Q1	Q2	Q3	Q4
newanthro	-7.74	16.72	17.83	-12.27
base02bnew	-3.95	-6.40	-17.54	-10.43

VISTAS (16 IMPROVE sites)
OCM

	Q1	Q2	Q3	Q4
newanthro	-44.88	-27.53	-17.23	-47.71
base02bnew	-46.87	-63.09	-74.50	-51.98

Figure 3-12. Model performance for OCM for the IMPROVE monitoring sites by geographical region (RPO states).

3.2. Impact on Policy-Related Criteria for Ozone and $PM_{2.5}$

Natural background levels of ozone and $PM_{2.5}$ can limit the effectiveness of air quality control measures in attaining NAAQS. If natural background levels are close to the NAAQS levels, substantially larger emissions controls will be required to attain the NAAQS. Although there is large uncertainty in the actual background levels, it is useful to evaluate the model simulated background because air quality models are an important tool in developing emissions control strategies. Even if the model predictions are not accurate, the model background level represents a floor in the simulated ozone and $PM_{2.5}$ levels, and if the floor exceeds the NAAQS levels, it will not be possible to demonstrate attainment of NAAQS levels using modeling studies. In this section we review the natural background levels for two simulations for both the natural and anthropogenic emissions cases.

3.2.1. 4th highest 8-hour Average Ozone

Figure 3-13 shows the model simulated 4th highest 8-hour average ozone for the Current and Revised Natural simulations, and the bottom plot in Figure 3-13 shows the difference between the two model simulations. In the Current Natural simulation, there were areas in the California and Oregon for which the 4th highest 8-hour average ozone exceeded 75 ppb, with a maximum value of 80.1 ppb in eastern Oregon. In the Revised Natural simulation, which had reduced NOx emissions in the MEGAN biogenic model, the maximum 4th highest 8-hour average ozone was 68.7 ppb, also in eastern Oregon. Figure 3-13 (bottom) shows that ozone levels decreased in the western US for the Revised Natural simulation compared to the Current Natural simulation, with the largest increase of 18.3 ppb occurring in northern CA. Even with these reductions, model simulated ozone levels still exceeded 50 ppb in the several areas in the southwestern US in the Revised Natural case.

There were also large areas in the eastern US where ozone increased in the Revised Natural simulation, and ozone levels exceeded 50 ppb in the southeastern US in the Revised Natural simulation. As shown in the bottom plot of Figure 3-13, the ozone levels in the southeastern US were substantially increased in the Revised Natural simulation compared to the Current Natural simulation, primarily from the effect of including lightning NOx emissions. Ozone levels increased in the Revised Natural simulation by more than 10 ppb in the southeastern US, with a maximum increase of 25.3 ppb in western Mexico.

For much of the central and northern US, the 4th highest 8-hour average ozone levels were between 20 to 35 ppb. Ozone levels in the upper Midwest increased by 3 to 6 ppb in the Revised Natural simulation compared to the Current Natural.

Figure 3-14 shows the model predicted 4th highest 8-hour average ozone for the Current Standard and the Revised Standard simulations. As in the natural emissions simulations, the differences between the two simulations are reduced ozone in the western US as result of the lower NOx emissions in the MEGAN model used in the Revised Standard simulation, and increased ozone in the eastern US as a result of the addition of the lightning NOx emissions.

Current Natural Simulation

Revised Natural Simulation

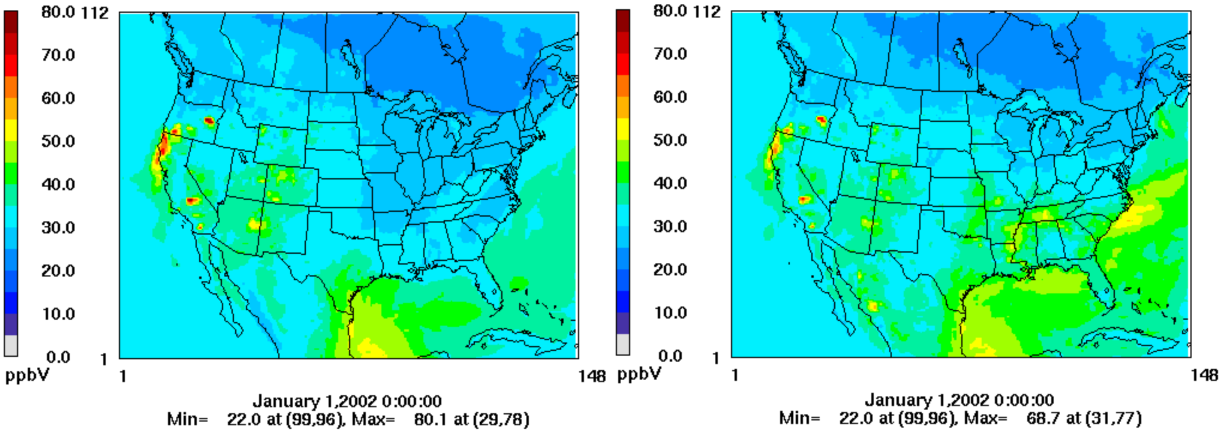

Revised Natural – Current Natural

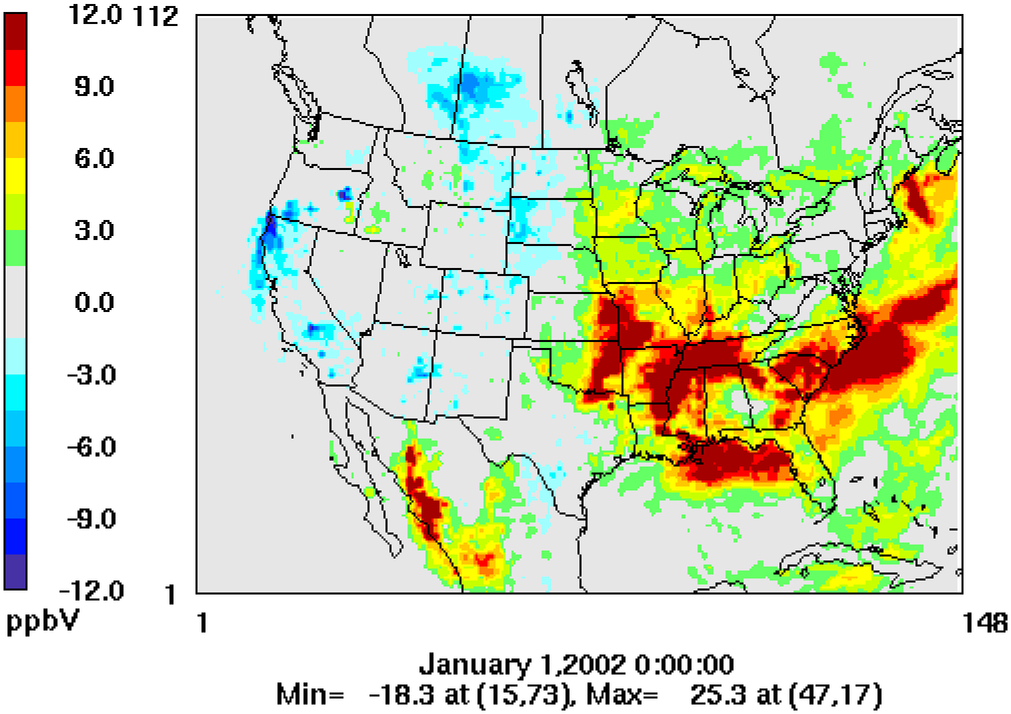

Figure 3-13. Model predicted 4th highest 8-hour average ozone for the natural emissions simulations: Current Natural case (top-left); Revised Natural case (top-right); and the difference between the two cases (bottom).

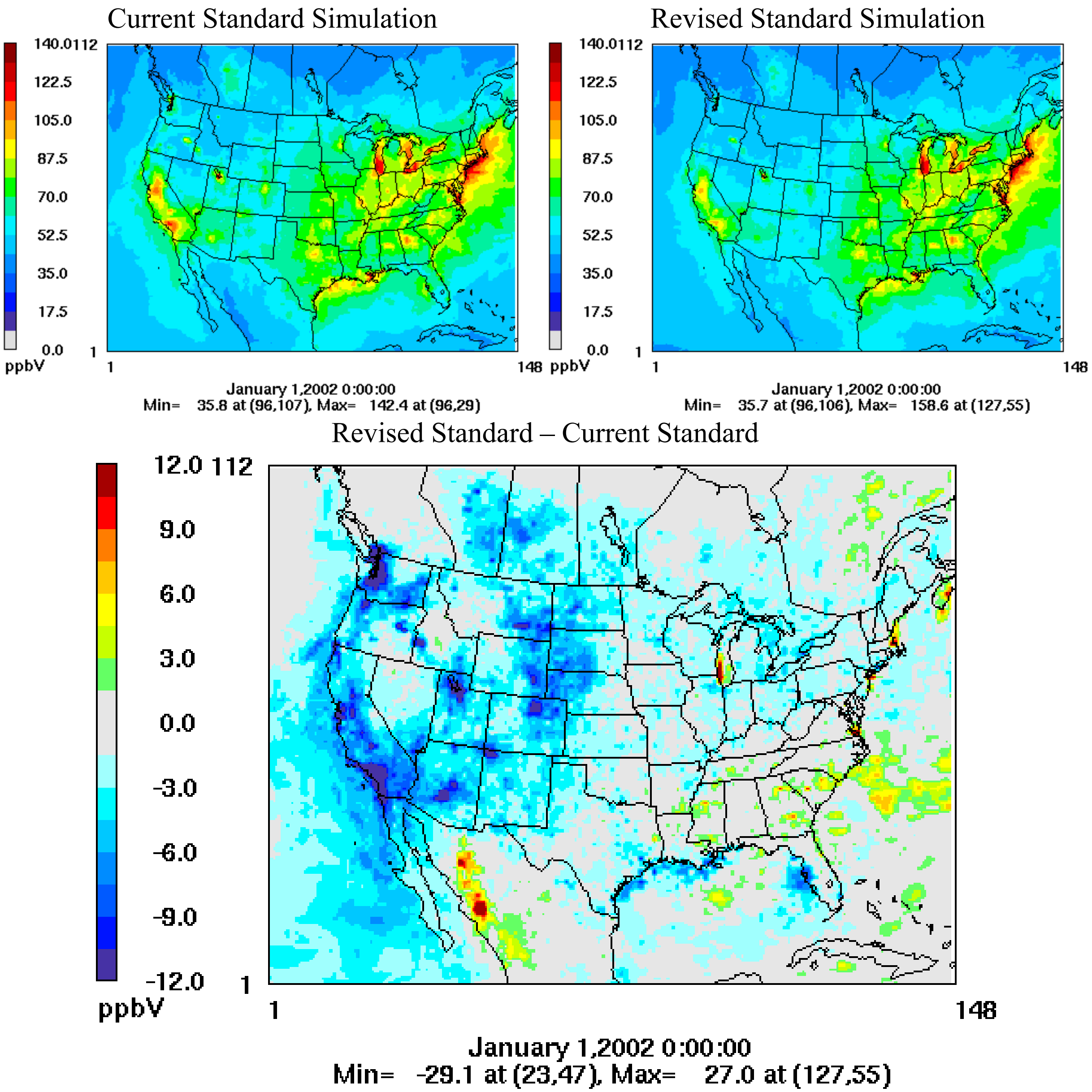

Figure 3-14. Model predicted 4th highest 8-hour average ozone for the anthropogenic emissions simulations: Current Standard case (top-left); Revised Standard case (top-right); and the difference between the two cases (bottom).

3.2.2. 8th highest 24-hour Average $PM_{2.5}$

Figure 3-15 shows the model simulated 8th highest 24-hour average $PM_{2.5}$ for the Current and Revised Natural simulations, and the bottom plot in Figure 3-15 shows the difference between the two model simulations. For both simulations, the maximum 8th highest 24-hour average $PM_{2.5}$ is about 345 $\mu g/m^3$ and it occurs in eastern Arizona. Wildfires are the primary source of $PM_{2.5}$ for these simulations and high $PM_{2.5}$ values also occur in other areas in the western US where there are large wild fires. In areas that are not immediately influenced by large fires, the 8th highest 24-hour average $PM_{2.5}$ concentrations vary from about 5 to 15 $\mu g/m^3$. We note that the fire emissions inventories used in these simulations were developed from actual 2002 fires, and the locations of the high $PM_{2.5}$ concentrations would differ for other modeling periods.

The bottom plot in Figure 3-15 shows the difference between the two simulations. There is an increase in the boundary concentrations of $PM_{2.5}$ on the western boundary in the Revised Natural case compared to the Current Natural case (see Section 2.1), and the simulated 8th highest 24-hour average concentrations for the Revised Natural case were about 1 to 2 $\mu g/m^3$ greater than the Current Natural case through most of the model domain. There were some small areas of reductions in $PM_{2.5}$ in the Revised Natural case compared to the Current Natural case, mostly in areas of large wildfires, and it is possible that the reduced ozone levels in the Revised Natural simulation might have resulted in less formation of secondary $PM_{2.5}$ in the fire plumes.

Figure 3-16 shows the model predicted 8th highest 24-hour average $PM_{2.5}$ for the Current and Revised Standard simulations, and the bottom plot in Figure 3-16 shows the difference between the two model simulations. There were increased in $PM_{2.5}$ of more than 4 $\mu g/m^3$ in the Revised Standard case in large areas in the Midwest, Appalachia and Texas.

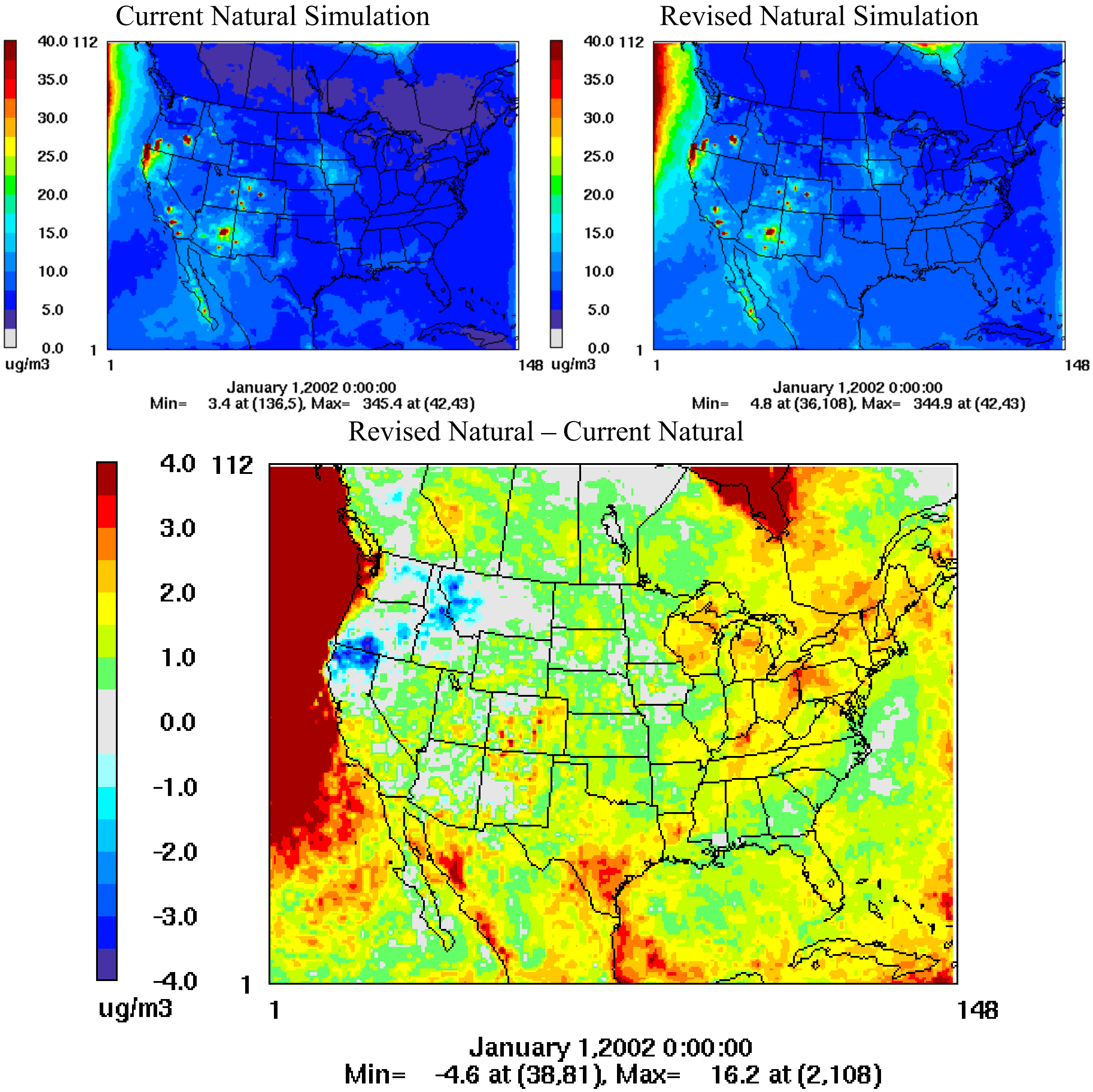

Current Natural Simulation

Revised Natural Simulation

Revised Natural – Current Natural

Figure 3-15. Model predicted 8th highest 24-hour average $PM_{2.5}$ for the natural emissions simulations: Current Natural case (top-left); Revised Natural case (top-right); and the difference between the two cases (bottom).

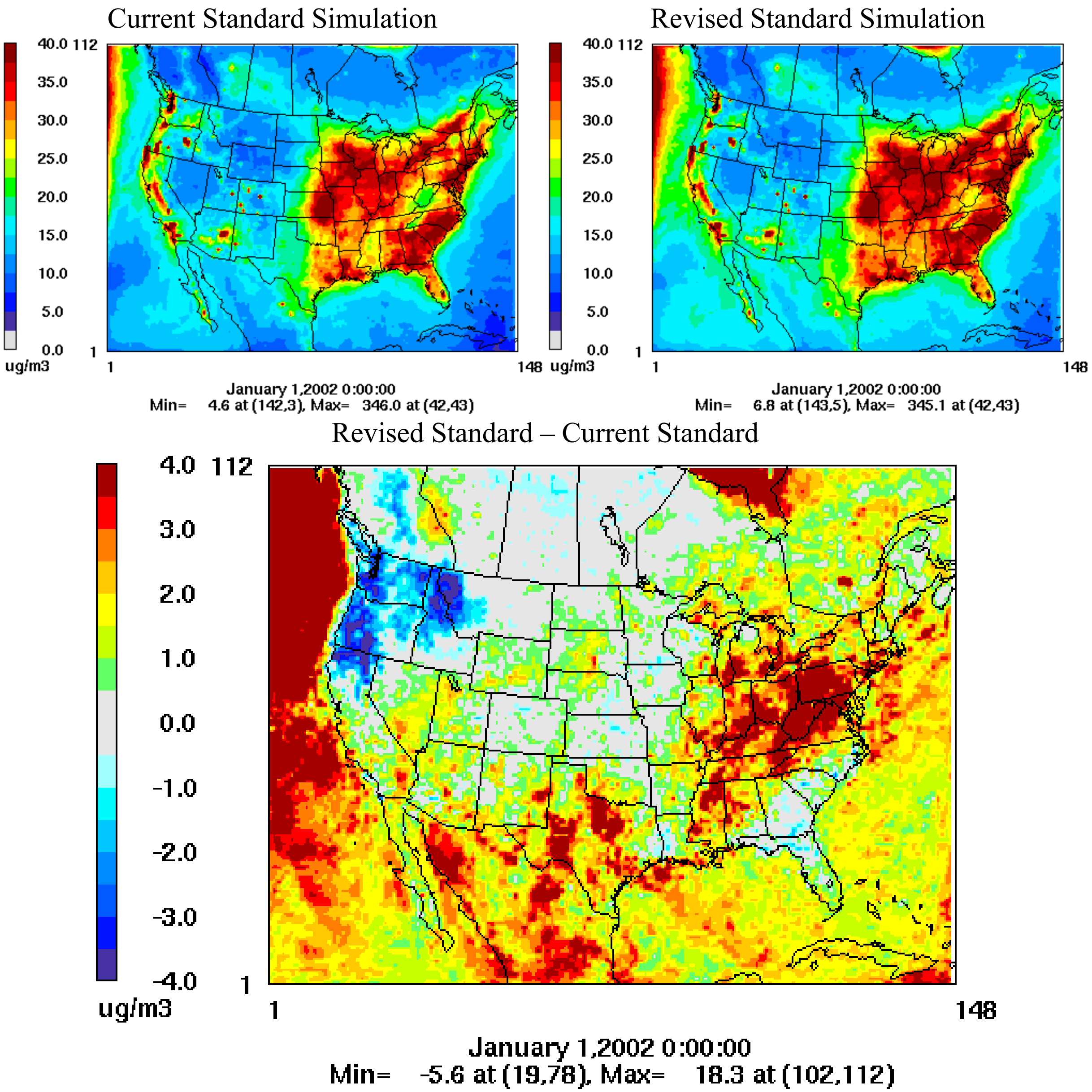

Figure 3-16. Model predicted 8th highest 24-hour average $PM_{2.5}$ for the anthropogenic emissions simulations: Current Standard case (top-left); Revised Standard case (top-right); and the difference between the two cases (bottom).

4. SUMMARY

Based on the literature review and findings from the previous WRAP "clean" simulation, the following natural components were added to the current modeling practice for ozone and $PM_{2.5}$:

- Sulfur emissions from ocean (DMS and MSA)
- NOx emissions from lightning
- Alternative sea salt emissions using the CAMx external sea salt generator
- Updated SOA model with the MEGAN biogenic emissions
- Pre-industrial level of methane

The largest impact on background ozone concentrations comes from inclusion of lightning NOx emissions which result in significant increases in ozone over southeastern US and Gulf of Mexico. MEGAN estimates less NO emissions from biogenic sources than SMOKE BEIS3, thus causes ozone decreases in central and western US. Background $PM_{2.5}$ generally increases with the revised natural sources. Additional SOA from the new SOA processes (e.g., SOA from sesquiterpenes and polymerization) is the major part of $PM_{2.5}$ increases in southeastern US.

The model performance evaluation for ozone and $PM_{2.5}$ showed results similar to previous performance evaluations completed in the WRAP modeling (Tonnesen et al., 2006a). The model tended to over-predict nitrate in the winter and under-predict nitrate in the summer. However, the MPE results for the Revised Standard simulation showed better performance for sulfate, EC and summer OCM compared to the Current Standard simulation. There was less negative bias for sulfate in the Revised Standard case compared to the Current Standard case. The Revised Standard simulation showed significant performance improvement for OCM over the southeastern US in summer time, whereas it showed greater negative bias in the western US in winter.

There remains large uncertainty in all model simulations of natural background levels of ozone, because of uncertainty in the biogenic emissions of VOC and NOx. As shown in the previous section, different biogenic NO emissions from BEIS3 and MEGAN result in contrary conclusions on whether it is possible to achieve the 75 ppb ozone NAAQS solely by controlling anthropogenic precursor emissions. Note that we have more confidence on MEGAN estimates as they are based on more updated land use data. Lightning NOx is also a critical uncertainty, especially for the southeastern US where there are large biogenic VOC emissions and where ozone formation is especially sensitive to changes in NOx emissions. The assumptions for lightning NOx emissions may significantly change the modeled natural ozone level and may also change the relative effectiveness of VOC and NOx emissions controls. Finally, the role of stratospheric ozone intrusion remains an important uncertainty. In all of the model simulations performed in this study, the ozone concentration in the top layers of the boundary concentration files were reduced because overly vigorous vertical circulations diagnosed by the CMAQ model are incorrectly transporting the high altitude ozone to the surface. Improvements on the model's vertical transport scheme should be preceded before the impact of stratospheric ozone intrusion is properly studied.

5. NEXT STEP

As stated in Section 1.1, the focus of the CRC Project A-65 is to assess ozone and PM responses to emissions reductions under the revised natural background conditions. For this, we will conduct a series of sensitivity simulations using the VISTAS 2002 36 and 12 km CMAQ modeling database. VISTAS uses the same national RPO 36 km domain as used by WRAP and a 12 km grid that covers the eastern US, from Houston and Minneapolis in the west to all of Florida and New York City in the east. The 36 and 12 km modeling will have different focus:

36 km simulation:

- Runs for the full year of 2002;
- Focuses on ozone and $PM_{2.5}$.

12 km simulation:

- Runs only for the third quarter (Q3) of 2002;
- Focuses on ozone; could be used for checking consistency of the PM results with the 36 km annual run.

We will also conduct future year (2018) base case simulations using the 36 km (annual) and 12 km (Q3) grids with two sets of natural background conditions: with the "Current" and the "Revised" natural components. Then, the future year sensitivity runs will be performed with various anthropogenic emissions reductions for each of the two natural background conditions (Table 5-1).

The EPA Model Attainment Test Software (MATS) will process the base and control case runs to obtain the 2018 projected 8-hr ozone and $PM_{2.5}$ Design Values and regional haze metrics at Class I areas. The impacts of natural sources on the model responses of ozone and PM to the anthropogenic emissions controls will be examined and discussed.

Table 5-1. Level of anthropogenic emission reductions selected for the future year sensitivity runs.

	NOx	VOC	SO_2	NH_3	$PM_{2.5}$
$PM_{2.5}$ 36 km (Annual)	30%	-	-	-	-
	-	30%	-	-	-
	-	-	30%	-	-
	-	-	-	30%	-
	-	-	-	-	30%
Ozone 36/12 km (Q3)	30%	-	-	-	-
	-	30%	-	-	-
	30%	30%	-	-	-

6. REFERENCES

Blunier, T., J. A. Chappellaz, J. Schwander, J.-M. Barnola, T. Desperts, B. Stauffer, and D. Raynaud (1993) Atmospheric methane, record from a Greenland ice core over the last 1000 year, Geophys. Res. Lett., 20(20), 2219.

Boccippio, D. J., K. L. Cummins, H. J. Christian, and S. J. Goodman (2001) Combined Satellite- and Surface-Based Estimation of the Intracloud-Cloud-to-Ground Lightning Ratio over the Continental United States, Mon. Wea. Rev., 129, 108-122.

EPA (2003) Guidance for Estimating Natural Visibility Conditions Under the Regional Haze Rule, U.S. Environmental Protection Agency, Research Triangle Park, NC. EPA-454/B-03-005. September.

EPA (2007) Review of the National Ambient Air Quality Standards for Ozone: Policy Assessment of Scientific and Technical Information OAQPS Staff Paper. Research Triangle Park, NC: Office of Air Quality and Planning and Standards, EPA-452/R-07-003. January.

Grini, A., G. Myhre, J. K. Sundet, and I. S. A. Isaksen (2002) Modeling the annual cycle of sea salt in the Global 3D Model Oslo CTM-2: Concentrations, fluxes and radiative impacts, J. Climate, 15.

Gong, S. L. (2003) A parameterization for sea-salt aerosol source function for sub- and super-micron particle sizes, Biogeochemical Cycles, 17, 1097-1104.

Henze, D. K., and J. H. Seinfeld (2006) Global secondary organic aerosol from isoprene oxidation, Geophys. Res. Lett., 33, L09812.

Kroll, J. H., N. L. Ng, S. M. Murphy, R. C. Flagan, and J. H. Seinfeld (2005) Secondary organic aerosol formation from isoprene photooxidation under high-NOx conditions, Geophys. Res. Lett., 32, L18808.

Kroll, J. H., N. L. Ng, S. M. Murphy, R. C. Flagan, and J. H. Seinfeld (2005) Secondary organic aerosol formation from isoprene photooxidation, Environ. Sci. Technol., 40, 1869-1877.

Kuhn, U., M. O. Andreae, C. Ammann, A. C. Araujo, E. Brancaleon, P. Ciccioli, T. Dindorf, M. Frattoni, L. V. Gatti, L. Ganzeveld, B. Kruijt, J. Lelieveld, J. Lloyd, F. X. Meixner, A. D. Nobre, U. Poschl, C. Spirig, P. Stefani, A. Thielmann, R. Valentini, and J. Kesselmeier (2007) Isoprene and monoterpene fluxes from Central Amazonian rainforest inferred from tower-based and airborne measurements, and implications on the atmospheric chemistry and the local carbon budget, Atmos. Chem. Phys., 7, 2855-2879.

Lelieveld, J., T. M. Butler, J. N. Crowley, T. J. Dillon, H. Fischer, L. Ganzeveld, H. Harder, M. G. Lawrence, M. Martinez, D. Taraborrelli, and J. Williams (2008) Atmospheric oxidation capacity sustained by a tropical forest, Nature, 452, 737-740.

Monaghan, E. C., D. E. Spiel, and K. L. Davidson (1986) A model of marine aerosol generation via whitecaps and wave disruption, Oceanic Whitecaps, 167-174.

Morris, R. E., B. Koo, A. Guenther, G. Yarwood, D. McNally, T. W. Tesche, G. Tonnesen, J. Boylan and P. Brewer (2006) Model Sensitivity Evaluation for Organic Carbon using Two Multi-Pollutant Air Quality Models that Simulate Regional Haze in the Southeastern United States, *Atmos. Environ.*, 40, 4960-4972.

Orville, R. E., G. R. Huffines, W. R. Burrows, R. L. Holle, and K. L. Cummins (2002) The North American Lightning Detection Network (NALDN)-First Results: 1998-2000, Mon. Wea. Rev., 130, 2098-2109.

Shankar, U., P.V. Bhave, J.M. Vukovich, and S.J. Roselle (2005) Initial applications of sea salt aerosol emissions and chemistry algorithms in the CMAQ v4.5 - AERO4 module. Presented at 4th Annual CMAS Models-3 Users' Conference, Chapel Hill, NC.

Smith, M. H. and Harrison, N. M. (1998) The Sea Spray Generation Function, J. Aerosol. Sci., 29, S189-S190.

Tonnesen, G., Z. Wang, M. Omary, C-J. Jung, Y. Wang, R. Morris, S. Kemball-Cook, Y. Jia, S. Lau, B. Koo, Z. Adelman, A. Holland, and J. Wallace (2006a) Final Report for the Western Regional Air Partnership (WRAP) 2002 Visibility Model Performance Evaluation, University of California Riverside, Riverside, CA. (http://pah.cert.ucr.edu/aqm/308/reports/final/2002_MPE_report_main_body_FINAL.pdf)

Tonnesen, G., M. Omary, Z. Wang, C-J. Jung, R. Morris, G. Mansell, Y. Jia, B. Wang, and Z. Adelman (2006b) Report for the Western Regional Air Partnership Regional Modeling Center, University of California Riverside, Riverside, CA. (http://pah.cert.ucr.edu/aqm/308/reports/final/2006/WRAP-RMC_2006_report_FINAL.pdf)

APPENDIX

Modification of the Boundary Conditions from the GEOS-CHEM simulations

From the initial CMAQ simulations using the 2002 WRAP "actual" and "clean" modeling databases, we found unrealistically high ozone concentrations over some of the western states (Colorado, New Mexico, etc.) that were correlated to the highest terrain in the domain (Figure A-1). The highest concentrations occurred during the spring months. A series of investigations revealed that very high ozone concentrations of the lateral boundary conditions (BCs) in the uppermost model layers led to the over-estimation. The BCs extracted from the GEOS-CHEM global model simulations show very high concentrations in the top layer (layer 19), peaking in the spring, with much lower concentrations just below that level (Figure A-2). While this could be stratospheric ozone extending to lower altitudes due to a seasonally lower tropopause or mixing by tropopause folding events, the problem is that overly vigorous vertical circulations diagnosed by the CMAQ model in areas of the highest terrain are incorrectly transporting the high altitude ozone to the surface (this applies to CAMx, too). However, to fix the internal diagnosis of vertical velocity fields in CMAQ is beyond the scope of the current CRC project. Therefore, we decided to exclude the stratospheric ozone impact by duplicating lateral ozone boundary conditions in layer 16 up through layers 17-19. The impact of this reduction is shown in Figure A-3; as much as 50 ppb over the highest terrain is attributed to the stratospheric ozone coming in from the boundary conditions. Note that applying a simple reduction of the upper boundary conditions is a "patch" that does not address the fundamental problem. Ultimately, we will need to examine, implement, and test ways to reduce the strength of the diagnosed vertical circulations over the high-terrain regions.

(a) Actual condition

(b) Clean condition

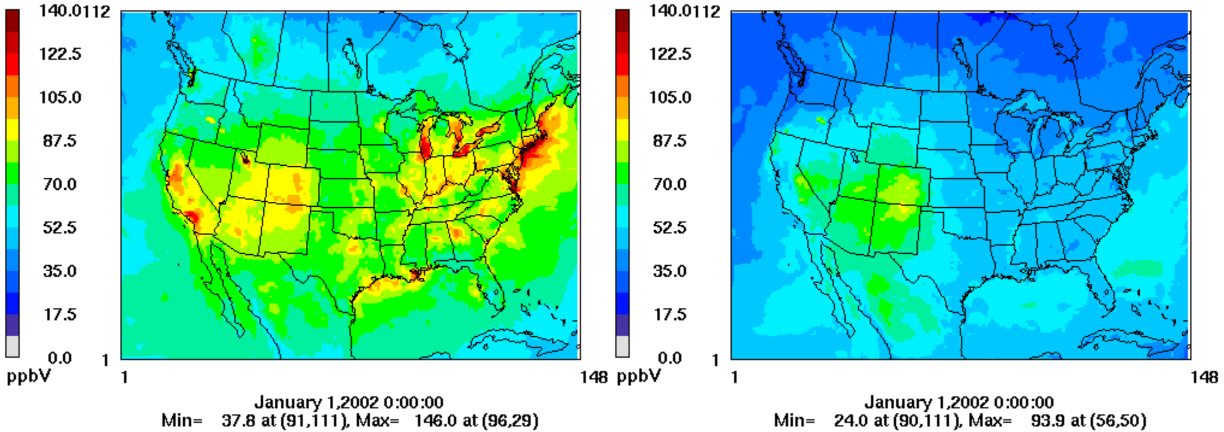

Figure A-1. Simulated 4th highest annual 8-hour ozone in the WRAP "actual" and "clean" CMAQ simulations.

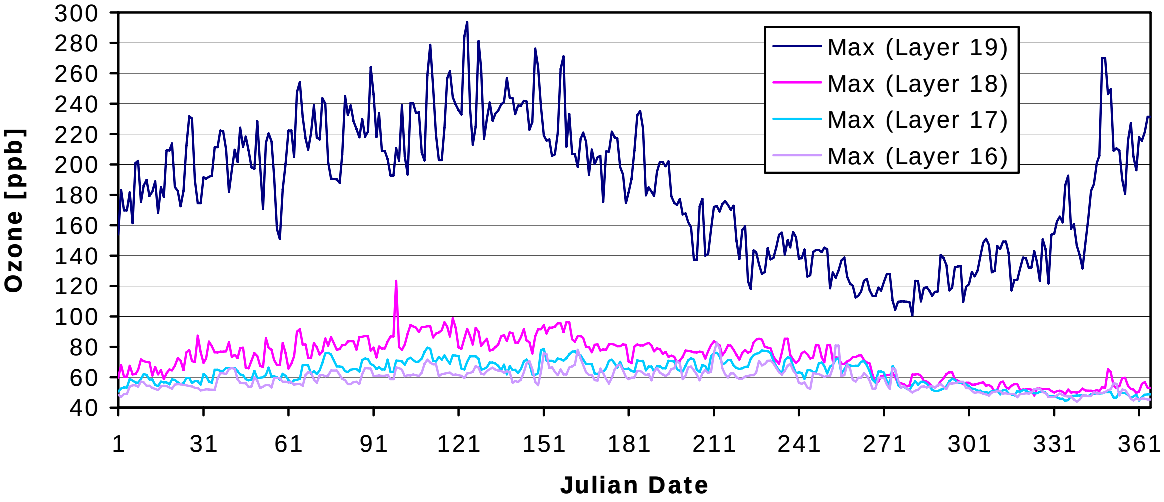

Figure A-2. Time series throughout 2002 of maximum ozone in layers 16-19 of the CMAQ lateral boundary conditions extracted from the GEOS-CHEM actual condition simulation.

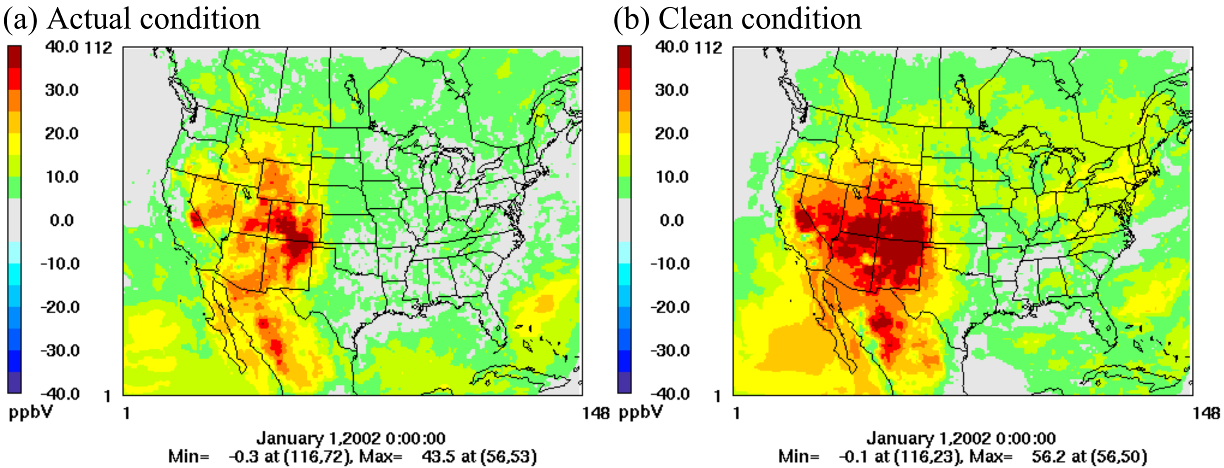
(a) Actual condition

(b) Clean condition

Figure A-3. Difference in simulated 4^{th} highest annual 8-hour ozone between the WRAP simulations with the original BCs and with the modified BCs.